UNCLASSIFIED

AD NUMBER
AD385912
CLASSIFICATION CHANGES
TO: unclassified
FROM: confidential
LIMITATION CHANGES
TO: Approved for public release, distribution unlimited
FROM: Distribution authorized to U.S. Gov't. agencies and their contractors; Critical Technology; DEC 1967. Other requests shall be referred to Air Force Rocket Propulsion Laboratory, Attn: RPPR-Stinfo], Edwards AFB, CA 93523.
AUTHORITY
AFRPL LTR 15 MAR 1971; AFRPL LTR 5 FEB 1986

THIS PAGE IS UNCLASSIFIED

AD 385 912

AUTHORITY: AFRPL

ltr, 5 Feb 86

Best Available Copy

SECURITY MARKING

The classified or limited status of this report applies to each page, unless otherwise marked.
Seperate page printouts MUST be marked accordingly.

THIS DOCUMENT CONTAINS INFORMATION AFFECTING THE NATIONAL DEFENSE OF THE UNITED STATES WITHIN THE MEANING OF THE ESPIONAGE LAWS, TITLE 18, U.S.C., SECTIONS 793 AND 794. THE TRANSMISSION OR THE REVELATION OF ITS CONTENTS IN ANY MANNER TO AN UNAUTHORIZED PERSON IS PROHIBITED BY LAW.

NOTICE: When government or other drawings, specifications or other data are used for any purpose other than in connection with a definitely related government procurement operation, the U. S. Government thereby incurs no responsibility, nor any obligation whatsoever; and the fact that the Government may have formulated, furnished, or in any way supplied the said drawings, specifications, or other data is not to be regarded by implication or otherwise as in any manner licensing the holder or any other person or corporation, or conveying any rights or permission to manufacture, use or sell any patented invention that may in any way be related thereto.

CSP-TC-2550-C, #2
LOD ... STA #2

PATENT SECRECY NOTICE

Material in this publication relating to DUAL ORIFICE INJECTION, LAMINATED CHAMBER COOLING MEANS, and A VARIABLE AREA INJECTOR CONCEPT

reveals subject matter contained in U.S. Patent Application Serial Nos. 426,711, 319,047, and 390,521 entitled "Rocket Injector," "High Pressure Rocket and Cooling Means" and "Controllable Injector for Rockets," respectively, which have been placed under Secrecy Orders issued by the Commissioner of Patents. These Secrecy Orders have been modified by SECURITY REQUIREMENTS PERMITS and a PERMIT "A", respectively.

A Secrecy Order prohibits publication or disclosure of the invention, or any material information with respect thereto. It is separate and distinct, and has nothing to do with the classification of Government contracts.

By statute, violation of a Secrecy Order is punishable by a fine not to exceed $10,000 and/or imprisonment for not more than two years.

A SECURITY REQUIREMENTS PERMIT authorizes disclosure of the invention or any material information with respect thereto, to the extent set forth by the security requirements of the Government contract which imposes the highest security classification on the subject matter of the application, except that export is prohibited.

A PERMIT "A" authorizes disclosure of the subject matter of the patent application to any person of the classes hereinafter specified if such person is known to be concerned directly in an official capacity with the subject matter, provided that all reasonable safeguards are taken to otherwise protect the invention from unauthorized disclosure. The specified classes are:

(a) Any officer or employee of any department, independent agency, or bureau of the Government of the United States.

(b) Any person designated specifically by the head of any department, independent agency or bureau of the Government of the United States, or by his duly authorized subordinate, as a proper individual to receive the disclosure of the above indicated application.

A PERMIT "A" also authorizes disclosure to the minimum necessary number of persons of known loyalty and discretion, employed by or working with United Aircraft Corporation or its licensees and whose duties involve cooperation in the development, manufacture or use of the subject matter by or for the Government of the United States, provided such persons are advised of the issuance of the Secrecy Order.

Disclosure of these inventions or any material information with respect thereto is prohibited except by written consent of the Commissioner of Patents or as authorized by the respective permits.

The foregoing does not in any way lessen responsibility for the security of the subject matter as imposed by any Government contract or the provisions of the existing laws relating to espionage and national security.

AD385912

CONFIDENTIAL

(UNCLASSIFIED TITLE)

ADVANCED CRYOGENIC ROCKET ENGINE PROGRAM STAGED-COMBUSTION CONCEPT

FINAL REPORT

R. R. ATHERTON

PRATT & WHITNEY AIRCRAFT
DIVISION OF UNITED AIRCRAFT CORPORATION
FLORIDA RESEARCH AND DEVELOPMENT CENTER

TECHNICAL REPORT AFRPL-TR-67-298-VOL III
DECEMBER 1967

DECLASSIFIED AFTER 12 YEARS, DOD DIR. 5200.10

PATENT SECRECY NOTICE

PORTIONS OF THIS DOCUMENT CONTAIN SUBJECT MATTER COVERED BY A U.S. PATENT OFFICE SECRECY ORDER WITH MODIFYING SECURITY REQUIREMENTS PERMIT AND MODIFYING PERMIT "A". HANDLING SHALL BE IN ACCORDANCE WITH THE PERMIT AS DESCRIBED ON PAGE A AND INDICATED HEREIN. VIOLATORS MAY BE SUBJECT TO THE PENALTIES PRESCRIBED BY, TITLE 35, U. S. C. (1952), SECTIONS 182 AND 186.

THIS DOCUMENT CONTAINS INFORMATION AFFECTING THE NATIONAL DEFENSE OF THE UNITED STATES WITHIN THE MEANING OF THE ESPIONAGE LAWS, TITLE 18 U. S. C., SECTIONS 793 AND 794. ITS TRANSMISSION OR THE REVELATION OF ITS CONTENTS IN ANY MANNER TO AN UNAUTHORIZED PERSON IS PROHIBITED BY LAW.

STATEMENT #2 CLASSIFIED

... security requirements which must be met, this ... to special export controls and each ... governments or foreign nationals ... approval of AFRPL (RPPR-STINFO) Edwards, Calif 93523

CONFIDENTIAL

APPENDIX I
ACCELERATION LOAD ANALYSIS

(U) A study of the 250X engine system with a fixed regeneratively cooled nozzle was made to determine the limiting values of acceleration loads for the basic engine components and assemblies. Particular attention was given to the rotating assemblies of the turbopumps and the major flanges between components.

(U) All engine components are capable of withstanding loads in excess of those required. (See figure 621.) The allowable accelerations (table LIII) were computed using the loads derived from the engine environment, including gimbal loads, vibration loads, pressure loads, and bolt preloads. This analysis did not include items such as control actuators, which have not been defined in mechanical detail.

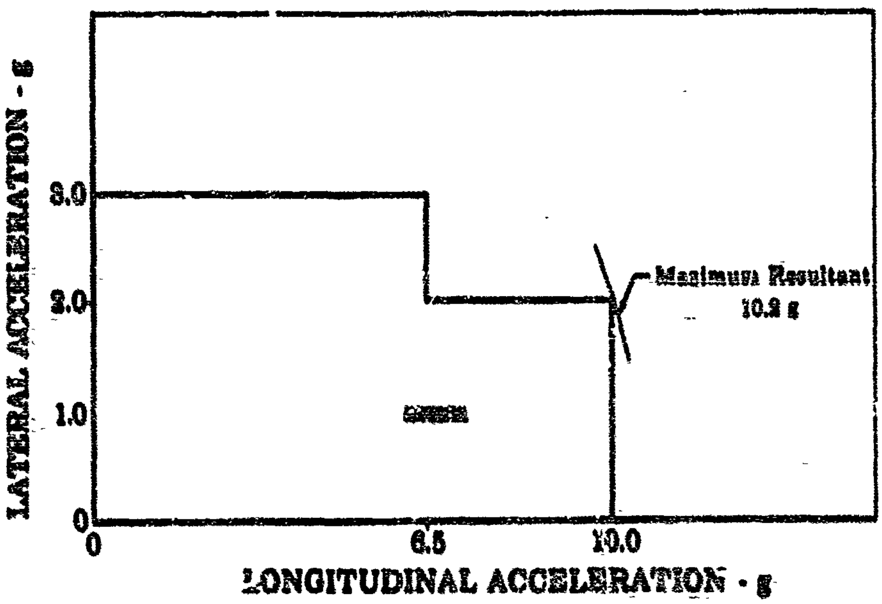

Figure 621. Operating or Nonoperating Engine Acceleration Requirements FD 20021

(C) Table LIII. Allowable g Load (10 hr)

Component	Longitudinal	Lateral	Resultant
Oxidizer Pump:			
Front Bearing			19
Rear Bearing			30
Housing			100+
Transition Case Flange			71
Transition Case Bolts			49
Shaft			*
Seals			15.8 (Parallel to Centerline)
Fuel Pump:			
Front Bearing			37
Rear Bearing			30
Thrust Balance Piston			15+ (Parallel to Centerline)
Housing			100+
Transition Case Flange			71
Transition Case Bolts			49
Shaft			*
Transition Case:			
Gimbal Actuator Loads	15+	3+	
Liner-Ducting	*	*	
Main Chamber Flange Bolts	15+	5	
Preburner Flow Divider Valve:			
Shaft Bearing			100+
Housing			187
Main Combustion Chamber:			
Nozzle Flange Bolts at $\epsilon = 4.75$	15+	5	
Nozzle:			
Transpiration Heat Exchanger:			
Outer Shell	15+	21	
Tube Buckling	15+	38	

*The allowable acceleration for these items is very large compared to the area of interest.

CONFIDENTIAL

(C) Table LXII. Allowable g Load (10 hr) (Continued)

Component	Longitudinal	Lateral	Resultant
Controls:			
Mixture Ratio Control:			
Shaft and Bearings	*		132
Housing			
Thrust Control:			
Butterfly Attachment			30+
Chamber Coolant Valve:			
Housing			20+
Low-Speed Inducers:			
Bearing Thrust Load	15+	4	

*The allowable acceleration for these items is very large compared to the area of interest.

(U) The main turbopump bearings are life and load limited. The oxidizer turbopump bearings used for this analysis were single ball bearings in both the front and rear locations. The fuel pump bearings were roller bearings in both locations.

(C) From this analysis the following conclusions can be made:

1. The engine system is capable of meeting the proposed maximum acceleration and environmental loads.

2. Accelerations to 15g longitudinal and 5g lateral can be accepted with no major change in the engine configuration. Minor changes in the transition case design to increase the structural rigidity may be required to accept the increased lateral loading.

CONFIDENTIAL

APPENDIX II

A SIMULATION FOR CONTROLS STUDY OF THE
ADVANCED CRYOGENIC ROCKET ENGINE

APPENDIX II
A SIMULATION FOR CONTROLS STUDY OF THE
ADVANCED CRYOGENIC ROCKET ENGINE

A. INTRODUCTION

(U) An analog mathematical model of the High Pressure Rocket Engine was developed in conjunction with a dynamically compatible digital model to study engine characteristics critical to the establishment of suitable control systems. The decision to provide both an analog and digital engine simulation was based on the relatively high operational cost of the more accurate digital transient program and the fixed resolution problem associated with throttling the analog program over the required operational range. It is, therefore, anticipated that the digital program will be used to evaluate transient characteristics of the engine-control system, while the analog program will be used to determine steady-state stability and response.

(U) This report describes (1) the engine cycle and engine operational limits or component physical constraints that cannot be exceeded throughout the required engine operating range, (2) the complete mathematical description of the analog program, including equations, constants, functions, and block diagrams, and (3) predicted engine performance obtained from the analog model. The assumptions and bases used in deriving the equations for the analog mathematical model and the P&WA-FRDC computer wiring diagram are included.

(U) Paragraph E describes in detail the equivalent digital mathematical model.

B. ENGINE CYCLE DESCRIPTION

(U) The High Pressure Rocket Engine uses a stage-combustion cycle in which the fuel is burned with a portion of the oxygen in a preburner. These gaseous products are used to drive the main turbopumps before final combustion with the remainder of the oxygen in the main chamber. A propellant flow schematic illustrating the principle flow paths and functional component arrangement of this engine is shown in figure 622.

(U) Hydrogen enters at the engine-driven fuel low-speed inducer where sufficient pressure rise must be provided to satisfy the main fuel pump NPSH requirements. The low-speed inducers are used to minimize vehicle NPSH (i.e., tank pressure) requirements and allows high-speed main propellant pump operation for high turbopump efficiencies. Hydrogen is pumped to the system operating pressure by the main fuel pump. It is then ducted to cool two regenerative sections of the nozzle. The principal hydrogen flow from the pump is used in the rear regeneratively cooled nozzle section, and then ducted to the preburner. The remainder of the hydrogen is used in the forward regeneratively cooled nozzle section. This heated hydrogen then passes through the low-speed fuel inducer drive turbine prior to being passed into the main chamber as a transpiration coolant. A small amount of hydrogen is bled off at the fuel low-speed inducer discharge to provide dump coolant for the translatable secondary

nozzle. This cooling flow is ducted from the discharge of the fuel low-speed inducer through a flow regulating valve and a quick-disconnect fitting, which is provided to stop the flow when the secondary nozzle is in the retracted position.

(U) Oxygen enters at the oxidizer low-speed inducer where sufficient pressure rise must be produced to satisfy the main oxidizer pump NPSH requirements. The oxygen is then pumped to system operating pressure levels by the main oxidizer pump. Pump discharge flow is then divided between the preburner and the main chamber. The main chamber oxygen flow is the principal oxidizer flow and is used as the oxygen low-speed inducer turbine working fluid. The smaller portion of the oxygen is ducted to the preburner where it is burned with the hydrogen. The resulting combustion products are ducted to the two main turbines, which are arranged in parallel, where the work required to drive the main pumps is extracted. The turbine exhaust gases rejoin in the transition case and pass through the main injector where they mix and burn with the main chamber oxidizer flow. The resulting combustion gas is then expanded through the bell nozzles.

(U) The low-speed fuel turbopump is a single shaft unit with an axial-flow inducer driven by a single-stage, gaseous hydrogen turbine. The oxygen low-speed turbopump is also a single shaft unit with an axial-flow inducer driven by a variable-admission, single-stage liquid oxygen turbine.

(U) The main fuel turbopump is a single shaft unit with two back-to-back centrifugal pump stages driven by a two-stage, pressure-compounded turbine. A double-acting thrust balance piston is provided between the pump and turbine.

(U) The oxidizer turbopump is a single shaft unit with a single, shrouded centrifugal pump stage driven by a two-stage, pressure-compounded turbine. A single-acting thrust balance piston is provided between the pump and turbine.

(U) The preburner injector consists of dual-orifice oxidizer injector elements and variable-area fuel injector elements. A flow divider valve is incorporated at the inlet to the injector assembly to vary the total preburner oxidizer flow rate, and to regulate the flow split to the dual orifice oxidizer elements. The preburner combustion chamber is an integral part of the transition case.

(U) The main chamber propellants are supplied through fixed area injection elements. The fuel side (preburner products after expansion through the turbine) guides the fuel-rich gas around the oxidizer elements. The main combustor chamber wall consists of a hydrogen transpirationally cooled liner extending from the injector face to a point downstream of the chamber throat.

(U) The exhaust nozzle attaches immediately downstream of the transpiration cooled section and is composed of two regenerative cooled sections followed by the translating secondary nozzle.

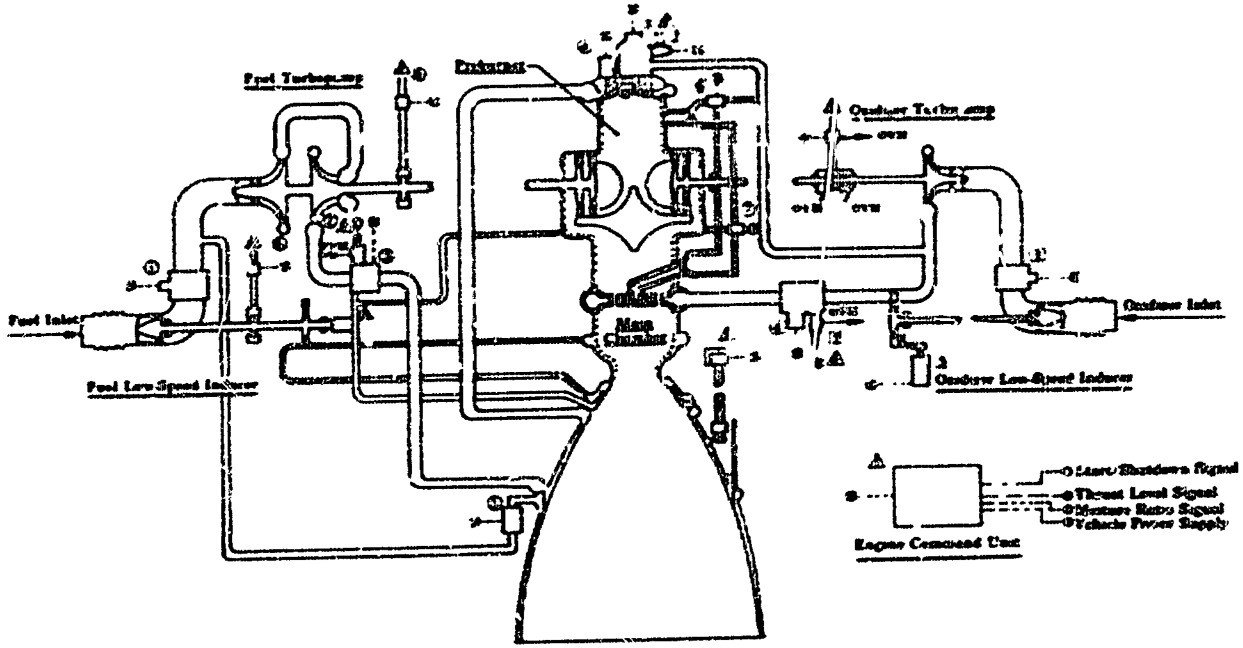

CONTROL SYSTEM COMPONENTS

Fuel Components ○

1. Total Fuel Flowmeter
2. Fuel Vent Valve
3. Main Fuel Control and Shutoff Valve (Fuel Pump Discharge Valve)
4. Fuel Injector Actuator (Preburner Fuel Injector Control)
5. Nozzle Skirt Coolant Control and Shutoff Valve (Dome Coolant Control)
6. Liftoff Seal Actuation Valves (2 req'd)
7. Igniter Fuel Valve

Oxidizer Components □

1. Total Oxidizer Flowmeter
2. Oxidizer Vent Valves (2 req'd)
3. Preburner Oxidizer Control & Shutoff Valve (Preburner Oxidizer Flow Divider Valve)
4. Main Chamber Oxidizer Control & Shutoff Valve (Main Chamber Oxidizer Control)
5. Oxidizer Inducer Turbine Actuator (Oxidizer Inducer Turbine Area Control)
6. Igniter Oxid. Valve

Miscellaneous Components △

1. Engine Command Unit
2. Translating Nozzle Actuator
3. Electric Power Source
4. Helium Supply & Vent Valves

Symbols & Abbreviations

FVM - Fuel Vent Manifold
OVM - Oxidizer Vent Manifold
Ⓒ Control-Command Electrical Connection
|| -- Helium Connection

Figure 622. Demonstrator Engine Control System

FD 2100SD

(U) Preliminary analysis of the 250K rocket engine cycle, AF-1111A, indicates the following six control points are required for steady-state operation. These six control points as shown in figure 622 are:

1. Fuel pump discharge valve
2. Preburner fuel injector control
3. Dump coolant control
4. Preburner oxidizer flow divider valve
5. Main chamber oxidizer control
6. Oxidizer inducer turbine area control.

1. Fuel Pump Discharge Valve

(U) The main fuel control is located downstream of the fuel pump in the hydrogen coolant supply to the lower regenerative nozzle. The function of this control is to distribute the hydrogen flow between the preburner and the chamber transpiration supply section. This control regulates most of the hydrogen flow. Therefore, it has a strong influence on chamber mixture ratio and a minimal influence on thrust, because fuel flow is a small fraction of total propellant flow. By regulating the fuel flow entering the preburner, it also influences available turbine power. Because the main fuel valve controls the magnitude of transpiration flow, it will influence the low-speed inducer available power (i.e., main fuel pump NPSH) as well as the adequacy of the transpiration cooling. Further, the discharge valve is positioned to produce sufficient pressure loss to ensure fuel system stability at all operating conditions.

2. Preburner Fuel Injector Control

(U) The preburner fuel control is an integral part of the fuel preburner injector. Modulation of this control varies the area of the fuel injector.

(U) The velocity of the fuel entering the preburner must be controlled at all flow rates to ensure stable, efficient preburner combustion. This fuel injector area is in series with the main fuel control and affects the fuel system in a similar manner.

3. Dump Coolant Control

(U) The dump coolant control is located in the dump cooled two-position nozzle hydrogen supply. This control is used to regulate the fuel supply to the secondary nozzle. The percentage of total fuel flow regulated by this area is small, and its influence on the overall system is small.

4. Preburner Oxidizer Flow Divider Valve

(U) The preburner oxidizer flow divider valve regulates the total oxidizer flow to the preburner as well as the flow split to the primary and secondary elements of the injector. Oxidizer preburner flow determines available turbine power by controlling turbine flow rate and inlet temperature. The oxidizer flow split determines the velocity of the oxidizer entering the preburner and must be controlled to ensure stable efficient preburner combustion.

5. Main Chamber Oxidizer Control

(U) The main chamber oxidizer control is located in the oxidizer supply to the main chamber. Because this control regulates most of the oxidizer flow, and in turn the majority of the total propellant flow, it has a strong influence on both chamber mixture ratio and thrust.

6. Oxidizer Inducer Turbine Area Control

(U) This control schedules the area of the low-speed inducer turbine that is in series with the main oxidizer control, and therefore affects the system in a similar manner. Modulation of this control affects available main oxidizer pump NPSH because turbine area determines turbine nozzle velocity, which influences turbine power and low-speed inducer performance.

7. Engine Operating Limits

(C) The operational limits and engine/control accuracy requirements for this engine-control system are as follows:

Thrust

1. Range - 100% to 20%
2. Engine/Control Accuracy

   Engine/Control Accuracy at 100% thrust - ± 3% full scale
   Engine/Control Accuracy at 20% thrust - ± 3% full scale

Mixture Ratio

1. Range - 5 to 7
2. Engine/Control Accuracy[7]

   Engine/Control Accuracy at 100% thrust - 3% of mixture ratio
   Engine/Control Accuracy at 20% thrust - 3% of mixture ratio

a. Thrust and Mixture Ratio Transient Response

(C) Changes between any combination of thrust and mixture ratio must be accomplished in less than 5 seconds within the limits as specified in the following paragraph.

b. Operational Limits

(C) The accompanying operational envelope (figure 623) reflects the steady-state component limitations for this engine cycle within the required operation range. These limits are as indicated below:

1. Main fuel turbopump maximum speed (NFP) - 48,000 rpm
2. Main oxidizer turbopump maximum speed (NLP) - 25,800 rpm
3. Main turbine inlet temperature - 2325°R.

[7] Engine/Control Accuracy is defined as total inaccuracy and includes deviations in engine trim, control valve areas, computer nonrepeatability and control sense precision.

(C) In addition to the steady-state limitations determined by the operational envelope:

1. A 4.5% minimum pressure drop exists for the main oxidizer injector, main fuel injector and preburner oxidizer and fuel injectors. This limitation will ensure combustion stability throughout the operating range.
2. Steady-state maximum transpiration cooling flow will not exceed the schedule shown in figure 624.

(C) Other physical limitations that apply to transient as well as steady-state operation are:

1. Minimum mixture ratio is set at 2.0 for the main chamber and 0.25 for the preburner.
2. Maximum main chamber mixture ratio is set at 8.0.
3. Minimum required net positive suction head for the main fuel pump and main oxidizer pump is a function of pump operation condition, as shown in figures 625 and 626.
4. Minimum transpiration cooling flow is a function of main chamber operating conditions and will be defined at a later date.

C. ANALOG SIMULATION

1. General

(U) In addition to the equations, constants, and functions that define this analog simulation, results from operation of this simulation on the P&WA-FRDC computer, and details of this operation, are presented in the following paragraphs.

2. Equations, Constants, and Functions

(C) The analog simulation of the High Performance Rocket Engine is defined in this section. The simulation consists of nine point-programs that allow limited operation about combinations of thrust at 100%, 50%, or 20% with mixture ratios of 5, 6, or 7.

(U) The building block method of simulation has been used. Individual component functions are separately developed and then interrelated into the engine system. The complete engine analog definition is accomplished within 12 groups of related engine components. These groups, called Engine Analog Sections, are illustrated and identified by letter and name in the accompanying Engine Section Diagram, figure 627. The parameter symbols used in this diagram show the location of parameters within the engine system. These same parameter symbols are used in the analog equations appearing as part of the analog definition within each of these Engine Analog Sections.

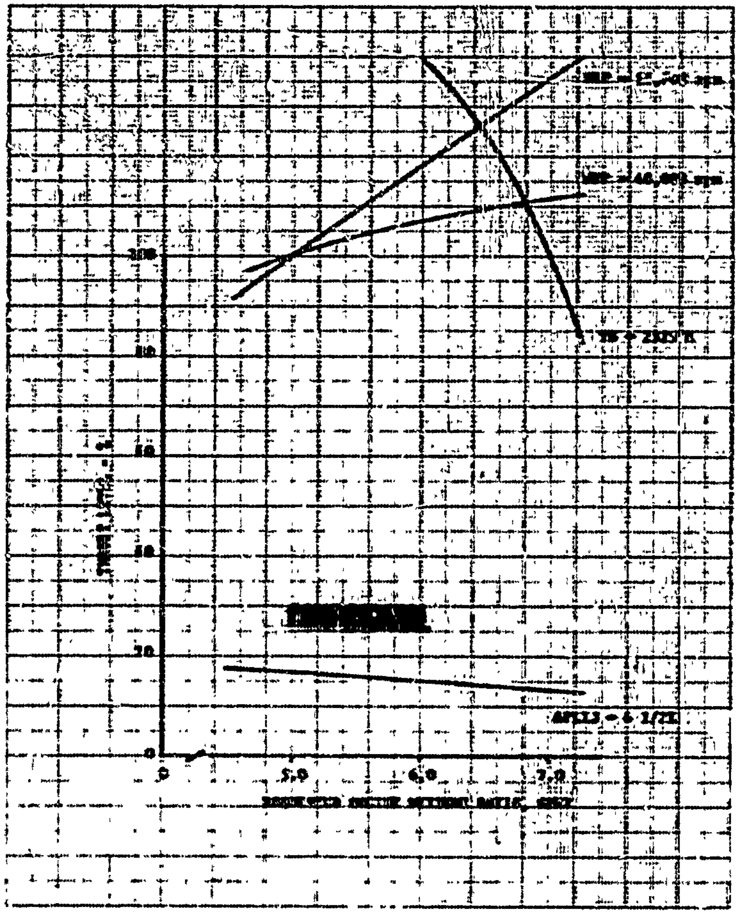

Figure 623. Operational Envelope DF 59703

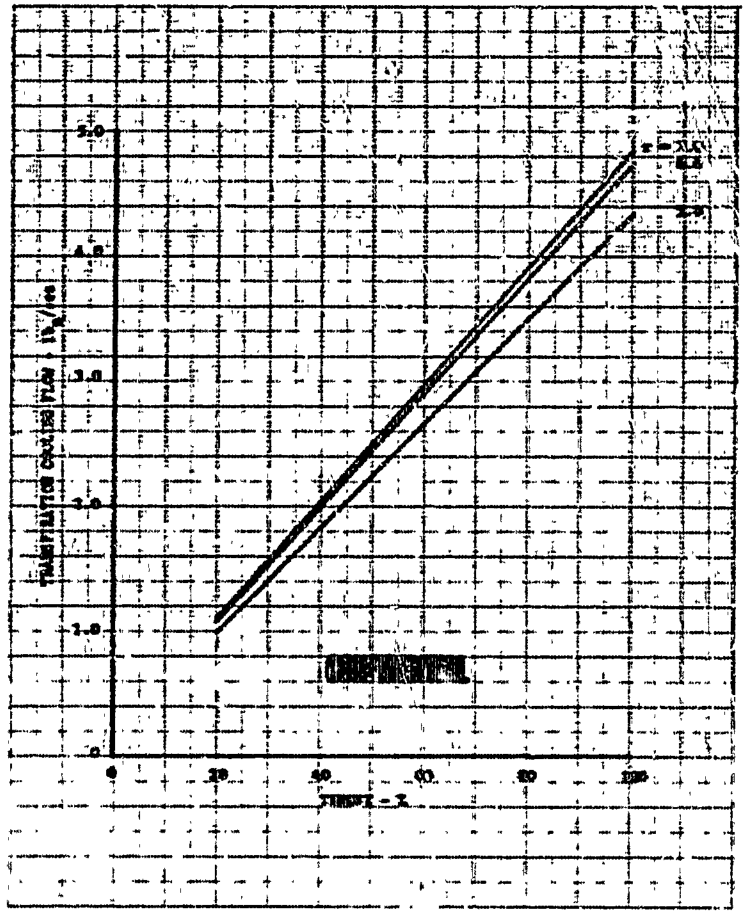

Figure 624. Transpiration Cooling Flow vs Thrust and Mixture Ratio DF 59706

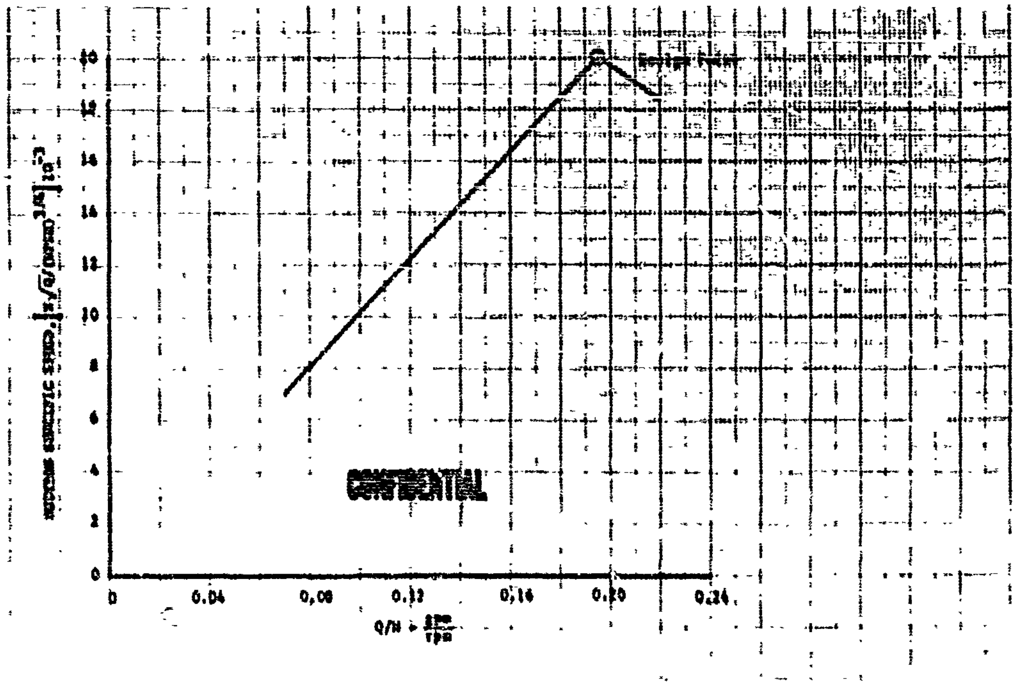

Figure 625. Main Fuel Pump Design Suction Capability DF 59705

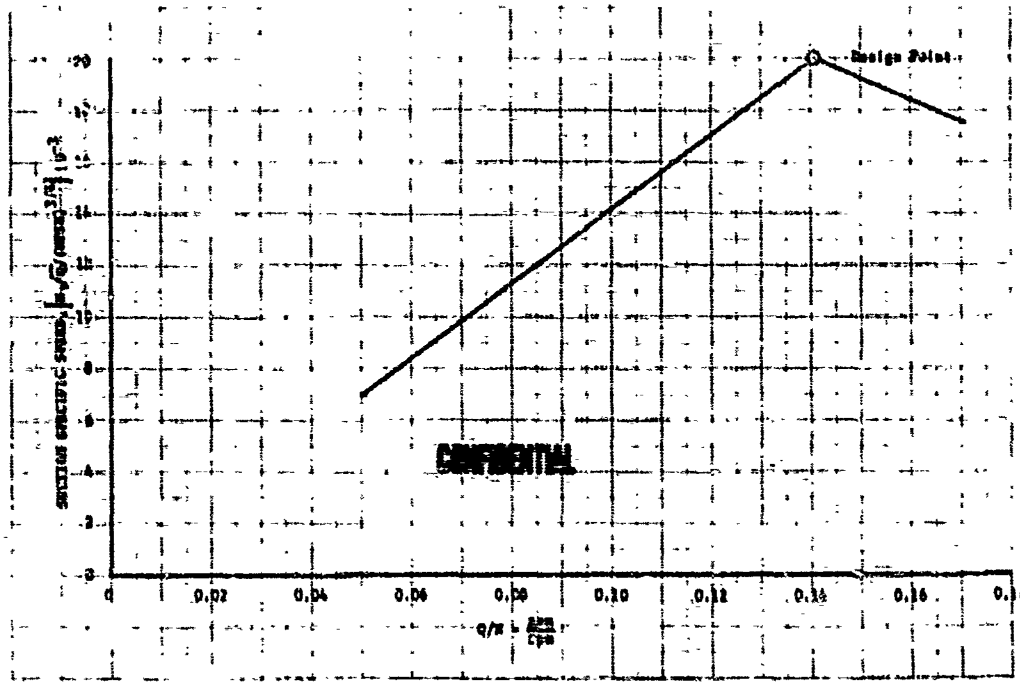

Figure 626. Main Oxidizer Pump Design Suction Capability DF 59706

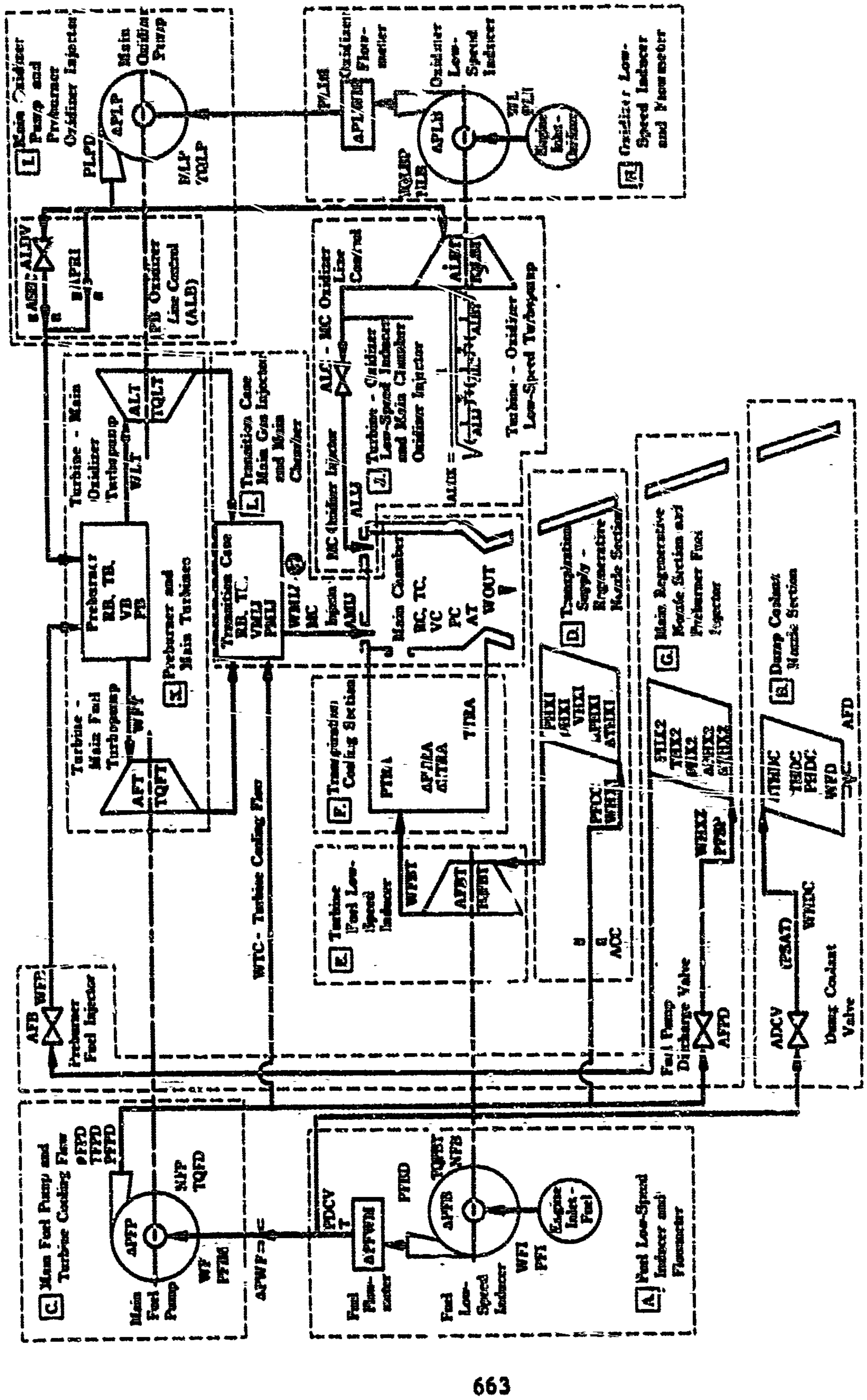

FD 23082

Figure 6?7. Engine Section Diagram

(U) The complete analog definition for each lettered Engine Analog Section appears within the following, correspondingly lettered, paragraphs. In addition to a set of analog equations expressed in terms of constants, functions, and parameter symbols, the definition includes numerical values for the constants, curves for the functions, and word definitions for the parameter symbols. Also included is a representative block diagram for the fuel low-speed inducer and flowmeter section.

(U) For analog operation at P&WA-FRDC the univariate functions were matched as straight lines between the points listed in the tables shown for each univariate curve. Records of the P&WA-FRDC match achieved for each of the bivariate functions (the eight pump curves) are included as broad (wavy) lines on each bivariate curve.

(U) $\boxed{A.}$ FUEL LOW-SPEED INDUCER AND FLOWMETER

Refer to figure 628 for block diagram.

EQUATIONS

$$WFI = WF + WHDC$$
$$\dot{NFB} = C_5 \cdot (TQFBT - TQFBP)$$
$$TQFBP = f_{1-x}$$
$$\Delta PFB = f_{2-x}$$
$$PFBD = PFI + \Delta PFB$$
$$\Delta PFWM = C_6 \cdot (WFI)^2$$
$$PDCV = PFBD - \Delta PFWM$$

CONSTANTS AND FUNCTIONS

$$C_5 = 9.55/JFBP = 0.267 \times 10^3$$
$$C_6 = (1.496)^2/\left[\rho_F \cdot (AWFM)^2\right] = 0.1776 \times 10^{-2}$$
f_{1-x} = f(NFB, WFI): See figure 629 for f_{1-100}

f_{2-x} = f(NFB, WFI): See figure 630 for f_{2-100}

$$PFI = 0.3180 \times 10^2$$

PARAMETER DEFINITIONS

WFI = Flow - Fuel, Inlet, (Engine Total)	:	lb_m/sec
WF = Flow - Fuel, Main Pump	:	lb_m/sec
WHDC = Flow - (Fuel), Heat Exchanger, Dump Coolant	:	lb_m/sec
NFB = Speed - Fuel Low-Speed Inducer	:	rpm
$\dot{NFB}$ = Speed Change Rate - Fuel Low-Speed Inducer	:	d(rpm)/d(t)

PARAMETER DEFINITIONS (Continued)

TQFBT	=	Torque - Fuel Low-Speed Inducer Turbine (Delivered)	: $lb_f \cdot ft$
TQFBP	=	Torque - Fuel Low-Speed Inducer (Required)	: $lb_f \cdot ft$
ΔPFB	=	Pressure Rise - Fuel Low-Speed Inducer (Pump)	: $lb_f/in.^2$
PFBD	=	Pressure - Fuel Low-Speed Inducer Discharge	: $lb_f/in.^2$
PFI	=	Pressure - Fuel, (Engine) Inlet	: $lb_f/in.^2$
ΔPWFM	=	Pressure Drop - Fuel Flowmeter	: $lb_f/in.^2$
PDCV	=	Pressure - Dump Coolant Valve (Upstream)	: $lb_f/in.^2$
JFBP	=	Rotor Polar Moment of Inertia, Fuel Low-Speed Inducer	: $ft \cdot lb_f \cdot sec^2$
ρ_F	=	Fuel Density, (Low-Speed Inducer Inlet)	: lb_m/ft^3
AWFM	=	Area (Effective), Fuel Flowmeter	: $in.^2$

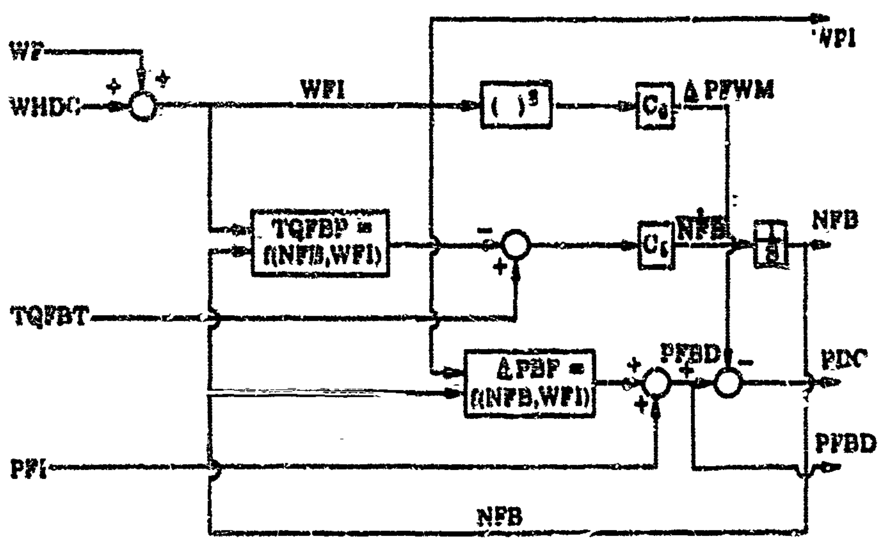

Figure 628. Fuel Low-Speed Inducer and Flowmeter Analog Section — FD 23063

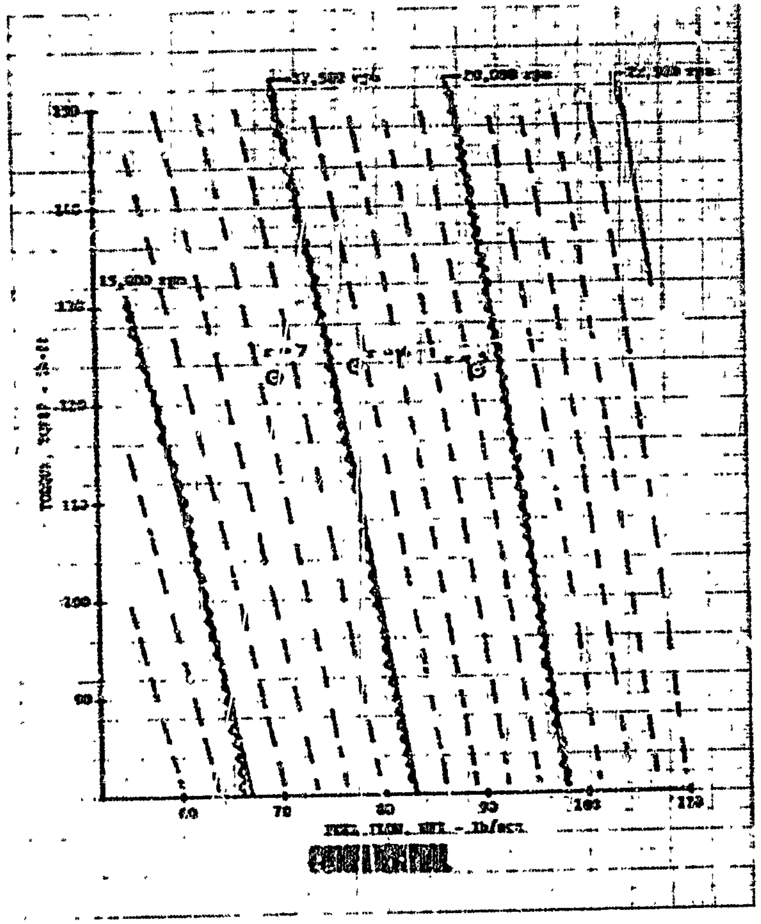

Figure 629. Fuel Low-Speed Inducer Characteristics Curve (Sheet 1) DF 59707

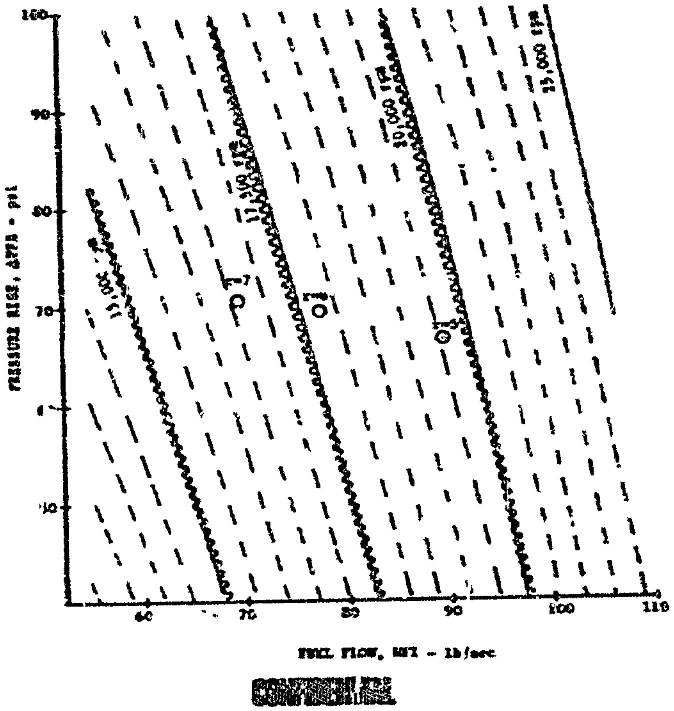

Figure 630. Fuel Low-Speed Inducer Characteristics Curve (Sheet 2) DF 59708

(U) [B.] DAMP COOLANT NOZZLE SECTION (HEAT EXCHANGER, DUMP COOLANT)

EQUATIONS

$$WHDC = C_7 \cdot ADCV \cdot \sqrt{(PDCV - C_{93})}$$

$$\Delta THDC = C_8 \cdot (PFG)^{0.87} \cdot f_{14}/WHDC$$

$$(PFG)^{0.87} = (C_{81-x} \cdot PFG) + C_{82-x} \quad \text{(See Section [D], Heat Exchanger No. 1)}$$

$$THDC = (C_{89} + \Delta THDC) \cdot 1/(1 + C_9 \cdot S)$$

$$\dot{PHDC} = C_{10} \cdot THDC \cdot (WHDC - WFD)$$

$$WFD = C_{11} \cdot f_6 \cdot PHDC/\sqrt{THDC}$$

CONSTANTS AND FUNCTIONS

$C_7 = \sqrt{\rho FDD}/1.496 = 0.1375 \times 10$

$C_8 = 0.2704 \times 10^4$

C_{9-x} = (Temp. Time Constant): $C_{9-100} = 0.2500$

$C_{10} = RH/VHDC = 0.7660 \times 10$

$C_{11} = AFD = 0.9714 \times 10$

C_{89} - $TFBD = 0.4220 \times 10^2$

$ADCV_{-x/y}$: $ADCV_{-100/5} = 0.1683$, $ADCV_{-100/6} = 0.1527$. $ADCV_{-100/7} = 0.1344$

f_{14} : KOFHT = f(OFC), Refer to table LIV

f_6 : $W \cdot \sqrt{T}/(A \cdot P)$ = f(PHDC/PAMB), Refer to table LV

C_{93} = PSAT = 3.300

(U) Table LIV f_{14} (KOFHT) as a Function of (OFC)

OFC	f_{14}	OFC	f_{14}
2.0	0.61	6.5	0.96
2.5	0.75	7.0	0.912
3.0	0.865	7.5	0.86
3.5	0.955	8.0	0.81
4.0	1.008	8.5	0.76
4.5	1.03	9.0	0.71
5.0	1.04	9.5	0.655
5.5	1.028	10.0	0.605
6.0	1.00		

(U) Table LV. $f_6\left[W\sqrt{T}/(AP)\right]$ as a Function of (PHDC/PAMB)

$\gamma = 1.39$

$\frac{PHDC}{PAMB}$	f_6	$\frac{PHDC}{PAMB}$	f_6
1.03	0.045	1.45	0.1315
1.05	0.06	1.6	0.1370
1.10	0.0829	1.75	0.139
1.15	0.097	1.89	0.1399
1.25	0.115	2.0	0.1399
1.35	0.1252		

PARAMETER DEFINITIONS

WHDC =	Flow - (Fuel), Heat Exchanger, Dump Coolant (Inlet)	:	lb_m/sec
ADCV =	Area - Dump Coolant Valve	:	$in.^2$
PDCV =	Pressure - Dump Coolant Valve (Upstream), See Section $\boxed{A}$	:	$lb_f/in.^2$
ΔTHDC =	Temperature Rise - Heat Exchanger, Dump Coolant	:	°R
THDC =	Pressure - Heat Exchanger, Dump Coolant (Exit)	:	°R
PHDC =	Pressure - Heat Exchanger, Dump Coolant (Exit)	:	$lb_f/in.^2$
WFD =	Flow - Fuel, Dump (Heat Exchanger, Dump Coolant, Exit)	:	lb_m/sec
ρFBD =	Density - Fuel (Main) Pump Discharge (See Section $\boxed{C}$)	:	$[illegible]_m/ft^3$
RH =	Gas Constant for Hydrogen (See Section $\boxed{D}$)		
VHDC	Volume - (Fuel Passage), Heat Exchanger, Dump Coolant	:	$in.^3$
AFD =	Area (Effective) - Heat Exchanger, Dump Coolant	:	$in.^2$
TFBD =	Temperature - Fuel Low-Speed Inducer Discharge	:	°R
PAMB	Pressure, Ambient - 14.7	:	$lb_f/in.^2$

(U) $\boxed{C.}$ MAIN FUEL PUMP AND TURBINE

EQUATIONS

$$\Delta PWF = C_{12} \cdot (WF)^2$$

$$PFIM = PDCV - \Delta PWF$$

$$WF = WHX2 + WHX1 + WTC$$

$$\overset{\cdot}{NFP} = C_{14} \cdot (TQFT - TQFP)$$

$$TQFP = f_{8-x}$$

$$\Delta PFP = f_{9-x}$$

$$PFPD = PFIM + \Delta PFP$$

$$WTC = f_{49}$$

$$TFPD = (C_{75} \cdot PFPD) + C_{76}$$

$$\sqrt{\rho FPD} = (C_{77-x} \cdot PFPD) + C_{78-x}$$

CONSTANTS AND FUNCTIONS

$$C_{12} = (1.496)^2 / \left[\rho_F \cdot (AFPI)^2\right] = 0.8474 \times 10^{-3}$$

$$C_{14} = 9.55/JFP = 0.1230 \times 10^3$$

$$C_{75} = 0.1400 \times 10^{-1}$$

$$C_{76} = 0.5110 \times 10^{\circ}$$

$$C_{77-x} : C_{77-100} = 0.2800 \times 10^{-4}$$

$$C_{78-x} : C_{78-100} = 1.917$$

$f_{8-x} = f(NFP, WF)$: See figure 631 for f_{8-100}

$f_{9-x} = f(NFP, WF)$: See figure 632 for f_{9-100}

$f_{49} = WTC = f(PFPD)$: Refer to table LVI.

PARAMETER DEFINITIONS

ΔPWF	=	ressure Drop - Fuel Flow (Main Pump Inlet Line)	: $lb_f/in.^2$
WF	=	Flow - Fuel, (Main Pump)	lb_m/sec
PFIM	=	Pressure - Fuel Inlet, Main (Pump)	: $lb_f/in.^2$
PDCV	=	Pressure - Dump Coolant Valve (Upstream)	: $lb_f/in.^2$
WHX2	=	Flow - (Fuel), Heat Exchanger No. 2 (Main Regenerative Nozzle)	: lb_m/sec

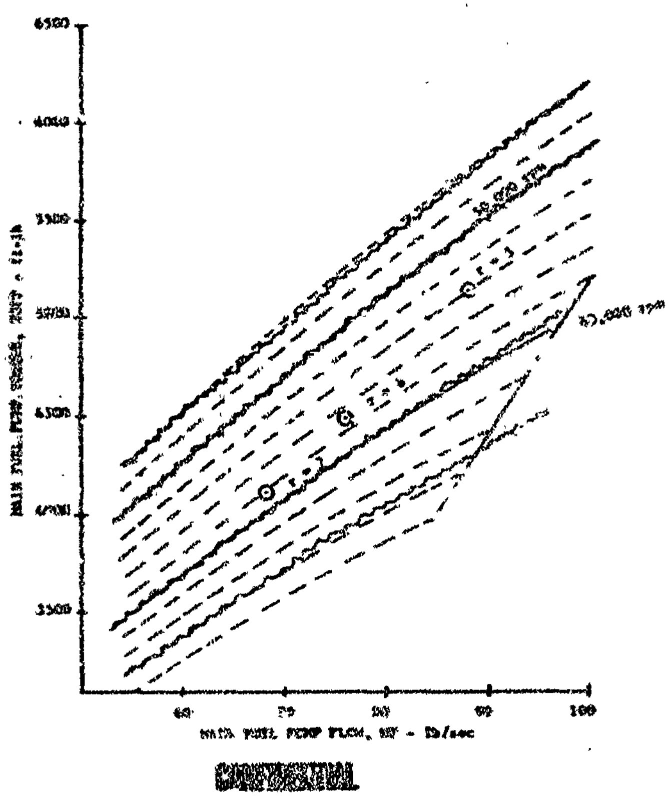

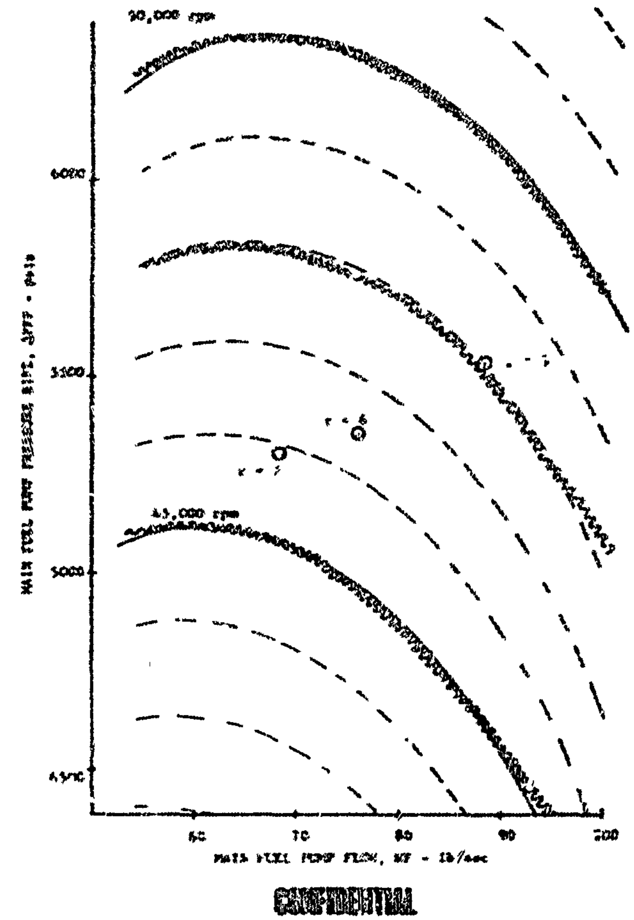

Figure 631. Main Fuel Pump and Turbine Characteristics Curve (Sheet 1) DF 59709

Figure 632. Main Fuel Pump and Turbine Characteristics Curve (Sheet 2) DF 59710

PARAMETER DEFINITIONS (Continued)

WHX1 = Flow - (Fuel) Heat Exchanger No. 1 (Transpiration Supply Regenerative Nozzle) : lb_m/sec

WTC = Flow - (Fuel), Turbine Cooling (Etc.) : lb_m/sec

NFP = Speed - (Main) Fuel (Turbo) Pump : rpm

$\dot{N}FP$ = Speed Change Rate - (Main) Fuel (Turbo) Pump : d(rpm)/d(t)

TQFT = Torque - (Main) Fuel Turbine (Delivered). (See Section K) : $lb_f \cdot ft$

TQFP = Torque - (Main) Fuel Pump (Required) : $lb_f/in.^2$

ΔPFP = Pressure Rise - Fuel Pump (Main) : $lb_f/in.^2$

PFPD = Pressure - Fuel (Main) Pump Discharge : $lb_f/in.^2$

TFPD = Temperature - (Main) Fuel Pump Discharge : °R

ρFPD = Density - Fuel, (Main) Pump Discharge : lb_m/ft^3

ρ_F = Fuel Density, (Main Fuel Pump Inlet) : lb_m/ft^3

AFPI = Area (Effective), Main Fuel Pump Inlet Line : $in.^2$

JFP = Rotor Polar Moment of Inertia, Main Fuel Turbopump : $ft \cdot lb_f \cdot sec^2$

(U) Table LVI. f_{49}(WTC) as a Function of (PFPD)

WTC	PFPD
1.85	900
2.07	1130
2.75	1925
3.32	2655
4.40	4000
5.42	5443
6.54	7000
7.25	8000

(U) D. TRANSPIRATION SUPPLY REGENERATIVE NOZZLE SECTION (HEX. NO. 1 - COOLANT SIDE)

EQUATIONS

$$WHX1 = C_{15} \cdot \sqrt{\rho FPD} \cdot \sqrt{(PFPD - PFCC)}$$

$$PFCC = PHX1 + \Delta PHX1$$

$$\dot{PHX1} = C_{18} \cdot THX1 \cdot (WHX1 - WFBT)$$

$$\Delta PHX1 = C_{74} \cdot (PFG)^{0.05} \cdot (WHX1)^2/\rho HX1$$

$$\rho HX1 = C_{100} \cdot PHX1/THX1$$

$$\Delta THX1 = C_{16} \cdot (PFG)^{0.87} \cdot f_{14} \cdot (1/WHX1)$$

$$THX1 = (TFPD + \Delta THX1) \cdot \left[1/(1 + C_{17} \cdot S)\right]$$

$$(PFG)^{0.05} = (C_{79-x} \cdot PFG) + C_{80-x}$$

$$(PFG)^{0.87} = (C_{81-x} \cdot PFG) + C_{82-x}$$

$$PFG = PC/\left[C_{84-x} - (C_{83-x} \cdot OFER)\right]$$

CONSTANTS AND FUNCTIONS

C_{15} = ACC/1.496 = 0.7192×10^{-1}

C_{16} = 0.1671×10^4

C_{17-x} = (Temperature Time Constant): C_{17-100} = 0.2500

C_{18} = RH/VHX1 = 9200/300 = 0.3067×10^2

C_{74} = 0.7252×10

C_{79-x} : C_{79-100} = 0.4930×10^{-4}

C_{80-x} : C_{80-100} = 0.9507

C_{81-x} : C_{81-100} = 0.8667

C_{82-x} : C_{82-100} = 0.1333

C_{83-x} : C_{83-100} = 0.6130×10^2

C_{84-x} : C_{84-100} = 0.3094×10^4

C_{100} = 0.1878

f_{14} : KOFHT = f(OFC), Refer to table LIV.

PARAMETER DEFINITIONS

PFCC =	Pressure - Fuel, Transpiration Orifice, (Orifice-Downstream)	: $lb_f/in.^2$
PHX1 =	Pressure - (Fuel), Heat Exchanger No. 1, (Exit)	: $lb_f/in.^2$
THX1 =	Temperature - (Fuel) Heat Exchanger No. 1 (Exit)	: °R

PARAMETER DEFINITIONS (Continued)

WFBT =	Flow - Fuel, Low-Speed Inducer Turbine - See Section E	: lb_m/sec
WHX1 =	Flow - Fuel, Heat Exchanger No. 1 (Transpiration Supply)	: lb_m/sec
ρFPD =	Density - Fuel Pump (Main Discharge), (See Section C)	: lb_m/ft^3
PFPD =	Pressure - Fuel Pump (Main) Discharge, (See Section C)	: $lb_f/in.^2$
ΔPHX1 =	Pressure Loss - (Fuel), Heat Exchanger No. 1	: $lb_f/in.^2$
PFG =	PC/(PC @ 100% Thrust Level)	: D'less
ρHX1 =	Density - (Fuel), Heat Exchanger No. 1	: lb_m/ft^3
ΔTHX1 =	Temperature Rise - Heat Exchanger No. 1 (Trans. Supply Fuel)	: °R
TFPD =	Temperature - Fuel (Main) Pump Discharge	: °R
OFER =	Mixture Ratio - Engine (Overall), Requested	: D'less
ACC =	Area (Effective), Transpiration Orifice	: $in.^2$
RH =	Gas Constant for Hydrogen	: in. · lb_f/lb_m · °R
VHX1 =	Volume - Heat Exchanger No. 1 (Fuel Passage)	: $in.^3$
KOFHT =	Correction Factor - Mixture Ratio, (Heat Exchanger Fuel Temperature)	: D'less
OFC =	Mixture Ratio - (Main) Chamber, (Chamber Overall), See Sec. L	: D'less
PC =	Pressure - (Main) Chamber, See Section L	: $lb_f/in.^2$
S =	Laplace Operator	

(U) E. TURBINE - FUEL LOW-SPEED INDUCER

EQUATIONS

$$WFBT = C_{19} \cdot f_{15} \cdot PHX1 \cdot (1/\sqrt{THX1})$$

$$\sqrt{\Delta HFBT} = f_{17} \cdot \sqrt{THX1} \cdot \sqrt{CPBT}$$

$$\sqrt{CPBT} = (C_{20-x} \cdot THX1) + C_{21-x}$$

$$TQFBT = WFBT \cdot \left| (C_{22-x} \cdot \sqrt{\Delta HFBT}) - (C_{23-x} \cdot NFB) \right|$$

CONSTANTS AND FUNCTIONS

Where:

C_{19} = AFBT = 0.2006

C_{20-x} : C_{20-100} = 0.7550×10^{-3}

C_{21-x} : C_{21-100} = 0.2330×10

C_{22-x} : C_{22-100} = 0.3389×10

C_{23-x} : C_{23-100} = 0.6546×10^{-3}

f_{15} : $W \cdot \sqrt{T}/(A \cdot P)$ = f(PHX1/PTRA), Refer to table LVII

f_{17} : $\sqrt{1 - (PTRA/PHX1)^{\gamma-1/\gamma}}$ = f(PTRA/PHX1), Refer to table LVIII.

(U) Table LVII. $f_{15}\left[W\sqrt{T}/(AP)\right]$ as a Function of (PHX1/PTRA)

$\gamma = 1.39$

PHX1/PTRA	f_{15}	PHX1/PTRA	f_{15}
1.03	0.045	1.45	0.1315
1.05	0.06	1.6	0.1370
1.10	0.0829	1.75	0.139
1.15	0.097	1.89	0.1399
1.25	0.115	2.00	0.1399
1.35	0.1252		

(U) Table LVIII. $f_{17}\left(\sqrt{1 - (PTRA/PHX1)^{\gamma-1/\gamma}}\right)$ as a Function of (PTRA/PHX1)

PTRA/PHX1	f_{17}	PTRA/PHX1	f_{17}
0.0	1.0	0.3	0.5354
0.015	0.8500	0.75	0.2784
0.03	0.8000	0.9	0.1706
0.05	0.7540	0.95	0.1195
0.1	0.6898	1.00	0.0
0.2	0.6028		

PARAMETER DEFINITIONS

WFBT =	Flow - Fuel, Low-Speed Inducer Turbine	: lb_m/sec
ΔHFBT =	Enthalpy Drop - Fuel, Low-Speed Inducer Turbine	: Btu/lb_m
CPBT =	Specific Heat at Constant Pressure - (Fuel), Low-Speed Inducer Turbine	: $Btu/lb_m \cdot {}^\circ R$
TQFBT =	Torque - Fuel Low-Speed Inducer Turbine (Delivered)	: $lb_f \cdot ft$
THX1 =	Temperature - (Fuel) Heat Exchanger No. 1 (Exit) (See Section $\boxed{D}$)	: °R
NFB =	Speed - Fuel Low-Speed Inducer, (See Section $\boxed{A}$)	: rpm
γ =	Ratio of Specific Heats	: D'less
AFBT =	Area (Effective) - Fuel Low-Speed Inducer	: $in.^2$
PHX1 =	Pressure - (Fuel) Heat Exchanger No. 1 (Exit) (See Section $\boxed{D}$)	: $lb_f/in.^2$
PTRA =	Pressure - (Fuel) Transpiration Cooled Section Inlet (See Section $\boxed{D}$)	: $lb_f/in.^2$

(U) $\boxed{F.}$ TRANSPIRATION COOLING SECTION

EQUATIONS

$$\Delta TTRA = C_{67} \cdot (PFG)^{0.87} \cdot f_{43} \cdot (1/WFBT)$$

$$TTRA = THX1 + \Delta TTRA$$

$$\Delta PTRA = C_{25} \cdot (PFG)^{0.2} \cdot f_{50} \cdot (WFBT)^2 \cdot TTRA/PC$$

$$PTRA = PC + \Delta PTRA$$

$$(PFG)^{0.2} = (C_{85-x} \cdot PFG) + C_{86-x}$$

CONSTANTS AND FUNCTIONS

$(PFG)^{0.87} = (C_{81-x} \cdot PFG) + C_{82-x}$, (See Section $\boxed{D}$)

$C_{25} = 0.3976 \times 10^2$

$C_{67} = 0.6730 \times 10^4$

C_{81-x} : (See Section $\boxed{D}$)

C_{82-x} : (See Section $\boxed{D}$)

C_{85-x} : $C_{85-100} = 0.1950$

C_{86-x} : $C_{86-100} = 0.8050$

f_{43} : KOFTT = f(OFC), Refer to table LIX.

(U) Table LIX. f_{43} (KOFTT) as a Function of (OFC)

OFC	f_{43}	OFC	f_{43}
2.0	0.28	6.5	1.025
3.0	0.52	7.0	1.044
3.5	0.63	7.5	1.06
4.0	0.73	8.0	1.08
4.5	0.82	8.5	1.097
5.0	0.90	9.0	1.11
5.5	0.96	9.5	1.13
6.0	1.0	10.0	1.145

PARAMETER DEFINITIONS

ΔTTRA =	Temperature Rise - Transpiration Cooled Section (Fuel)	: °R
TTRA =	Temperature (Fuel) - Transpiration Cooled Section (Exit)	: °R
ΔPTRA =	Pressure Drop (Fuel) - Transpiration Cooled Section	: $lb_f/in.^2$
PTRA =	Pressure (Fuel) - Transpiration Cooled Section (Inlet)	: $lb_f/in.^2$
THX1 =	Temperature - (Fuel), Heat Exchanger No. 1 (Exit) (See Section $\boxed{D}$)	: °R
PFG =	Thrust Ratio (See Section $\boxed{D}$)	: D'less
f_{50} =	KOFTP = f(OFC), Refer to table LX.	
KOFTP =	Correction Factor - Mixture Ratio, Transpiration (Cooled Section) Pressure	: D'less
PC =	Pressure - (Main) Chamber, (See Section $\boxed{L}$)	: D'less
OFER =	Mixture Ratio - Engine (Overall) - Requested	: D'less
OFC =	Mixture Ratio - Main Chamber	: D'less
KOFTT =	Correction Factor - Mixture Ratio, Transpiration (Cooled Section) Temperature	: D'less
WFBT =	Flow - Fuel, Low-Speed Inducer Turbine (Calculated in Section $\boxed{E}$)	: lb_m/sec

(U) Table LX. f_{30} (KOFTP) as a Function of (OFC)

OFC	KOFTP	OFC	KOFTP
2.0	0.927	6.6	0.960
2.6	0.971	7.0	0.9214
3.6	1.008	7.6	0.840
4.0	1.016	8.0	0.778
4.6	1.020	8.6	0.673
5.0	1.0198	9.0	0.600
5.6	1.012	9.6	0.490
6.0	1.0	10.0	0.413

(U) C. ..IN REGENERATIVE NOZZLE SECTION (HEX NO. 2); AND PREBURNER INJECTOR (FUEL SIDE)

EQUATIONS

$$WHX2 = C_{27} \cdot AFPD_{x/y} \sqrt{\rho FPD} \cdot \sqrt{PFPD - PFSP}$$

$$PFSP = PHX2 + \Delta PHX2$$

$$\Delta PHX2 = C_{28} \cdot (PFG)^{0.05} \cdot (WHX2)^2/\rho HX2$$

$$\rho HX2 = C_{100} \cdot PHX2/THX2$$

$$\Delta THX2 = C_{29} \cdot (PFG)^{0.87} \cdot f_{14}/(WHX2)$$

$$THX2 = (TFPD + \Delta THX2) \cdot \left| 1/(1 + C_{30} \cdot S) \right|$$

$$\dot{PHX2} = C_{31} \cdot THX2 \cdot (WHX2 - WFB)$$

$$WFB = AF3_{x/y} \cdot f_{24} \cdot PHX2/\sqrt{THX2}$$

CONSTANTS AND FUNCTIONS

Where:

C_{27} = 1/1.496 = 0.6684

C_{28} = 0.6242×10^{-1}

C_{29} = 0.3972×10^{4}

C_{30-x} : Main Regenerative Heat Exchanger Temperature Time Constants, C_{30-100} = 0.2500

C_{31} = RH/VHX2 = 9200/1683 = 0.5466×10

C_{100} = 0.1878

f_{14} : KOFHT = f(OFC), Refer to table LIV.

PARAMETER DEFINITIONS

WHX2	=	Flow - (Fuel), Heat Exchanger No. 2 (Coolant In)	: lb_m/sec
ρFPD	=	Density - Fuel (Main) Pump Discharge (See Main Fuel Pump) C	: lb_m/ft^3

PARAMETER DEFINITIONS (Continued)

PFPD = Pressure - Fuel Pump Discharge (See Main Fuel Pump) $\boxed{C}$: $lb_f/in.^2$

PFSP = Pressure - Fuel (Heat Exchanger No. 2 Inlet) : $lb_f/in.^2$

PHX2 = Pressure - (Fuel), Heat Exchanger No. 2 (Exit) : $lb_f/in.^2$

ΔPHX2 = Pressure Drop - (Fuel), Heat Exchanger No. 2 : $lb_f/in.^2$

ρHX2 = Density - (Fuel), Heat Exchanger No. 2 (Exit) : lb_m/ft^3

ΔTHX2 = Temperature Rise - (Fuel), Heat Exchanger No. 2 : °R

THX2 = Temperature - (Fuel), Heat Exchanger No. 2, (Exit) : °R

AFPD = Area - Fuel Pump Discharge (Valve), (Effective) : $in.^2$

S = Laplace Operator

WFB = Flow - Fuel, Preburner (Injector) : lb_m/sec

AFB = Area - Fuel (Side), Preburner (Injector) (Effective) : $in.^2$

$AFB_{-x/y}$: $AFB_{-100/5} = 2.661$, $AFB_{-100/6} = 1.814$

$AFB_{-100/7} = 1.403$

f_{24} : $W \cdot \sqrt{T}/A \cdot P = f(PHX2/PB)$, Refer to table LXI.

AFPD · Area (Effective) - Fuel Pump Discharge (Valve) : $in.^2$

$AFPD_{-x/y}$: $AFPD_{-100/5} = 3.237$, $AFPD_{-100/6} = 3.237$,

$AFPD_{-100/7} = 3.216$

$(PFG)^{0.05} = (C_{79-x} \cdot PFG) + C_{80-x}$, See Section $\boxed{D}$: D'less

TFPD = Temperature - (Main) Fuel Pump Discharge, Section $\boxed{C}$: °R

RH = Gas Constant, Hydrogen : $in.-lb_f/lb_m-°R$

VHX2 = Volume - (Main Regenerative Nozzle Section - Coolant Side) Heat Exchanger No. 2 : $in.^3$

PFG = PC/(PC at 100% Thrust Level), See Section $\boxed{D}$: D'less

(U) Table LXI. $f_{24}\left[(W\sqrt{T}/AP)\right]$ as a Function of (PHX2/PB)

$\gamma = 1.39$

$\frac{PHX2}{PB}$	f_{24}	$\frac{PHX2}{PB}$	f_{24}
1.05	0.06	1.45	0.1315
1.078	0.0748	1.6	0.1370
1.10	0.0829	1.75	0.139
1.15	0.097	1.89	0.1399
1.25	0.115	2.0	0.1399
1.35	0.1252		

(U) H. OXIDIZER LOW-SPEED INDUCER AND FLOWMETER

EQUATIONS

$$WL = WLB + WLC$$

$$\dot{NLB} = C_{43} \cdot (TQLBT - TQLBP)$$

$$TQLBP = f_{27-x}$$

$$\Delta PLB = f_{28-x}$$

$$PLBD = PLI + \Delta PLB$$

$$\Delta PLWM = C_{44} \cdot (WL)^2$$

$$PLIM = PLBD - \Delta PLWM$$

CONSTANTS AND FUNCTIONS

$$PLI = 0.3760 \times 10^2$$

$$C_{43} = 9.55/JLBP = 0.2870 \times 10^3$$

$$C_{44} = (1.496)^2/\left[\rho_L \cdot (AWLM)^2\right] = 0.2912 \times 10^{-3}$$

$f_{27-x} = f(NLB, WL)$ See figure 633 for f_{27-100}

$f_{28-x} = f(NLB, WL) =$ See figure 634 for f_{28-100}

PARAMETER DEFINITIONS

JLBP = Rotor Polar Moment of Inertia, Oxidizer Low-Speed Inducer : $ft \cdot lb_f \cdot sec^2$

AWLM = Area (Effective), Oxidizer Flowmeter : $in.^2$

ρ_L = Oxidizer Density, (Low-Speed Inducer Inlet) : lb_m/ft^3

PARAMETER DEF. [illegible]TIONS (Continued)

WL =	Flow - Oxidizer, (Engine - Total)	: lb_m/sec
WLB =	Flow - Oxidizer, Preburner (Injector)	: lb_m/sec
WLC =	Flow - Oxidizer, Main Chamber (Injector)	: lb_m/sec
NLP =	Speed - Oxidizer Low-Speed Inducer	: rpm
TQLBP =	Torque - Oxidizer Low-Speed Inducer (Required)	: lb_f-ft
TQLBT =	Torque - Oxidizer Low-Speed Inducer Turbine (Delivered) Section $\boxed{J}$	: lb_f-ft
ΔPLB =	Pressure Rise - Oxidizer Low-Speed Inducer	: lb_f/in^2
PLBD =	Pressure - Oxidizer Low-Speed Inducer Discharge	: lb_f/in^2
ΔPLWM =	Pressure Drop - Oxidizer Flowmeter	: lb_f/in^2
PLIM =	Pressure - Oxidizer Inlet, Main (Pump)	: lb_f/in^2
PLI =	Pressure - Oxidizer, (Engine) Inlet	: lb_f/in^2

(U) $\boxed{I.}$ MAIN OXIDIZER PUMP AND PREBURNER INJECTOR (OXIDIZER SIDE)

EQUATIONS

$$\dot{NLP} = C_{45} \cdot (TQLT - TQLP)$$

$$TQLP = f_{29-x}$$

$$\Delta PLP = f_{30-x}$$

$$PLPD = PLIM + \Delta PLP$$

$$WLB = C_{46} \cdot ALB \cdot \sqrt{(PLPD - PB)}$$

$$ALB = C_{47} + \left| 1/\sqrt{C_{90} + \left[1/(ALDV)^2\right]} \right|$$

CONSTANTS AND FUNCTIONS

$C_{45} = 9.55/JLP = 9/40 \times 10^2$

C_{46-y} : $C_{46-5} = 5.470$, $C_{46-6} = 5.524$, $C_{46-7} = 5.539$

$C_{47} = APRI = 0.4150 \times 10^{-1}$

$C_{90} = 1/(ASEC)^2 = 0.8044$

f_{29-x} = f(NLP, WL) = See figure 635 for f_{29-100}

f_{30-x} = f(NLP, WL) = See figure 636 for f_{30-100}

$ALB_{-x/y}$: $ALB_{-100/5} = 0.3237$, $ALB_{-100/6} = 0.3939$, $ALB_{-100/7} = 0.5284$

$ALDV_{-x/y}$: $ALDV_{-100/5} = 0.2917$, $ALDV_{-100/6} = 0.3715$, $ALDV_{-100/7} = 0.5412$

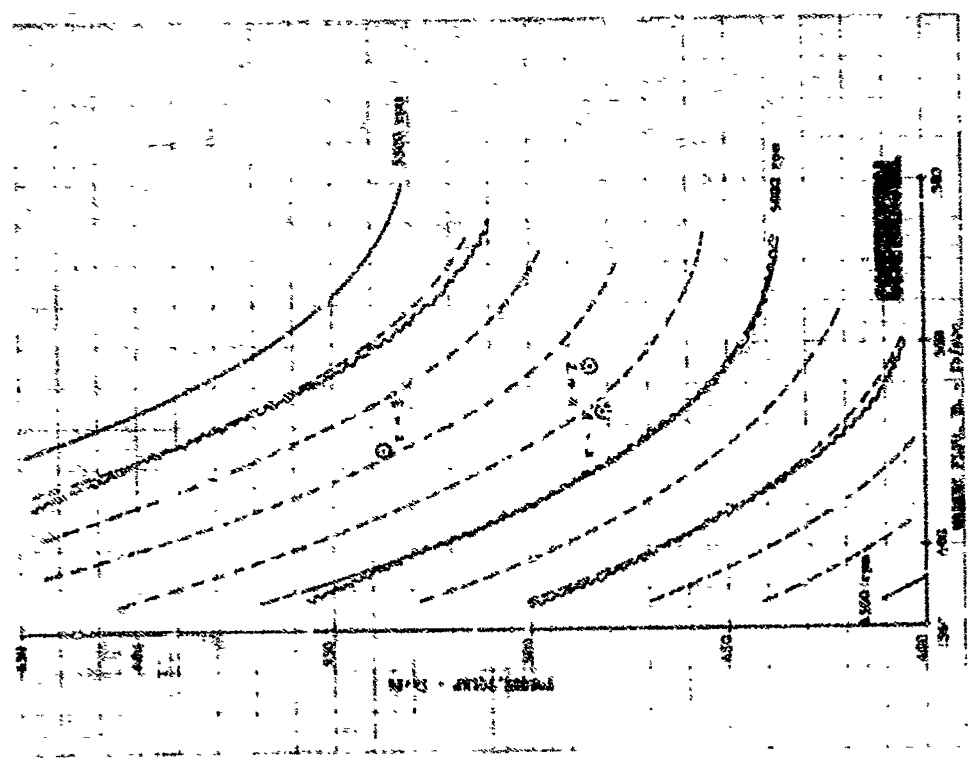

Figure 633. Oxidizer Low-Speed Inducer Characteristics Curve (Sheet 1) DF 59724

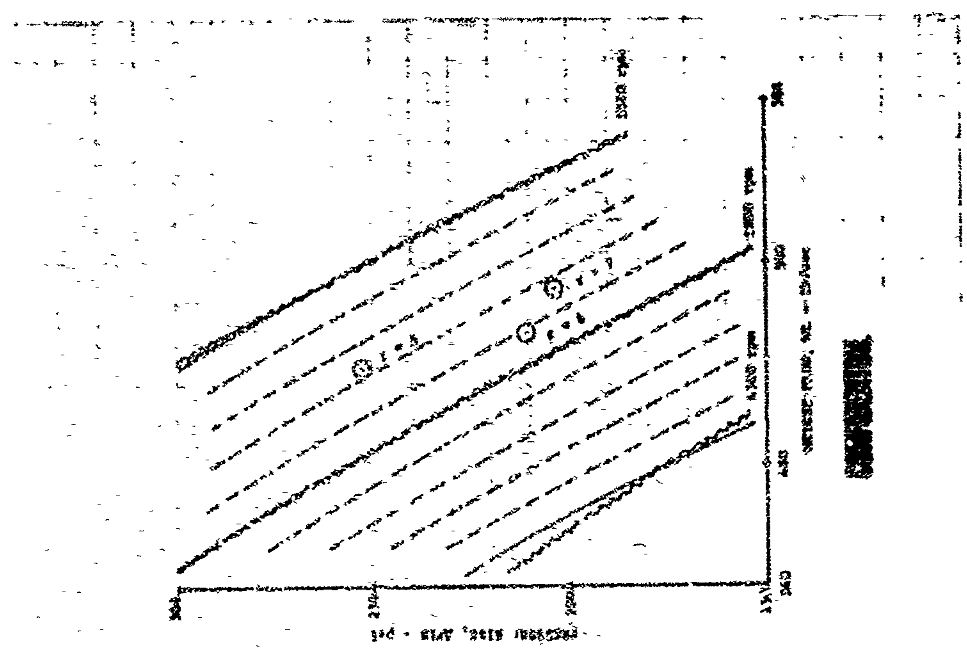

Figure 634. Oxidizer Low-Speed Inducer Characteristics Curve (Sheet 2) DF 59725

PARAMETER DEFINITIONS

NLP =	Speed - (Main) Oxidizer (Turbo) Pump	: rpm
TQLP =	Torque - (Main) Oxidizer Pump, (Required)	: ft-lb_f
TQLT =	Torque - (Main) Oxidizer Turbine, (Delivered) (See Section $\boxed{K}$)	: ft-lb_f
ΔPLP =	Pressure Rise - Oxidizer Pump (Main)	: $lb_f/in.^2$
PLPD =	Pressure - Oxidizer, (Main) Pump Discharge	: $lb_f/in.^2$
PLIM =	Pressure - Oxidizer Inlet, Main (Pump)	: $lb_f/in.^2$
WLB =	Flow - Oxidizer, Preburner (Injector)	: lb_f/sec
ALB =	Area - Oxidizer, Preburner (Line and Control - Effective)	: $in.^2$
APRI =	Area - Primary (Preburner Injector) (Effective)	: $in.^2$
ASEC =	Area - Secondary (Preburner Injector) (Effective)	: $in.^2$
ALDV =	Area - Oxidizer, (Flow) Divider Valve, (Effective)	: $in.^2$
PB =	Pressure - Preburner (See Section $\boxed{K}$)	: $lb_f/in.^2$
PLPD =	Pressure - Oxidizer, Main Pump Discharge	: $lb_f/in.^2$
JLP =	Rotor Polar Moment of Inertia, Main Oxidizer Pump	: ft lb_f sec^2

(U) $\boxed{J.}$ TURBINE - OXIDIZER LOW-SPEED INDUCER AND MAIN CHAMBER OXIDIZER INJECTOR

EQUATIONS

$$\sqrt{\Delta HLBT} = C_{48} \cdot (WLC/ALBT)$$

$$TQLBT = WLC \cdot \left[(C_{49-x} \cdot \sqrt{\Delta HLBT}) - (C_{50-x} \cdot NLB) \right]$$

$$WLC = C_{51} \cdot ALOX \cdot \sqrt{(PLPD - PC)} \cdot$$

$$ALOX = 1/\sqrt{C_{52} + (1/ALC^2) + (1/ALBT^2)}$$

CONSTANTS AND FUNCTIONS

where:

$C_{48-x/y}$: $C_{48-100/5} = 0.9675 \times 10^{-2}$, $C_{48-100/6} = 0.9489 \times 10^{-2}$

$C_{48-100/7} = 0.9436 \times 10^{-2}$

C_{49-x} : $C_{49-100} = 2.019$

CONSTANTS AND FUNCTIONS (Continued)

C_{50-x} : $C_{50-100} = 0.2677 \times 10^{-3}$

$C_{51-x/y}$: $C_{51-100/5} = 5.470$, $C_{51-100/6} = 5.524$,
$C_{51-100/7} = 5.539$

$C_{52-x/y} = \left(1/\overline{ALIJ}^2\right)$: $C_{52-100/5} = 0.1778$, $C_{52-100/6} = 0.1742$,
$C_{52-100/7} = 0.1714$

ALOX-x/y : ALOX-100/5 = 1.034, ALOX-100/6 = 1.276,
ALOX-100/7 = 1.550

ALBT-x/y : ALBT-100/5 = 2.514, ALBT-100/6 = 2.862,
ALBT-100/7 = 3.058

ALC-x/y : ALC-100/5 = 1.292, ALC-100/6 = 1.774,
ALC-100/7 = 2.694

PARAMETER DEFINITIONS

ΔHLBT =	Enthalpy Drop - Oxidizer Low-Speed Inducer Turbine	: Btu/lb_m
ALBT =	Area - Oxidizer Low-Speed Inducer Turbine (Variable)	: $in.^2$
TQLBT =	Torque - Oxidizer Low-Speed Inducer Turbine (Delivered)	: ft-lb_f
WLC =	Flow - Oxidizer, (Main) Chamber (Injector)	: lb_m/sec
ALOX =	Area - Oxidizer (Effective Total Area - Main Chamber Injector and Controls)	: $in.^2$
ALC =	Area - Oxidizer (Main Chamber Line) Control	: $in.^2$
ALIJ =	Area - Oxidizer (Main Chamber) Injector	: $in.^2$
NLB =	Speed - Oxidizer Low-Speed Inducer	: rpm
PLPD =	Pressure - Oxidizer Low-Speed Inducer Discharge	: $lb_f/in.^2$
PC =	Pressure - Main Chamber	: $lb_f/in.^2$

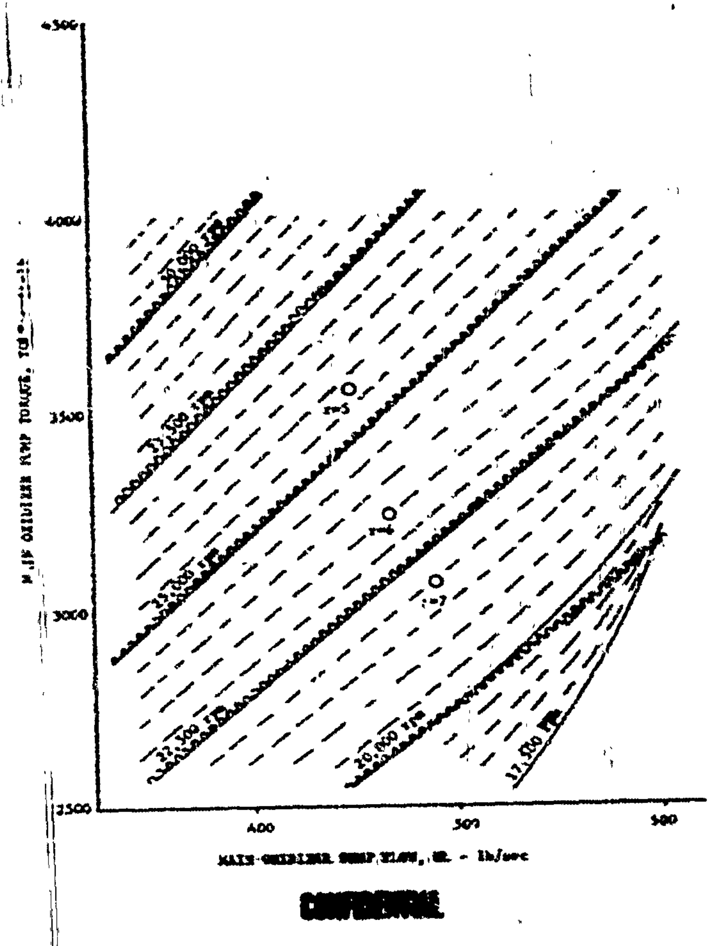

Figure 635. Main Oxidizer Pump and Preburner Injector Characteristics Curve (Sheet 1) DF 59726

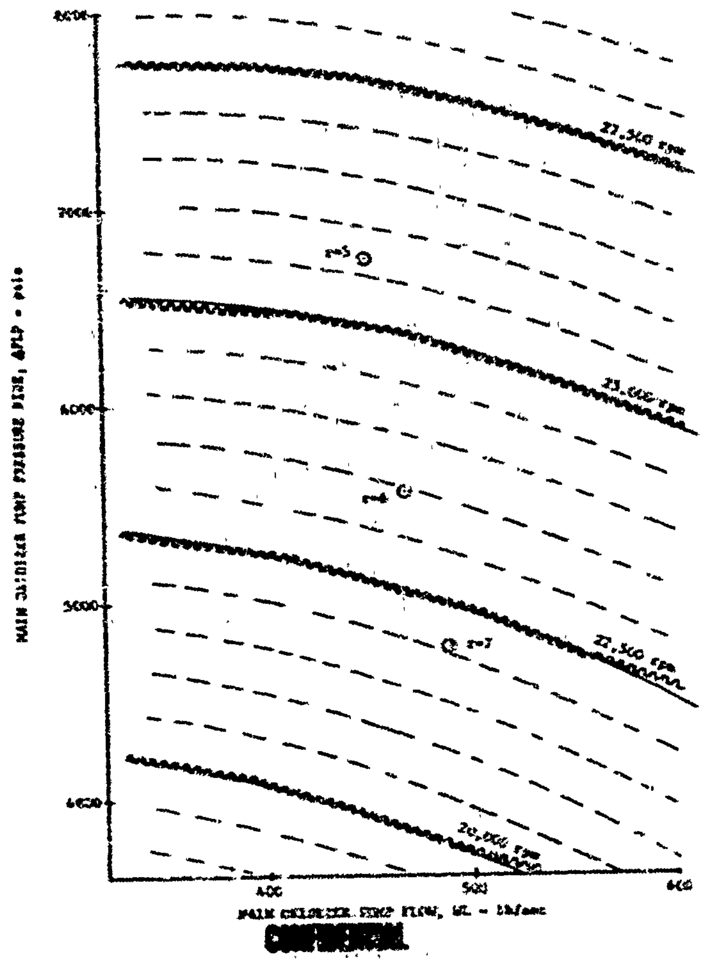

Figure 636. Main Oxidizer Pump and Preburner Injector Characteristics Curve (Sheet 2) DF 59727

(U) K. PREBURNER AND MAIN TURBINES

EQUATIONS

$$\dot{PB} = C_{56} \cdot f_{31} \cdot (WFB + WLB - WFT - WLT)$$

$$FLO = f_{32} \cdot f_{33} \cdot PB$$

$$\sqrt{\Delta HP} = f_{34} \cdot f_{35}$$

$$OFB = WLB/WFB$$

$$WFT = C_{57-x} \cdot FLO$$

$$TQFT = WFT \cdot \left| (C_{58-x} \cdot \sqrt{\Delta HP}) - (C_{59-x} \cdot NFP) \right|$$

$$\dot{W}LT = C_{60-x} \cdot FLO$$

$$TQLT = WLT \cdot \left| (C_{61-x} \cdot \sqrt{\Delta HP}) - (C_{62-x} \cdot NLP) \right|$$

CONSTANTS AND FUNCTIONS

where:

$C_{56} = 1/VB = 0.7143 \times 10^{-3}$

$C_{57-x} =$ AFT: $C_{57-100} = 1.581$

$C_{58-x/y} = C_{58-100/5} = 4.715$, $C_{58-100/6} = 4.678$,
$C_{58-100/7} = 4.618$

$C_{59-x} = C_{59-100} = 0.9517 \times 10^{-2}$

$C_{60-x} =$ ALT: $C_{60-100} = 0.7643$

$C_{61-x/y}$: $C_{61-100/5} = 6.324$, $C_{61-100/6} = 6.255$,
$C_{61-100/7} = 6.165$

C_{62-x} : $C_{62-100} = 0.2205 \times 10^{-2}$

f_{31} : $RB \cdot TB = f(OFB)$ Refer to table LXII

f_{32} : $1/\sqrt{RB \cdot TB} = f(OFB)$ Refer to table LXIII

f_{33} : $W \cdot \sqrt{R \cdot T}/(A \cdot P) = f(PB/PMIJ)$ Refer to table LXIV

f_{34} : $\sqrt{CPB \cdot TB} = f(OFB)$ Refer to table LXV

f_{35} : $\sqrt{1 - (PMIJ/PB)^{\gamma-1/\gamma}} = f(PMIJ/PB)$ Refer to table LXVI.

(U) Table LXII. f_{31} (RB · TB) as a Function of $(\overline{OFB})$

OFB	f_{31}	OFB	f_{31}
0.4	4.85	0.9	7.90
0.5	5.70	1.0	8.27
0.6	6.40	1.2	8.90
0.7	7.00	1.35	9.26
0.8	7.50	1.45	9.55

(U) Table LXIII. $f_{32}\left(1/\sqrt{RB \cdot TB}\right)$ as a Function of (OFB)

OFB	f_{32}	OFB	f_{32}
0.4	1.435	0.8	1.155
0.45	1.365	0.9	1.124
0.5	1.320	1.1	1.078
0.6	1.250	1.3	1.043
0.7	1.195	1.5	1.022

(U) Table LXIV. $f_{33}\left[W\sqrt{RT}/(AP)\right]$ as a Function of (PB/PMIJ)

$\gamma = 1.37$

$\frac{PB}{PMIJ}$	f_{33}	$\frac{PB}{PMIJ}$	f_{33}
1.0	1.00	1.40	12.3376
1.03	5.00	1.50	12.8195
1.10	7.9574	1.70	13.2747
1.15	9.3	1.8868	13.3645
1.20	10.2685	2.000	13.3645
1.30	11.5572		

(U) Table LXV. $f_{34}\left(\sqrt{CPB \cdot TB}\right)$ as a Function of (OFB)

OFB	f_{34}	OFB	f_{34}
0.4	46.0	0.8	57.0
0.5	49.4	0.9	58.8
0.6	52.4	1.0	60.3
0.7	54.9	1.4	65.5

(U) Table LXVI. $f_{35}\left(\sqrt{1 - (PMIJ/PB)^{\gamma-1/\gamma}}\right)$ as a Function of (PMIJ/PB)

$\gamma = 1.37$

$\frac{PMIJ}{PB}$	f_{35}	$\frac{PMIJ}{PB}$	f_{35}
0.0	1.000	0.7	0.3030
0.02	0.82	0.8	0.2418
0.05	0.7447	0.9	0.1674
0.1	0.6804	0.95	0.1172
0.2	0.5937	1.00	0.0000
0.3	0.5268		

PARAMETER DEFINITIONS

TB -	Temperature - Preburner Combustion Chamber	: °R
PB -	Pressure - Preburner	: $lb_f/in.^2$
VB =	Volume - Preburner Combustion Chamber	: in^3
FLO =	Intermediate Calculation for Turbine Gas Flow	: ---
RB =	Preburner Combustion Products - Gas Constant	: $in.-lb_f/lb_m-°R$
ΔHP =	Enthalpy Drop - Main Turbines	: Btu/lb_m
PMIJ =	Pressure - Main Fuel Injector (Transition [illegible]) (Section $\boxed{L}$)	: $lb_f/in.^2$
OFB =	Mixture Ratio - Preburner	: D'less
WFB =	Flow - (Fuel) - Preburner Injector (Section $\boxed{G}$)	: lb_m/sec
WFT =	Flow (Gas) - (Main) Fuel (Turbopump) Turbine	: lb_m/sec
NFP =	Speed - Main Fuel Turbopump (Section $\boxed{C}$)	: rpm
TQFT =	Torque - (Main) Fuel (Turbopump) Turbine	: lb_f-ft

PARAMETER DEFINITIONS (Continued)

WLB =	Flow - (Oxidizer) - Preburner Injector (Section $\boxed{I}$)	: lb_m/sec
WLT =	Flow (Gas) - (Main) Oxidizer (Turbopump) Turbine	: lb_m/sec
NLP =	Speed - Main Oxidizer Turbopump (Section $\boxed{I}$)	: rpm
TQLT =	Torque - (Main) Oxidizer (Turbopump) Turbine	: lb_f-ft
ALT =	Effective Area - Main Oxidizer Turbine	: in^2
AFT =	Effective Area - Main Fuel Turbine	: in^2
CPB =	Specific Heat (Constant Pressure) Preburner	: Btu/lb_m-°R
γ =	Ratio of Specific Heats	: D'less

(U) $\boxed{L}$ TRANSITION CASE, MAIN FUEL INJECTOR AND MAIN CHAMBER

EQUATIONS

$$\dot{PMIJ} = C_{63} \cdot f_{31} \cdot (WFT + WLT + WTC - WMIJ)$$
$$WMIJ = C_{64-x} \cdot f_{32} \cdot f_{38} \cdot PMIJ$$
$$WFIJ = WMIJ \cdot (WFB + WTC)/(WFB + WTC + WLB)$$
$$WLIJ = WMIJ \cdot (WLB)/(WFB + WTC + WLB)$$
$$OFC = (WLIJ + WLC)/WFIJ + WFBT)$$
$$\dot{PC} = C_{65} \cdot f_{39} \cdot (WMIJ + WFBT + WLC - WOUT)$$
$$WOUT = C_{66-x} \cdot f_{40} \cdot PC$$
$$OFE = WL/WF$$

CONSTANTS AND FUNCTIONS

$$C_{63} = 1/VMIJ = 0.5000 \times 10^{-3}$$
$$C_{64-x/y} = AMIJ : C_{64-100/5} = 5.068,\ C_{64-100/6} = 4.96\ ,$$
$$C_{64-100/7} = 4.935$$
$$C_{65} = 1/VC = 0.8333 \times 10^{-3}$$
$$C_{66-x/y} = AT \cdot g : C_{66-100/5} = 0.1496 \times 10^4,$$
$$C_{66-100/6} = 0.1502 \times 10^4,$$
$$C_{66-100/7} = 0.1514 \times 10^4$$

CONSTANTS AND FUNCTIONS (Continued)

f_{31} = RB · TB = f(OFB), See Preburner, Section $\boxed{K}$

f_{32} = $1/\sqrt{RB \cdot TB}$ = f(OFB), See Preburner, Section $\boxed{K}$

f_{39} = RC · TC = f(OFC), Refer to table LXVII

f_{40} = $1/(\eta_c{}^* \cdot C^*)$ = f(OFC), Refer to table LXVIII

f_{38} = $W \cdot \sqrt{R \cdot T}/(A \cdot P)$ = f(PMIJ/PC) Refer to table LXIX.

(U) Table LXVII. f_{39}(RC · TC) as a Function of (OFC)

OFC	f_{39}	OFC	f_{39}
2.0	10.23	4.25	10.05
3.0	10.20	4.50	9.95
4.0	10.12	10.00	7.08

(U) Table LXVIII. $f_{40}\left[1/(\eta_c{}^* \cdot C^*)\right]$ as a Function of (OFC)

OFC	f_{40}	OFC	f_{40}
2.0	0.0001295	4.75	0.0001271
2.35	0.0001275	5.25	0.0001283
2.75	0.0001263	5.75	0.0001300
3.25	0.0001259	7.50	0.0001390
3.75	0.0001259	10.00	0.0001338
4.25	0.0001262		

(U) Table LXIX. $f_{38}\left[W\sqrt{RT}/(AP)\right]$ as a Function of (PMIJ/PC)

$\frac{PMIJ}{PC}$	f_{38}	$\frac{PMIJ}{PC}$	f_{38}
1.0	0.00	1.40	12.3376
1.03	5.00	1.50	12.8195
1.10	7.9574	1.70	13.2747
1.15	9.3	1.8869	13.3645
1.20	10.2685	2.000	13.3645
1.30	11.5572		

PARAMETER DEFINITIONS

PMIJ =	Pressure - Main (Gas) Injector (Transition Case)	: $lb_f/in.^2$
$\dot{PMIJ}$	Pressure Change Rate - Main (Gas) Injector	: d(PMIJ)/dt
WMIJ =	Flow (Gas) - Main (Gas) Injector	: lb_m/sec
WFB =	Flow - Fuel, Preburner (Injector),	: lb_m/sec
	See Section [C]	: lb_m/sec
WFIJ =	Flow - Fuel, (Main Gas) Injector	: lb_m/sec
WTC =	Flow (Fuel), Turbine Cooling (Etc.), See Section [C]	: lb_m/sec
OFC	Mixture Ratio (Main) Chamber (Chamber-Overall)	: D'less
η_{c^*}	Characteristic Velocity Efficiency	: D'less
PC	Pressure - (Main) Chamber	: $lb_f/in.^2$
C^*	Characteristic Velocity	: ft/sec
WOUT	Flow - (Gas), (Main Chamber) Out	: lb_m/sec
WFT	Flow (Gas) - (Main) Fuel (Turbopump) Turbine Section [K]	: lb_m/sec
VMIJ	Volume - Main (Gas) Injector	: $in.^3$
WLT	Flow (Gas) - (Main) Oxidizer (Turbopump) Turbine Section [K]	: lb_m/sec
VC	Volume - (Main) Chamber	: $in.^3$
AMIJ	Area - (Effective) - Main Chamber Gas Injector	: $in.^2$
OFE	Mixture Ratio - Engine (Overall)	: D'less
AT	Area - (Effective) - Throat, Main Chamber	: $in.^2$
g	Gravitational Constant	: ft/sec^2
RC	Gas Constant, Main Chamber Gas	: $in\text{-}lb_f/lb_m\text{-}°R$
TC	Temperature (Gas) - (Main) Chamber	: °R
WLB =	Flow - Oxidizer, Preburner (Injector), (See Section [C])	: lb_m/sec
WLIJ	Flow - Oxidizer, (Main Gas) Injector	: lb_m/sec

3. EQUATION ASSUMPTIONS AND BASES

(U) A description of the assumptions and the bases for the equations used in the analog simulation of the Engine Cycle AF 1121A is included here along with a description of the technique employed in activating this simulation on the P&WA-FRDC analog computer.

(U) Certain assumptions have been made in arriving at the equations used in this analog simulation. A summary of the equations used is shown in figure 637, and the more significant assumptions made, along with the bases of the equations involved are discussed in the following paragraphs.

1. Fluid Flow - General

(U) When simulating the fluid flows through the engine, the oxidizer (oxygen) is considered to be liquid from the tank through the oxidizer injectors, and the fuel (hydrogen) is considered to be liquid from the tank up to the inlet of the nozzle sections, (heat exchangers). Beyond these points the fluids are considered to be gases.

(U) Where Bernoulli's equation is used in determining flow rates or pressure drops, the flow is assumed to be steady, irrotational, one-dimensional, frictionless and adiabatic; and differences in component elevation as well as any influence of external forces such as vehicle accelerations are disregarded.

(U) Certain line pressure drops have been consolidated with adjacent component pressure drops in this Engine Analog Simulation to reduce the amount of analog computer equipment involved. The following areas of consolidation should be noted:

a. Upstream line loss is included with the transpiration cooling flow orifice (ACC)

b. Downstream line loss is included with the main fuel pump discharge valve (AFPD)

c. Upstream line loss is included with the fuel preburner injector (AFB)

d. Downstream line loss is included with the transpiration heat exchanger

e. Downstream line loss is included with the fuel inducer turbine

f. Upstream line loss in included with the oxidizer preburner injector (ALB)

g. Upstream line loss is included with the oxidizer inducer turbine

h. Upstream line loss is included with the main oxidizer injector (ALIJ)

i. Upstream loss is included with the main turbines

j. Upstream loss is included with the main gas injector (AMIJ).

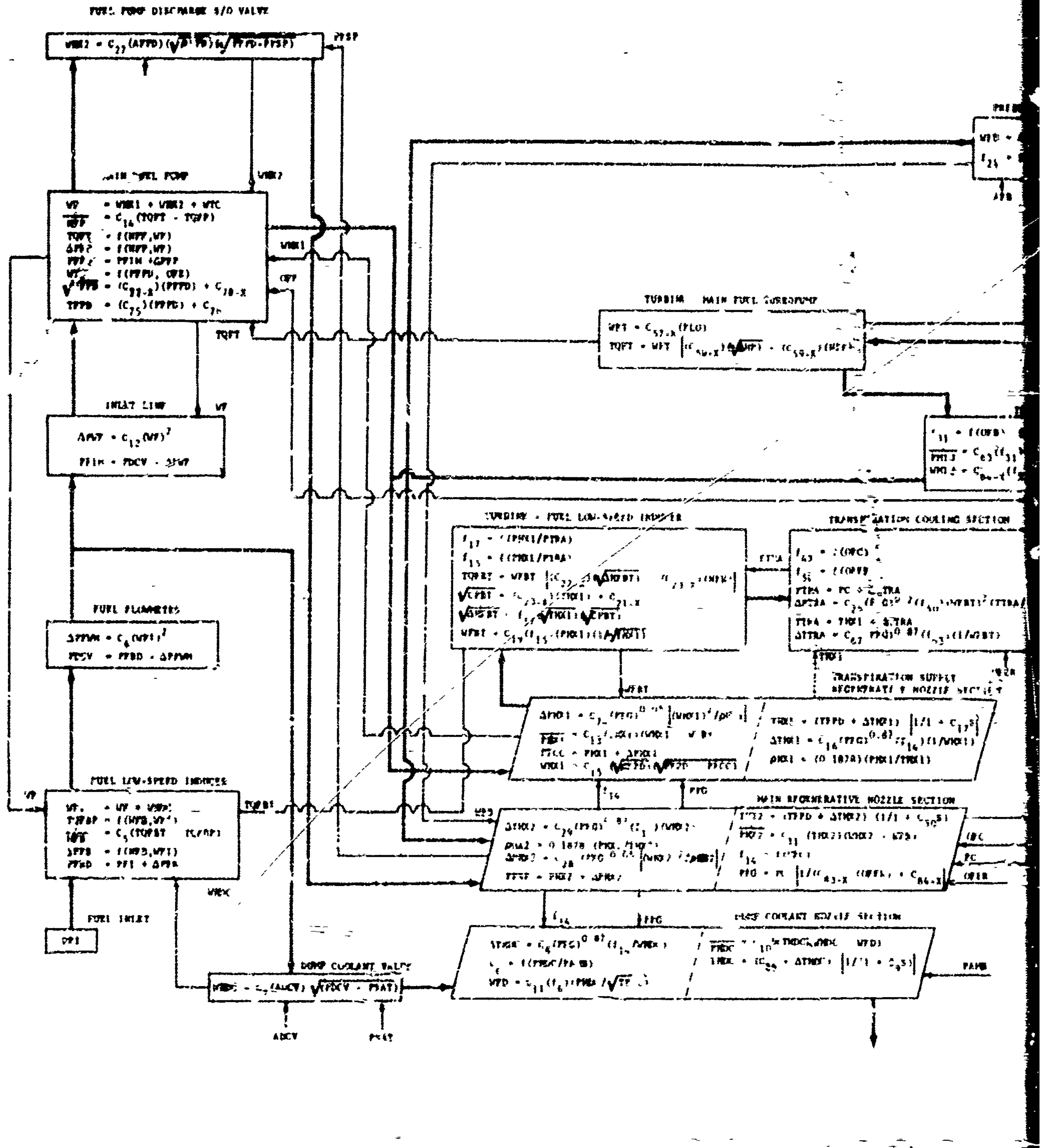

Figure 67. Logic Diagram Used for Analog Simulation

UNCLASSIFIED

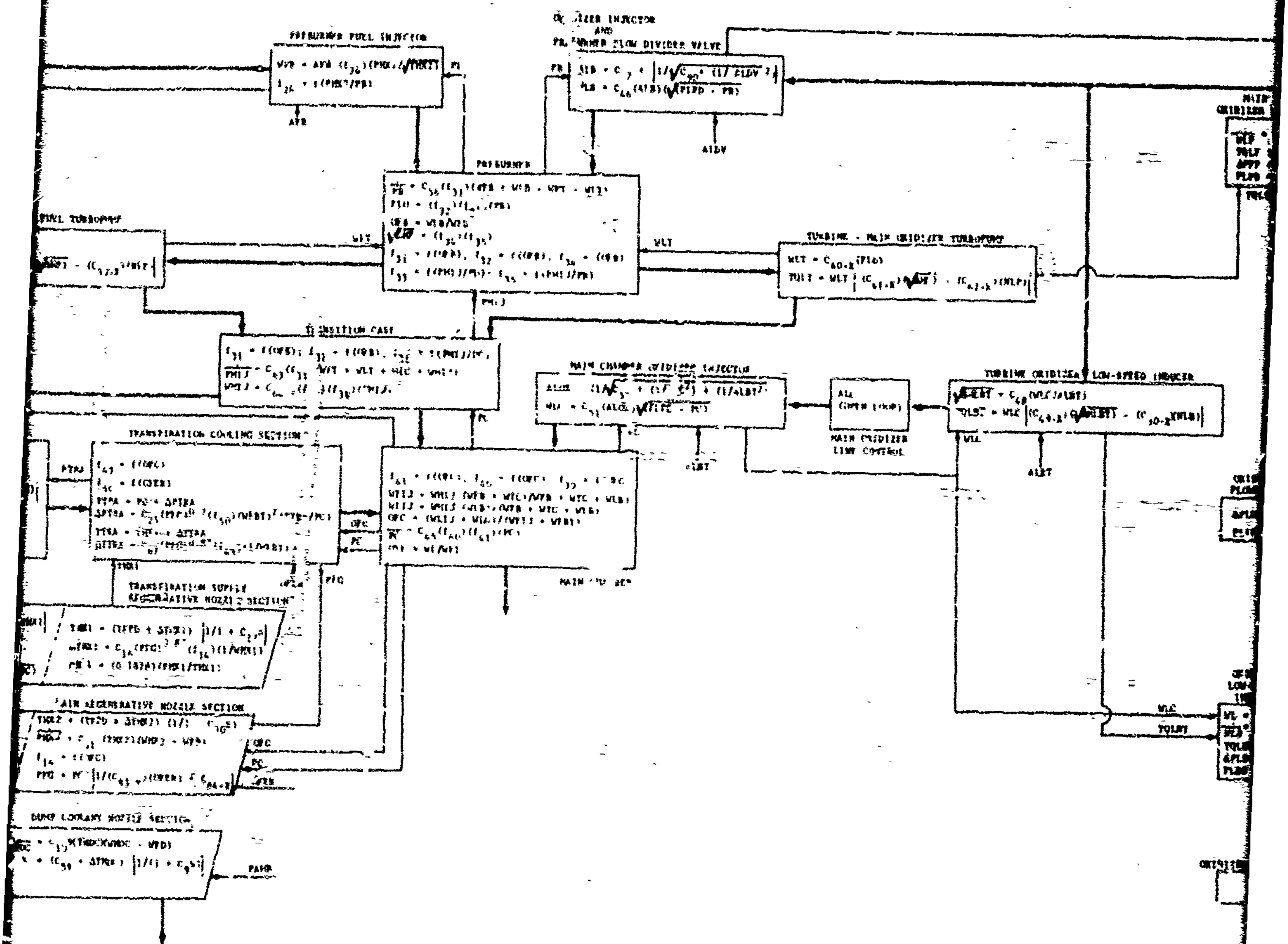

UNCLASSIFIED

2

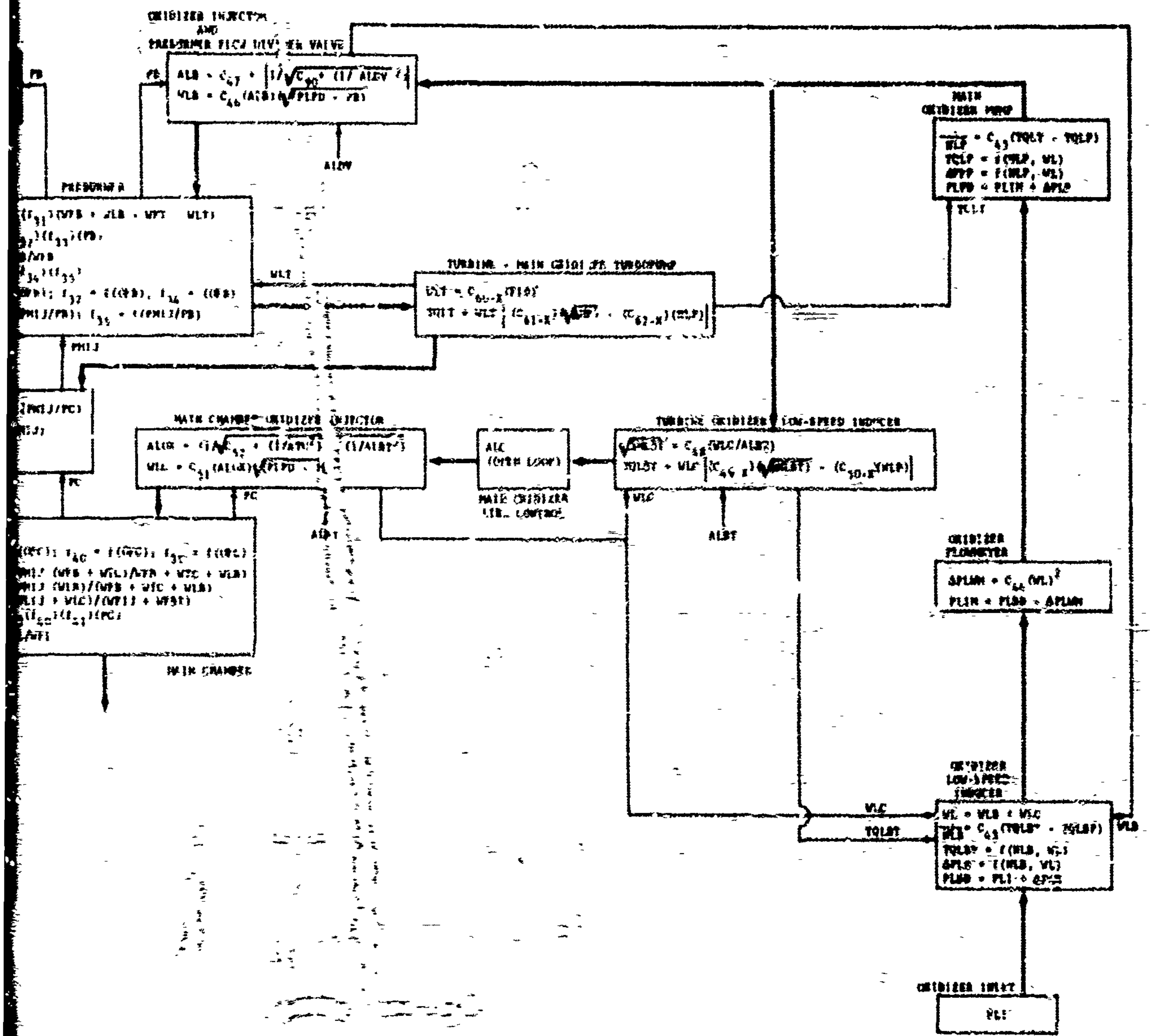

FD 23089

693/694

3

(C) Because flow through the dump coolant valve (ADCV) is subject to phase change during operation, particularly at the lower (20%) thrust levels, this valve is treated as a cavitating venturi type of valve with saturation pressure assumed to exist at the throat. The effective throat area (ADCV) was established on this basis.

(U) All flow areas used in the analog simulation were calculated using cycle flows and, where applicable, the consolidated pressure drops noted above.

2. Liquid Flow

(U) All liquid flow in this program is considered incompressible. The liquid flow rates up to and through the fuel valves and the oxidizer injectors are simulated in the following form by the combination of Bernoulli's equation and the Continuity equation.

Bernoulli's equation: $$V = \sqrt{\frac{2g_c \Delta P}{\rho}}$$

Continuity equation: $$\dot{w} = \rho A_{cd} V$$

therefore:

$$\dot{w} = \frac{A_{cd}}{1.496} \sqrt{\rho \Delta P}$$

where:

$\dot{w}$ = Flow rate, lb_m/sec

A_{cd} Effective area, $in.^2$

ρ = Density, lb_m/ft^3

ΔP = Pressure drop, $lb_f/in.^2$

g_c = Gravitational constant, $ft\text{-}lb_m/lb_f\text{-}sec^2$

3. Gas Flow

(U) Bernoulli's equation as formulated for an isentropic, perfect gas flow process is used in determining the gas flow rates through the preburner fuel and main-gas injectors as well as through the main turbines and the fuel boost turbine. Bernoulli's equation in this gas flow form is:

$$\frac{\dot{w} \cdot \sqrt{R \cdot T_1}}{A_{cd} \cdot P_1} = \sqrt{\frac{\left[2g_c\ \gamma/(\gamma-1)\right]\left[(P_1/P_2)^{\gamma-1/\gamma} - 1\right]}{(P_1/P_2)^{\gamma+1/2\gamma}}} = \text{Gas Flow Parameter}$$

where:

$\dot{w}$ = Flow rate, lb/sec

T_1 = Upstream temperature, °R

R = Gas constant, $ft\text{-}lb_f/lb_m\text{-}°R$

Acd = Effective area, $in.^2$

P_1 = Upstream pressure, $lb_f/in.^2$ (abs)

γ = Specific heat ratio (C_p/C_v), d'less

g_c = Gravitational constant, ft-lb_m/lb_f-sec^2.

(U) For hydrogen gas flow, the hydrogen gas constant, R, is constant and is included when calculating the hydrogen gas flow parameter as follows:

$$\frac{\dot{w} \cdot \sqrt{T_1}}{Acd \cdot P_1} \quad \frac{\sqrt{\left[2g_c\ \gamma/R(\gamma-1)\right]\ \left[(P_1/P_2)^{\gamma-1/\gamma} - 1\right]}}{(P_1/P_2)^{\gamma+1/2\gamma}} = \text{Hydrogen Gas Flow Parameter}$$

These flow parameters are calculated for the pertinent specific heat ratio (γ) and as functions of the total to static pressure ratio = P_1/P_2. It should be noted that in the analog simulation the pressure ratios used are total-to-total, which are not consistent with the flow parameters definition given above. This incompatibility has been found to be negligible in most cases, and when it was necessary it was compensated for in the program constants (i.e., turbine torque constants). This is the basis for these functions as used in the analog simulation.

(U) It was assumed that the preburner temperature can be used when calculating the main-gas injector flow (WMIJ) by slightly (3.5%) changing the main-gas injector area (AMIJ). The small sacrifice in dynamic accuracy resulting from this assumption is compensated for by the elimination of inaccuracies in the additional operations otherwise required to determine and incorporate the turbine downstream temperature into this gas flow calculation.

4. Gas Pressures

(U) The instantaneous gas pressures within such engine volumes as the preburner transition case, main chamber and the nozzle section fuel passages are obtained by continuously integrating the following expression.

$$\dot{P} = (R/V)T\left(\dot{w}_1 - \dot{w}_2\right)$$

where:

$\dot{P}$ = Rate of change of pressure - $lb_f/in.^2$-sec

V = Volume - $in.^3$

T = Temperature - °R

$\dot{w}_1$ = Flow rate, into volume - lb_m/sec

$\dot{w}_2$ = Flow rate, out of volume - lb_m/sec

R = Gas constant - in.-lb_f/lb_m-°R

(U) IC (initial condition) values are assigned to these pressures before the computer is switched to "compute." Thereafter these pressure values are controlled by computer integration.

(U) The above differential expression is derived from the perfect gas law as follows:

$$P = RTm/V$$

where:

P = Pressure - $lb_f/in.^2$-sec

R = Gas constant - $in.-lb_f/lb_m$-°R

T = Temperature - °R

m = Mass density - $lb_m/in.^3$

V = Volume - $in.^3$

Differentiating with respect to time

$$d(P)/dt = (RT/V)d(m)/dt + (MR/V)d(T)/dt$$

Because the temperature of an ideal gas is a function of the gas energy only, no change in stagnation temperature results from consideration of reversible adiabatic flow in and out of the volume. Therefore, dT/dt is zero and consequently

$$\dot{P} = d(P)/dt = (RT/V)dm/dt = (RT/V)(\dot{w}_1 - \dot{w}_2).$$

5. Pumps

(U) The pump characteristics are depicted by the Pressure Rise vs Flow and Torque vs Flow curves that are bivariate with speed. These curves are provided for each of the four pumps.

(U) Angular momentum is used in determining the pump speeds as follows:

$$J \cdot \dot{N} = T$$

where:

T = Torque

$\dot{N}$ = Time rate of change of angular velocity (angular acceleration)

J = Polar moment of inertia for turbopump rotor assembly

therefore:

$$\dot{N} = T/J = (\text{turbine torque} - \text{pump torque})/J.$$

(U) The analog computer continuously integrates this expression to develop the instantaneous pump speeds.

6. Regenerative Nozzle Sections (Heat Exchangers)

(U) The expressions for pressure drop and temperature rise of the coolant (fuel) passing through the different nozzle sections and the main chamber transpiration cooling section are empirically derived. This includes the time constant which adds a dynamic factor to these expressions.

(U) Another dynamic factor is introduced in the simulation by considering the equivalent volume of the nozzle sections and their manifolds as existing between two flow-regulating areas. The instantaneous gas pressures within these volumes are developed from the conservation of mass relationship as discussed in paragraph 4, Gas Pressures. The relatively small volume of the main chamber transpiration cooling section has been added to the volume of the transpiration supply nozzle section to provide for its dynamic effect on the tranrpiration flow.

7. Preburner and Main Turbines

(U) Pressure in the preburner is derived from the conservation of mass relationship discussed in paragraph 4, Gas Pressures.

(U) The FLO expression is an intermediate step in the calculation of gas flow through the main turbine areas as noted in paragraph 3, Gas Flow.

(U) The adiabatic flow of gases through a turbine was expressed as:

$$\Delta h' = C_p(T_1 - T_2)$$

where $\Delta h'$ is the ideal enthalpy drop across the turbine, C_p is the specific heat of the gas at constant pressure, and T_1, T_2 are the turbine inlet and outlet total temperatures. For isentropic flow of a perfect gas, the total pressure ratio corresponding to the temperature ratio is given by the equation

$$(P_1/P_2) = (T_1/T_2)^{\gamma/(\gamma-1)}$$

therefore, combination of these equations gives

$$\Delta h' = C_p T_1\left[1 - \left(\frac{P_2}{P_1}\right)^{(\gamma-1)/\gamma}\right]$$

This is the expression used in simulating the ideal enthalpy drop across the turbines.

(U) The efficiency of an impulse turbine is defined in terms of the ratio of mean wheel speed to the ideal nozzle exit velocity (u/c) as shown by the following parabolic curve.

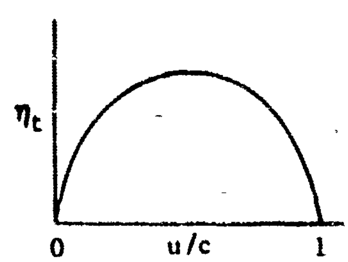

For fixed arc of admission

The parameter u/c is proportional to $(N/\sqrt{\Delta h'})$ where N is the turbine speed in rpm and $\Delta h'$ is the ideal enthalpy drop across the turbine.

(U) Therefore, the efficiency can be expressed in terms of the parameter $(N/\sqrt{\Delta h'})$ by a similar parabolic curve as follows:

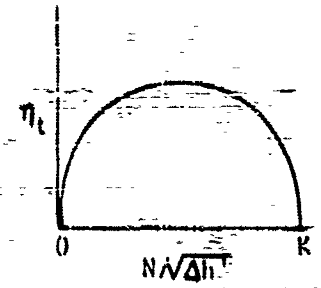

The equation defining this curve will have a paraboloid characteristic originating at the point (o,o) as follows:

$$\eta_T = K_2 \frac{N}{\sqrt{\Delta h'}} - K_1 \frac{N^2}{\Delta h'} \qquad (9)$$

Turbine torque is defined by the relationship:

$$TQ = \frac{\Delta h' \times \eta_T \times W_T}{0.00013466 \times N} \qquad (10)$$

where W_T = turbine mass flow, lb_m/sec and the constant 0.00013466 is the units conversion required to convert rpm to rad/sec and Btu to ft-lb_f.

Combination of equations (9) and (10) yields:

$$TQ = \frac{\Delta h' \times W_T}{0.00013466\ N} \left[K_2 \frac{N}{\sqrt{\Delta h'}} - K_1 \frac{N^2}{\Delta h'} \right], \qquad (11)$$

which can be reduced to the form

$$TQ = W_T \left| \left(K_3 \cdot \sqrt{\Delta h'}\right) - \left(K_4 \cdot N\right) \right|$$

This is the form in which the torque equation is used in the engine analog simulation.

8. Main Combustion Chamber

(U) The characteristic velocity, c*, is defined by the relation:

$$c^* = A_t P_c g / \dot{m}$$

where:

A_t = Throat area, in^2

P_c = Chamber pressure, lb_f/in^2

g = Gravitational constant, 32.17 ft·lb_m/lb_f sec^2

$\dot{w}$ = Mass flow rate, lb_m/sec

And from the choking equation for a perfect gas

$$c^* = A_t P_c g/\dot{w} = \sqrt{\frac{RT_g}{M}} / f(\gamma)$$

where:

R = Universal gas constant, 1544 ft.lb_f/lb-mole °R

T_g = Total gas temperature - °R

M = Molecular weight of gas.

The effect of γ is slight, so c* depends primarily upon the propellant combination, which determines the stagnation temperature and molecular weight of the product gases. The last expression gives a theoretical value of c* as calculated from the properties of the hot combustion gases and which is a function of mixture ratio.

(U) The characteristic exhaust velocity efficiency, η_c*, is the ratio of the actual c* (realized) to the theoretical c*. The theoretical c* values used in this simulation are based on calculations assuming complete chemical reaction within the chamber and a homogeneous gas mixture with equilibrium expansion to the throat. The η_c* values are based on empirical results based on P&WA-FRDC test experience. Therefore, in terms of theoretical c* and η_c*, the above expression becomes

$$c^* \cdot \eta_c^* = A_t P_c g/\dot{w}$$

or

$$(WOUT) = \frac{(A_t)(g)}{c^* \cdot \eta_c^*} (PC) = \frac{G_{?}}{66} f_{40} \cdot PC,$$

which is the analog equation used to calculate flow out of the main chamber. The function, 1/(c* · η_c*), is based on the particular propellant combination used and on predicted efficiencies and can be plotted as a function of the oxidizer to fuel mixture ratio.

(U) Because the gas flow from the preburner (volume) through the turbines (area), transition case (volume), and main gas injector (area) into the main chamber is subject to the dynamics of flow through two volumes and areas in series, and since these dynamics have been shown to have a significant effect on the main chamber mixture ratio (OFC), they were considered in the equation for OFC.

E. DIGITAL TRANSIENT PROGRAM

(U) The following sections describe the digital computer dynamic simulation of the demonstrator engine cycle. The engineering mathematical representations of the engine components are essentially the same as those incorporated in the previously described analog program. Basic differences in the two programs are the manner in which the time solutions are obtained and the operational procedures involved in execution of simulations. The analog solutions are based on continuous time, while the digital program solutions are based on numerical integration techniques. Results from both simulations show excellent agreement of data over comparable operations.

(U) This program was written for the IBM System 360 Model 65 and requires the following equipment:

1. Fortran IV, Level H
2. 100,000 Bytes or 25,000 words of storage
3. An additional 16,000 Bytes or 4000 words for systems subroutines, e.g., I/O control, exponential, zero, log, max - min
4. Extended binary coded decimal language
5. Multiple entry and return for subroutines
6. Sense light subroutine for testing
7. 120 characters per line of output
8. Initialization of data tables in assembly language
9. Assembly language subroutine to count arguments in a calling list.

1. Program Input Parameters

(U) The digital program input parameters are used to establish (1) the duration of the engine transient calculation (STIM-To), (2) time increments to be taken during the transient (DT), and (3) optional data print time (PTIM).

1.	To	Engine Transient Start Time
2.	DT	Time Increment
3.	PTIM	Increment of T Between Printout
4.	STIM	Engine Transient Stop Time

(U) The following engine control areas will be input through a separate subroutine and constitute the transient forcing parameters around which the control system will be developed.

5.	ALDV	Control Area	Preburner oxidizer flow divider valve	in^2
6.	ALC	Control Area	Main oxidizer line control valve	in^2
7.	ALBT	Control Area	Oxidizer low-speed inducer turbine	in^2
8.	AFPD	Control Area	Fuel valve at pump discharge	in^2
9.	AFB	Control Area	Preburner fuel injector	in^2
10.	ADCV	Control Area	Dump coolant control valve	in^2

(C) Engine initial conditions are required to establish the starting point of the transients and are input for each case. The following engine initial conditions for 20, 50 and 100 percent are contained in table LXX.

11.	OFV	Mixture Ratio	Into the low-speed inducers	D'less
12.	PBS	Pressure	Preburner injector face (static)	lb_f/in^2
13.	PB	Pressure	Preburner total	lb_f/in^2

14.	PC	Pressure	Main chamber throat total	lb_f/in^2
15.	PCP	Pressure	Main chamber throat total (steady-state)	lb_f/in^2
16.	PCS	Pressure	Main chamber injector face (static)	lb_f/in^2
17.	PHDC	Pressure	Dump coolant heat exchanger discharge	lb_f/in^2
18.	PHX2	Pressure	Downstream of the main nozzle regenerative heat exchanger	lb_f/in^2
19.	PMIJ	Pressure	Upstream of main chamber injecter	lb_f/in^2
20.	PTCV	Pressure	Turbine cooling flow volume	lb_f/in^2
21.	PTRA	Pressure	Transpiration section supply	lb_f/in^2
22.	RHX1	Density	Small nozzle heat exchanger discharge	lb_m/ft^3
23.	RHX2	Density	Main nozzle heat exchanger discharge	lb_m/ft^3
24.	ROFB	Density	Fuel low-speed inducer discharge	lb_m/ft^3
25.	ROFI	Density	Fuel Pump Interstage	lb_m/ft^3
26.	RFPD	Density	Main fuel pump discharge (2nd stage)	lb_m/ft^3
27.	ROL	Density	Main oxidizer pump discharge	lb_m/ft^3
28.	ROLB	Density	Oxidizer low-speed inducer discharge	lb_m/ft^3
29.	NFP	Speed	Main fuel turbopump	rpm
30.	NFB	Speed	Fuel low-speed inducer	rpm
31.	NLP	Speed	Main oxidizer turbopump	rpm
32.	NLB	Speed	Oxidizer low-speed inducer	rpm
33.	THDC	Temperature	Dump cooling nozzle exit	°R
34.	TFBTD	Temperature	Fuel low-speed inducer turbine discharge	°R
35.	THX1	Temperature	Small nozzle heat exchanger discharge	°R
36.	THX2	Temperature	Main nozzle heat exchanger discharge	°R
37.	TMJ	Temperature	Upstream of main chamber injector (dome)	°R
38.	WUC	Flow	Out of the transpiration section volume	lb_m/sec
39.	WFI	Flow	Fuel low-speed inducer	lb_m/sec
40.	WL	Flow	Oxidizer low-speed inducer	lb_m/sec
41.	PFI	Pressure	Fuel low-speed inducer inlet	lb_f/in^2
42.	WHDC	Flow	Into the dump cooling heat exchanger	lb_m/sec
43.	HFI	Enthalpy	Fuel Inlet	Btu/lb_m
44.	OFC	Mixture Ratio	Main chamber, including all transpiration flow	D'less
45.	PLIM	Pressure	Main oxidizer pump inlet	lb_f/in^2
46.	TLI	Temperature	Oxidizer inlet	°R
47.	PLI	Pressure	Oxidizer low-speed inducer inlet	lb_f/in^2
48.	WMIJ	Flow	Exit from the dome volume	lb_m/sec
49.	TAUC	Time Constant	Main chamber	sec

(C) Table LXX. Engine Initial Conditions at Engine Mixture Ratio of 6 and Thrust Levels of 20, 50, and 100 Percent

	THRUST LEVEL		
	20%	50%	100%
OFV	$\left(\frac{93.84}{15.64}\right) = 6.000$	$\left(\frac{233.52}{38.92}\right) = 6.000$	$\left(\frac{465.77}{77.63}\right) = 6.000$
[illegible]	721.8	1,976.8	4,516.5
Pt	$\left(\frac{721.8}{1.00836}\right) = 715.8$	$\left(\frac{1976.8}{1.00836}\right) = 1960.4$	$\left(\frac{4516.5}{1.00836}\right) = 4479.1$
PC	538.1	1,355.3	2,726.4
PCP	538.1	1,355.3	2,725.4
PCS	558.8	1,407.2	2,830.9
PHDC	10.9	25.5	48.6
PHX2	924.8	2,385.6	[illegible],174.3
PMJ	577.2	1,467.6	3,003.6
PTCY	700.	1,700.	3,580.
PTRA	767.	1,737.3	3,350.5
RHX1	0.47	0.90	1.42
RHX2	1.17	2.41	3.33
ROFB	4.20	4.21	4.23
ROF1	3.95	4.11	4.24
RFPD	3.80	4.04	4.28
ROL	68.38	68.77	68.29
ROLS	69.00	69.09	69.20
NFP	20,984.	32,125.	46,471.
NFB	6,099.	11,002.	17,861.
NLP	9,931.	15,817.	23,509.
NLB	1,697.	3,004.	5,087.
THDC	1,901.	1,799.3	1,726.
TFBTD	368.3	416.5	458.5
THX1	375.2	428.0	474.9
THX2	142.6	158.8	187.
TMJ	1,279.2	1,494.5	1,847.6
WCC	1.33	2.68	4.76
WF	15.64	38.92	77.63
WL	93.84	233.52	465.77

(C) Table LXX. Engine Initial Conditions at Engine Mixture Ratio of 6 and Thrust Levels of 20, 50, and 100 Percent (Continued)

	THRUST LEVEL		
	20%	50%	100%
PFI	31.8	31.8	31.8
WHDC	0.34	0.81	1.59
HFI	-97.08	-97.08	-97.08
OFC	[illegible]	6.128	6.125
PLIM	76.3	118.0	185.7
TLI	175.6	175.6	175.6
PLI	37.6	37.6	37.6
WMIJ	23.29	64.56	147.95
TC	0.01	0.01	0.01

2. Program Output Parameters

(U) The output parameter list is arranged according to the output format shown below. The block of output data is printed at time intervals specified by PTIM and is labeled with the actual time in the engine simulation.

PROGRAM OUTPUT FORMAT

1.	PFI	PHXI	PBS	PLI	WFI	WL	ROFB	TFBD	TQFT	QXF	NFP
2.	PFBD	PFBTD	PB	[illegible]	WHDC	WLLEK	RFPD	TFPD	TQLT	QXL	NLP
3.	PFIM	PZRA	PFTIN	PLIM	WFD	WLC	RHX2	THX2	TQFBT	QXFB	NFB
4.	XFNPSP	FTCV	PFTD	XLNPSP	WF	WLB	RHX1	THX1	TQLBT	QXLB	NLB
5.	PFPD		PLTIN	PLPD	WHX2	WFT	ROLB	TFBTD	DPFP	DPFDV	ALDV
6.	PFSL	OFL	PLTD	PLSP	WFB	WLT	ROL	TLBD	DPLP	DPLCV	ALC
7.	PFSP	OFC	PMIJ	PLBTU	WTCS	WFTD	WMJI	TLD	DPFB	DPLBT	ALBT
8.	PHX2	OFB	PCS	PLBTD	WTC	WLTD	WMIJ	TB	DPLB	DPFV	AFPD
9.	PFBI	OFV	PC	PLCV	WFBT	WFJI	WFIJ	TMJ	HPFP	DPFBI	AFB
10.	PDCVU	PFO	PCP	PLIJ	WCC	WCCX	WLCH	THDC	HPLP	DPDCV	ADCV

PROGRAM OUTPUT PARAMETERS

PFI	Pressure	Fuel low-speed inducer inlet	lb_f/in^2
PFBD	Pressure	Fuel low-speed inducer discharge	lb_f/in^2
PFIM	Pressure	Main fuel pump inlet (1st Stage)	lb_f/in^2
XFNPSP	Pressure	Excess NPSP at main fuel pump inlet	lb_f/in^2
PF2D	Pressure	Main fuel pump discharge (2nd stage)	lb_f/in^2
PFSL	Pressure	Split point of the cooling flows and P/B fuel flow	lb_f/in^2
PFSP	Pressure	Downstream of the fuel control valve	lb_f/in^2
PHX2	Pressure	Downstream of the main nozzle regenerative heat exchanger	lb_f/in^2

PROGRAM OUTPUT PARAMETERS (Continued)

PFBI	Pressure	Inlet to the preburner fuel injector	lb_f/in^2
PDCVU	Pressure	Inlet to the dump coolant control	lb_f/in^2
PHX1	Pressure	Fuel low-speed inducer turbine inlet	lb_f/in^2
PFBTD	Pressure	Fuel low-speed inducer turbine discharge	lb_f/in^2
PTRA	Pressure	Transpiration section supply	lb_f/in^2
PTCV	Pressure	Turbine cooling flow volume	lb_f/in^2
OFI	Mixture Ratio	Main chamber injector	D'less
OFC	Mixture Ratio	Main chamber, including all transpiration flow	D'less
OFB	Mixture Ratio	Preburner	D'less
OFV	Mixture Ratio	Into the low speed inducers	D'less
PFG	Ratio	Chamber pressure/design chamber pressure	D'less
PBS	Pressure	Preburner injector face (static)	lb_f/in^2
PB	Pressure	Preburner total	lb_f/in^2
PFTIN	Pressure	Main fuel turbine inlet	lb_f/in^2
PFTD	Pressure	Main fuel turbine discharge	lb_f/in^2
PLTIN	Pressure	Main oxidizer turbine inlet	lb_f/in^2
PLTD	Pressure	Main oxidizer turbine discharge	lb_f/in^2
PMIJ	Pressure	Upstream of main chamber injector	lb_f/in^2
PCS	Pressure	Main chamber injector face (static)	lb_f/in^2
PC	Pressure	Main chamber throat total	lb_f/in^2
PCP	Pressure	Main chamber throat total (steady state)	lb_f/in^2
PLI	Pressure	Oxidizer low-speed inducer inlet	lb_f/in^2
PLBD	Pressure	Oxidizer low-speed inducer discharge	lb_f/in^2
PLIM	Pressure	Main oxidizer pump inlet	lb_f/in^2
XLNPSP	Pressure	Excess NPSP at main oxidizer pump inlet	lb_f/in^2
PLPD	Pressure	Main oxidizer pump discharge	lb_f/in^2
PLSP	Pressure	Split point of the oxidizer P/B and main chamber flows	lb_f/in^2
PLBTU	Pressure	Oxidizer low-speed inducer turbine inlet	lb_f/in^2
PLBTD	Pressure	Oxidizer low-speed inducer turbine discharge	lb_f/in^2
PLCV	Pressure	Downstream of the main oxidizer control	lb_f/in^2
PLIJ	Pressure	Inlet to the main oxidizer injector	lb_f/in^2
WFI	Flow	Fuel low-speed inducer	lb_m/sec
WHDC	Flow	Into the dump cooling heat exchanger	lb_m/sec
WFD	Flow	Discharge of the dump cooling nozzle	lb_m/sec
WF	Flow	Main fuel pump	lb_m/sec
WHX2	Flow	Fuel pump valve	lb_m/sec
WFB	Flow	Preburner fuel flow	lb_m/sec
WTCS	Flow	Into the turbine cooling volume	lb_m/sec
WTC	Flow	Out of the turbine cooling volume	lb_m/sec
WFBT	Flow	Into the transpiration section volume	lb_m/sec
WCC	Flow	Out of the transpiration section volume	lb_m/sec

PROGRAM OUTPUT PARAMETERS (Continued)

WL	Flow	Oxidizer lo[illegible]ed i[illegible]ducer	lb_m/sec
WLLEK	Flow	Oxidizer [illegible] which dumps overboard	lb_m/sec
WLC	Flow	Oxidizer main chamber injector	lb_m/sec
WLB	Flow	Oxidizer into the preburner	lb_m/sec
WFT	Flow	Preburner products through the main fuel turbine	lb_m/sec
WLT	Flow	Preburner products through the main oxidizer turbine	lb_m/sec
WFTD	Flow	Main fuel turbine discharge including cooling	lb_m/sec
WLTD	Flow	Main oxidizer turbine discharge including cooling	lb_m/sec
WFJI	Flow	Fuel flow in the transition case	lb_m/sec
WCCX	Flow	Excess transpiration cooling flow	lb_m/sec
ROFB	Density	Fuel low-speed inducer discharge	lb_m/ft^3
RFPD	Density	Main fuel pump discharge (2nd stage)	lb_m/ft^3
RHX2	Density	Main nozzle heat exchanger discharge	lb_m/ft^3
RHX1	Density	Small nozzle heat exchanger discharge	lb_m/ft^3
ROLB	Density	Oxidizer low-speed inducer discharge	lb_m/ft^3
ROL	Density	Main oxidizer pump discharge	lb_m/ft^3
WMJI	Flow	Total turbine discharge into the dome volume	lb_m/sec
WMIJ	Flow	Exit from the dome volume	lb_m/sec
WFIJ	Flow	Fuel flow out of the main chamber injector	lb_m/sec
WLCH	Flow	Total oxidizer flow in the main chamber	lb_m/sec
TFBD	Temperature	Fuel low-speed inducer discharge	°R
TFPD	Temperature	Main fuel pump discharge	°R
THX2	Temperature	Main nozzle heat exchanger discharge	°R
THX1	Temperature	Small nozzle heat exchanger discharge	°R
TFBTD	Temperature	Fuel low-speed inducer turbine discharge	°R
TLBD	Temperature	Oxidizer low-speed inducer turbine discharge	°R
TLD	Temperature	Main oxidizer pump discharge	°R
TB	Temperature	Preburner	°R
TMJ	Temperature	Upstream of main chamber injector (dome)	°R
THDC	Temperature	Dump cooling nozzle exit	°R
TQFT	Torque	Main fuel turbine	lb_m-ft
TQLT	Torque	Main oxidizer turbine	lb_m-ft
TQFBT	Torque	Fuel low-speed induce[illegible] turbine	lb_m-ft
TQLBT	Torque	Oxidizer low-speed inducer turbine	lb_m-ft
DPFP	Pressure Rise	Main fuel pump	lb_f/in^2
DPLP	Pressure Rise	Main oxidizer pump	lb_f/in^2
DPFB	Pressure Rise	Fuel low-speed inducer	lb_f/in^2
DPLB	Pressure Rise	Oxidizer low-speed inducer	lb_f/in^2
HPFP	Horsepower	Main fuel pump	hp
HPLP	Horsepower	Main oxidizer pump	hp
CXF	Excess Torque	Main fuel (turbine torque - pump torque)	lb_m-ft

PROGRAM OUTPUT PARAMETERS (Continued)

QXL	Excess Torque	Main oxidizer (turbine torque - pump torque)	lb_m-ft
QXFB	Excess Torque	Fuel boost low-speed inducer - (turbine torque - pump torque)	lb_m-ft
QXLB	Excess Torque	Oxidizer low-speed inducer - (turbine torque - pump torque)	lb_m-ft
DPFDV	Pressure Drop	Preburner oxidizer flow divider valve	lb_f/in^2
DPLCV	Pressure Drop	Main oxidizer line control valve	lb_f/in^2
DPLBT	Pressure Drop	Oxidizer low-speed inducer turbine	lb_f/in^2
DPFV	Pressure Drop	Fuel valve at pump discharge	lb_f/in^2
DPFBI	Pressure Drop	[illegible]	lb_f/in^2
DPDCV	Pressure Drop	Dump coolant control	lb_f/in^2
NFP	Speed	Main fuel turbopump	rpm
NLP	Speed	Main oxidizer turbopump	rpm
NFB	Speed	Fuel low-speed inducer	rpm
NLB	Speed	Oxidizer low-speed inducer	rpm
ALDV	Control Area	Preburner oxidizer flow divider valve	in^2
ALC	Control Area	Main oxidizer line control valve	in^2
ALBT	Control Area	Oxidizer low-speed inducer turbine	in^2
AFPD	Control Area	Fuel valve at pump discharge	in^2
AFB	Control Area	Preburner fuel injector	in^2
ADCV	Control Area	Dump coolant control valve	in^2

3. Program Formulation

(U) The following engineering formulation includes the series of calculation of which the program execution cycles through each time increment (DT). The numerical integration technique has proven quite accurate, with DT = 0.001 second. However, some calculations have required mathematical iteration loops to assure proper balances in each program cycle pass. This is particularly true in the liquid flow - pressure balances where extremely small DT's would be required to eliminate mathematical oscillations. These iteration loops are designated in the formulation.

(U) 1. Fuel side

$$PFG = PC/2716.4$$

Assume WFI

$$DPFB = f_1(NFB,\ WFI,\ ROFB)$$

$$PFBD = PFI + DPFB$$

$$PFIN = PFBD - 0.01139603 \cdot (WFI)^2/ROFB$$

$$PDGVU = PFBD - (0.005698 \cdot WFI^2 + 4.28 \cdot WHDC^2)/ROFB$$

$$WHDC = 1.3645 \cdot ADGV \cdot \sqrt{PDGVU - 33.}$$

$$WF = WFI - WHDC$$

$$DPFP = f_2(NFP,\ WF,\ ROFP,\ RFPD)$$

$$PFPD = PFIN + DPFP$$

$$PFSL = PFPD - 0.01 \cdot (WF)^2/RFPD$$

$$ATCS = f(PFG)$$

Assume PTCV

$$WTCS = ATCS \sqrt{(PFSL - PTCV) \cdot RFPD/1.496}$$

$$WTC = 0.1228 \sqrt{(PTCV - PHC1) \cdot RTCV}$$

where: $RTCV = f_3(PTCV)$

$$PTCVX = PTCVP + BTCV \cdot (WTCS - WTC) \cdot 8.64 \cdot (DT)/RFPD$$

where: $PTCVP = PTCV$ at time $= T - DT$

$BTCV = f_4(PTCV)$

Iterate on PTCV until PTCVX = PTCV ± tolerance.

Assume WCC

$$PTRA = 0.5\left(PC + \sqrt{PC^2 + 787.378 \cdot SOT \cdot WC \cdot TFBTD}\right)$$

where: $SOT = 32.119(WCC\sqrt{PTRA}/PC) - 0.182$

$$WFBT = WCC + \frac{0.332816 \cdot (PTRA - PTRAP)}{PTRA\ (DT)}$$

where: $PTRAP = PTRA$ at time $= T - DT$

$$PFBTD = \sqrt{PTRA^2 + 22.20267 \cdot (WFBT)^2 \cdot TFBTD}$$

$$PHX1 = 476.799 \cdot WFBT \cdot \sqrt{THX1}/f_5(PFBTS)$$

where: $PFBTS = 0.5\left(PFBTD + \sqrt{PFBTD^2 - 43.71 \cdot TFBTD \cdot (WFBT)^2}\right)$

$$PFBTX = \sqrt{PBHXD^2 - 19.2674 \cdot RHX1\,(WFBT)^2}$$

where: $PBHXD = PFSL + \left(\frac{131.385}{RFPD} + \frac{0.4}{RHX1} + \frac{21.3}{(RFPD + RHX1)}\right) WFBT^2$

Iterate on WCC until PFBTX = PHX1 ± tolerance

$$[illegible] = WF - WTCB - WFBY$$

$$PFSP = PFSL - \frac{2.238}{RFPD} \cdot \left(\frac{WA\,2}{AFPD}\right)^2$$

$$DPFV = PFSL - PFSP$$

$$PHXDX = PFSP - WHX2^2 \left(\frac{0.02775}{RFPD} + \frac{6.04(PFG)^{0.05}}{RHX2}\right)$$

$$WFB = \sqrt{\frac{(PHXDX - PBS)\,RHX2}{0.089 + \left(\frac{1.495}{AFB}\right)^2}}$$

$$PFBI = PBS + \frac{2.238}{RHX2} \cdot \left(\frac{WFB}{AFB}\right)^2$$

$$DPFBI = PFBI - PBS$$

$$PHX2 = PHXDP + 1.02676 \cdot BFHX \cdot (WHX2 - WFB) \cdot (DT)/RHX3$$

where: $BFHX = f_6(PHXDX)$

$PHXDP$ = PHX2 of time = T - DT

Iterate on WFI until PHX2 = PHXDX ± tolerance.

$$TFBD = f_7(PFBD, HFB)$$

where: $HDFB;\ ETFB = f_1(WFI, NFB)$

$HFB = HFI + \frac{HDFB}{778\,(ETFB)}$

$$ROFB = f_8(PFBD, TFBD)$$

$$TFPD = f_9(PFPD, HFP)$$

where: $HDFP,\ EFP = f(WF, NFP)$

$HFP = HF[illegible] + \frac{HDFP}{778\,(EFP)}$

$$RFPD = f_8(PFPD, TFPD)$$

$$\mathrm{THX2} = \mathrm{THXDP} - (\mathrm{THXDP} - \mathrm{THX2})\ \exp\left(-\frac{\mathrm{DT}}{\mathrm{TAUM}}\right)$$

where: $\mathrm{HHXD} = \mathrm{HF2} + 13840\ (\mathrm{PFG})^{0.87}\ \mathrm{SKOF}/\mathrm{WHX2}$

$\mathrm{SKOF} = f_9(\mathrm{OFC})$

$\mathrm{THXDP} = f_7(\mathrm{PHX2},\ \mathrm{HHXD})$

$\mathrm{TAUM} = f_{10}(\mathrm{WFB})$

$$\mathrm{RHX2} = f(\mathrm{PHX2},\ \mathrm{THX2})$$

$$\mathrm{THX1} = \mathrm{TBHXDP} - (\mathrm{TBHXDP} - \mathrm{THX1})\ \exp\left(-\frac{\mathrm{DT}}{\mathrm{TAUB}}\right)$$

where: $\mathrm{HBHXD} = \mathrm{HF2} + 6500 \cdot (\mathrm{PFG})^{0.87} \cdot \mathrm{SKOF}/\mathrm{WFBT}$

$\mathrm{SKOF} = f_5(\mathrm{OFC})$

$\mathrm{TBHXDP} = f_7(\mathrm{PBHXD},\ \mathrm{HBHXD})$

$\mathrm{TAUB} = f_{10}(\mathrm{WFBT})$

$$\mathrm{RHX1} = f_8(\mathrm{PBHXD},\ \mathrm{THX1})$$

$$\mathrm{TQFBT} = 7426.11 \cdot \mathrm{DHFBT} \cdot \mathrm{ETFBT} \cdot \mathrm{WFBT}/\mathrm{NFB}$$

where: $\mathrm{DHFBT} = 3.616 \cdot \mathrm{THX1}\left(1 - (\mathrm{PFBTE}/\mathrm{PHX1})^{0.2642}\right)$

$\mathrm{ETFBT} = f_{11}(\mathrm{NFB},\ \sqrt{\mathrm{DHFBT}})$

$$\mathrm{QXFB} = \mathrm{TQFBT} - \mathrm{TQFB}$$

where: $\mathrm{RDFB},\ \mathrm{ETFB} = f_1(\mathrm{WFI},\ \mathrm{NFB})$

$$\mathrm{TQFB} = \frac{1.34861 \cdot \mathrm{WFI} \cdot \mathrm{RDFB}}{\mathrm{NFB} \cdot \mathrm{ETFB}}$$

$$\mathrm{NFB} = 266.74 \cdot \mathrm{QXFB} \cdot \mathrm{DT} + \mathrm{NFB}$$

$$\mathrm{TFBTD} = \mathrm{THX1} - \mathrm{DHFBT} \cdot \mathrm{ETFBT}/3.616$$

$$\mathrm{WFD} = f_8(\mathrm{THDC},\ \mathrm{PHDC})$$

$$\mathrm{PHDC} = \mathrm{PHDC} + 3.8325 \cdot (\mathrm{TFBD} + \mathrm{THDC}) \cdot (\mathrm{WDC} - \mathrm{WFD}) \cdot \mathrm{DT}$$

$$\mathrm{THDC} = 1726./(\mathrm{PFG})^{0.06}$$

$$\mathrm{DPDCV} = \mathrm{PDCVU} - \mathrm{PHDC} - 28.(\mathrm{PFG})^{0.98} \cdot \mathrm{SKLP} - 4.28(\mathrm{WHDC})^2/\mathrm{ROFB}$$

$$\mathrm{PFNPSP} = \mathrm{PFIN} - 30. - \frac{\mathrm{ROFB}}{144.}\left(4.391 \times 10^{-7} \cdot \mathrm{NFP}^2 \cdot \sqrt{\frac{\mathrm{ROFB}}{\mathrm{WF}}}\right)^{4/3}$$

$$XLNPSP = PLIM - 30. - \frac{ROL}{144} \cdot \left(3.?? \times 10^{-7}\ WLP^2 \sqrt{\frac{ROLB}{WL}}\right)^{4/3}$$

$$WCCX = WCC - \frac{24130.}{6600.} \cdot \frac{(WB)^{0.87} \cdot SNOFT}{ASMD + SNFRT}$$

where: $SNOFT = f_{22}(OFC)$

(U) 2. Oxidizer Side

Assume WL

DPLB $= f_{10}$(WL, WLH, ROLB)

PLBD $=$ PLB + DPLB

PLIM $=$ PLBD $-$ 0.0004542 $\cdot$ $(WL)^2$/ROLB

DPLP $= f_{11}$(WL, ..., ROL)

PLPD $=$ PLIM + DPLP

PLSP $=$ PLPD $-$ 0.011009 $\cdot$ $(WL)^2$/ROL

$$WLB = \sqrt{\frac{(PLSP - PBS)\ ROL}{0.38??75 + \left(\frac{1.496}{ALBI}\right)^2}}$$

where: $ALBI = 0.039345 \cdot \frac{1.496}{\sqrt{3.3993 + \left(\frac{1.496}{ALOV}\right)^2}}$

$$WLC = \sqrt{\frac{(PLSP - PCS) \cdot ROL}{0.322037 + \left(\frac{1.496}{ALBT}\right)^2 + \left(\frac{1.496}{ALC}\right)^2}}$$

WLLEK $=$ 0.9375 $\cdot$ (PFG) + 0.0625

WLPX $=$ WLB + WLC + WLLEK

Iterate on WL until WLPX = WL ± Tolerance

TLBD $=$ TLB + (1.0/ETAB $-$ 1.0) $\cdot$ 0.0047697 $\cdot$ (HDLB)

where: HDLB, ETAB $= f_{12}$(WLB, WL)

ROLB $= f_{1?}$(PLBD, TLBD)

$$TLD = \frac{316.646 \cdot TLBD \cdot ROL - ... \cdot DPLP \cdot (1. - EL1)}{EL1(316.646 \cdot ROL - 0.33634 \cdot DPLP)}$$

where: $EL1 = f_{13}$(DPLP, WL, ROL)

ROL $= f_{14}$(PLPD, TLD)

$$PLBTU = PLSP - 0.0027184(WLC)^2/ROL$$

$$DPLBT = \frac{2.238}{ROL}\left(\frac{WLC}{ALBT}\right)^2$$

$$PLBTD = PLBTU - DPLBT$$

$$TQLBT = 7426.1\ (DHLBT \cdot ETLBT \cdot WLC)/NLB$$

where: $DHLBT = 0.18\text{[illegible]}\ DPLBT/ROL$

$$ETLBT = f_{15}\left(NLB, \frac{1}{\sqrt{DHLBT}}, ALBT\right)$$

$$QXLB = TQLBT - TQLB$$

where: $HDLB, ETLB = f_{12}(NLB, WL)$

$$TQLB = \frac{\text{[illegible]}.54861 \cdot WL \cdot HDLB}{NLB \cdot ETLB}$$

$$NLB = 286.482 \cdot QXLB \cdot DT + NLB$$

$$PLIJ = PCS + 0.31\text{[illegible]}94(WLC)^2/ROL$$

$$PLCV = PLIJ + 0.0036245(WLC)^2/ROL$$

$$DPLCV = PLBTD - PLCV$$

$$DPFDV = \left(\frac{1.496}{ALDV}\right)^2 \cdot \left(\left(1 - \frac{0.029345}{ALBI}\right) \cdot WLB\right)^2$$

(U) 3. Preburner and Main Turbines

a. Preburner

$$OFB = WLB/WFB$$

$$TB = f(OFB, THX2)$$

Also: $GMB, CPB, RB = f_{16}(OFB, THX2)$

$$(WFT + WLT) = \frac{7.452 \cdot \text{[illegible]}}{\text{[illegible]} \cdot RB} \cdot f_{17}\left(\frac{PB}{PMIJ}, GMB\right)$$

$$PB = 0.0007145 \cdot RB \cdot TB \cdot \left[WFB + WLB - (WFT + WLT)\right] \cdot DT + PB$$

$$PBS = 1.00836 \cdot PB$$

b. Fuel Turbine

$$WFT = 0.67408 \cdot (WFT + WLT)$$

$$WFTD = WFT + 0.359\ WTC$$

$$PFTD = \sqrt{PMIJ^2 + 8.0452 \times 10^{-6} \cdot (WFTD)^2 \cdot RB \cdot TMJ}$$

$$PFTIN = \sqrt{PB^2 - 2.0828 \times 10^{-6} \cdot (WFT)^2 \cdot RB \cdot TB}$$

$$TQFT = 7426.11 \cdot DHFT \cdot ETAFT \cdot WFT/NFP$$

where:

$$PFTS = 0.5 \left(PFTD^2 + \sqrt{PFTD^2 - 3.6444 \times 10^{-5} \cdot RB \cdot TMJ \cdot (WFTD)^2} \right)$$

$$DHFT = CPB \cdot TB \left[1. - \left(\frac{PFTS}{PFTIN} \right)^{\frac{GMB-1}{GMB}} \right]$$

$$ETAFT = f_{18}\left(NFP, \frac{1}{\sqrt{DHFT}} \right)$$

$$QXF = TQFT - TQRF$$

where: $DHFP, EFP = f_2(WF, NFP)$

$$TQRF = \frac{9.54861 \cdot WF \cdot DHFP}{NFP \cdot EFP}$$

$$NFP = 123.22 \cdot QXF \cdot DT + NFP$$

$$HPFP = TQRF \cdot NFP/5250$$

c. Oxidizer Turbine

$$WLT = (WFT + WLT) - WFT$$

$$WLTD = WLT + 0.359\ WTC$$

$$PLTD = \sqrt{PMLJ^2 + 4.04672 \times 10^{-5} \cdot (WLTD)^2 \cdot RB \cdot TMJ}$$

$$PLTIN = \sqrt{PB^2 - 2.12476 \times 10^{-5} \cdot (WLT)^2 \cdot RB \cdot TB}$$

$$TQLT = 7426.11 \cdot DHLT \cdot ETALT \cdot WLT/NLP$$

where:

$$PLTS = 0.5 \left(PLTD^2 + \sqrt{PLTD^2 - 1.29235 \times 10^{-5} \cdot RB \cdot TMJ \cdot (WLTD)^2} \right)$$

$$DHLT = CPB \cdot TB \left[1. - \left(\frac{PLTS}{PLTIN} \right)^{\frac{GMB-1}{GMB}} \right]$$

$$ETALT = f_{19}(NLP, \sqrt{DHLT})$$

$$QXL = TQLT - TQRL$$

where: $DHLP, ELP = f_{13}(WL, NLP)$

$$TQRL = \frac{9.54861 \cdot WL \cdot DHLP}{NLP \cdot ELP}$$

$$NLP = 97.4418 \cdot QXL \cdot DT + NLP$$

$$HPLP = TQRL \cdot NLP/5250$$

(U) 4. Main Injector and Chamber Dome

$$WMJI = WTC + WFT + WLT$$

$$TMJ = \frac{WFTD \cdot TFT + WLTD \cdot TLT}{\frac{3.816}{CPB} \cdot WTC + WFT + WLT}$$

where: $$TFT = TB - \frac{DHFT \cdot ETAFT}{CPB}$$

$$TLT = TB - \frac{DHLT \cdot ETALT}{CPB}$$

Assume: WMIJ

$$PMIJ = PMIJP + 0.0005(WMJI - WMIJ) \cdot RMIX \cdot TMJ \cdot DT$$

where: $$RMIX = \frac{9198. \cdot WTC + RB\ (WFT + WLT)}{WMJI}$$

$$PMIJP = PMIJ \text{ of time } = T - DT$$

$$WMJOP = \frac{21.837 \cdot PMIJ}{\sqrt{TMJ \cdot RMIX}}\ f_{17}(PMJ/PCS,\ GAMIX)$$

where: $$CPMIX = \frac{3.816 \cdot WTC + CPB(WFT + WLT)}{WMJI}$$

$$GAMIX = \frac{CPMIX \cdot 9336.}{CPMIX \cdot 9336. - RMIX}$$

Iterate on WMIJ until WMJOP = WMIJ ± Tolerance

$$WFJI = \frac{WFT + WLT}{(OPB + 1)} + WTC$$

$$WFIJ = \frac{WMIJ}{\left(\frac{WMIJ - WFJI}{WFJI}\right) + 1}$$

$$WLCH = WLC + WMIJ - WFIJ$$

$$OFI = WLCH/WFIJ$$

$$OFC = \frac{WLCH}{WFIJ + WCC}$$

$$PCP = (WLCH + WFIJ + WCC) \cdot CSTR \cdot ETAC/1497.3$$

where: $$CSTR = f_{20}(OFC,\ PC)$$

$$ETAC = f_{21}(OFI)$$

$$PC = PCP - (PCP - PC)\exp\left(-\frac{DT}{TC}\right)$$

$$PCS = PC \cdot 1.03833$$

$$OFV = WL/WFI$$

V. PROGRAM OPERATING INSTRUCTIONS

(U) The 250K digital transient deck consists of the following program blocks:

1. A "START" subroutine will be provided as a source deck and will allow the users prime authority over the selection of available control areas and sense parameters. For example, the dump coolant control area (ADCV) can be programed as a function of chamber pressure, and preburner fuel injector area (AFB) can be set to a constant. The named common block "CINPUT" is contained in the subroutine "START" and must be retained in its present form.

2. The engine mathematical simulation "ENGINE" will be provided as an object deck and will not require program changes unless cycle modifications are encountered.

(U) The input items in "CINPUT" are initialized by the first 40 cards of input. These cards are followed by a blank card to indicate the end of the data for the first case. The number in column 1-2 determines the location in the "CINPUT" common block where the value is to be stored. The number should be right adjusted in the field. The name in columns 25-30 is for references only. The value for each input can be in either a decimal form or decimal exponent form. This value must be punched between columns 5 and 20 and must contain a decimal point. The input listing always prints the input values in the decimal exponent form.

(U) The data are read in until the blank card is processed. The program then enters subroutine "START" to obtain the engine control areas. Subroutine "ENGINE" is called to perform the engine simulation calculations for the input start time. Upon completion of these calculations, the time increment (DT) is added to the start time and subroutine "START" is recalled to change the control areas, if necessary. Subroutine "ENGINE" is again entered and the computation for the new time is completed. At this point the sum of the time increments is checked against the print time (PTIM). If they are equal, the results of the simulation at that time are printed. The process of adding the time increment and completing the simulation is repeated until the stop time (STIM) is reached. At any time during any of the steps, if a situation occurs that would terminate the run, "EPRINT" is called to print the results at that point and a statement is printed indicating that Error Print was called.

(U) The next card is read for a second case. If multiple cases are desired they must be separated by a blank card and only the input items that are to be changed from the previous case need be included for the next case. If there is no additional case to be run, a card with -1 punched in columns 1-2 is placed following the blank card of the first case. The data package must have a blank card and a -1 card at the end.

(U) The time increment, DT, (input card No. 2 of the data package) should remain 0.001 because the calculations and convergence loops in the program are based on this increment. The start time, T, (card No. 1) can be changed providing the initial conditions established by the other input cards are adjusted to give reasonable engine conditions at the start time input. The print time, PTIM, (card No. 3) may be changed to reduce the printed output, if desired. The print time must be some multiple of the time increment (DT).

APPENDIX III
PARAMETRIC DATA

APPENDIX III
PARAMETRIC DATA

A. PERFORMANCE DATA

1. General

(C) These data are for high-pressure, two-position bell-nozzle engines, using the staged-combustion (preburner) cycle and are based on technology that could be realized during a full engine development program. The use of dump cooling downstream of an expansion ratio of 35 was assumed in computing these parametric engine data. For high expansion ratio nozzles, radiation cooling is used aft of the lowest expansion ratio allowed by heat flux consideration. (This expansion ratio varies over the range, but is approximately 300.) Performance, weight, and dimensional data are based on the following:

1. High pressure, staged-combustion, two-position bell-nozzle engines
2. Main turbopumps and preburner, mounted in a transition case
3. Lo[illegible] speed inducers with:
   a. Minimum hydrogen net positive suction head (NPSH) = 60 ft
   b. Minimum oxygen net positive suction head (NPSH) = 60 ft
4. Throttling capability - continuous between 100 and 20% of rated thrust
5. Mixture ratio range of 5 to 7 at all thrust levels
6. Thrust vector control provided by gimbaling
7. Durability of 10 hours time between overhaul (TBO), 100 reuses, 300 starts, 300 thermal cycles, 10,000 valve cycles
8. The lightweight extendable secondary nozzle translates to provide high sea level performance and altitude compensation capability.

(C) The ranges of engine parameters included in the parametric data are:

1. Vacuum thrust - 100,000 to 350,000 lb
2. Chamber pressure - 2000 to 3500 psia
3. Overall engine mixture ratio - 5 to 7
4. Overall expansion ratio - 50 to 400

5. Nozzle contour - maximum performance (MC_s), base, and minimum surface area (MSA)

6. Primary expansion ratio - 35.

(U) Values of specific impulse are given for an altitude range from sea level to vacuum conditions.

(C) Data are presented for engines where the secondary nozzle skirt is translated from primary expansion ratios of 35 for a range of overall nozzle area ratios of 30 to 150. In addition, data are presented for primary area ratios that result in the minimum stowed engine length (i.e., the secondary nozzle skirt fully retracted). The primary expansion ratio for minimum stowed length varies with thrust level, chamber pressure, overall expansion ratio, and nozzle contour. For these data, the overall nozzle area ratio range is 80 to 400. The secondary nozzle can be translated over the turbopump for those engines where the primary area ratio is greater than 80. For the nozzles translating at primary area ratios between 35 and 80, the secondary nozzle is retracted to the point where it is limited by the turbomachinery.

(U) Parametric data over the complete thrust and chamber pressures range and for minimum surface area, base, and amximum performance nozzle contours are presented in the following paragraphs.

2. Performance

(U) Delivered vacuum specific impulse as a function of thrust, mixture ratio, chamber pressure, and nozzle area ratio is shown in figure 638 through 658 for minimum surface area, base, and maximum performance nozzle contours.

(C) Performance from sea level to 200,000 ft is shown as a ratio of delivered specific impulse to vacuum specific impulse plotted as a function of the ratio of chamber pressure to ambient pressure for primary area ratios of 35 (the data are independent of chamber pressure when primary area ratio is constant). These data are presented in figures 659 through 667. Altitude to vacuum performance for minimum stowed length engines (i.e., primary area ratio is a varible) is shown in figures 668 through 703 as a function of altitude.

(C) The delivered specific impulse at other than vacuum conditions can be calculated using figures 659 through 703, which show the ratio of altitude to vacuum performance as a function of altitude or pressure ratio and nozzle expansion ratio for mixture ratios of 5, 6, and 7. The delivered specific impulse at any altitude up to 200,000 ft (200,000 ft is the reference altitude for vacuum conditions) is calculated by:

$$I_{s_{alt}} = \left[\frac{I_{s_{alt}}}{I_{vac}}\right] I_{vac}$$

where:

$I_{s_{alt}}$ = delivered specific impulse at the altitude of interest

$I_{s_{alt}}/I_{vac}$ = ratio of altitude to vacuum performance for the altitude and mixture ratio of interest (figures 659 through 703)

also

$$F_{alt} = \frac{I_{s_{alt}}}{I_{vac}} F_{vac}$$

(U) In cases where altitude performance is plotted versus pressure ratio, the pressure ratio can be calculated by:

$$PR = \frac{P_c}{P_a}$$

where:

P_c = chamber pressure, psia

P_a = ambient pressure at the altitude of interest, psia

(U) The curves present altitude performance for the engines with the secondary nozzle extended at high altitudes and with the secondary nozzle retracted at low altitudes. Low altitude primary nozzle data have not been included for cases where the primary nozzle exhaust would be expected to reattach to the secondary nozzle (acting as a shroud).

B. WEIGHT AND ENVELOPE

(C) This paragraph contains parametric data showing the effect of nozzle contour, area ratio, and mixture ratio changes on the weight and envelope of oxygen-hydrogen, high-pressure (3000-psia chamber pressure), pump-fed, staged combustion cycle rocket engines with transpiration cooled main combustion chambers and dump-cooled two-position nozzles. Data are presented for vacuum thrust levels of 100,000 lb to 350,000 lb, with nozzle contour, chamber pressure, and area ratio as independent variables. The nozzle contours covered are the following truncations of perfect bell nozzles: (1) minimum surface area (MSA); (2) base nozzle; and (3) maximum performance (MC_g).

(U) Engine weights are presented in figures 704 through 721.

(U) Figure 722 illustrates the engine configuration with a two-position nozzle. Engine length with a two-position nozzle is presented as stowed length, minimum stowed length (upper stage), and overall length (nozzle fully extended). These data are presented in figures 723 through 749.

(U) Exit envelope diameters are presented in figures 750 through 7[illegible].

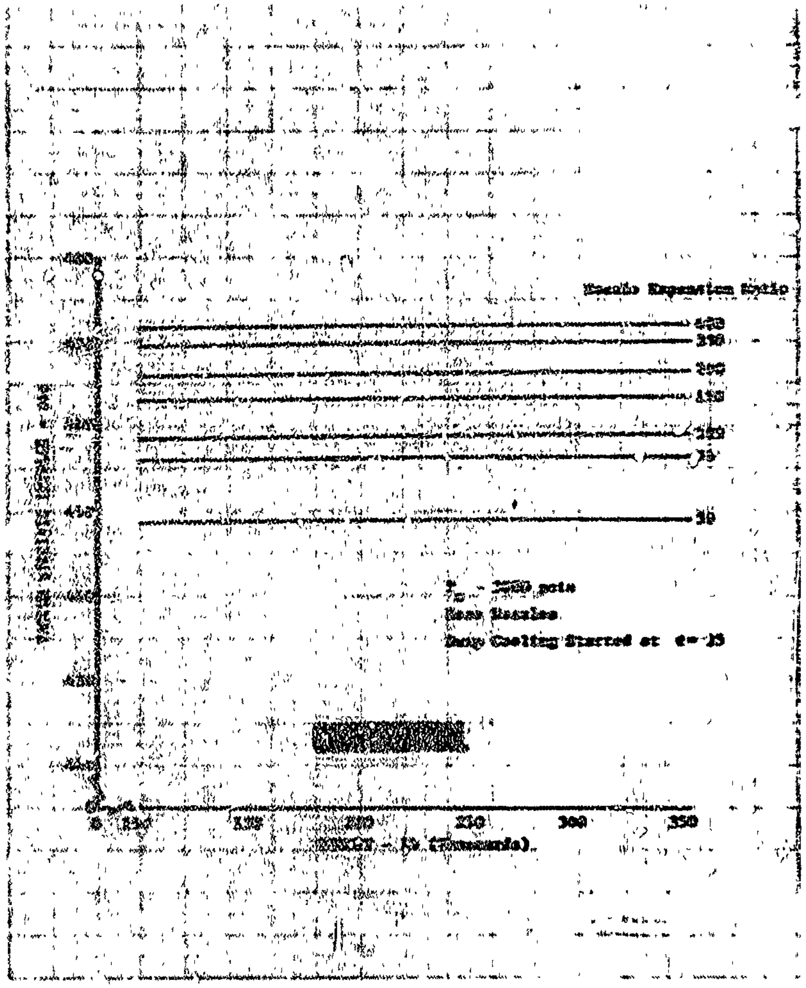

Figure 638. Vacuum Specific Impulse vs Thrust With Base Contour Two-Position Nozzle (r = 5.0) DF 56328

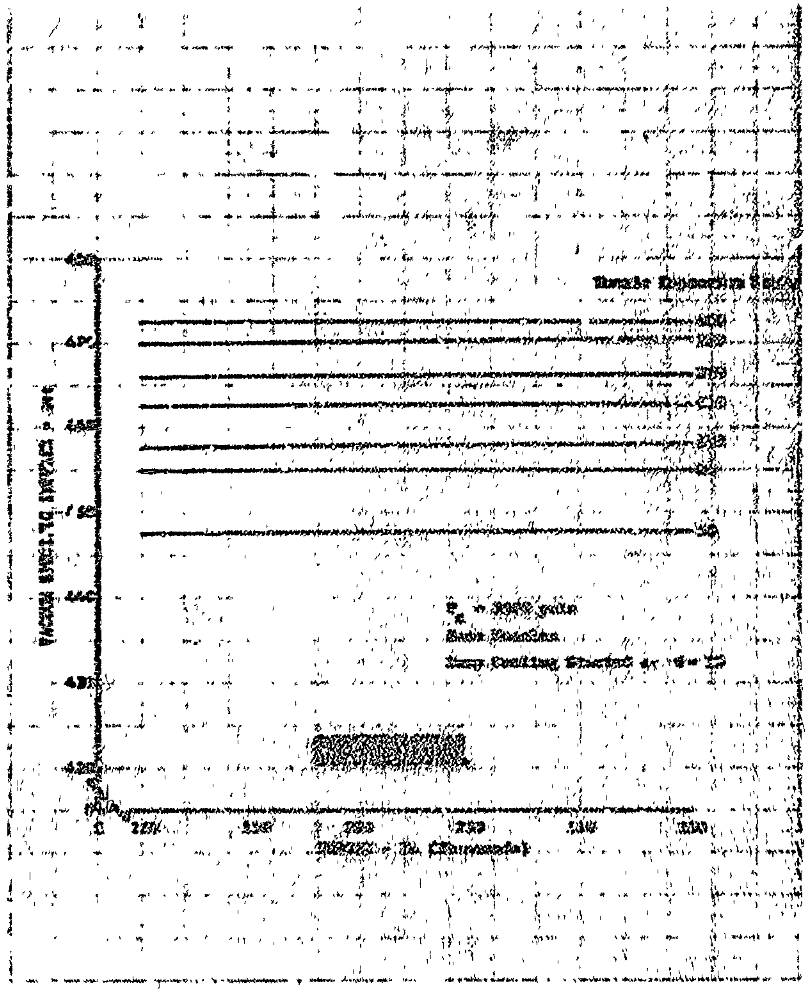

Figure 639. Vacuum Specific Impulse vs Thrust With Base Contour Two-Position Nozzle (r = 5.5) DF 56285

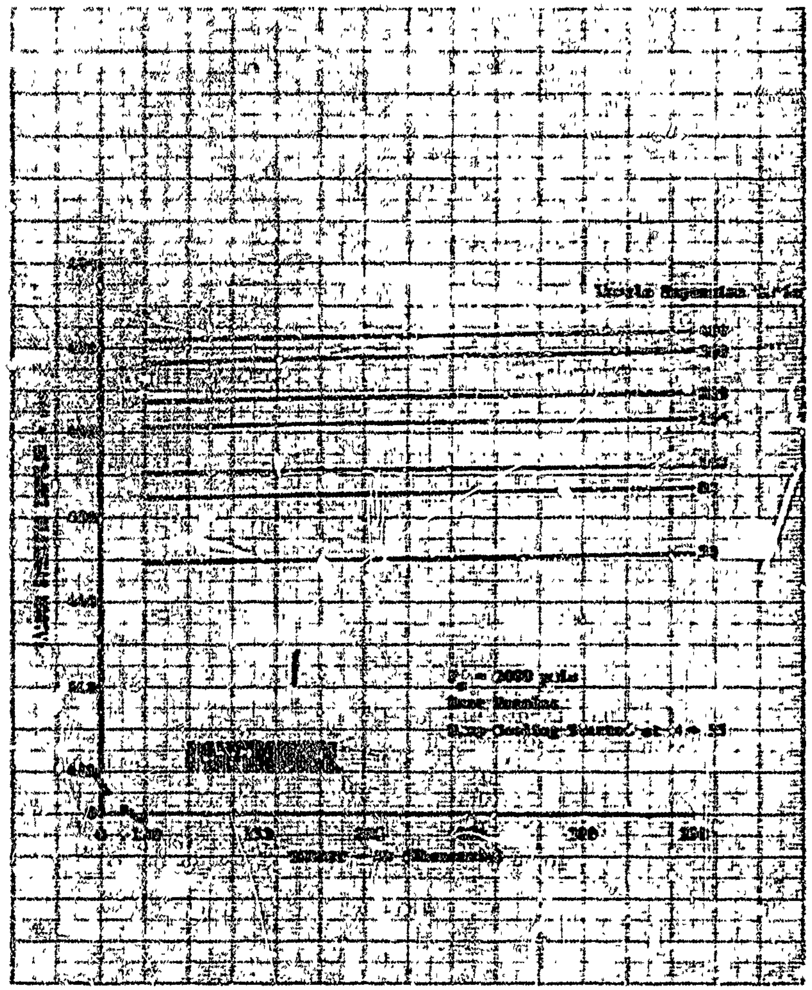

Figure 640. Vacuum Specific Impulse vs Thrust With Base Contour Two-Position Nozzle (r = 6.0) DF 56286

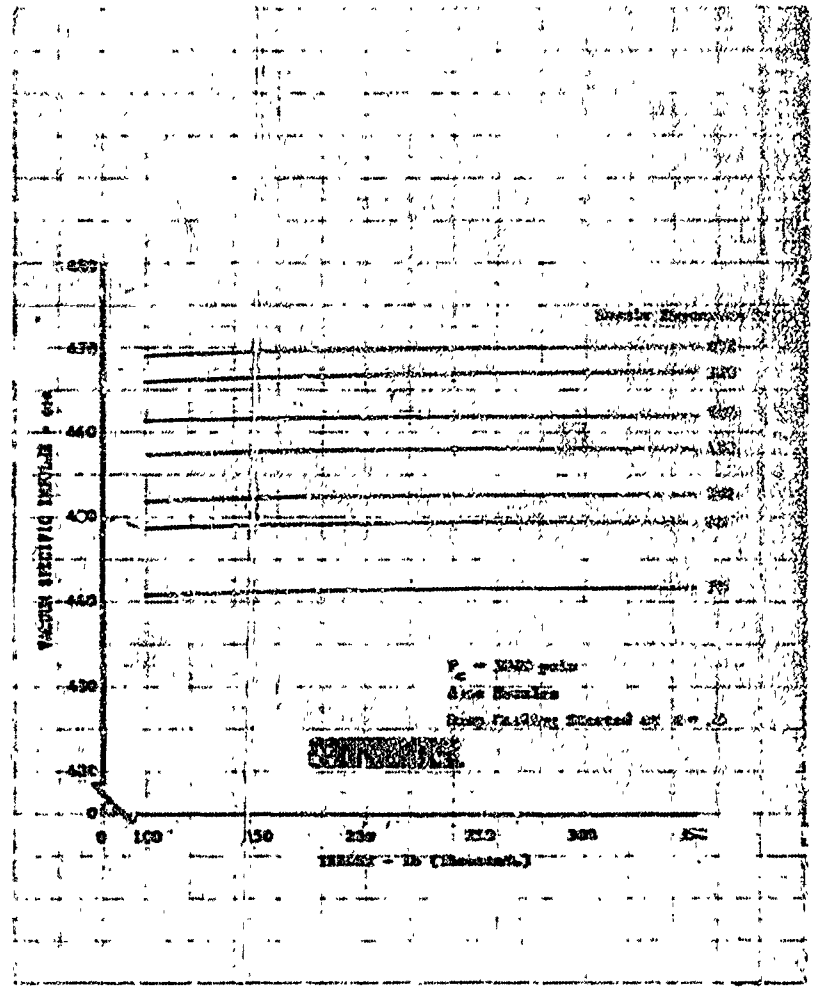

Figure 641. Vacuum Specific Impulse vs Thrust With Base Contour Two-Position Nozzle (r = 6.5) DF 56287

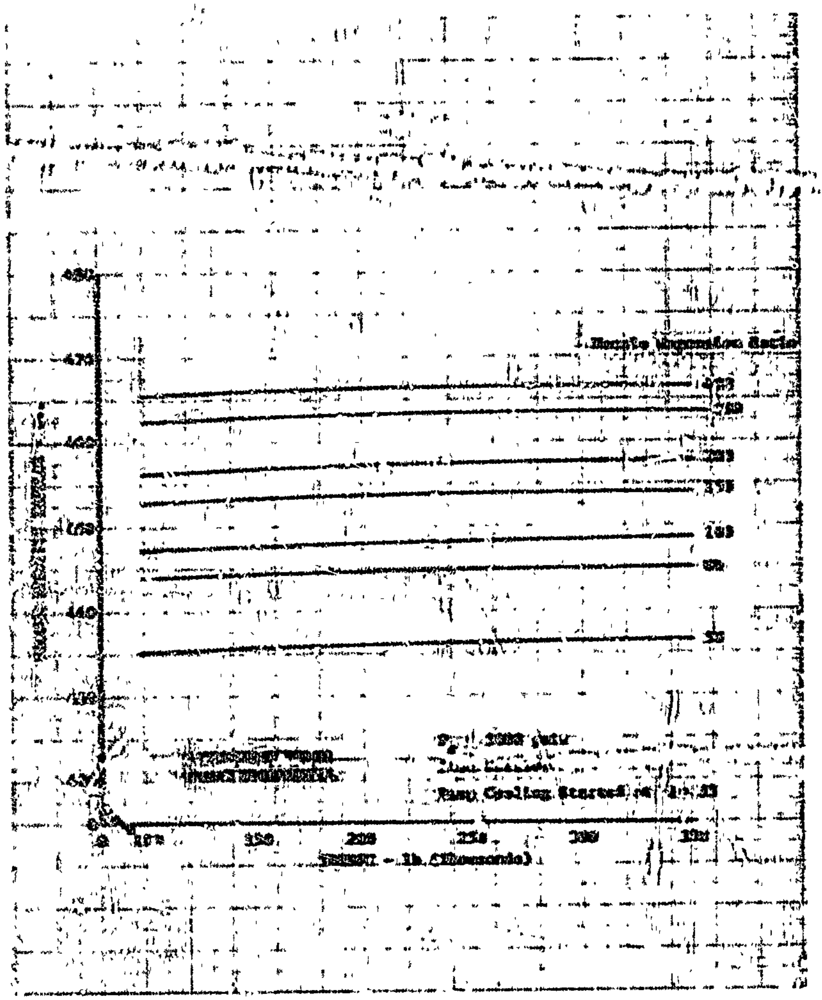

Figure 642. Vacuum Specific Impulse vs Thrust With Base Contour Two-Position Nozzle (r = 7.0) DF 56288

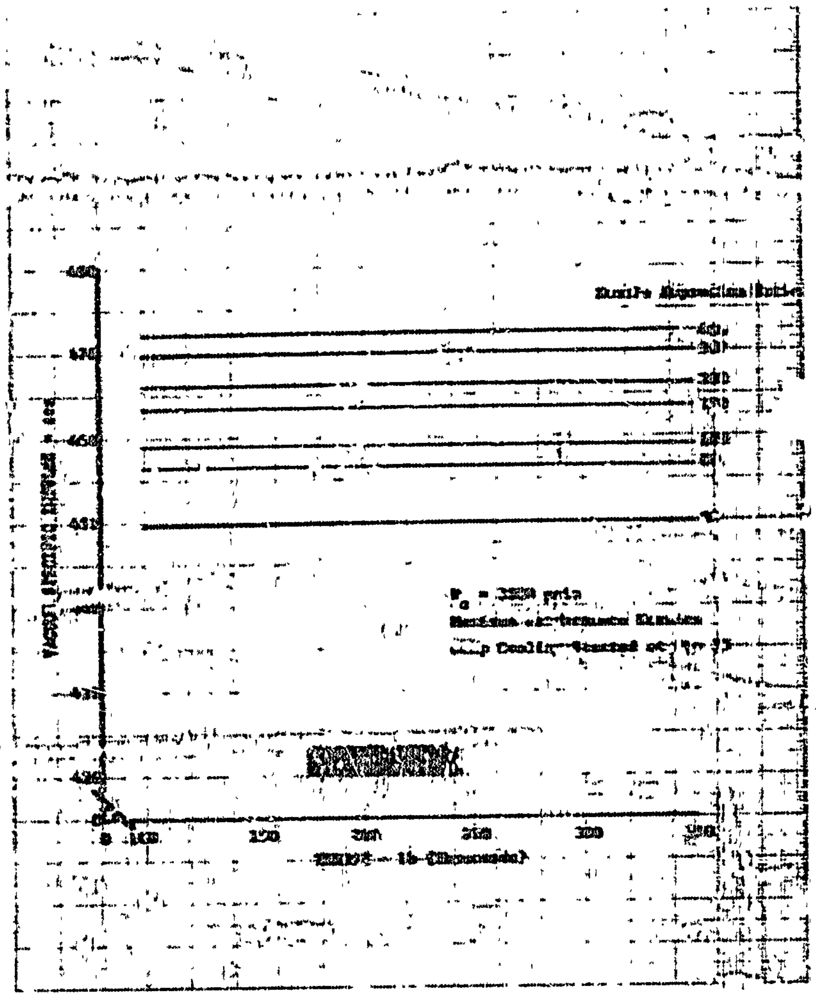

Figure 643. Vacuum Specific Impulse vs Thrust With Maximum Performance Contour Two-Position Nozzle (r = 5.0) DF 56294

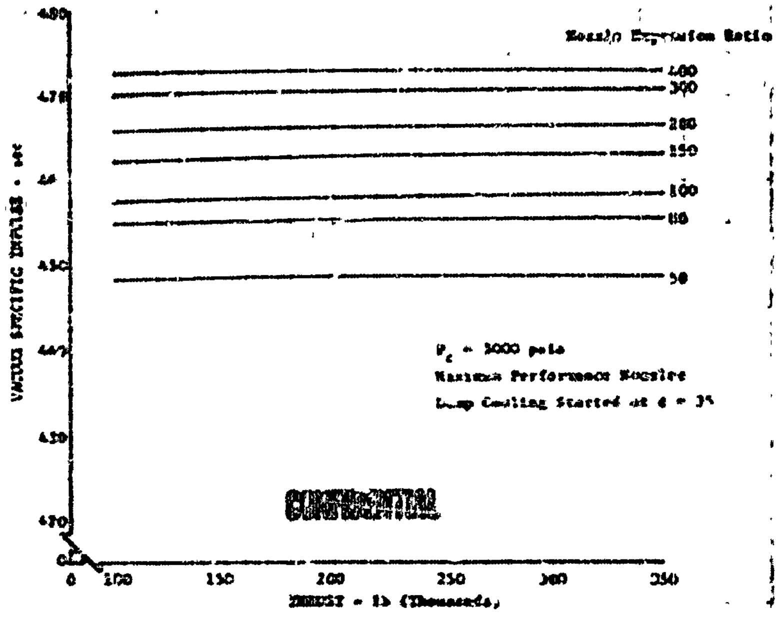

Figure 644. Vacuum Specific Impulse vs Thrust With Maximum Performance Contour Two-Position Nozzle (r = 5.5) DF 56295

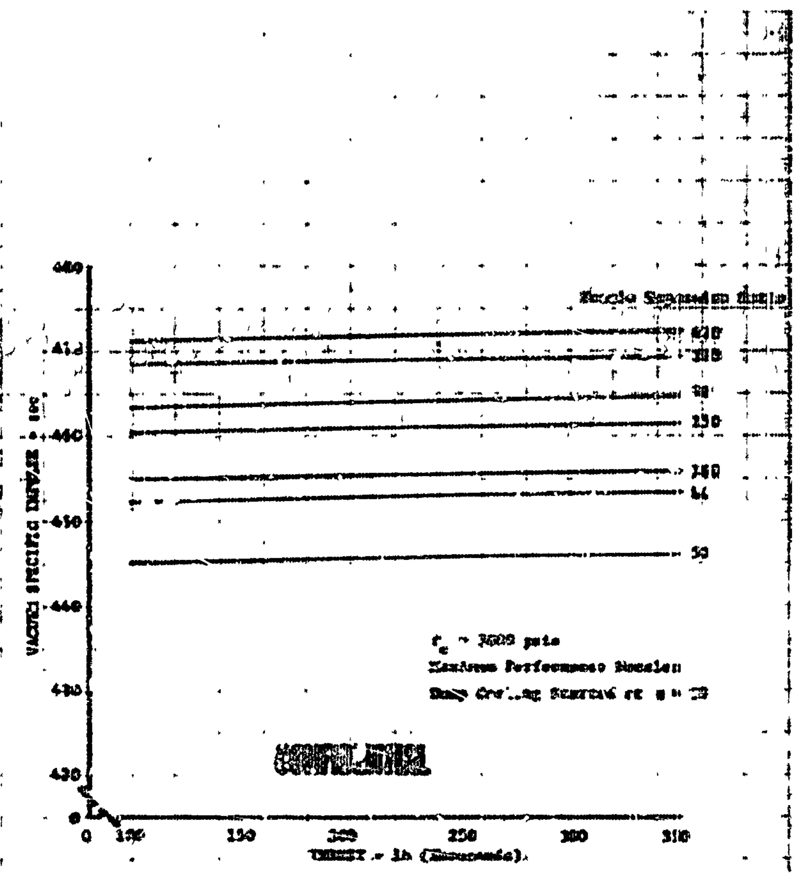

Figure 645. Vacuum Specific Impulse vs Thrust With Maximum Performance Contour Two-Position Nozzle (r = 6.0) DF 56296

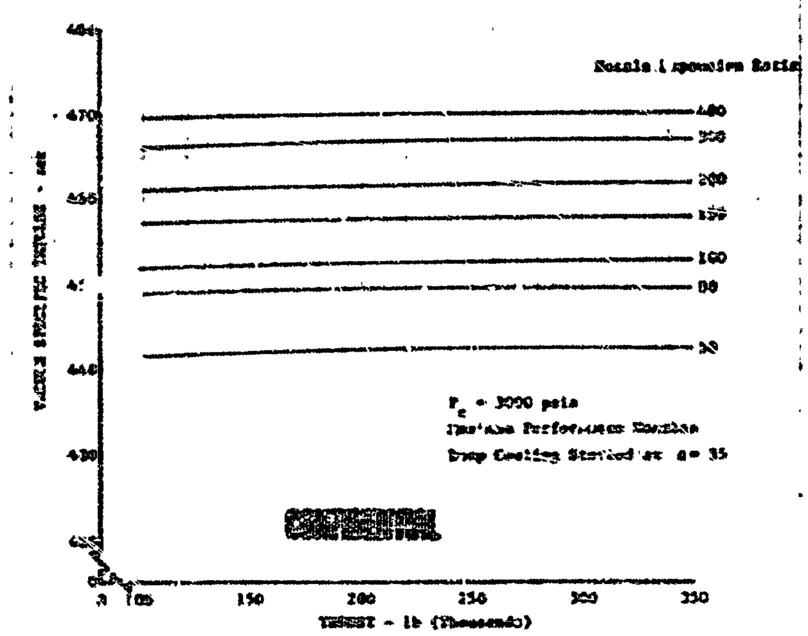

Figure 646. Vacuum Specific Impulse vs Thrust With Maximum Performance Contour Two-Position Nozzle (r = 6.5) DF 56297

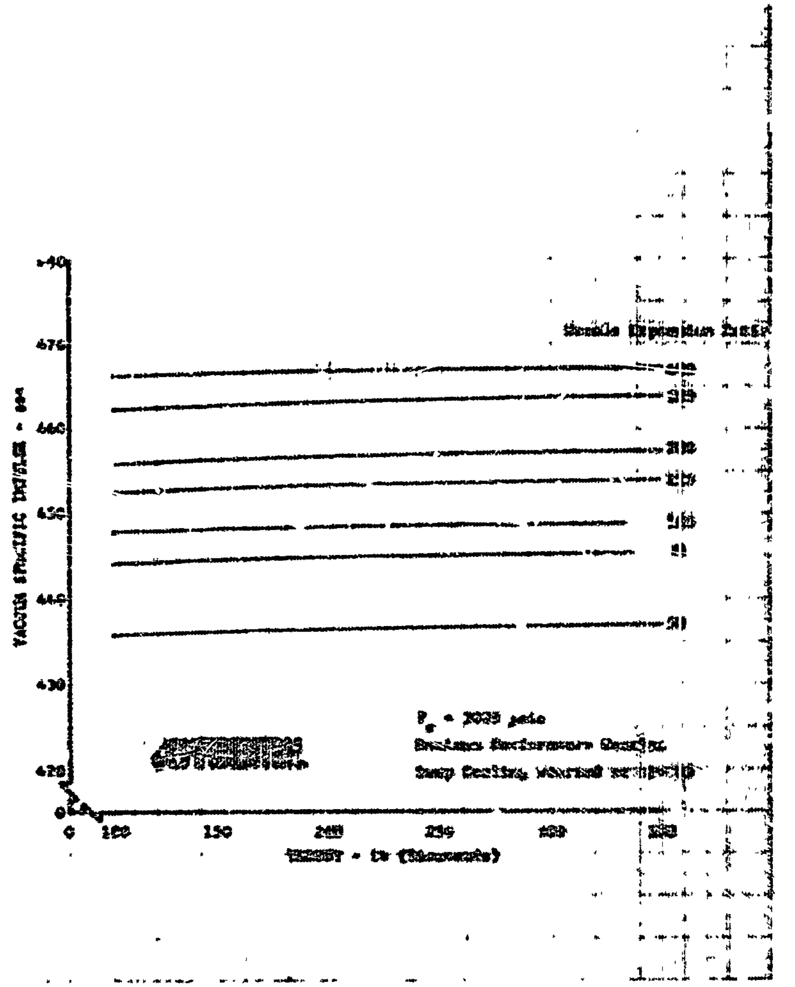

Figure 647. Vacuum Specific Impulse vs Thrust With Maximum Performance Contour Two-Position Nozzle (r = 7.0) DF 56298

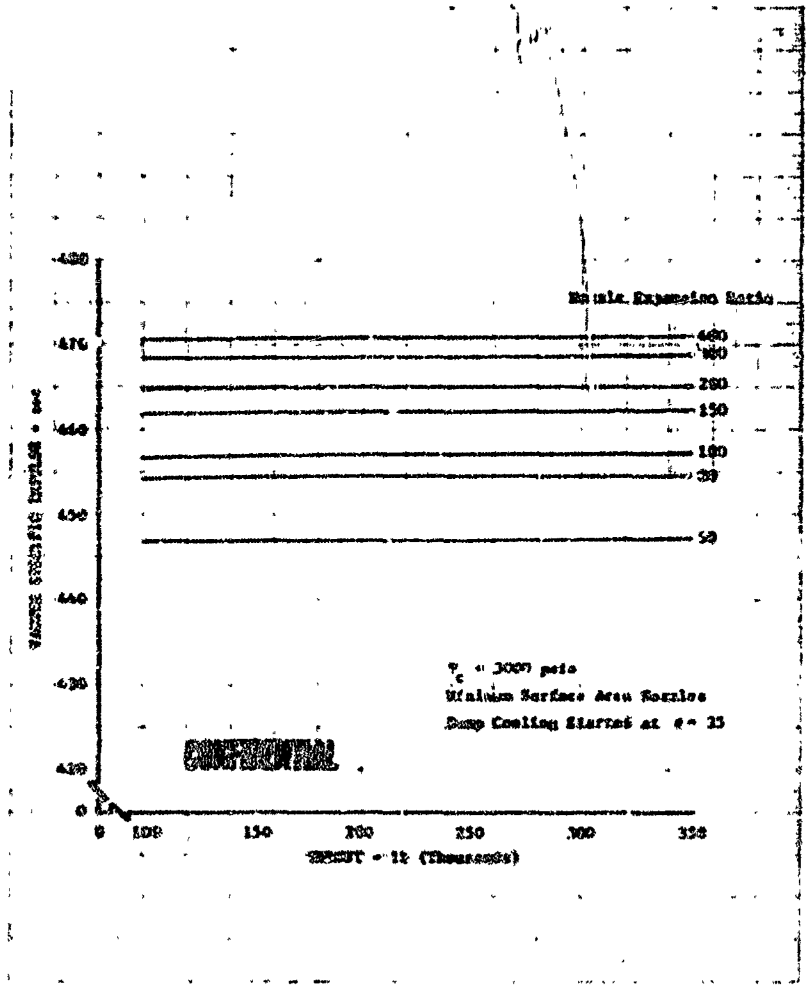

Figure 648. Vacuum Specific Impulse vs Thrust With Minimum Surface Area Contour Two-Position Nozzle (r = 5.0) DF 56289

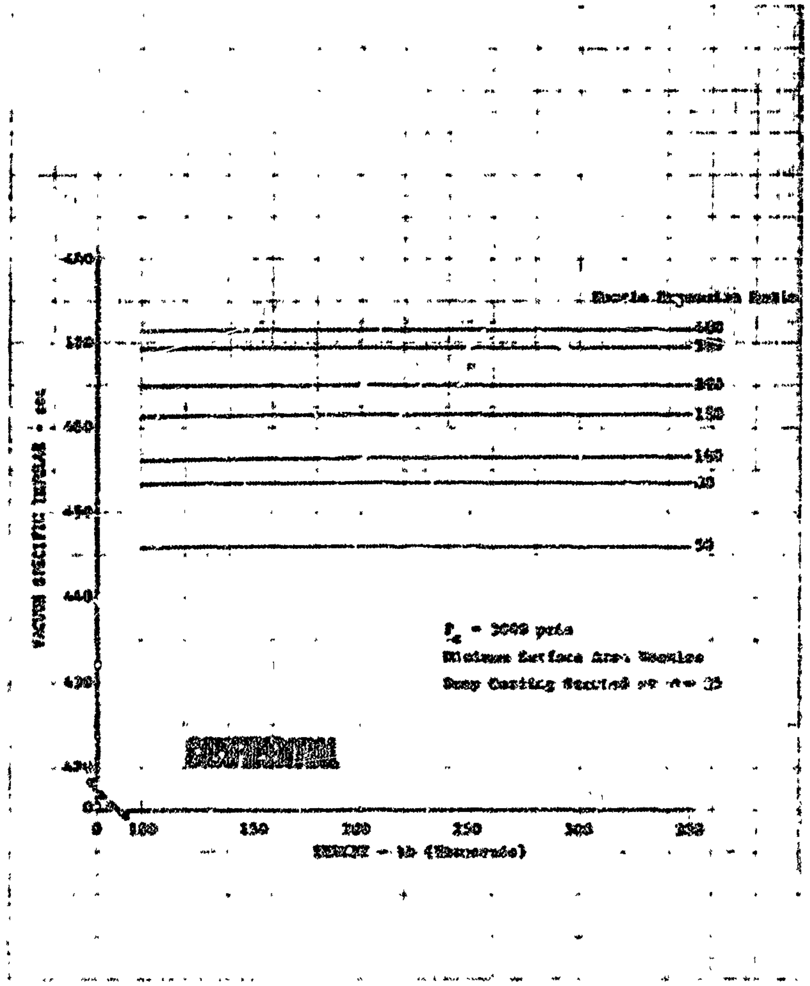

Figure 649. Vacuum Specific Impulse vs Thrust With Minimum Surface Area Contour Two-Position Nozzle (r = 5.5) DF 56290

CONFIDENTIAL

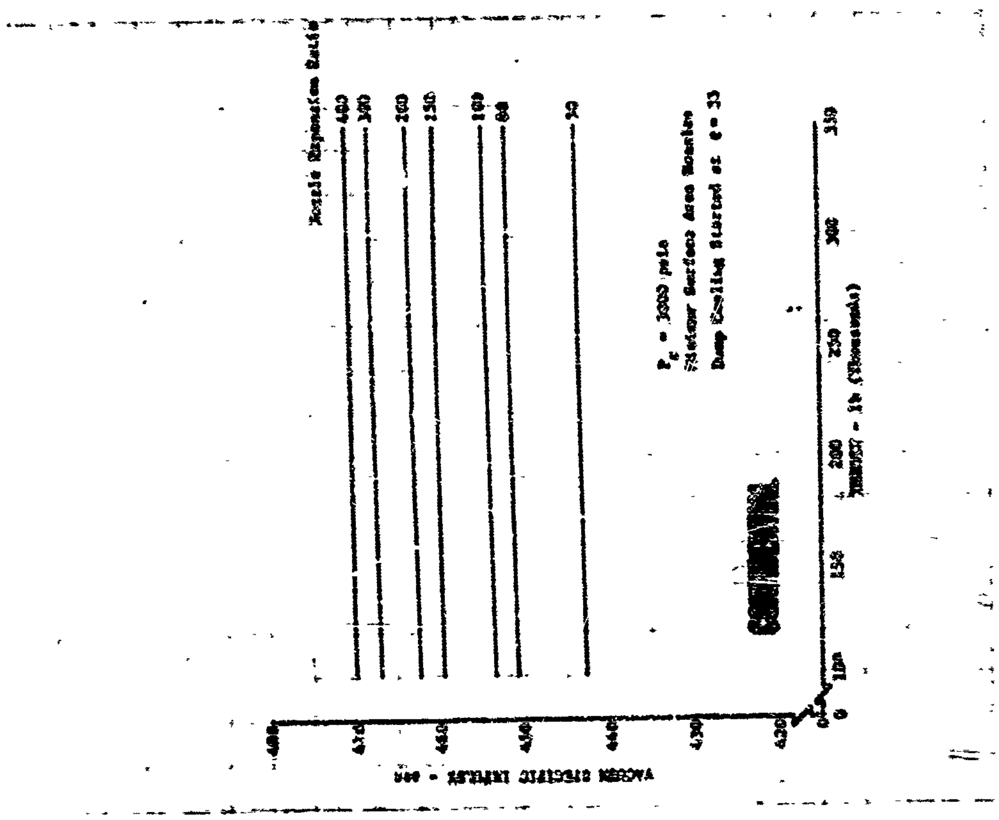

Figure 650. Vacuum Specific Impulse vs Thrust With Minimum Surface Area Contour Two-Position Nozzle (r = 6.0) DF 56291

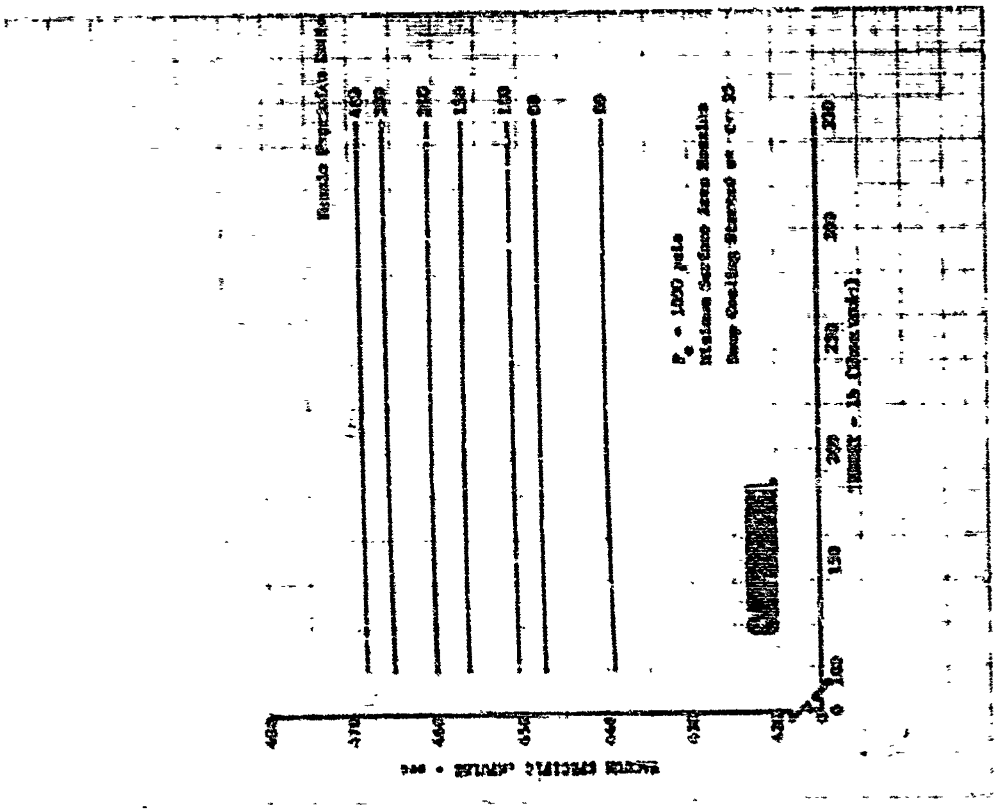

Figure 651. Vacuum Specific Impulse vs Thrust With Minimum Surface Area Contour Two-Position Nozzle (r = 6.5) DF 56297

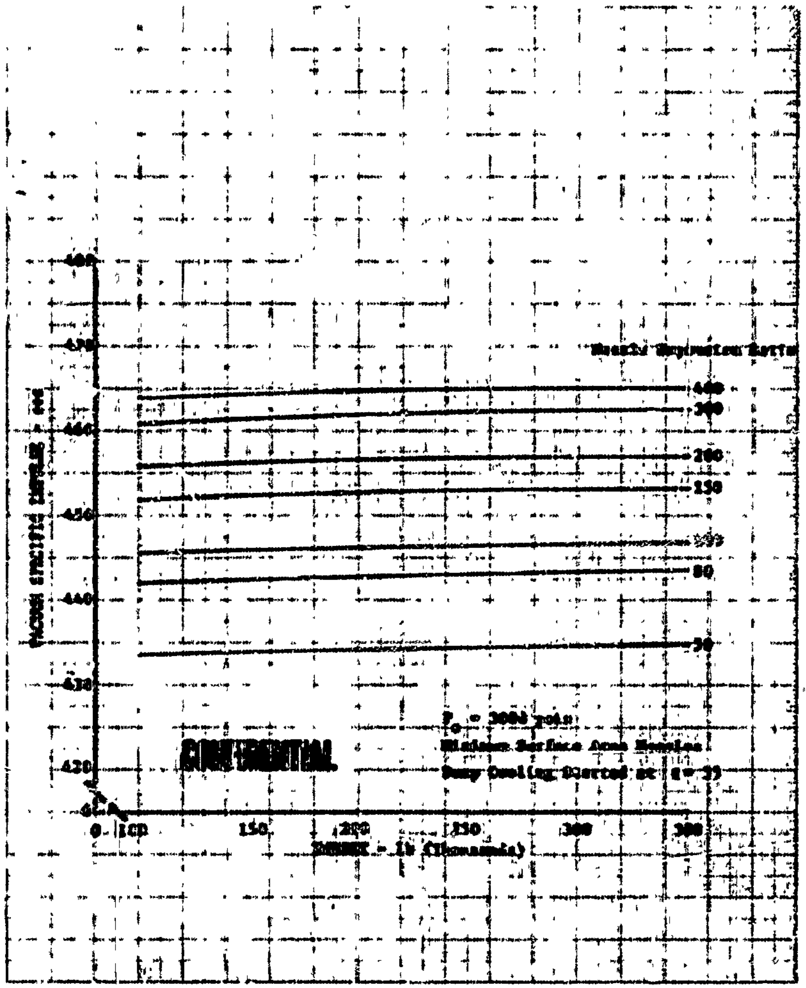

Figure 652. Vacuum Specific Impulse vs Thrust With Minimum Surface Area Contour Two-Position Nozzle (r = 7.0) DF 56293

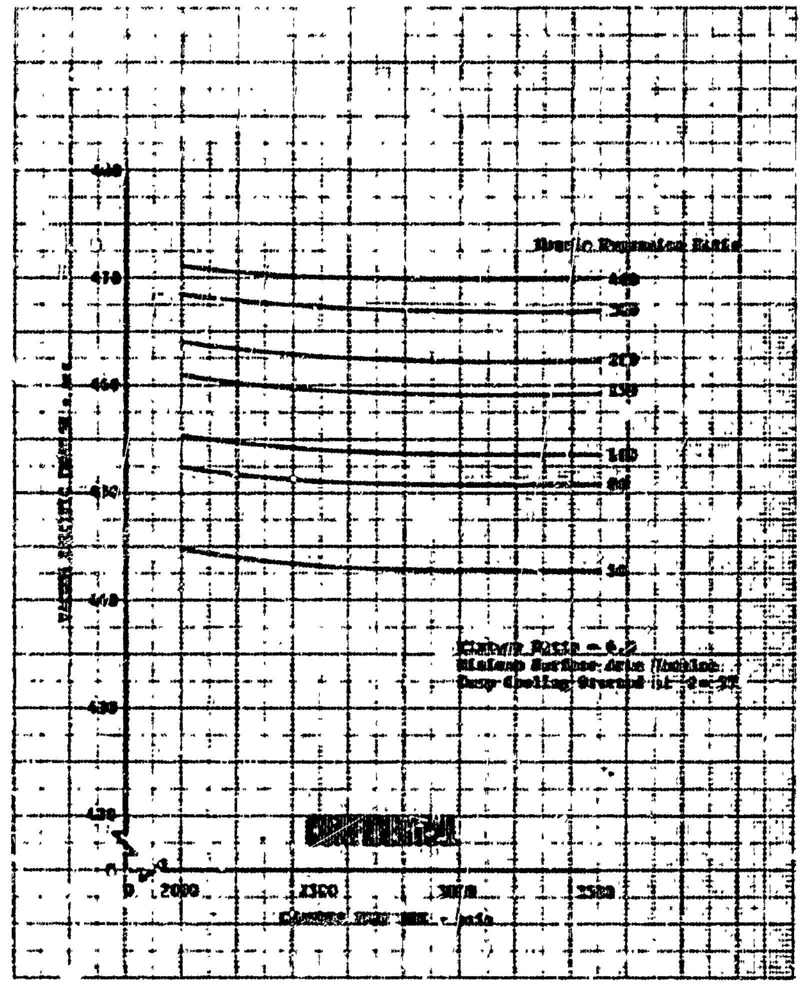

Figure 653. Vacuum Specific Impulse vs Chamber Pressure (100,000-lb Thrust) DF 56224

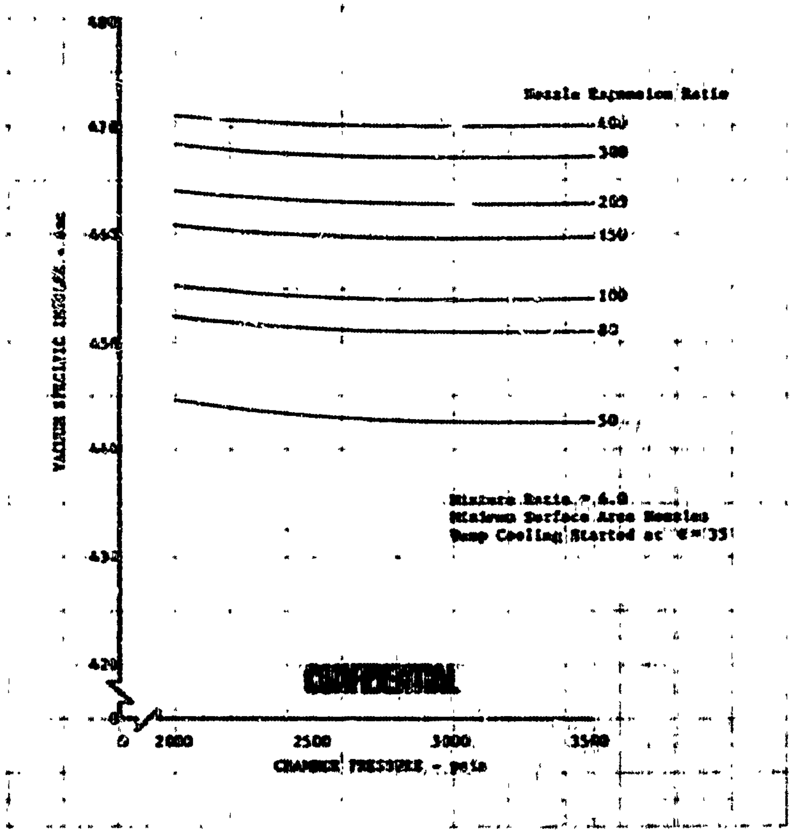

Figure 654. Vacuum Specific Impulse vs Chamber Pressure (150,000-lb Thrust) DF 56223

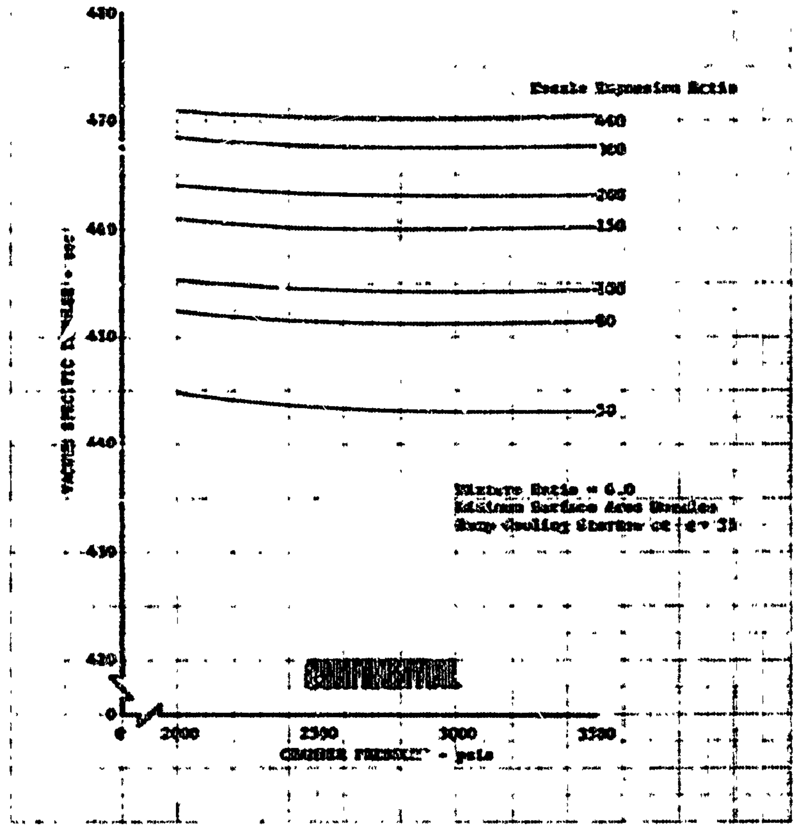

Figure 655. Vacuum Specific Impulse vs Chamber Pressure (200,000-lb Thrust) DF 56222

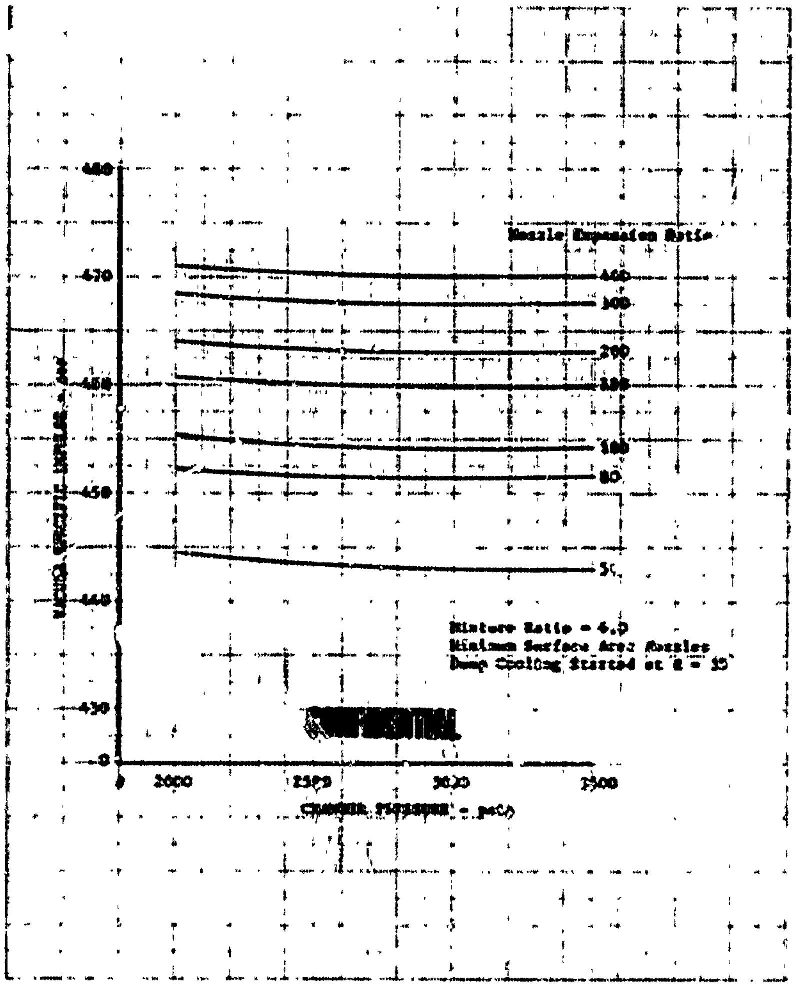

Figure 656. Vacuum Specific Impulse vs Chamber Pressure (250,000-lb Thrust) DF 56221

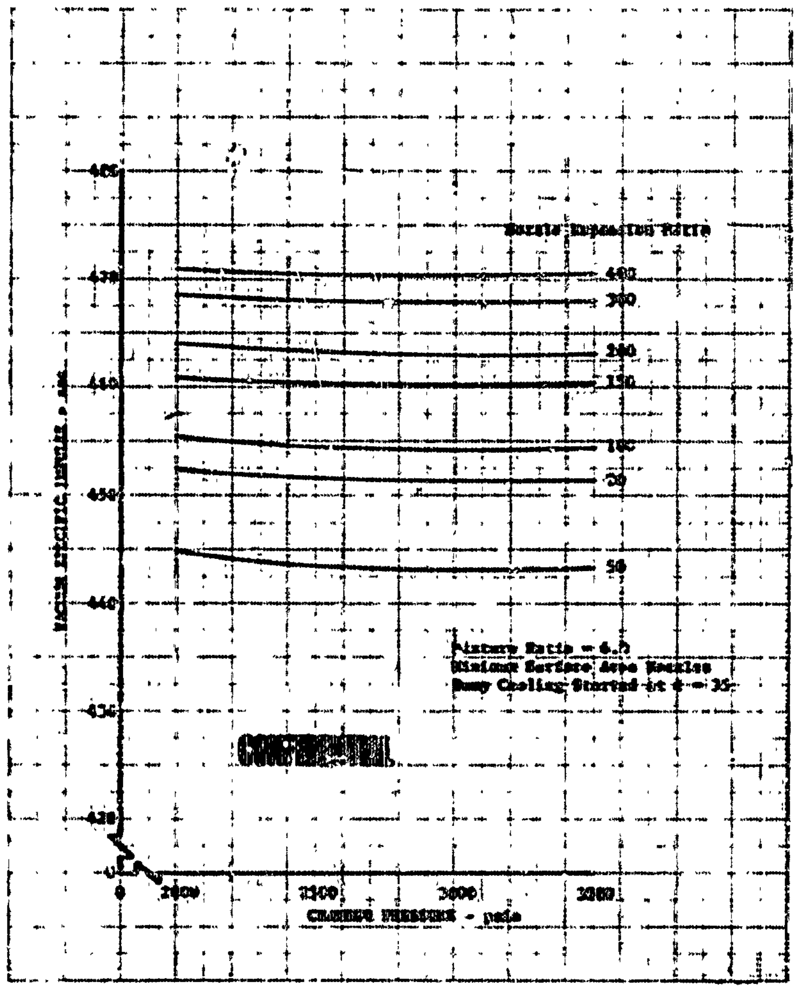

Figure 657. Vacuum Specific Impulse vs Chamber Pressure (300,000-lb Thrust) DF 56220

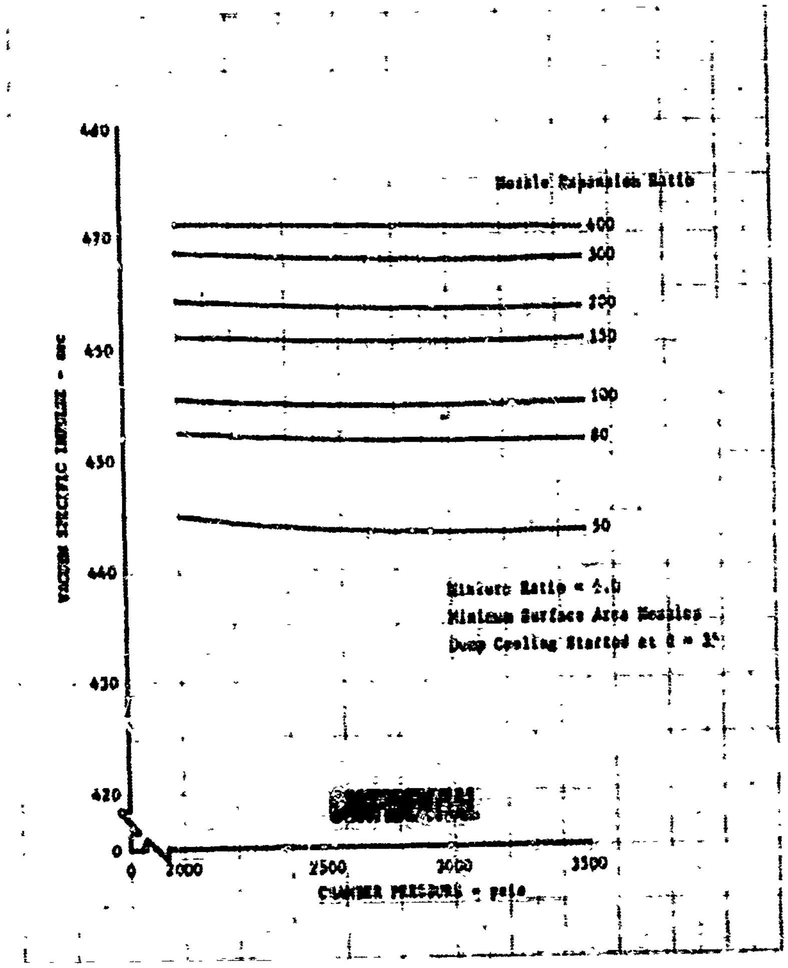

Figure 658. Vacuum Specific Impulse vs Chamber Pressure (350,000-lb Thrust) DF 56279

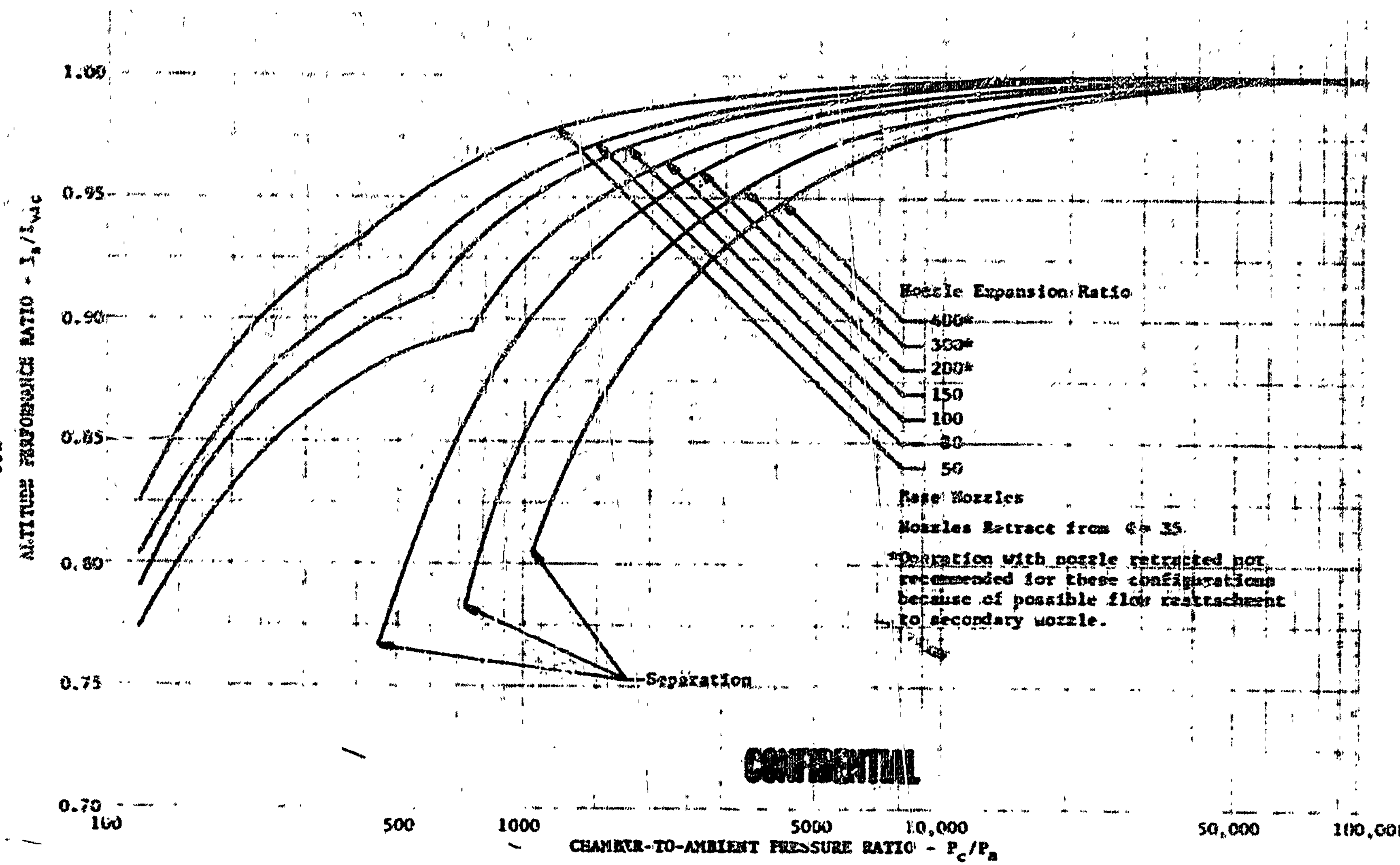

Figure 659. Altitude Performance With Base Contour Two-Position Nozzle (r = 5.0)

DF 56031

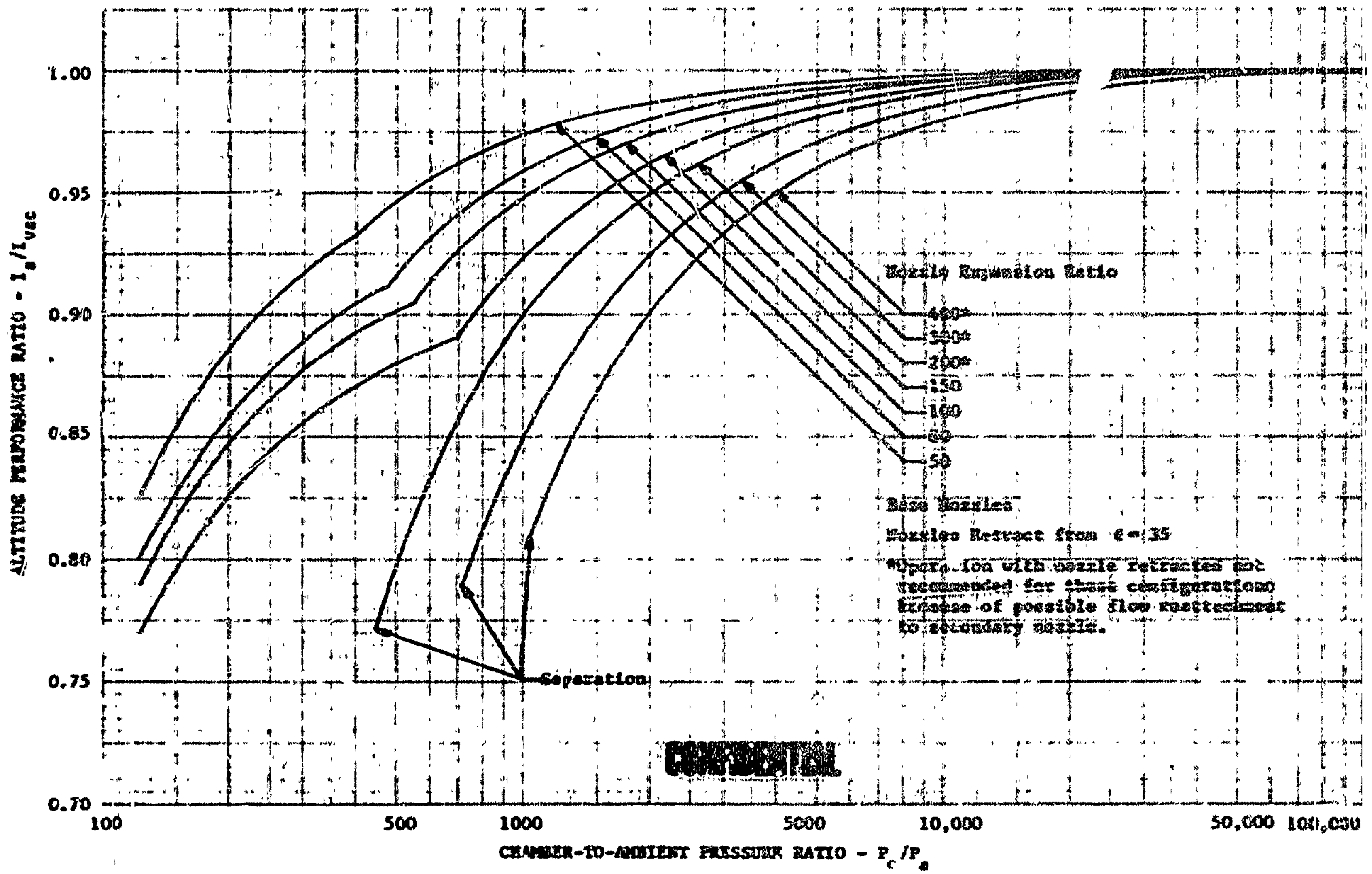

Figure 660. Altitude Performance With Base Contour Two-Position Nozzle (r = 6.0)

DF 56032

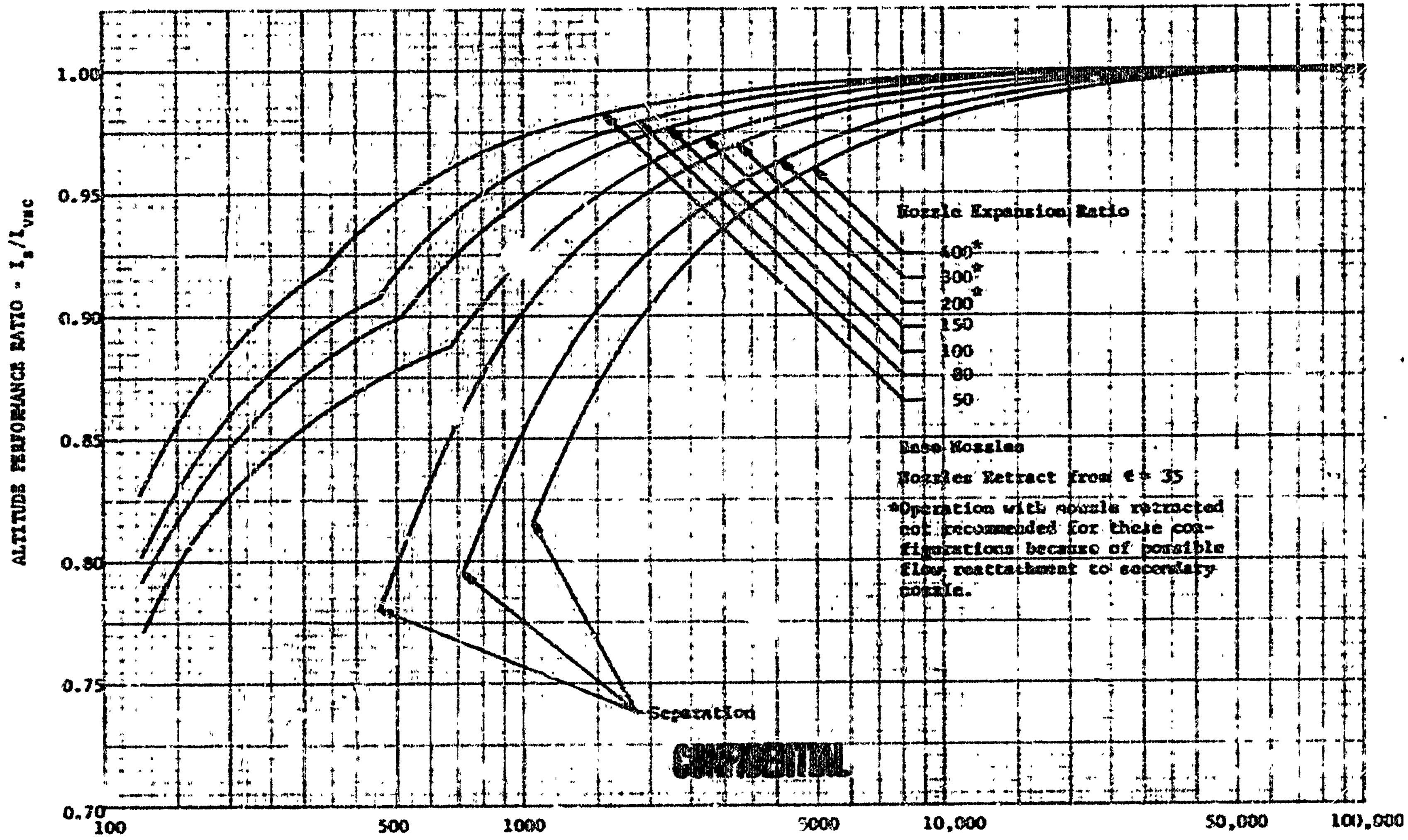

Figure 661. Altitude Performance With Base Contour Two-Position Nozzle (r = 7.0)

DF 56033

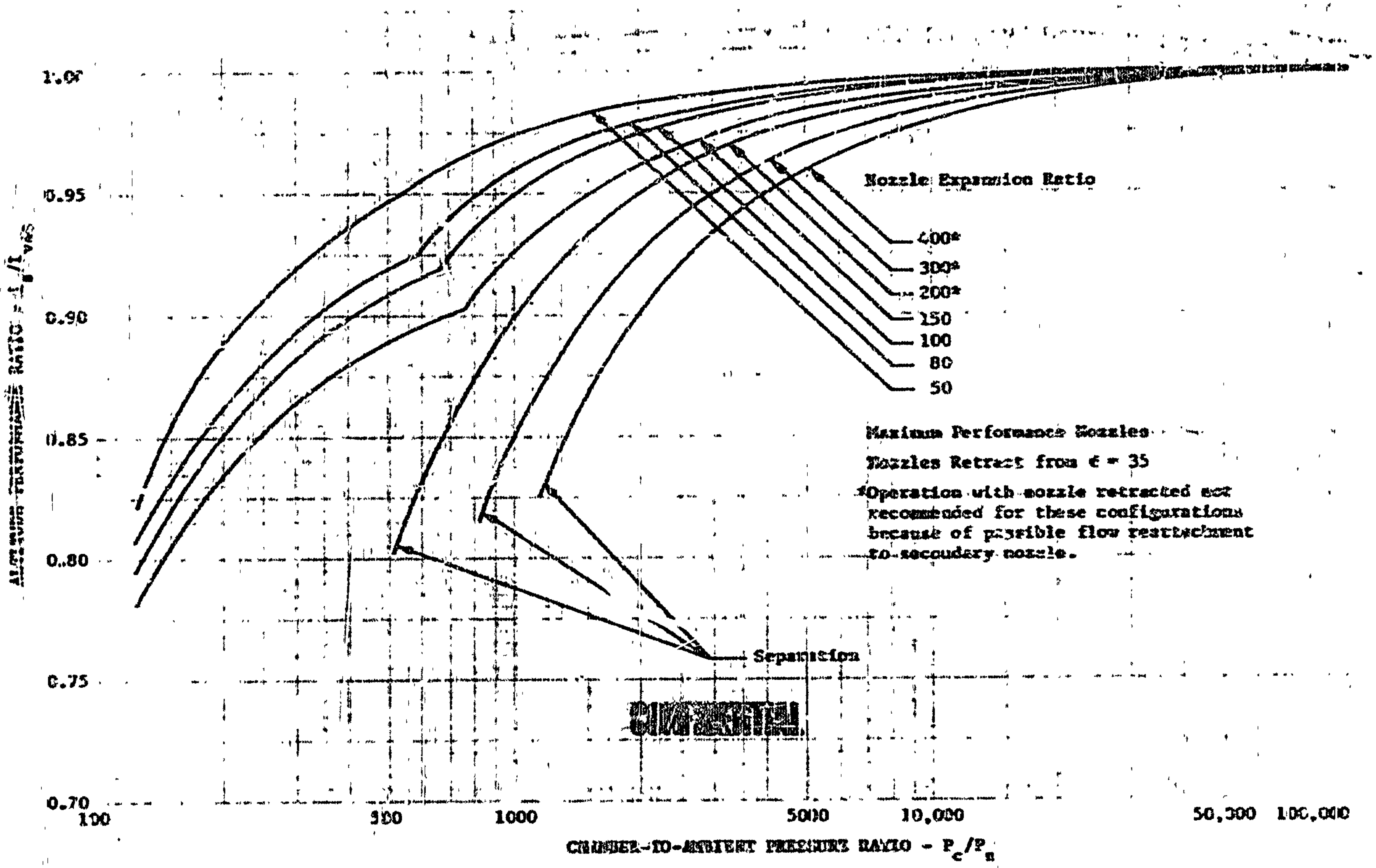

Figure 662. Altitude Performance With Maximum Performance Contour Two-Position Nozzle (r = 5.0) DF 56028

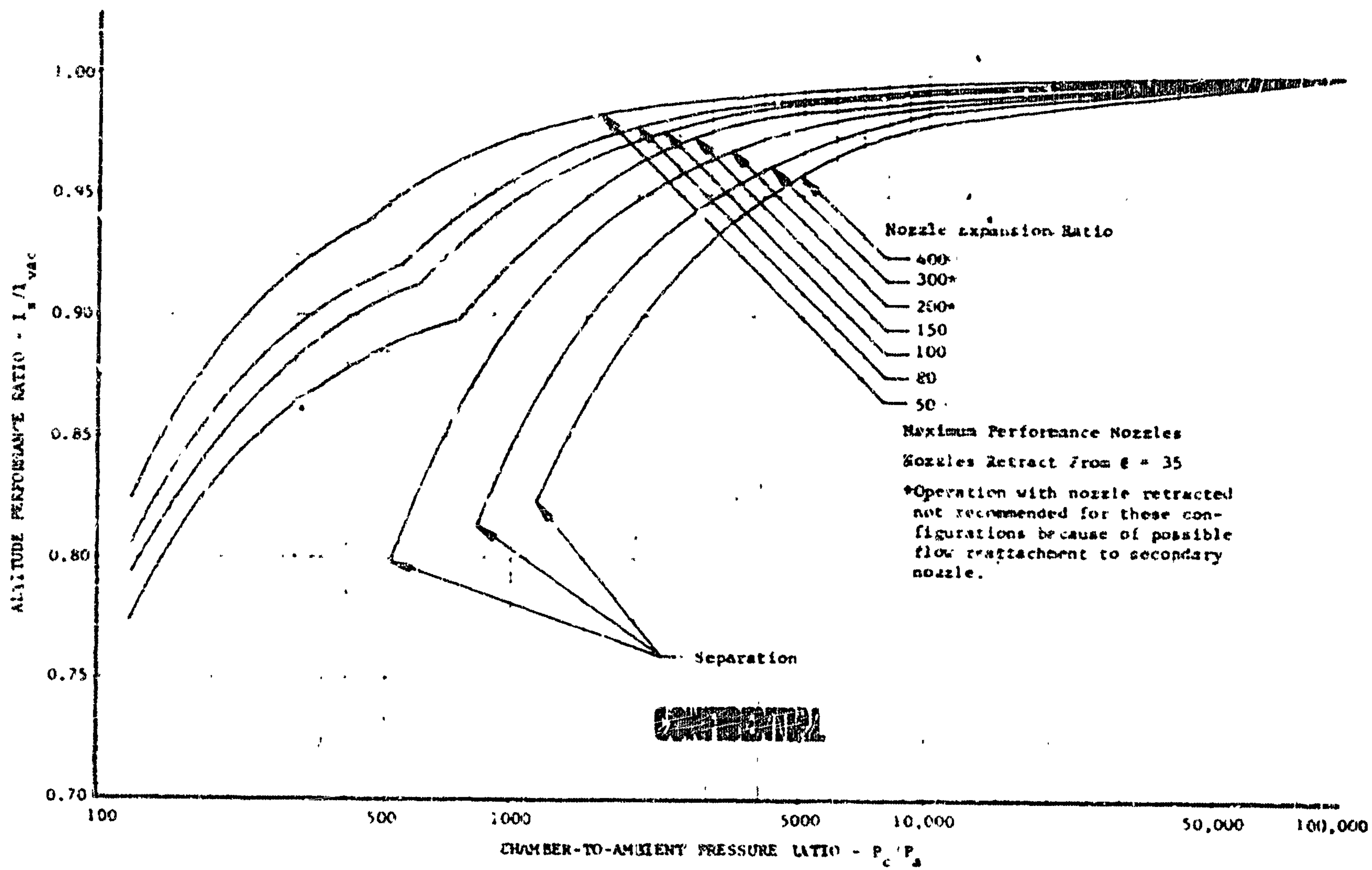

Figure 663. Altitude Performance With Maximum Performance Contour Two-Position Nozzle (r = 6.0) DF 56029

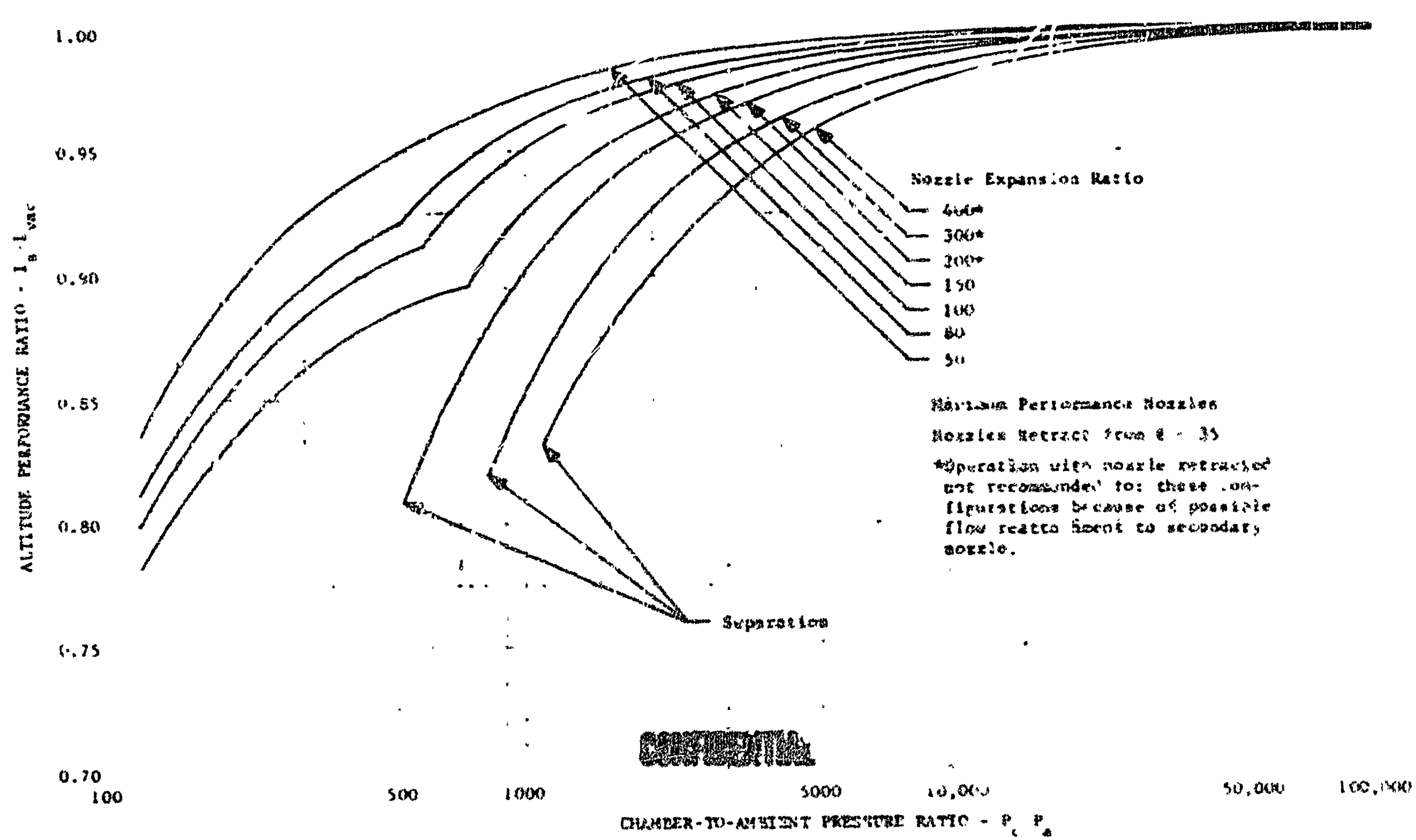

Figure 664. Altitude Performance With Maximum Performance Contour Two-Position Nozzle (r = 7.0) DF 56030

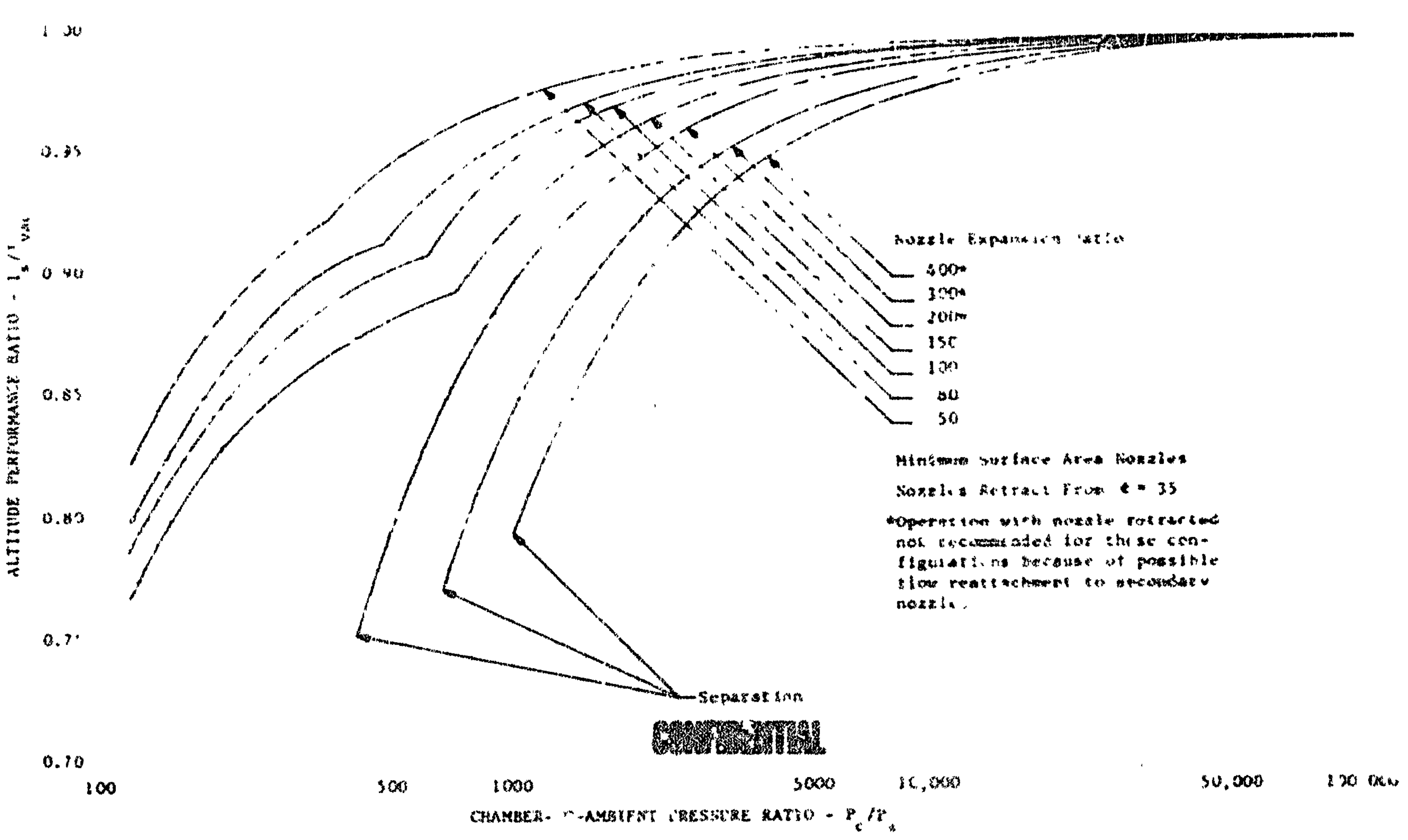

Figure 665. Altitude Performance With Minimum Surface Area Contour Two-Position Nozzle (r = 5.0) DF 56034

CONFIDENTIAL

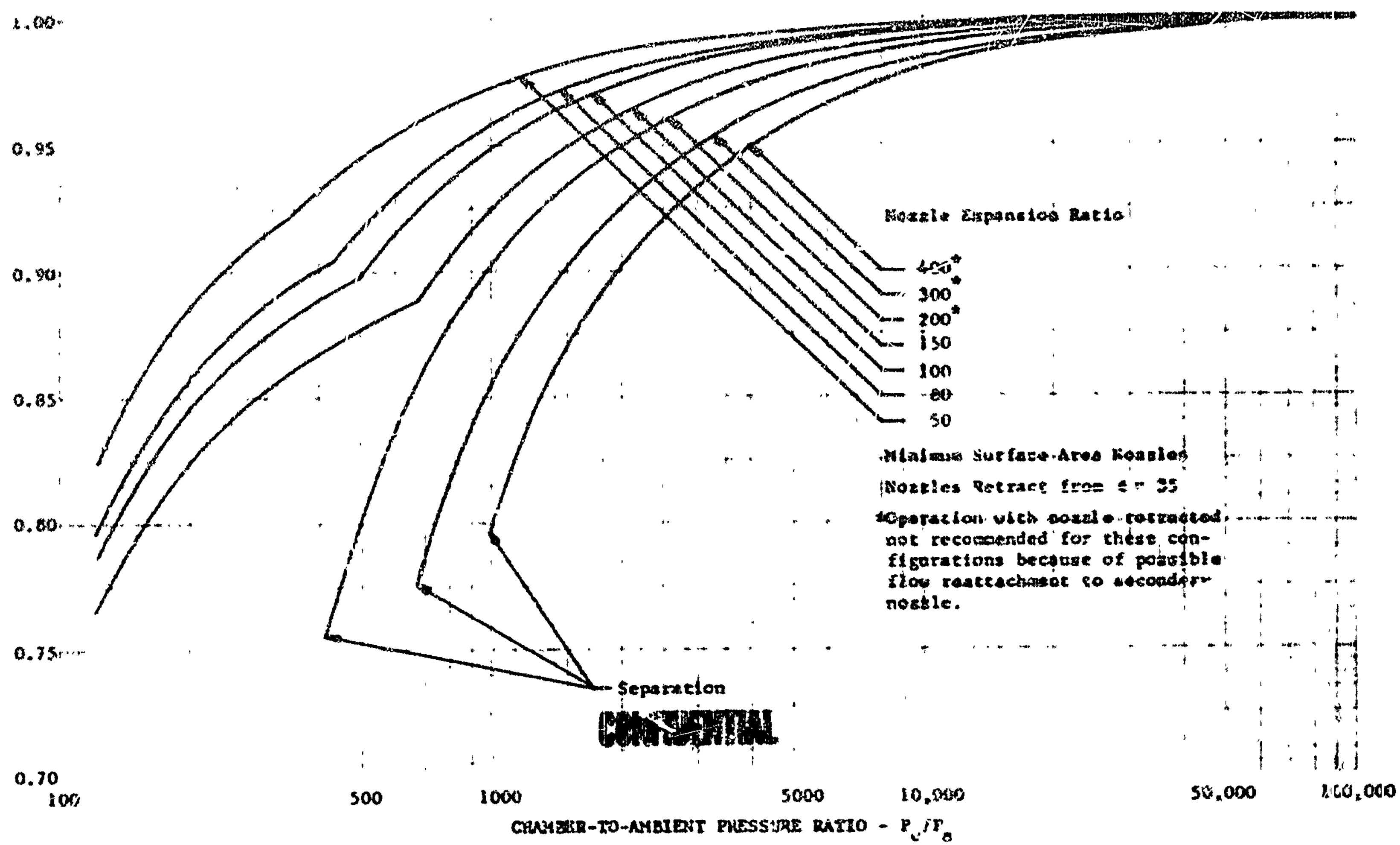

Figure 666. Altitude Performance With Minimum Surface Area Contour Two-Position Nozzle (r = 6.0) DF 56035

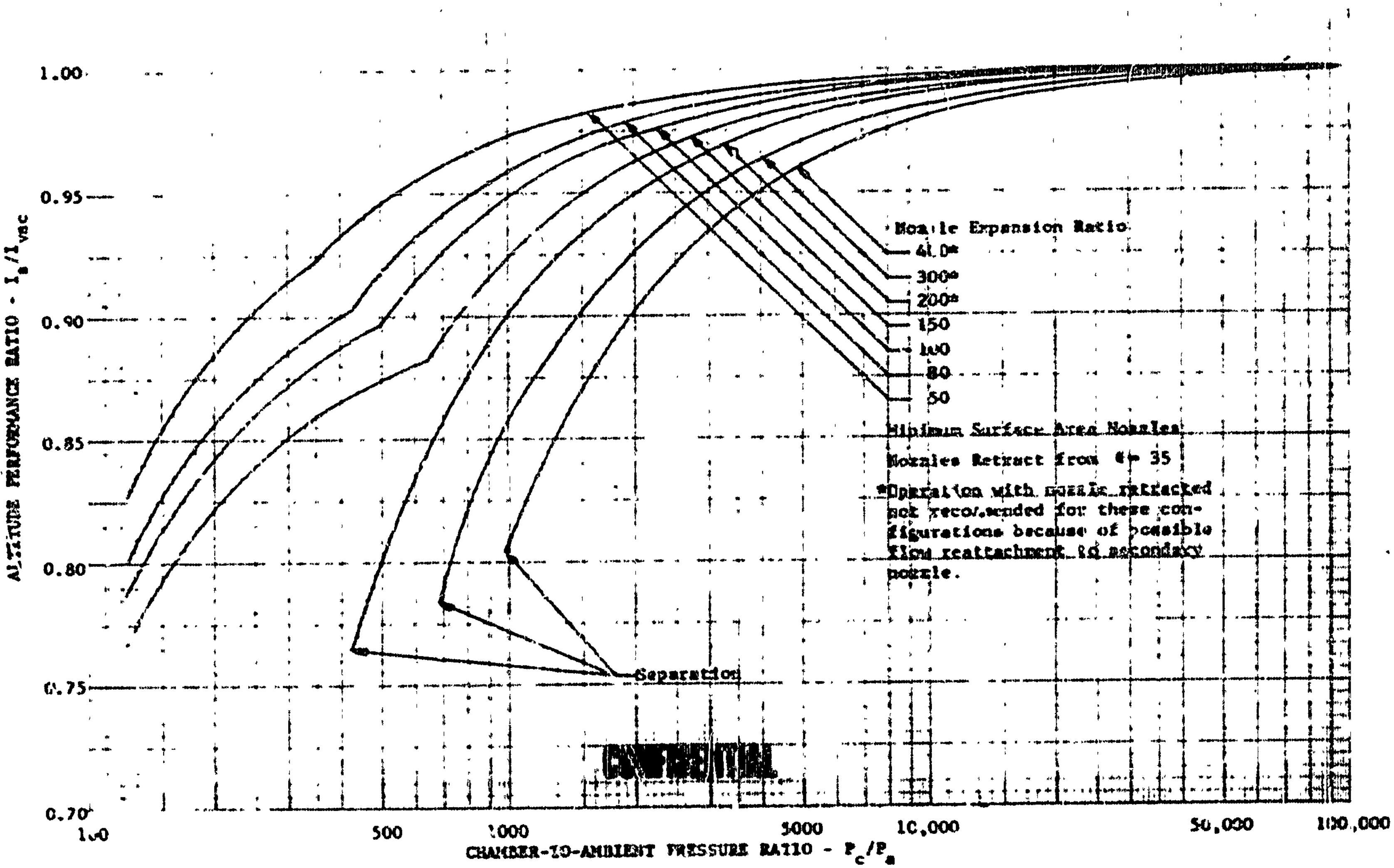

Figure 667. Altitude Performance With Minimum Surface Area Contour Two-Position Nozzle (r = 7.0) DF 56036

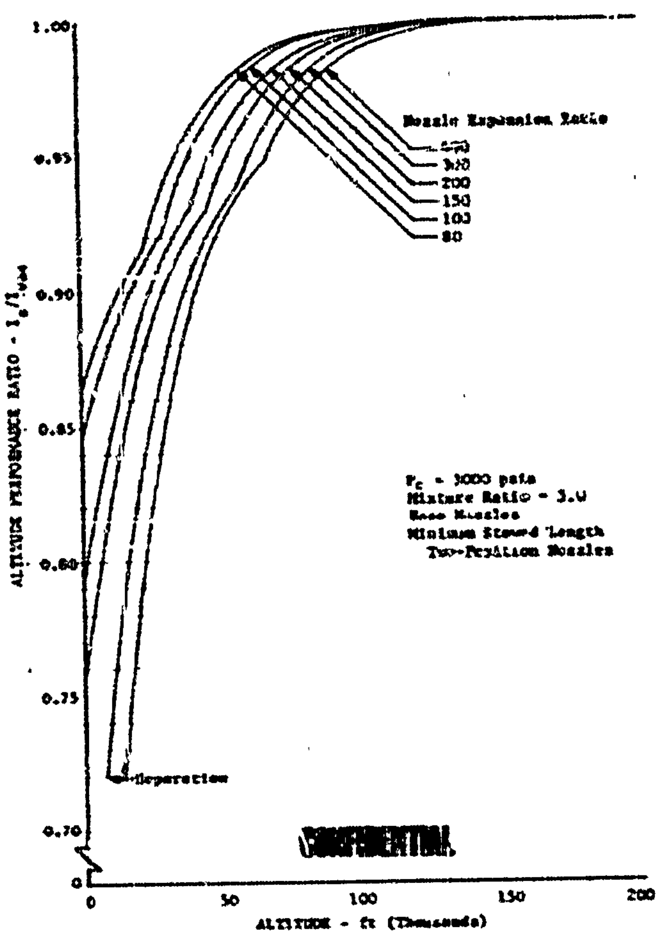

Figure 668. Altitude Performance With Base Contour Nozzle, 100,000-lb Thrust, r = 5.0 DF 56172

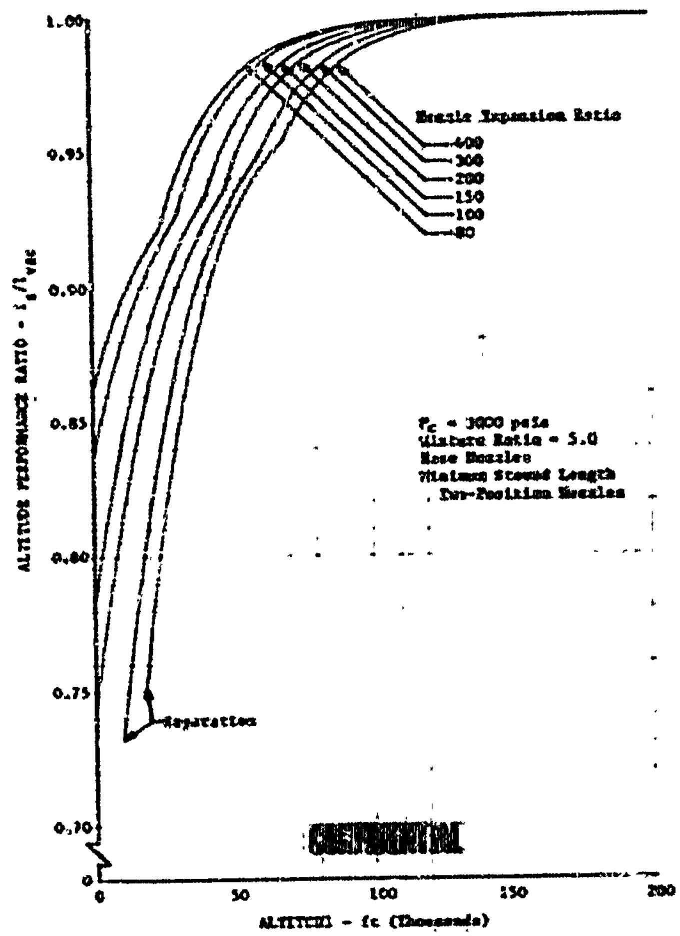

Figure 669. Altitude Performance With Base Contour Nozzle, 250,000-lb Thrust, r = 5.0 DF 56171

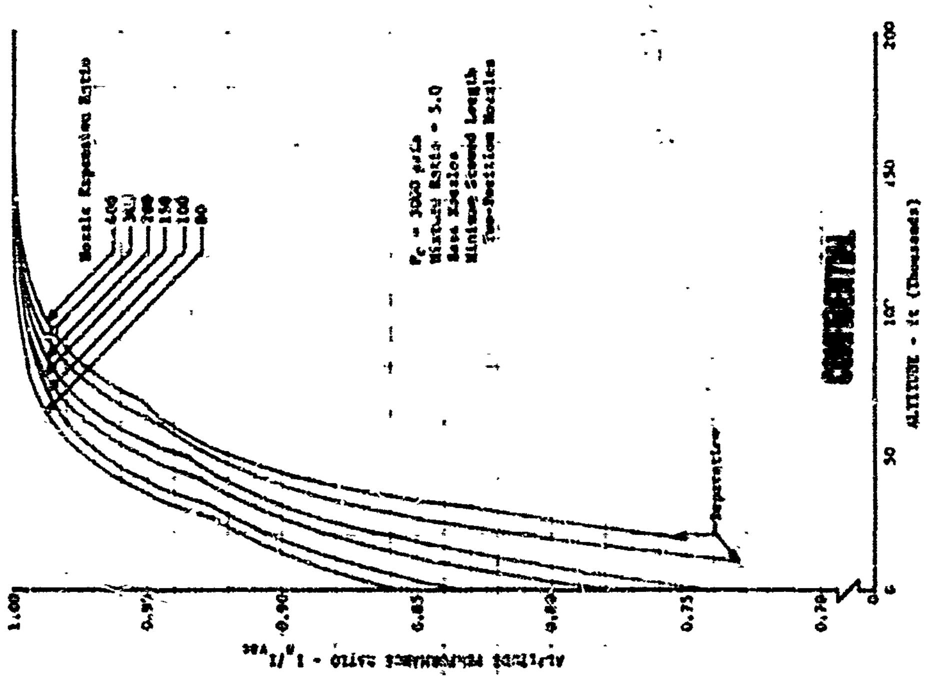

Figure 670. Altitude Performance With Base Contour Nozzle, 350,000-lb Thrust, r = 5.0 DF 56170

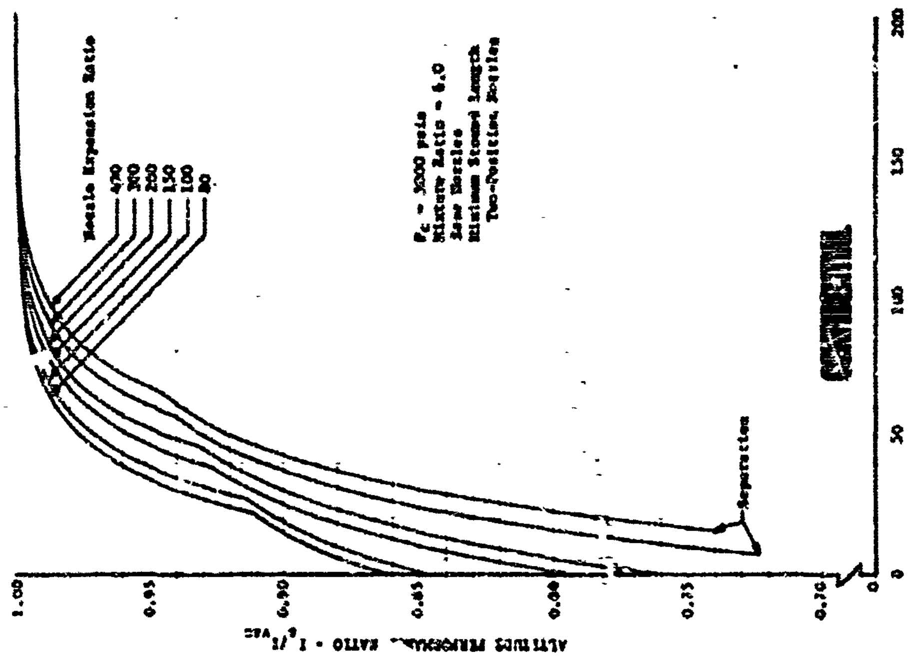

Figure 671. Altitude Performance With Base Contour Nozzle, 100,000-lb Thrust, r = 6.0 DF 56169

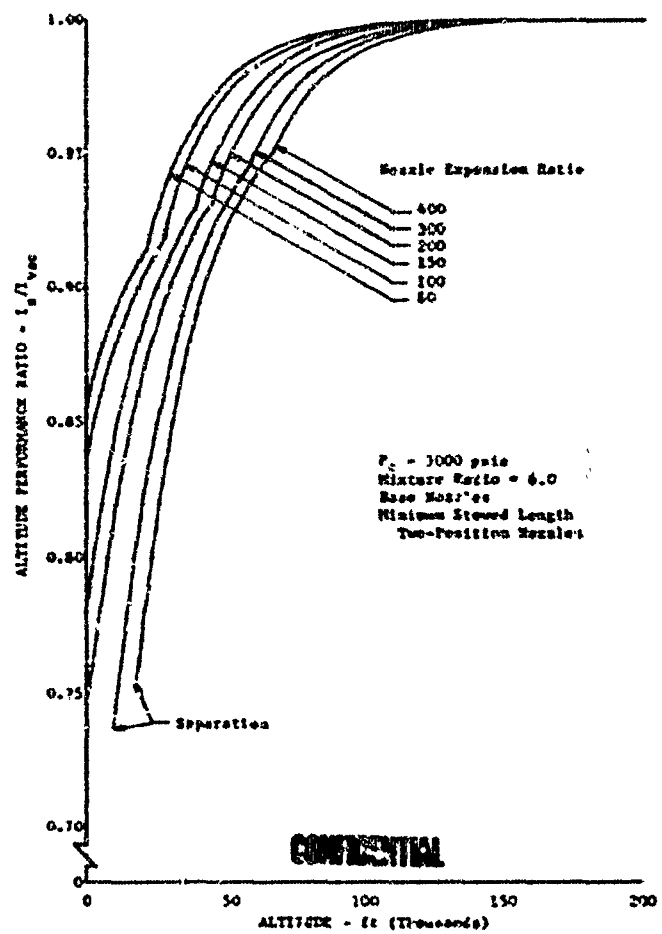

Figure 672. Altitude Performance With Base Contour Nozzle, 250,000-lb Thrust, r = 6.0 DF 56168

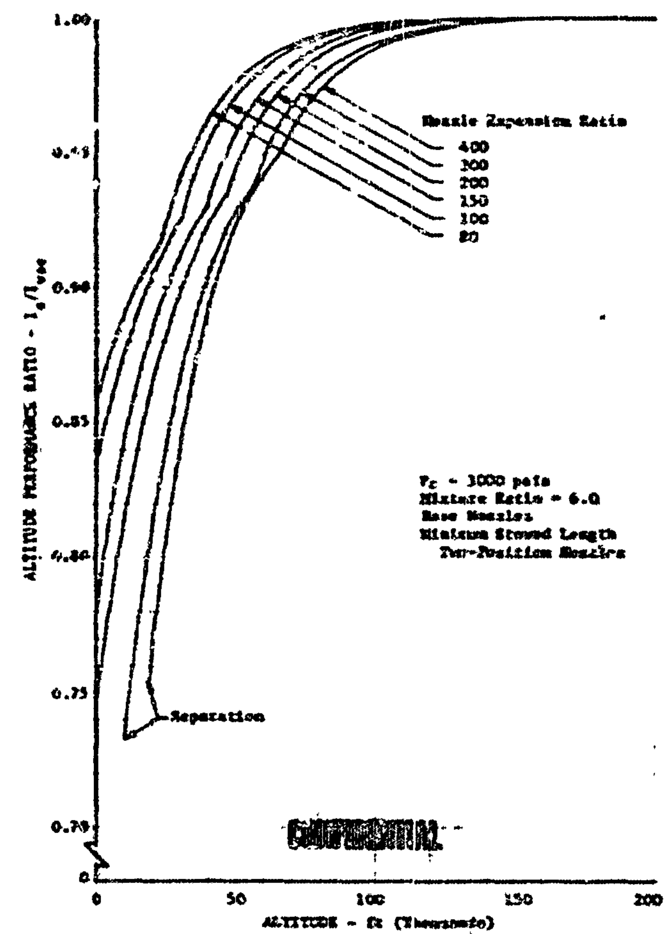

Figure 673. Altitude Performance With Base Contour Nozzle, 350,000-lb Thrust, r = 6.0 DF 56167

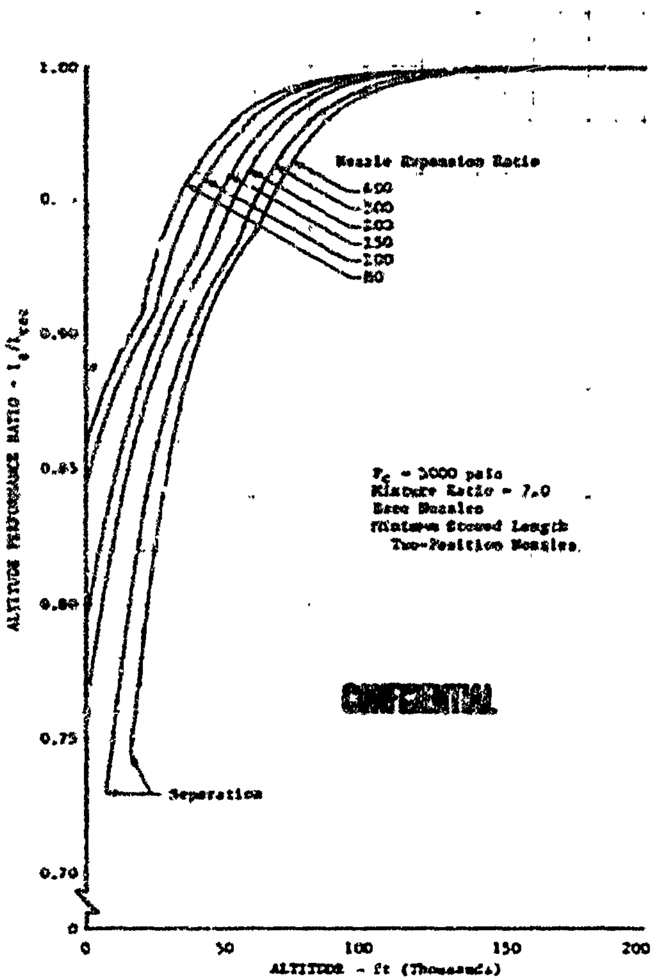

Figure 674. Altitude Performance With Base Contour Nozzle, 100,000-lb Thrust, r = 7.0 DF 56184

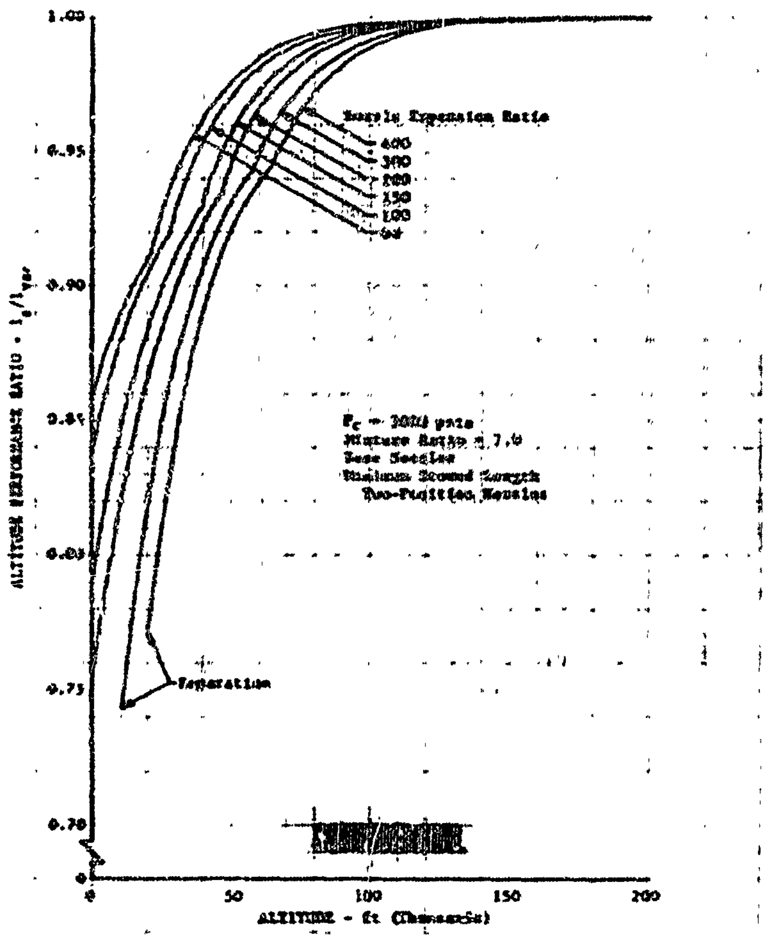

Figure 675. Altitude Performance With Base Contour Nozzle, 250,000-lb Thrust, r = 7.0 DF 56183

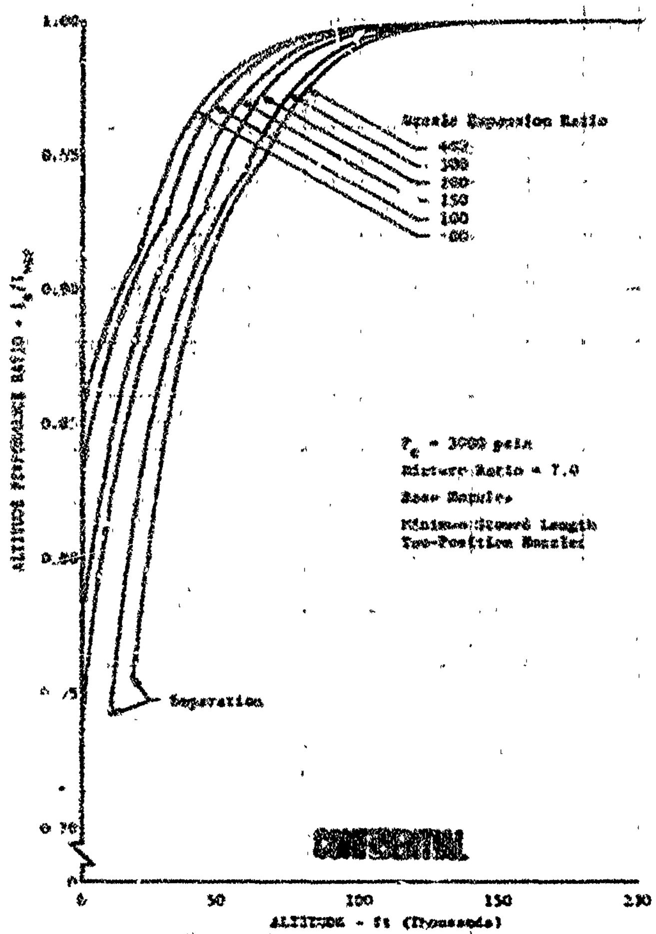

Figure 676. Altitude Performance With Base Contour Nozzle, 350,000-lb Thrust, r = 7.0 DF 56182

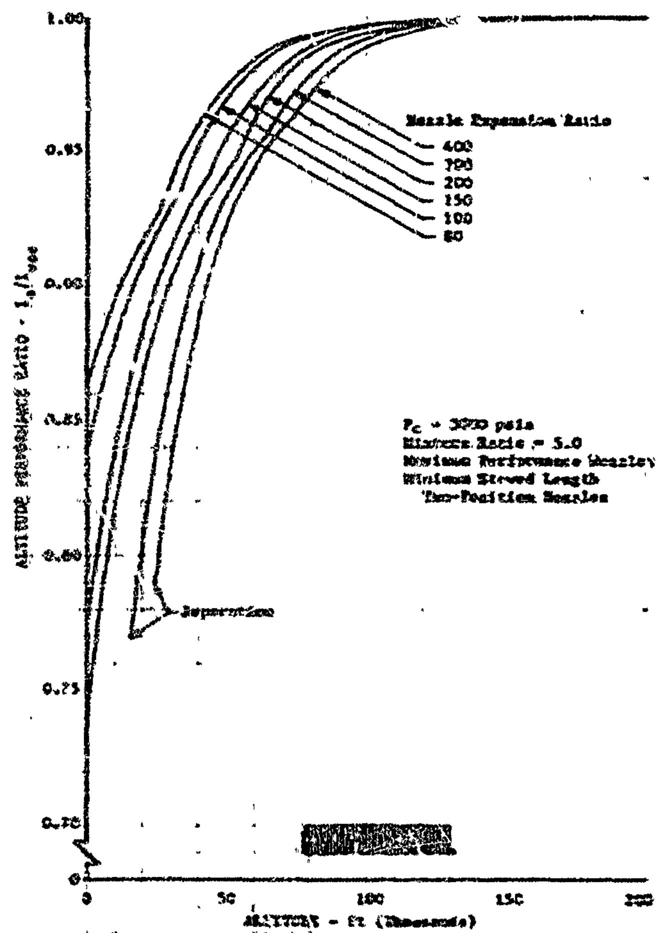

Figure 677. Altitude Performance With Maximum Performance Contour Nozzle, 100,000-lb Thrust, r = 5.0 DF 56181

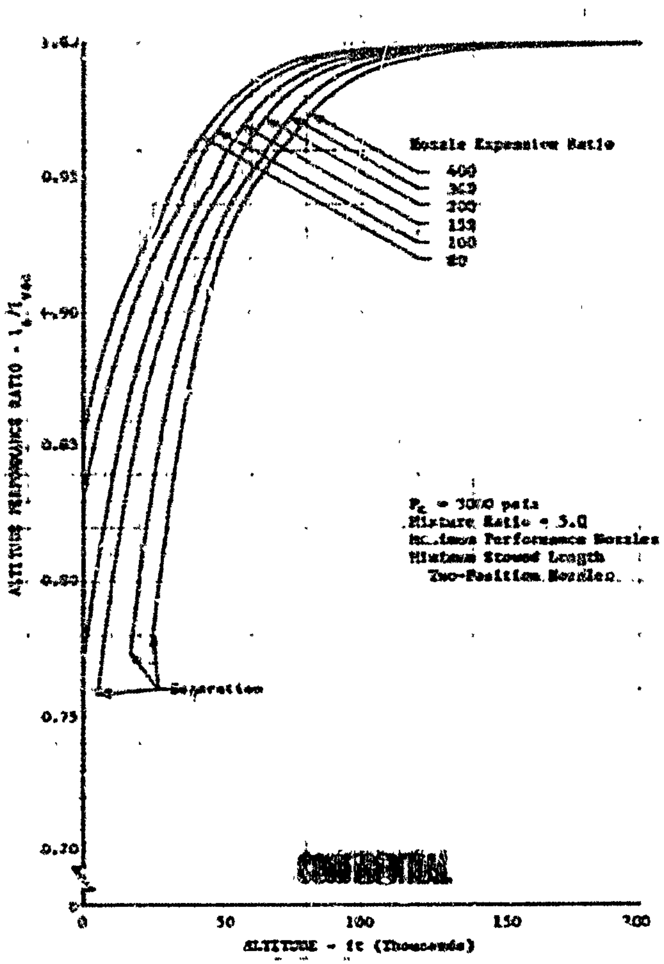

Figure 678. Altitude Performance With Maximum Performance Contour Nozzle, 250,000-lb Thrust, r = 5.0

DF 56180

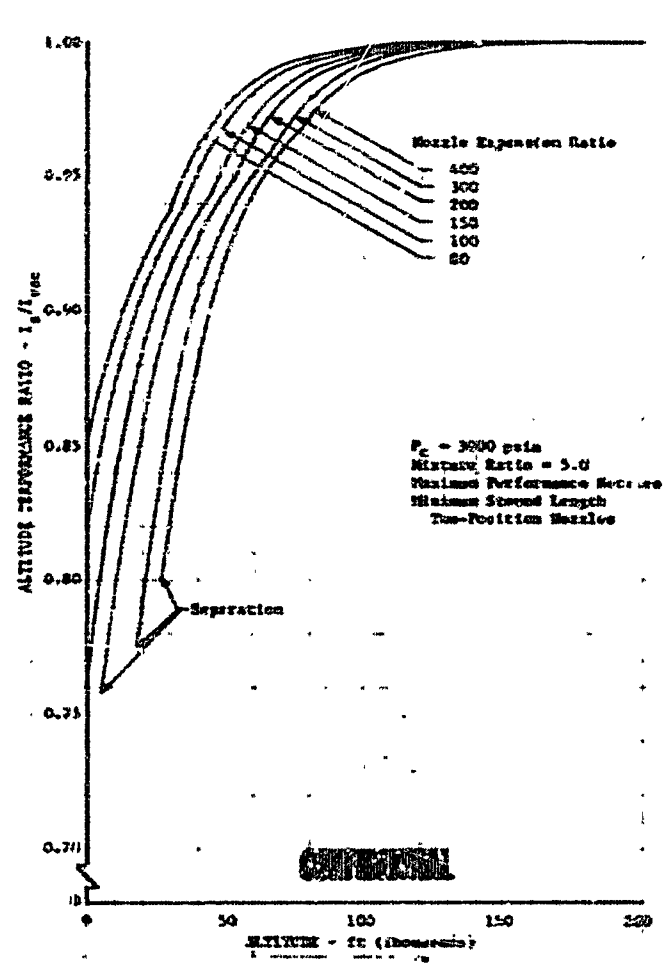

Figure 679. Altitude Performance With Maximum Performance Contour Nozzle, 350,000-lb Thrust, r = 5.0

DF 56179

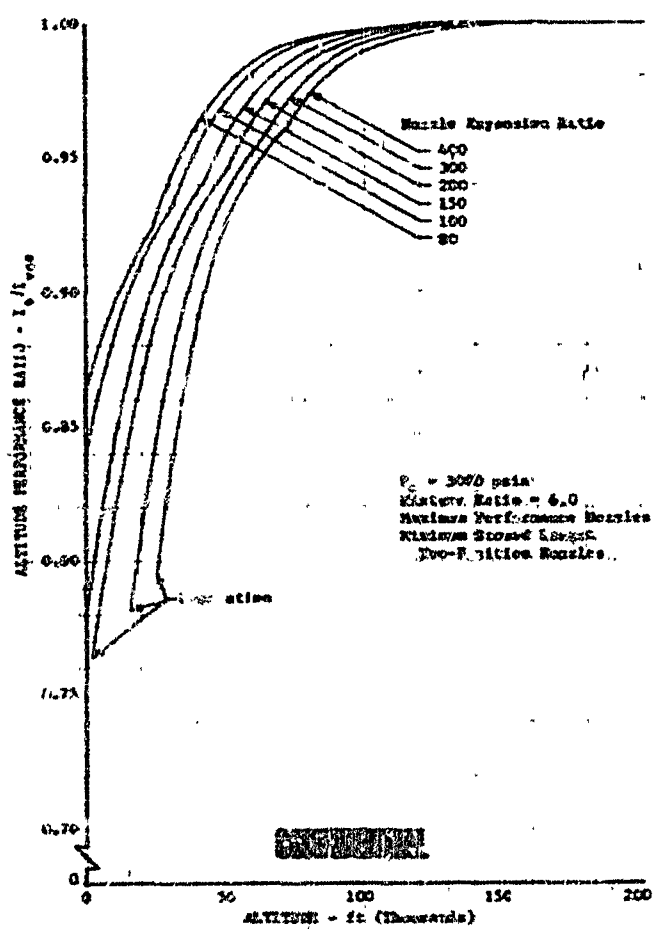

Figure 680. Altitude Performance With Maximum Performance Contour Nozzle, 100,000-lb Thrust, r = 6.0 DF 56178

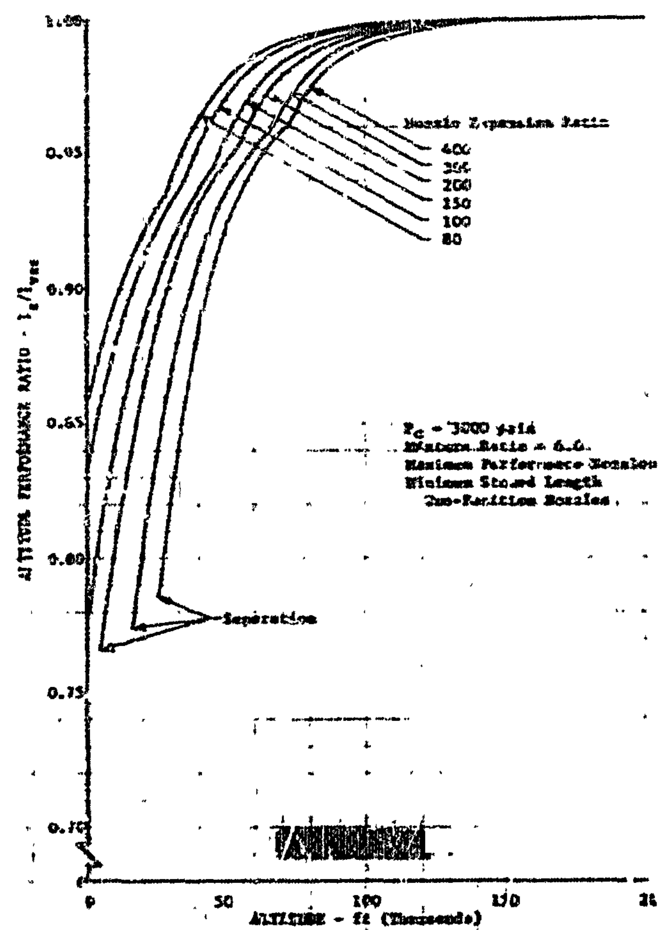

Figure 681. Altitude Performance With Maximum Performance Contour Nozzle, 250,000-lb Thrust, r = 6.0 DF 56177

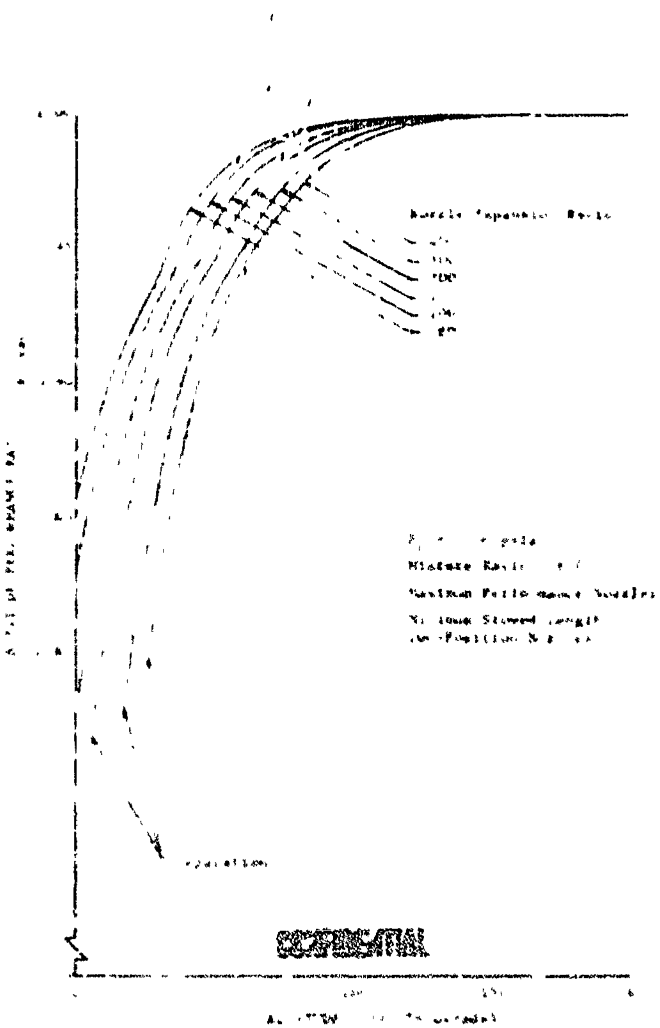

Figure 682. Altitude Performance With Maximum Performance Contour Nozzle, 350,000-lb Thrust, r = 6.0 DF 56176

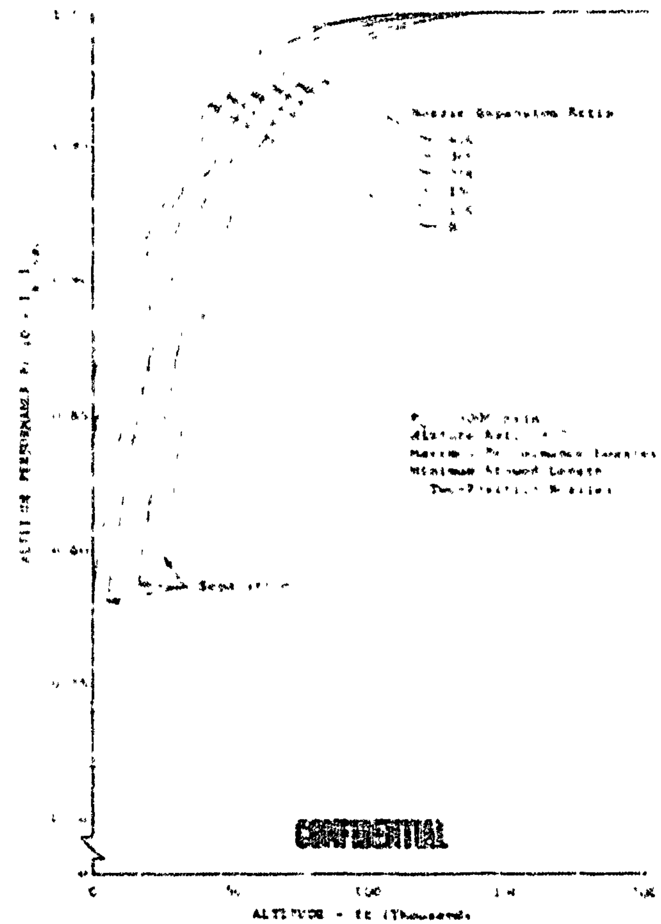

Figure 683. Altitude Performance With Maximum Performance Contour Nozzle, 400,000-lb Thrust, r = 7.0 DF 56175

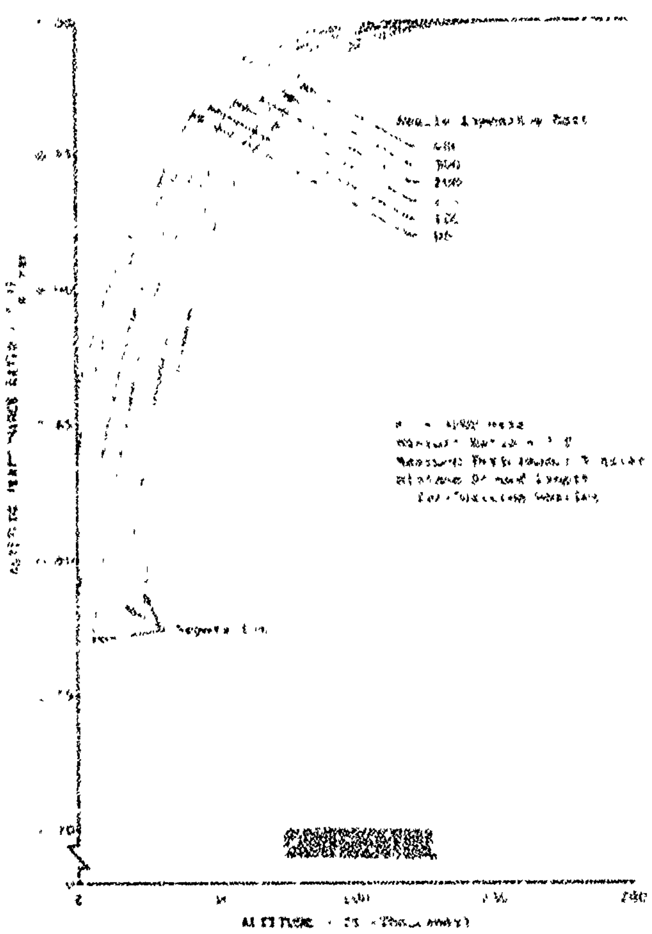

Figure 684. Altitude Performance With Maximum Performance Contour Nozzle, 250,000-lb Thrust, r = 7.0 DF 56174

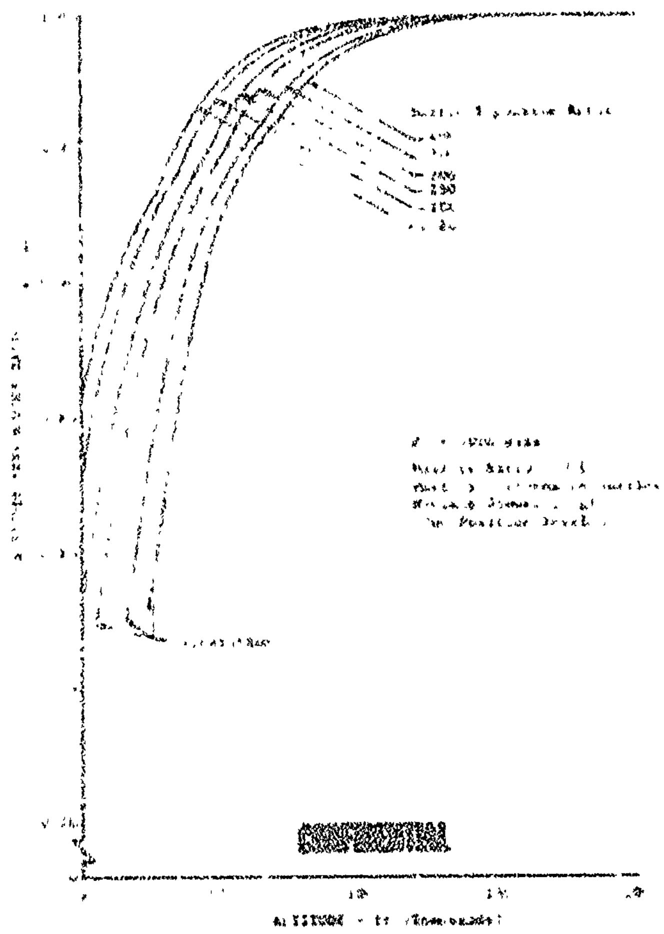

Figure 685. Altitude Performance With Maximum Performance Contour Nozzle, 300,000-lb Thrust, r = 7.0 DF 5617?

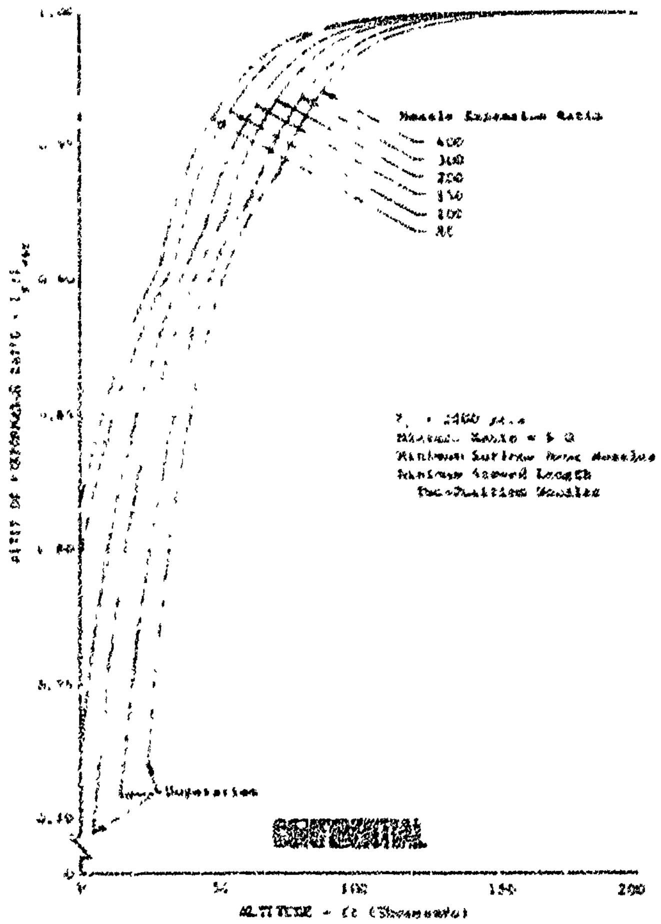

Figure 686. Altitude Performance With Minimum Surface Area Contour Nozzle, 100,000-lb Thrust, r = 6.0, P_c = 2000 psia DF 56189

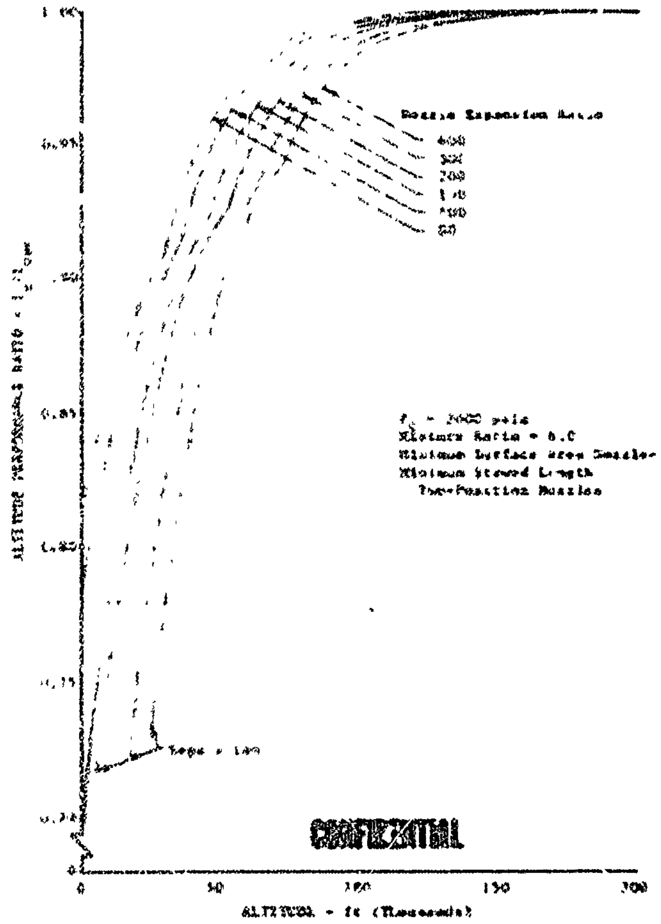

Figure 687. Altitude Performance With Minimum Surface Area Contour Nozzle, 250,000-lb Thrust, r = 6.0, P_c = 2000 psia DF 56190

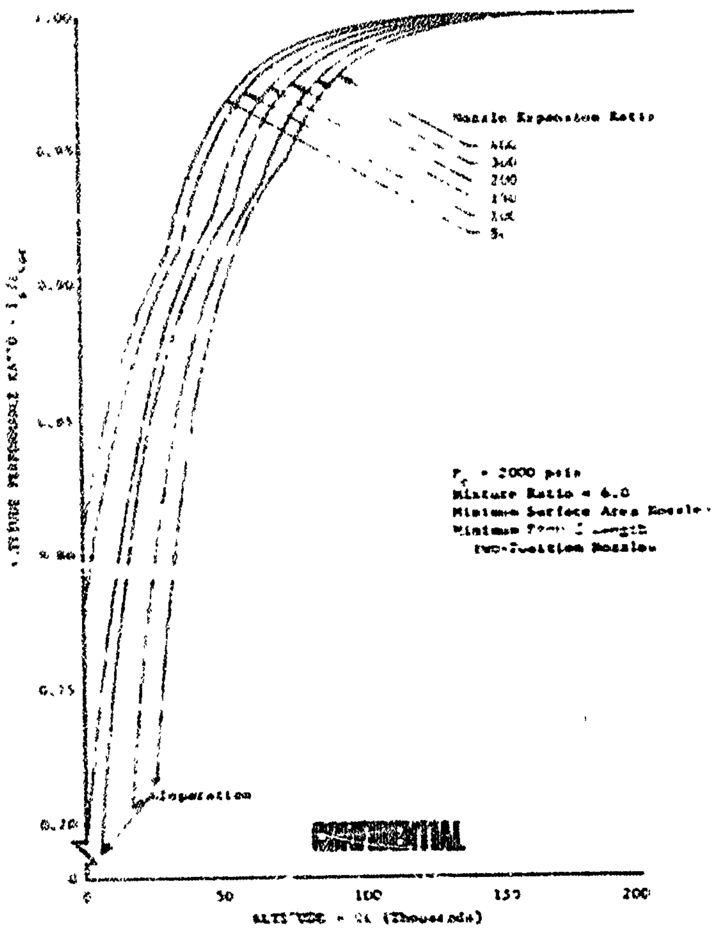

Figure 688. Altitude Performance With Minimum Surface Area Contour Nozzle, 350,000-lb Thrust, r = 6.0, P_c = 2000 psia DF 56191

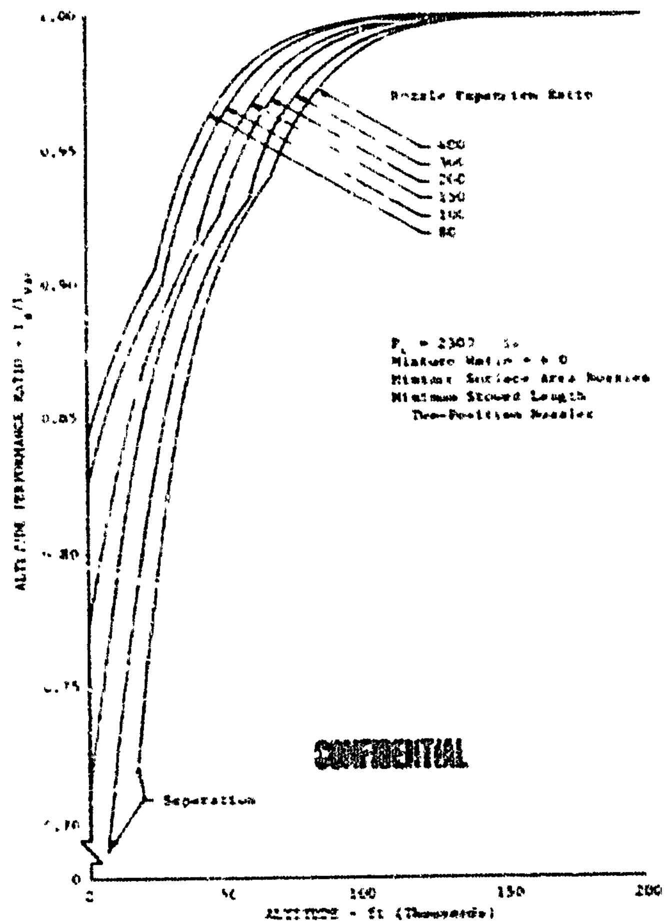

Figure 689. Altitude Performance With Minimum Surface Area Contour Nozzle, 100,000-lb Thrust, r = 6.0, P_c = 2500 psia DF 56192

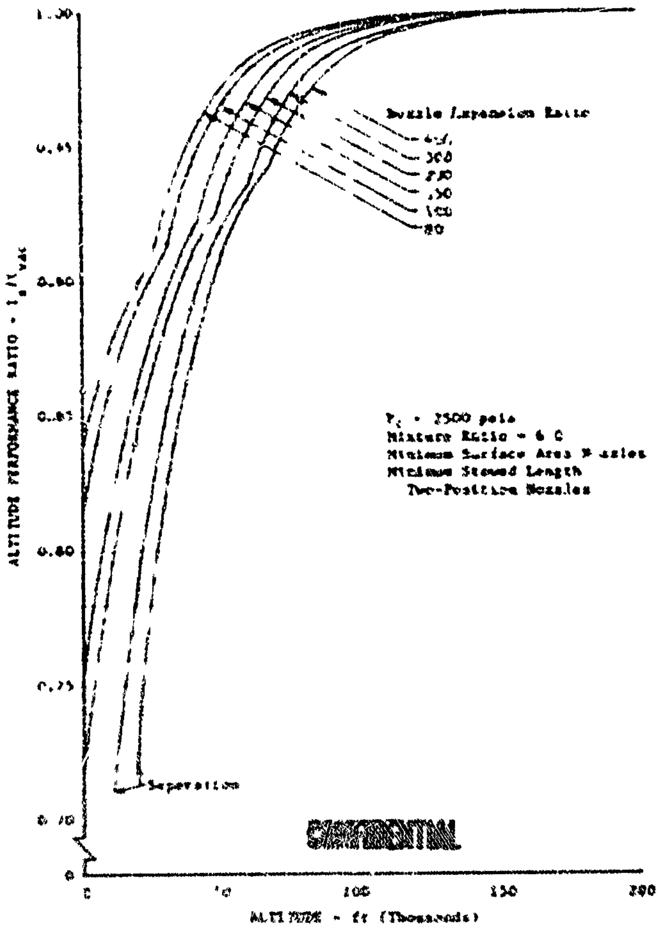

Figure 690. Altitude Performance With Minimum Surface Area Contour Nozzle, 250,000-lb Thrust, r = 6.0, P_c = 2500 psia DF 56193

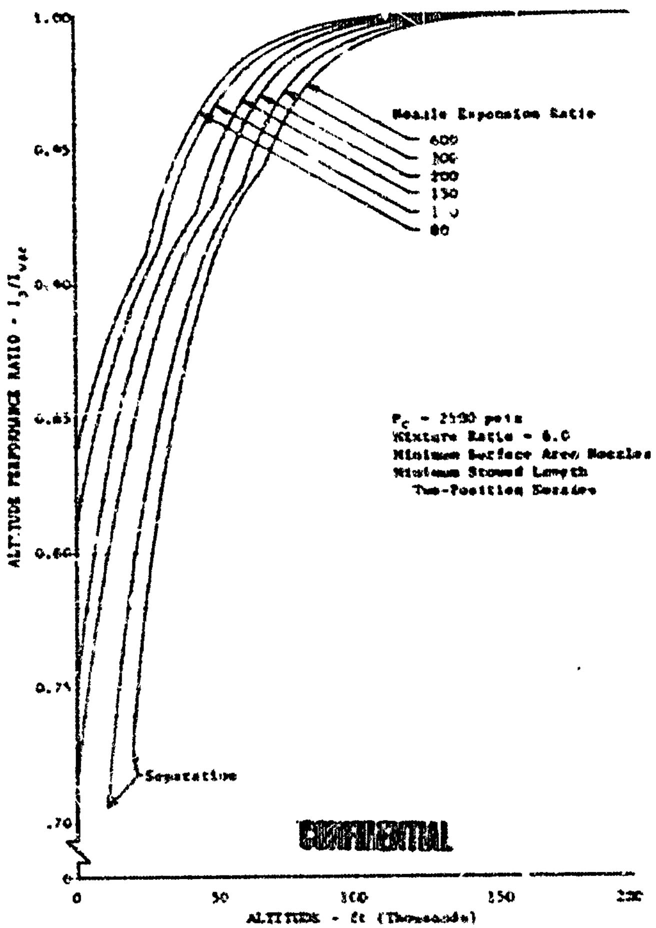

Figure 691. Altitude Performance With Minimum Surface Area Contour Nozzle, 350,000-lb Thrust, r = 6.0, P_c = 2500 psia DF 56194

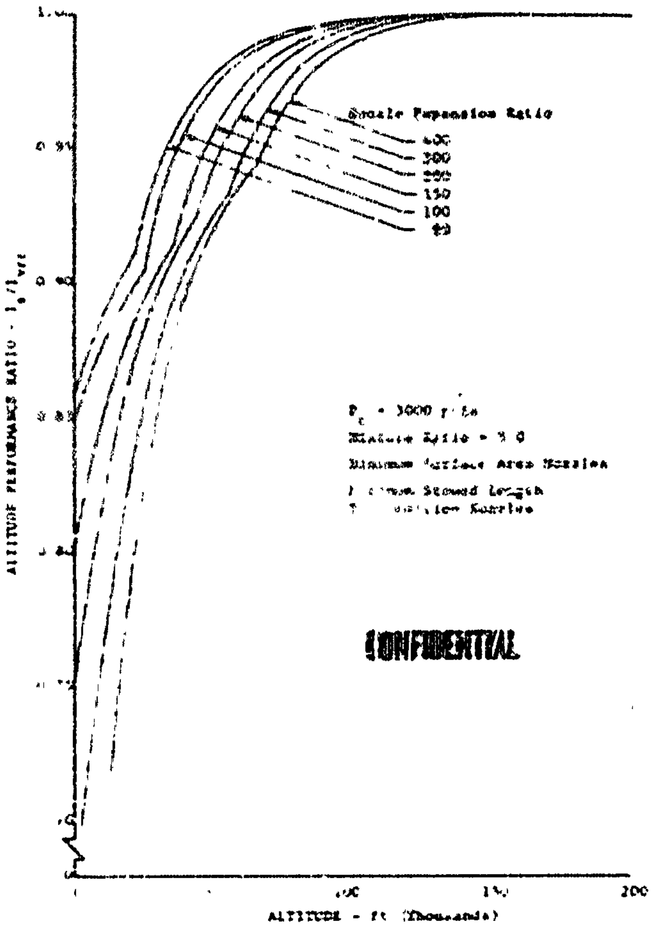

Figure 692. Altitude Performance With Minimum Surface Area Contour Nozzle, 100,000-lb Thrust, r = 5.0, P_c = 3000 psia   DF 56405

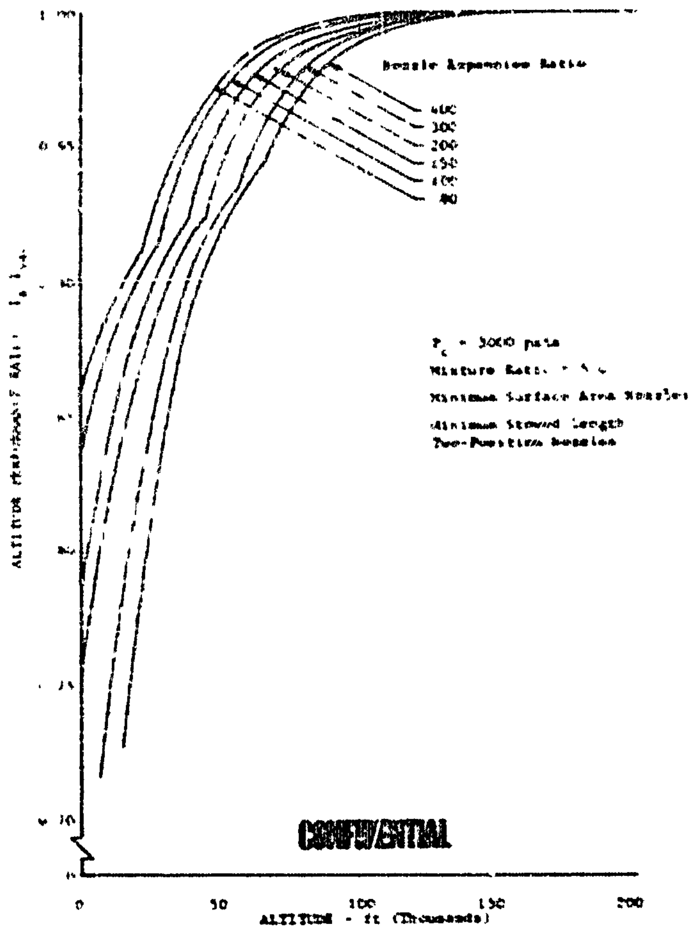

Figure 693. Altitude Performance With Minimum Surface Area Contour Nozzle, 250,000-lb Thrust, r = 5.0, P_c = 3000 psia   DF 56402

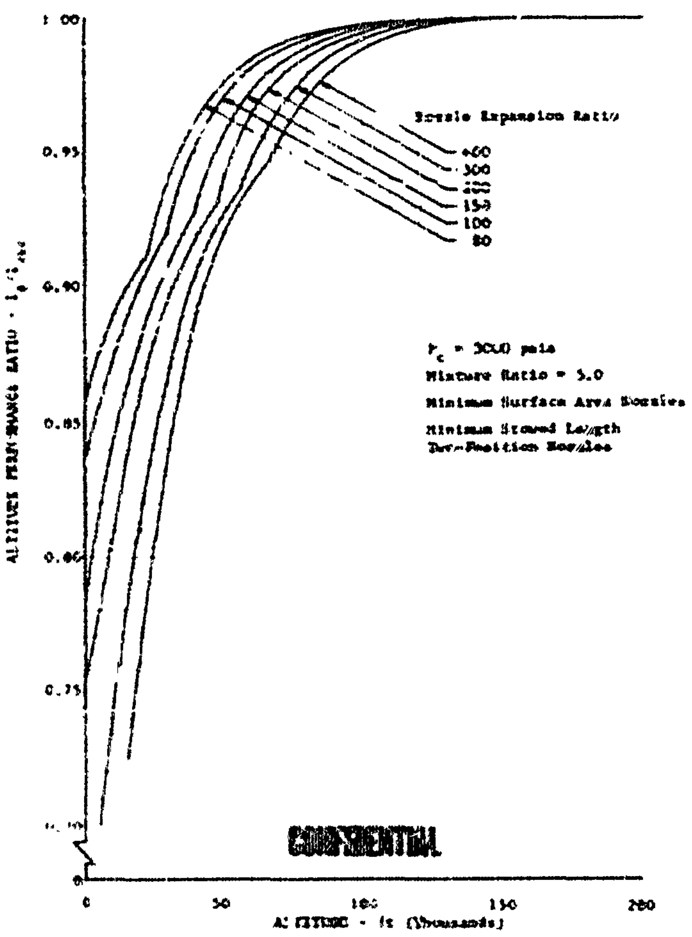

Figure 694. Altitude Performance With Minimum Surface Area Contour Nozzle, 350,000-lb Thrust, r = 6.0, P_c = 3000 psia DF 56403

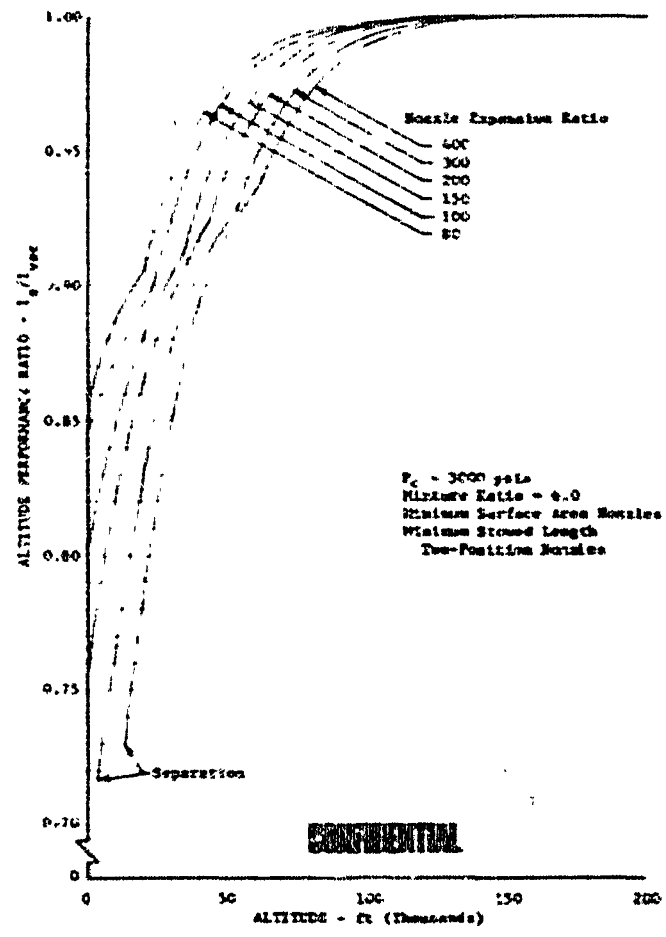

Figure 695. Altitude Performance With Minimum Surface Area Contour Nozzle, 10',000-lb Thrust, r = 6.0, P_c = 3000 psia DF 56195

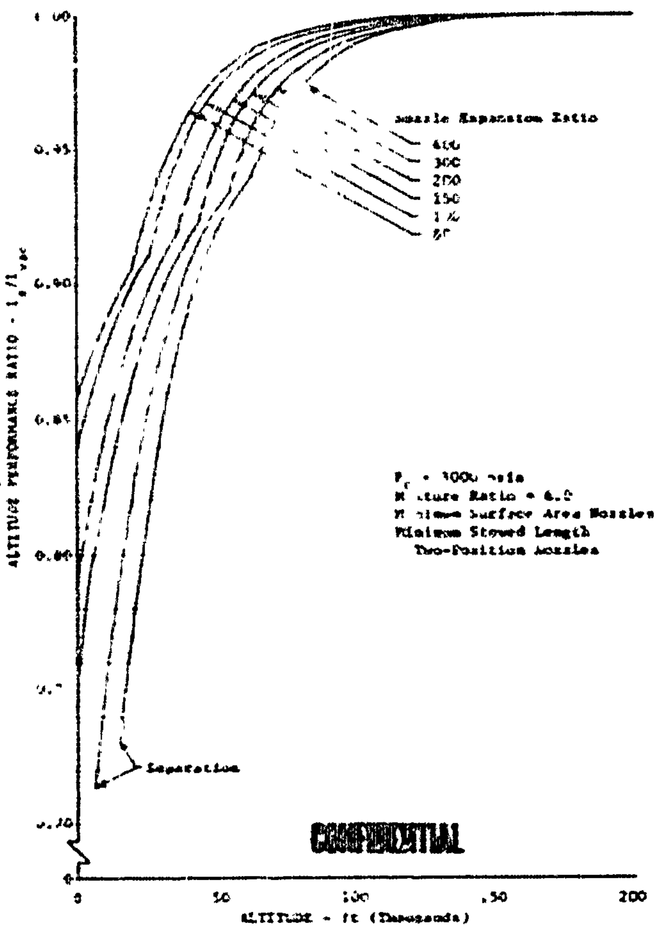

Figure 696. Altitude Performance With Minimum Surface Area Contour Nozzle, 250,000-lb Thrust, $r = 6.0$, $P_c = 3000$ psia DF 56196

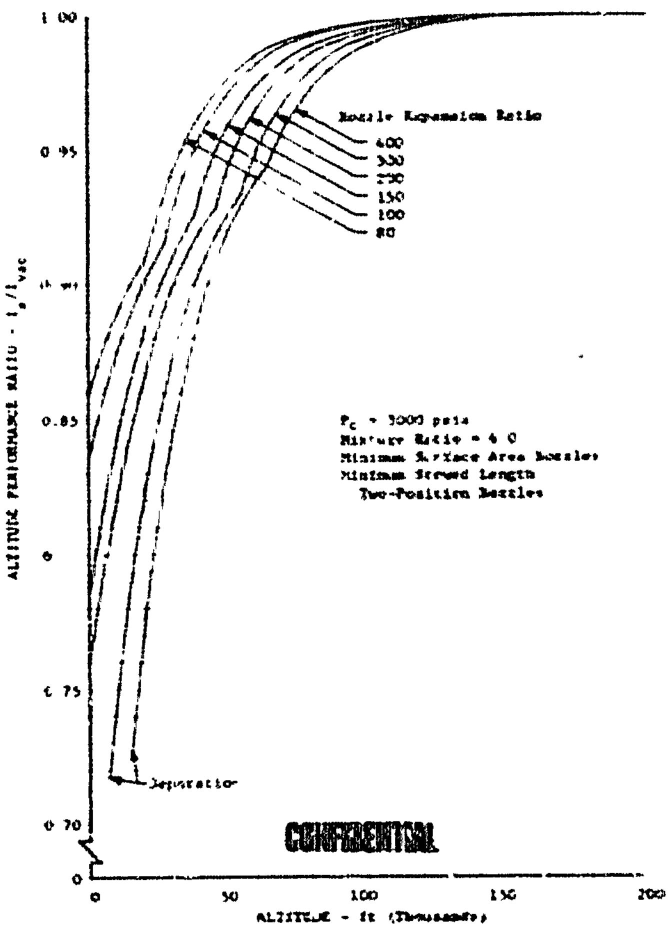

Figure 697. Altitude Performance With Minimum Surface Area Contour Nozzle, 350,000-lb Thrust, $r = 6.0$, $P_c = 3000$ psia DF 56188

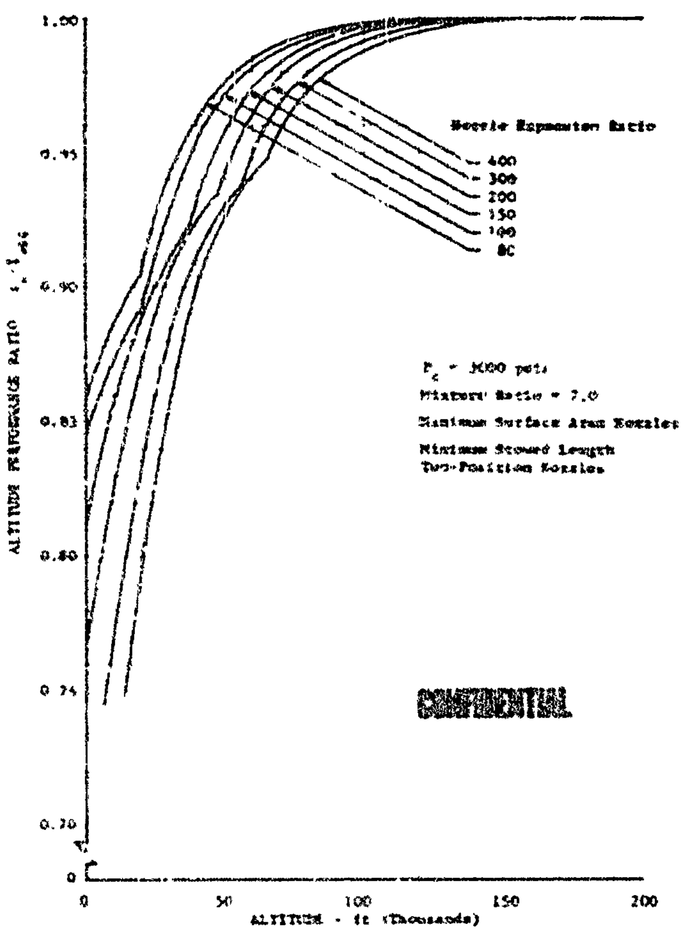

Figure 698. Altitude Performance With Minimum Surface Area Contour Nozzle, 100,000-lb Thrust, r = 7.0, P_c = 3000 psia DF 56404

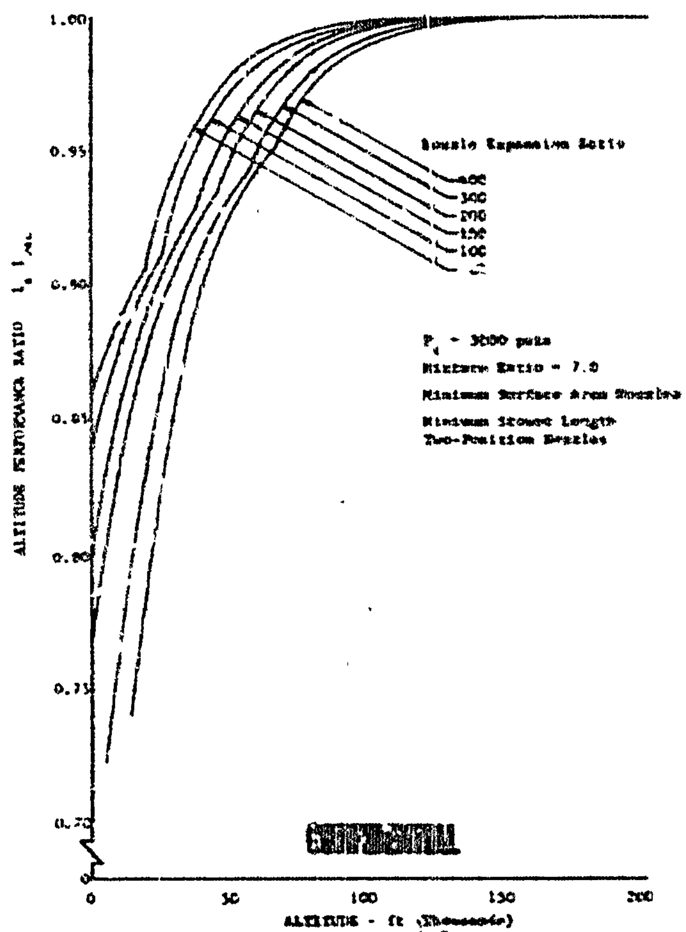

Figure 699. Altitude Performance With Minimum Surface Area Contour Nozzle, 250,000-lb Thrust, r = 7.0, P_c = 3000 psia DF 56401

CONFIDENTIAL

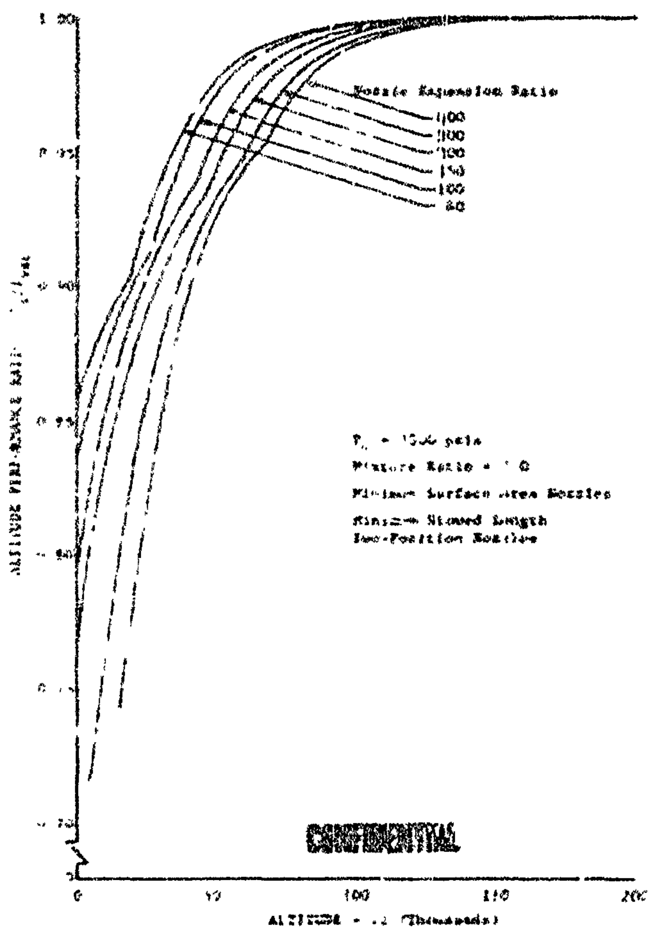

Figure 700. Altitude Performance With Minimum Surface Area Contour Nozzle, 350,000-lb Thrust, r = 7.0, P_c = 3000 psia DF 56406

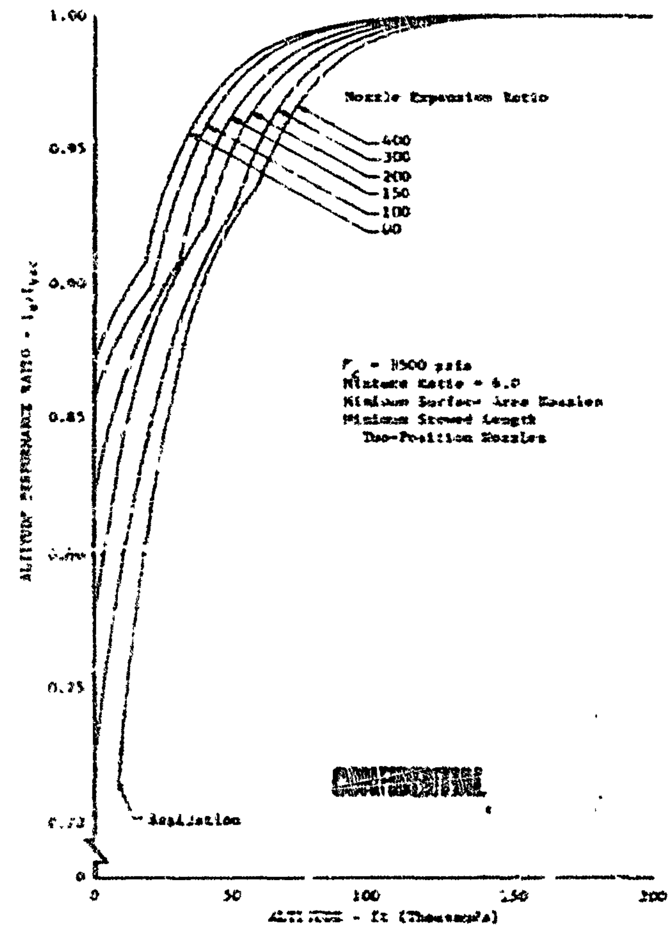

Figure 701. Altitude Performance With Minimum Surface Area Contour Nozzle, 100,000-lb Thrust, r = 6.0, P_c = 3500 psia DF 56187

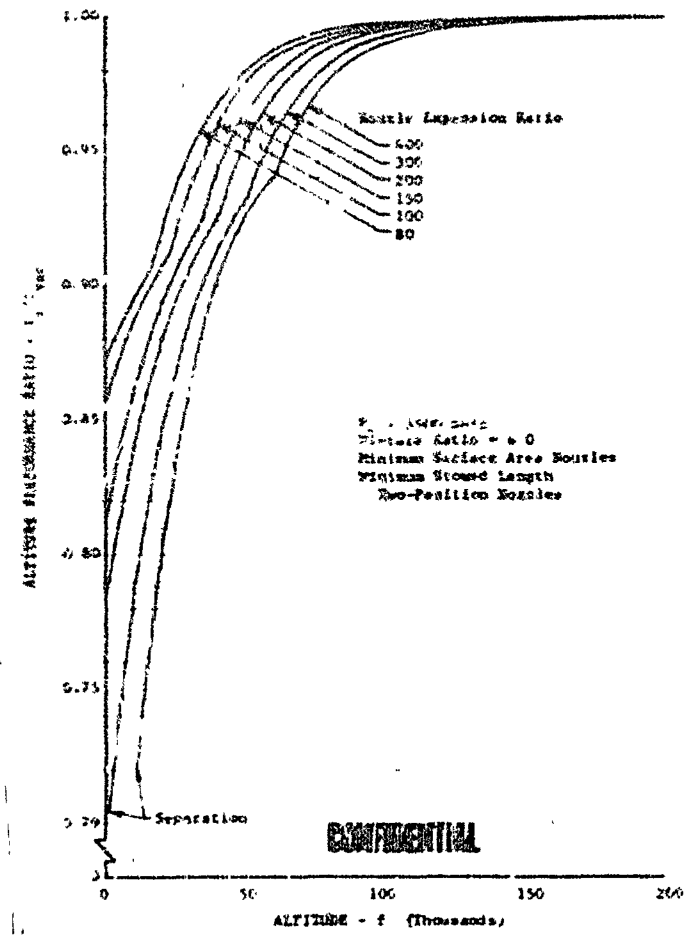

Figure 702 Altitude Performance With Minimum Surface Area Contour Nozzle, 250,000-lb Thrust, $r = 6.0$, $P_c = 3500$ psia

FF 56186

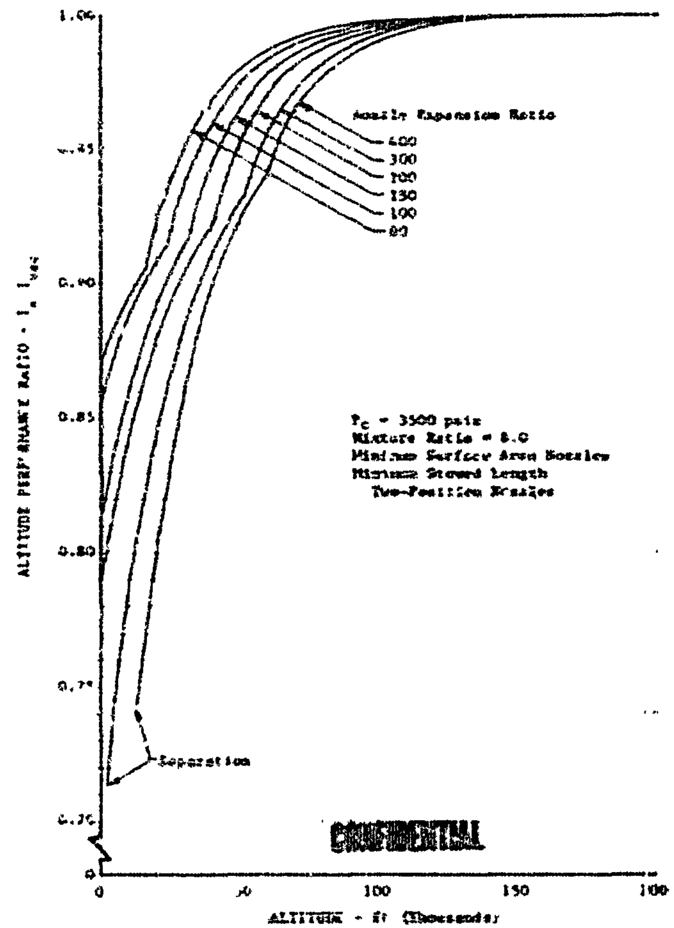

Figure 703. Altitude Performance With Minimum Surface Area Contour Nozzle, 350,000-lb Thrust, $r = 6.0$, $P_c = 3500$ psia

DF 56185

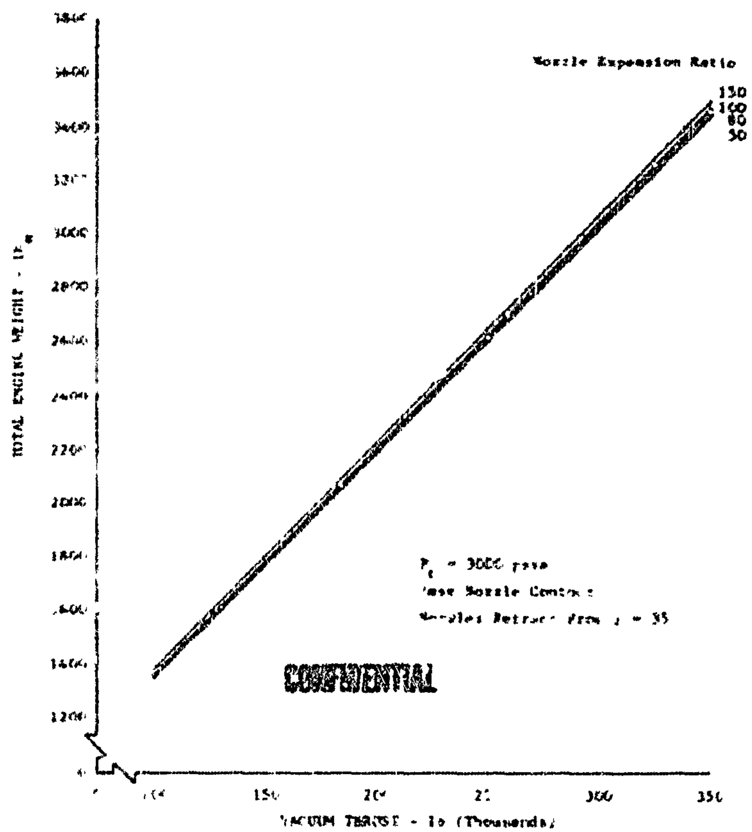

Figure 704. Total Engine Weight vs Vacuum Thrust for Engine With Base Contour Two-Position Nozzle (ϵ_p = 35) DF 56357

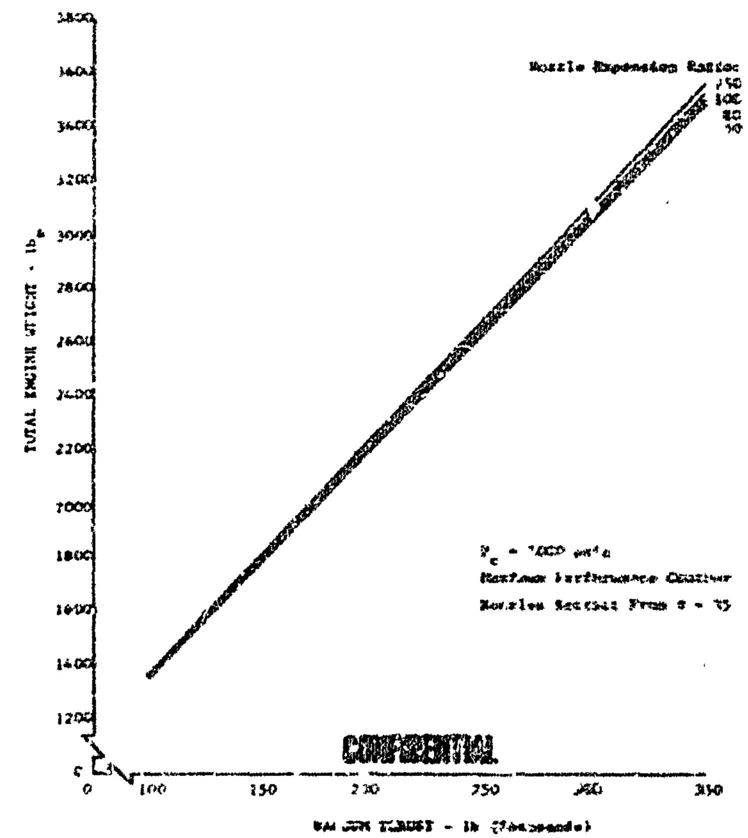

Figure 705. Total Engine Weight vs Vacuum Thrust for Engine With Maximum Performance Contour Two-Position Nozzle (ϵ_p = 35) DF 56356

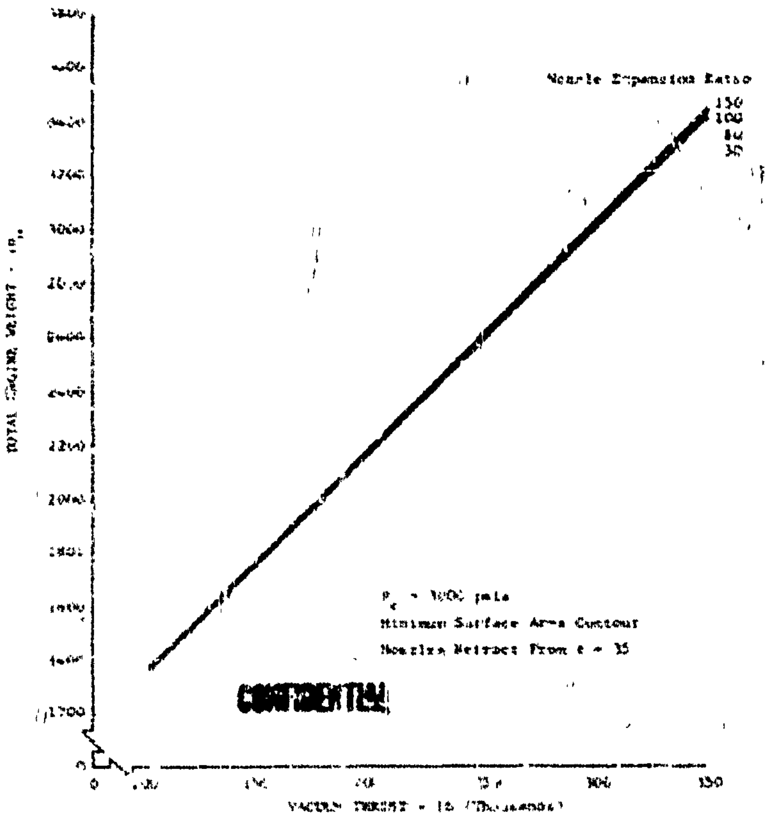

Figure 706. Total Engine Weight vs Vacuum Thrust for Engine With Minimum Surface Area Contour Two-Position Nozzle (ϵ_r = 35) DF 56358

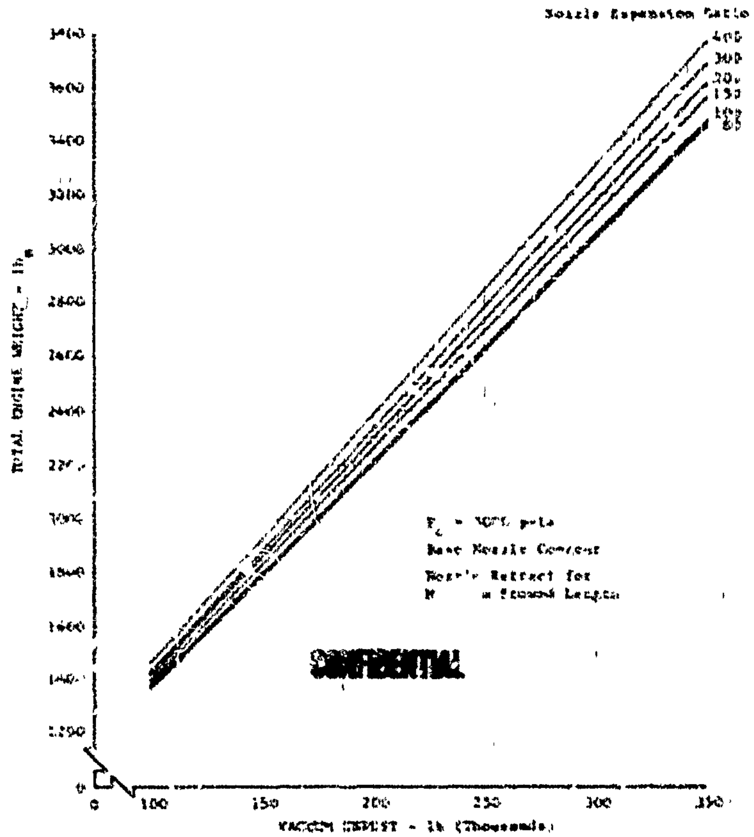

Figure 707. Total Engine Weight vs Vacuum Thrust for Engine With Base Contour Two-Position Nozzle (ϵ_p = Minimum) DF 56354

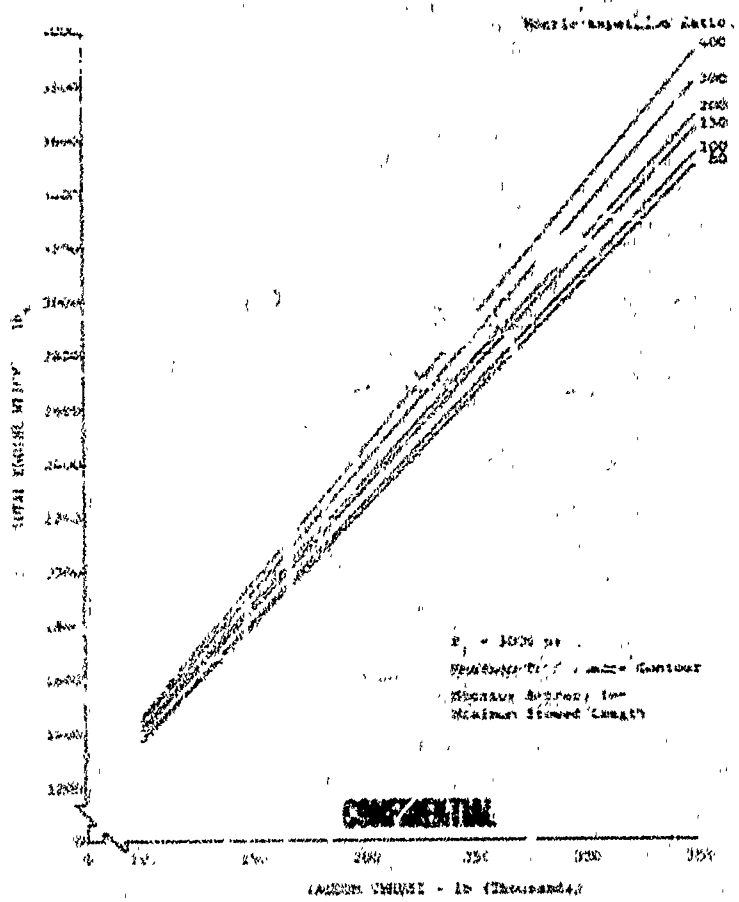

Figure 708. Total Engine Weight vs Vacuum Thrust for Engine With Maximum Performance Contour Two-Position Nozzle (ϵ_p = Minimum) DF 56353

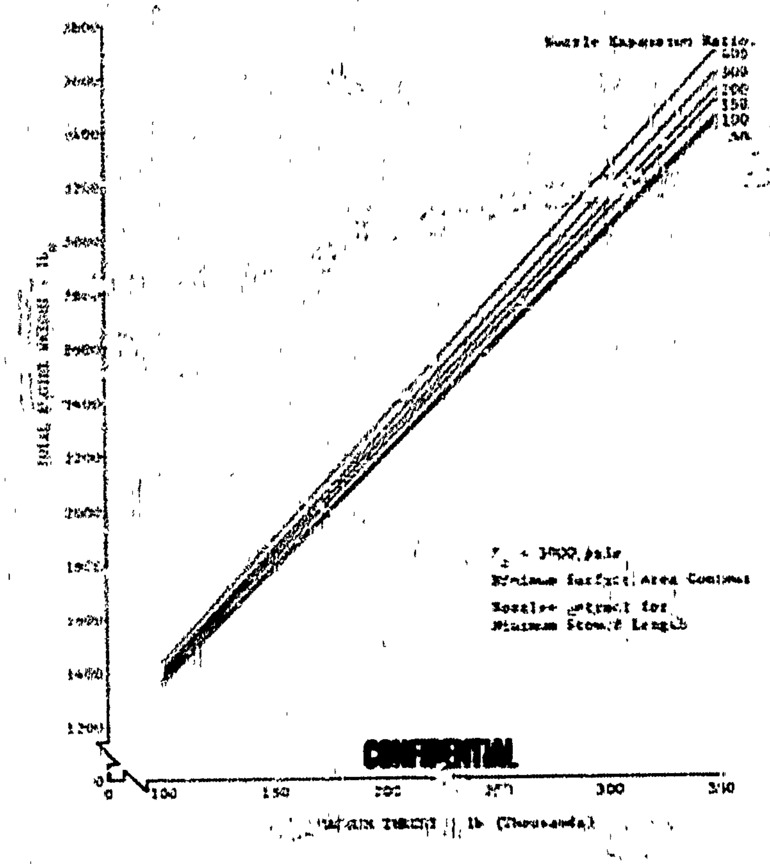

Figure 709. Total Engine Weight vs Vacuum Thrust for Engine With Minimum Surface Area Contour Two-Position Nozzle (ϵ_p = Minimum) DF 56355

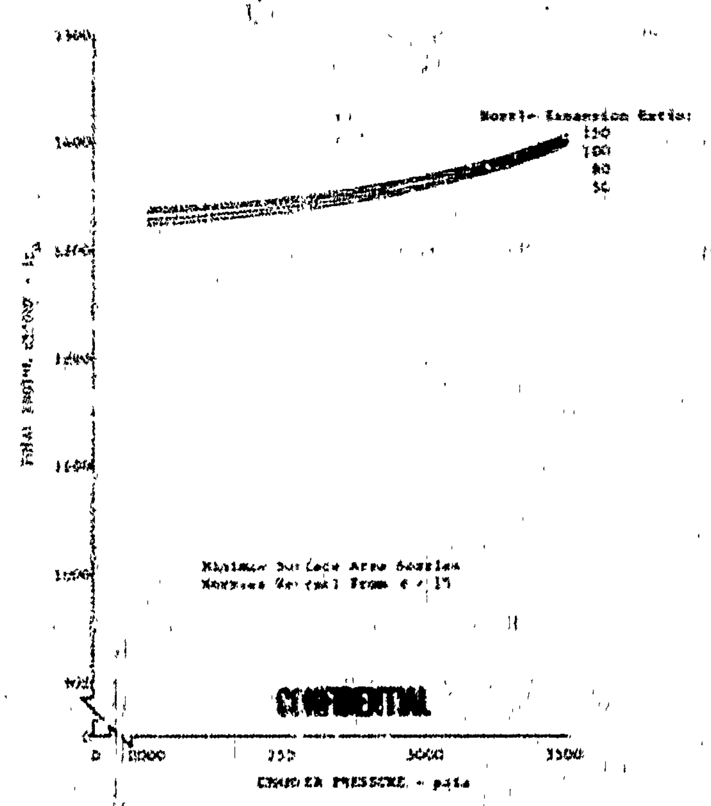

Figure 710. Total Engine Weight vs Chamber Pressure for 100,000-lb Thrust Engine (ϵ_p = 35

DF 56347

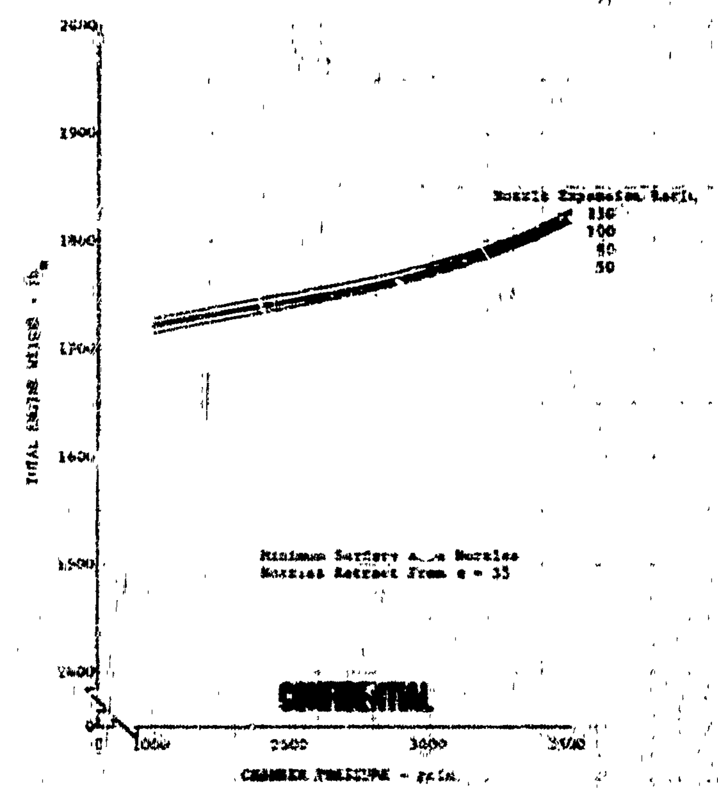

Figure 711. Total Engine Weight vs Chamber Pressure for 150,000-lb Thrust Engine (ϵ_p = 35)

DF 56348

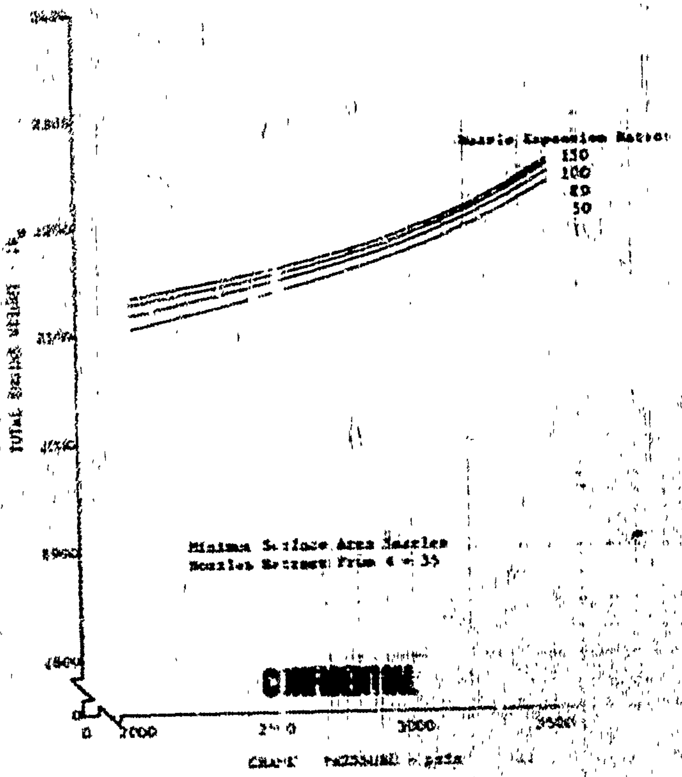

Figure 712. Total Engine Weight vs Chamber Pressure for 200,000-lb Thrust Engine ($\epsilon_p = 35$)

DF 56349

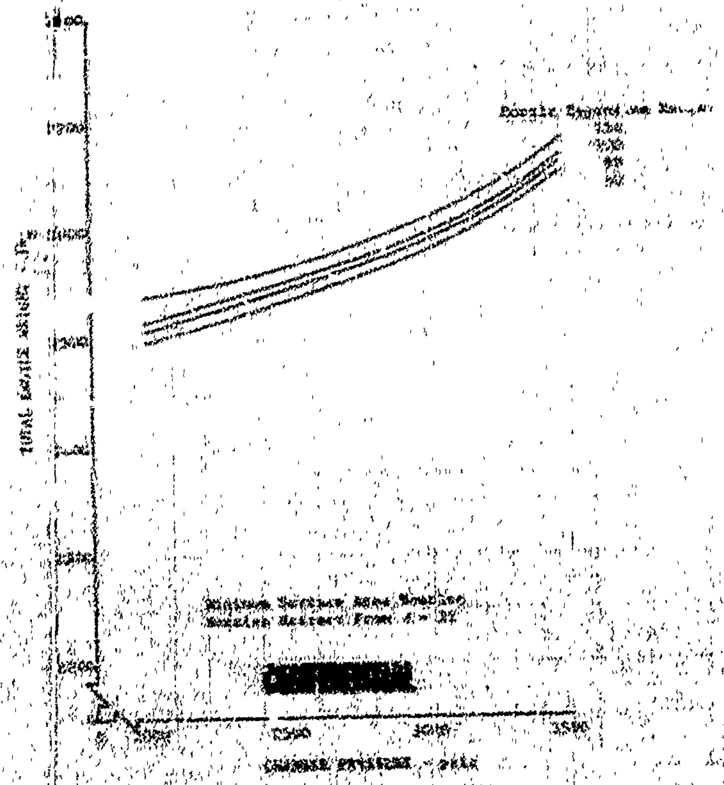

Figure 713. Total Engine Weight vs Chamber Pressure for 250,000-lb Thrust Engine ($\epsilon_p = 35$)

DF 56350

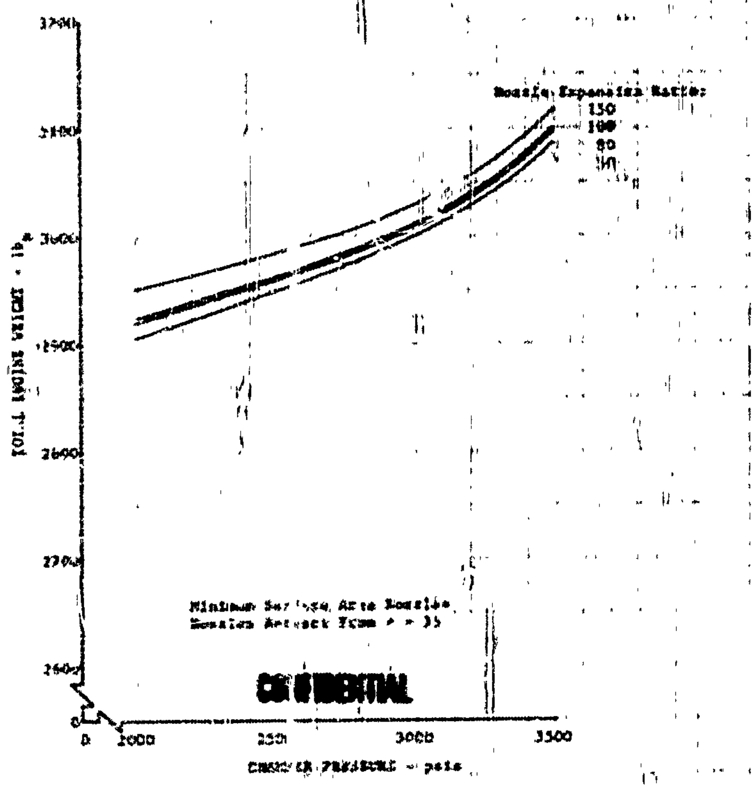

Figure 714. Total En ine Weight vs Chamber Pressure for 300,000- b Thrust Engine (ϵ_p = 35 DF 56351

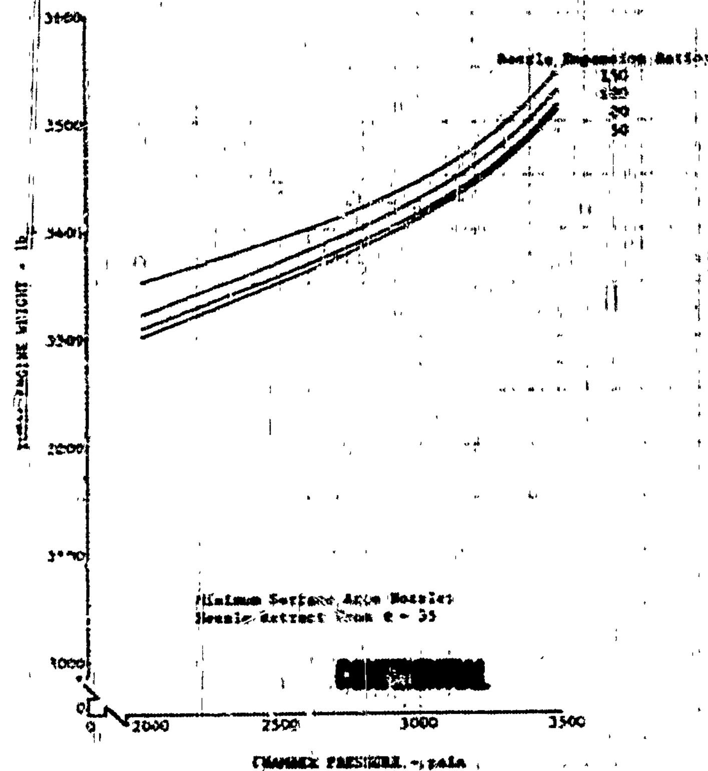

Figure 715. Total Engine Weight vs Chamber Pressure for 350,000-lb Thrust Engine (ϵ_p = 35) DF 56352

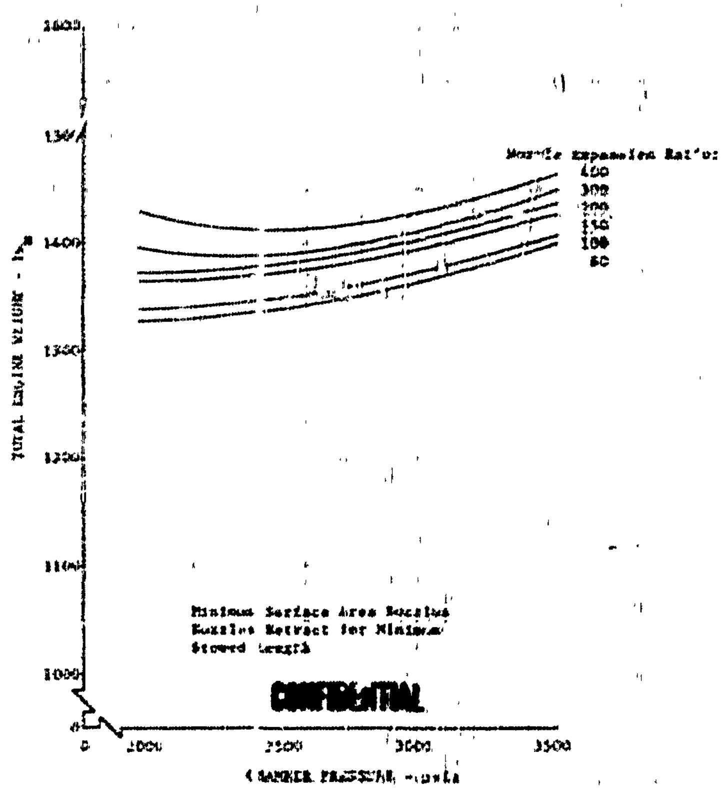

Figure 716. Total Engine Weight vs Chamber Pressure for 100,000-lb Thrust Engine (ϵ_p = Minimum) DF 56342

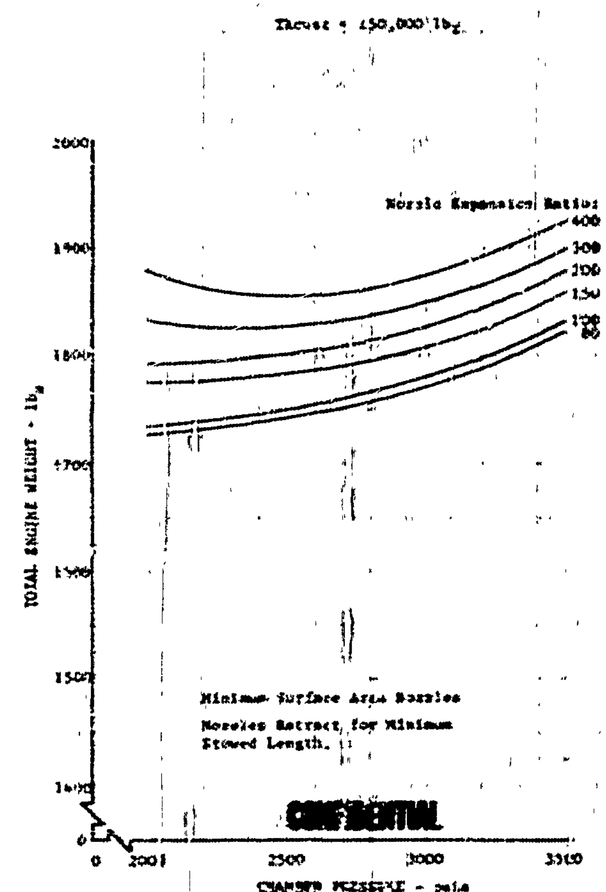

Figure 717. Total Engine Weight vs Chamber Pressure for 150,000-lb Thrust Engine (ϵ_p = Minimum) DF 56359

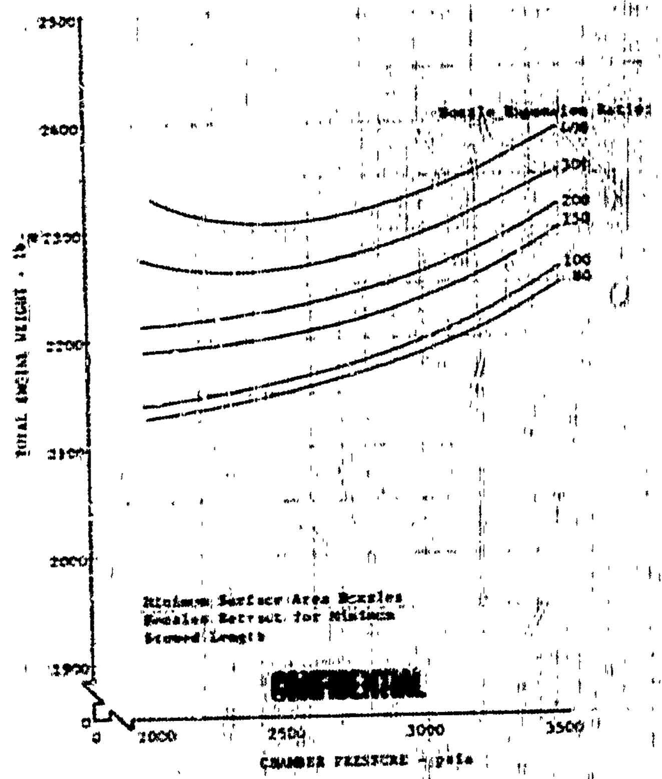

Figure 718. Total Engine Weight vs Chamber Pressure for 200,000-lb Thrust Engine (ϵ_p = Minimum)

DF 56343

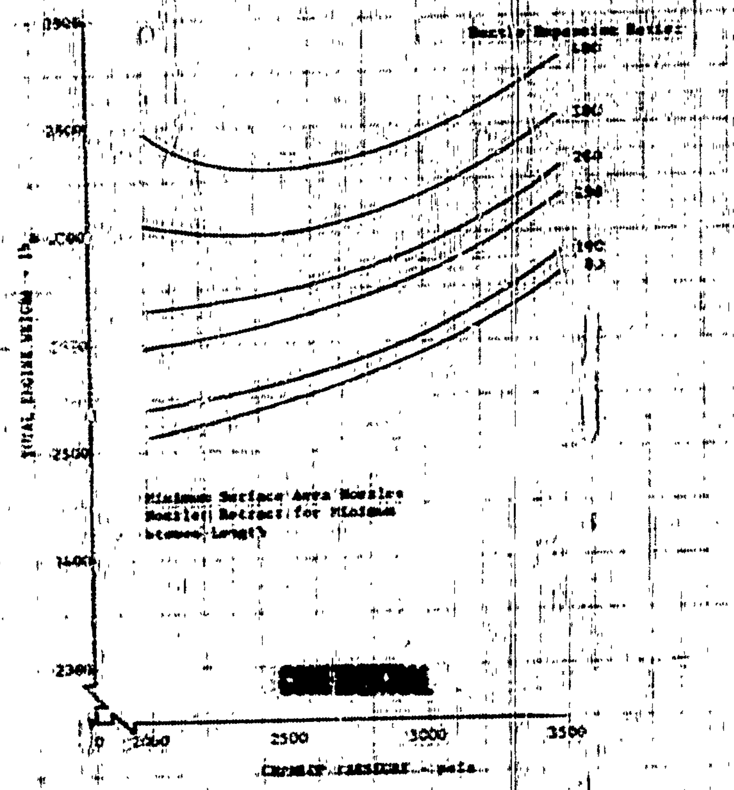

Figure 719. Total Engine Weight vs Chamber Pressure for 250,000-lb Thrust Engine (ϵ_p = Minimum)

DF 56344

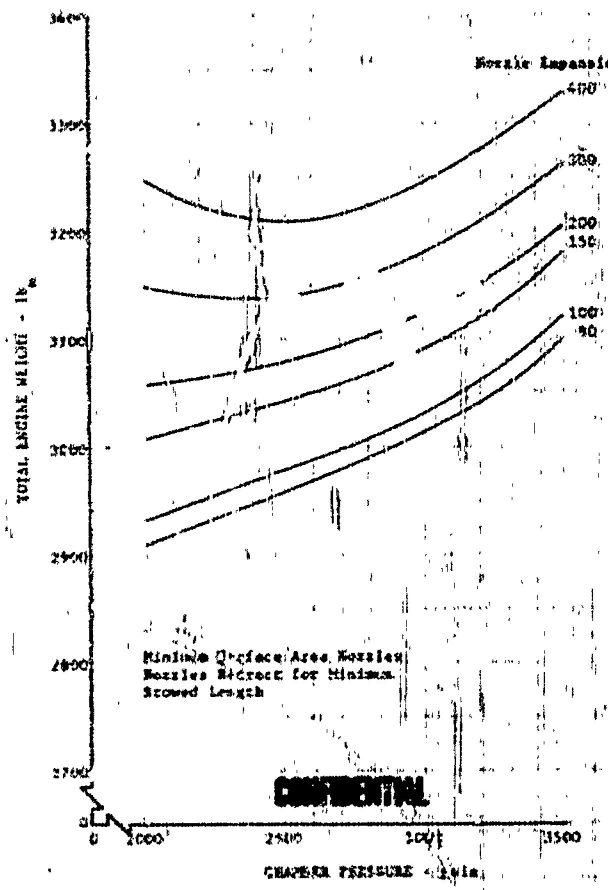

Figure 720. Total Engine Weight vs Chamber Pressure for 300,000-lb Thrust Engine (ϵ_p = Minimum)

DF 56345

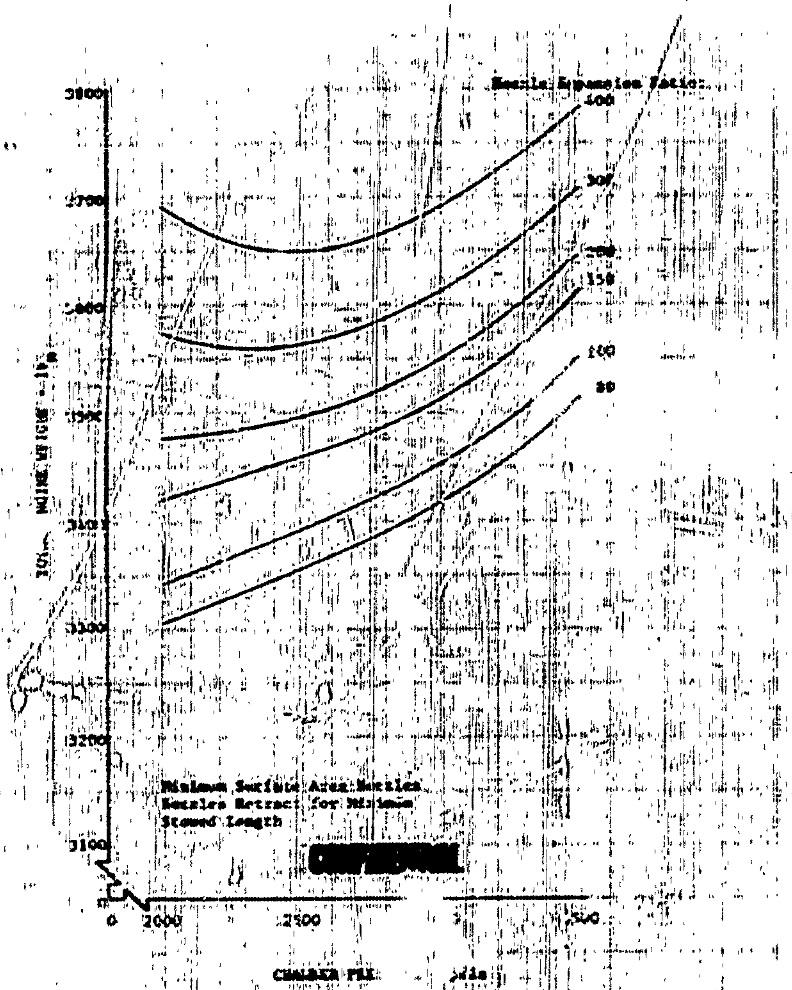

Figure 721. Total Engine Weight vs Chamber Pressure for 350,000-lb Thrust Engine (ϵ_p = Minimum)

DF 56346

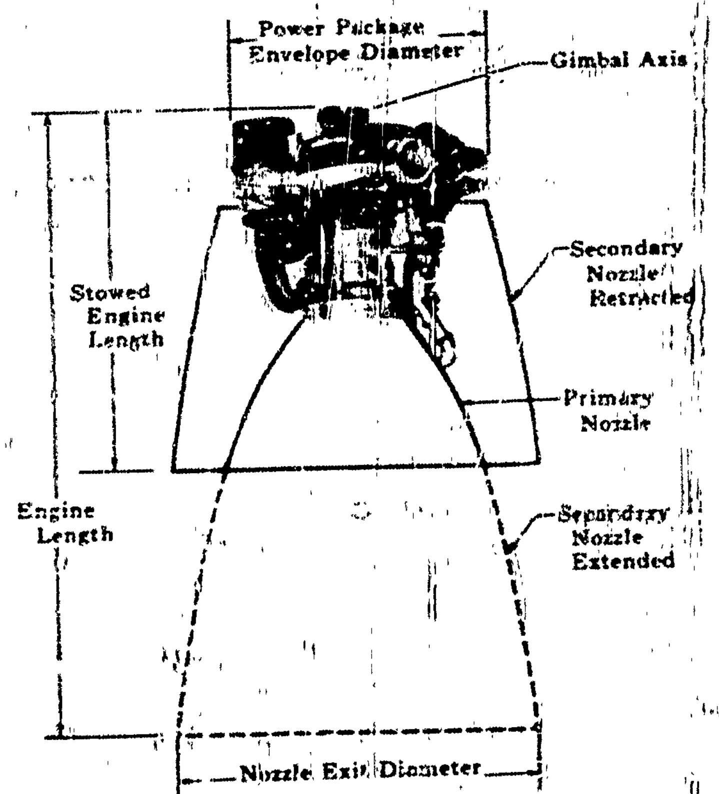

Figure 722. Engine Configuration With Two-Position Nozzle FD 21152

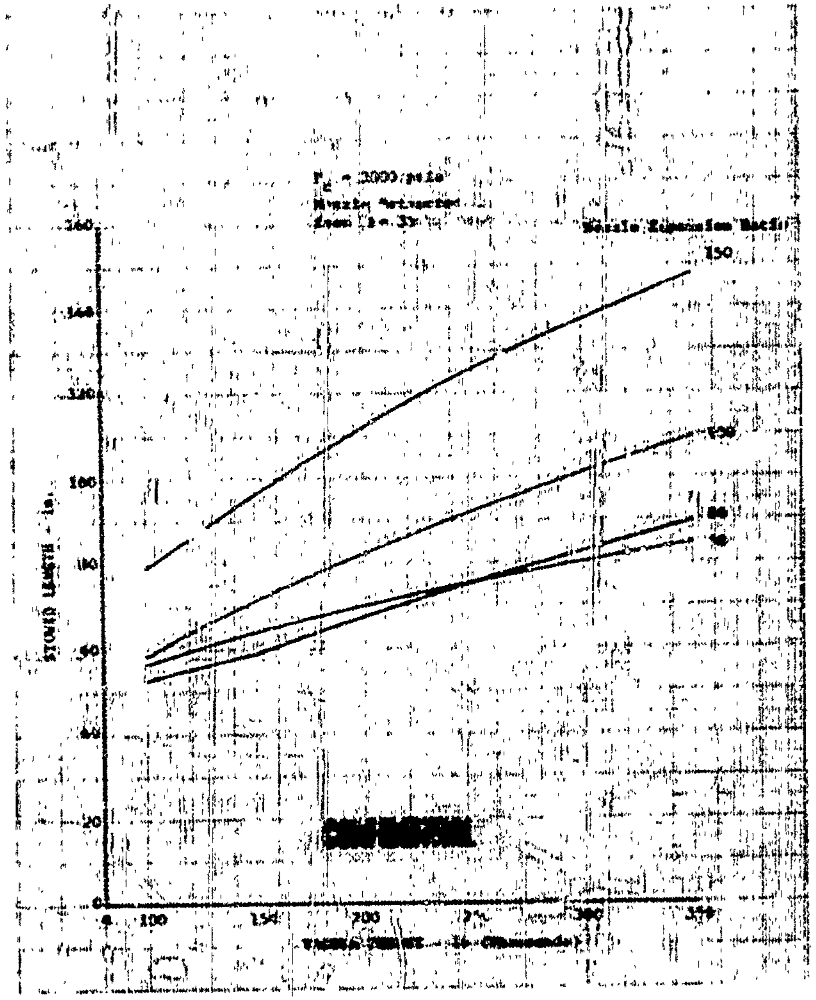

Figure 723. Stowed Length vs Vacuum Thrust for Engine With Base Contour Two-Position Nozzle ($\epsilon_p = 35$) DF 56239

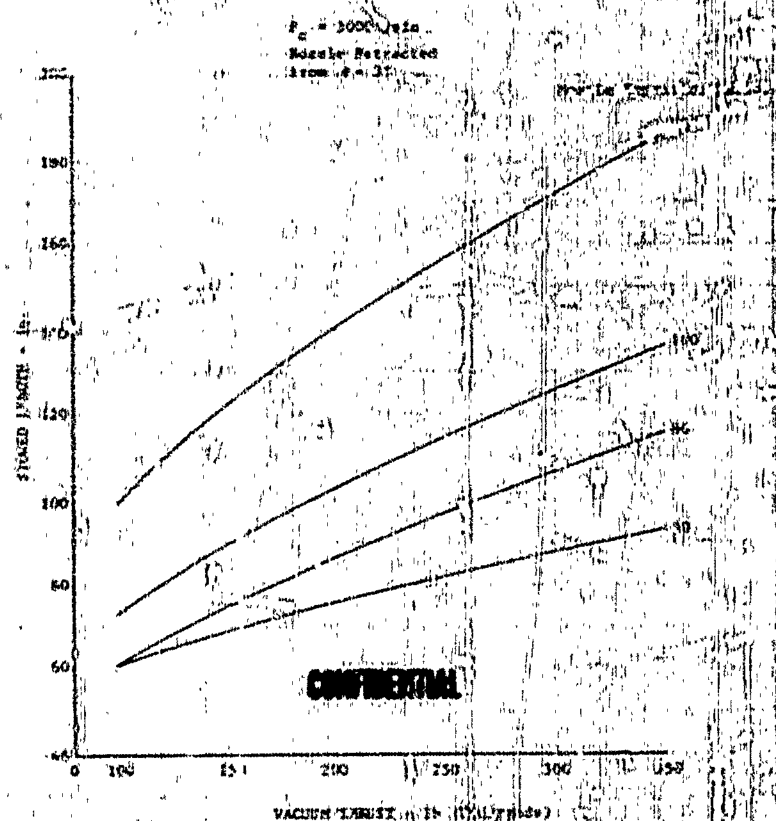

Figure 724. Stowed Length vs Vacuum Thrust for Engine With Maximum Performance Contour Two-Position Nozzle ($\epsilon_p = 35$) DF 56238

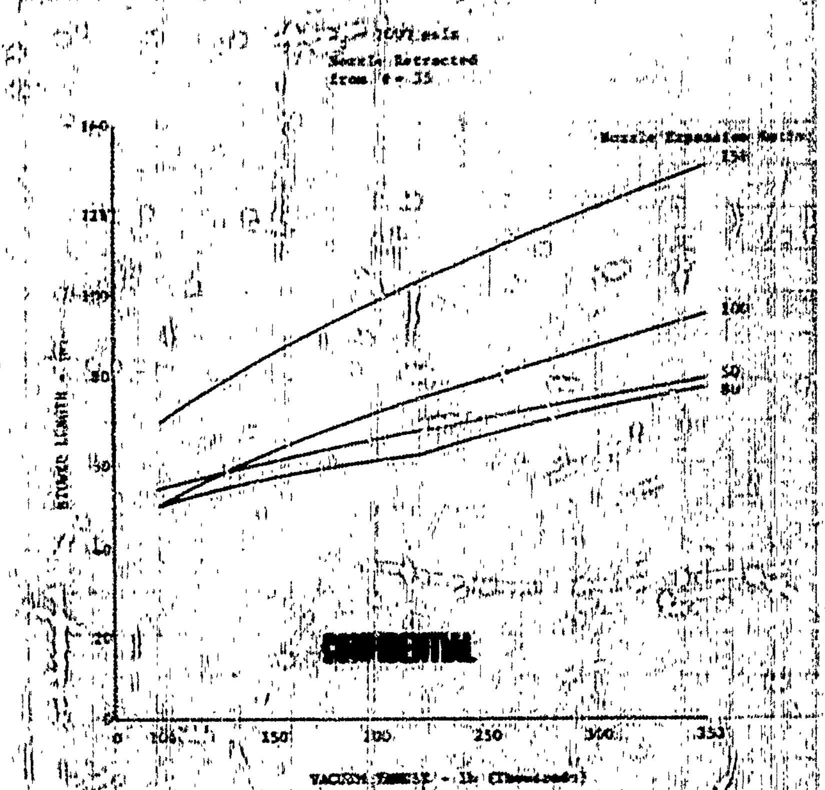

Figure 725. Stowed Length vs Vacuum Thrust for Engine With Minimum Surface Area Contour Two-Position Nozzle ($\epsilon_p = 35$) DF 56237

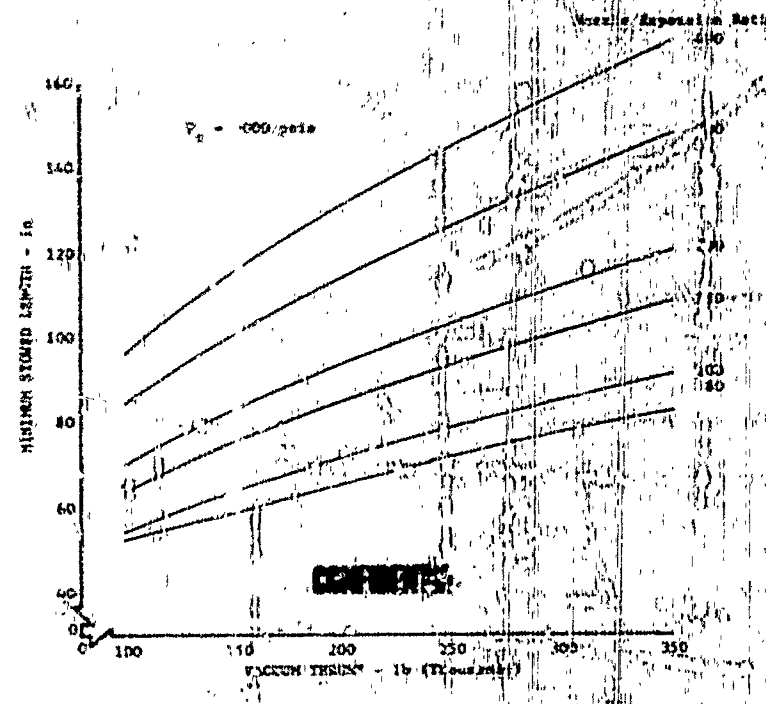

Figure 726. Minimum Stowed Length vs Vacuum Thrust for Engine With Base Contour Two Position Nozzle DF 56210

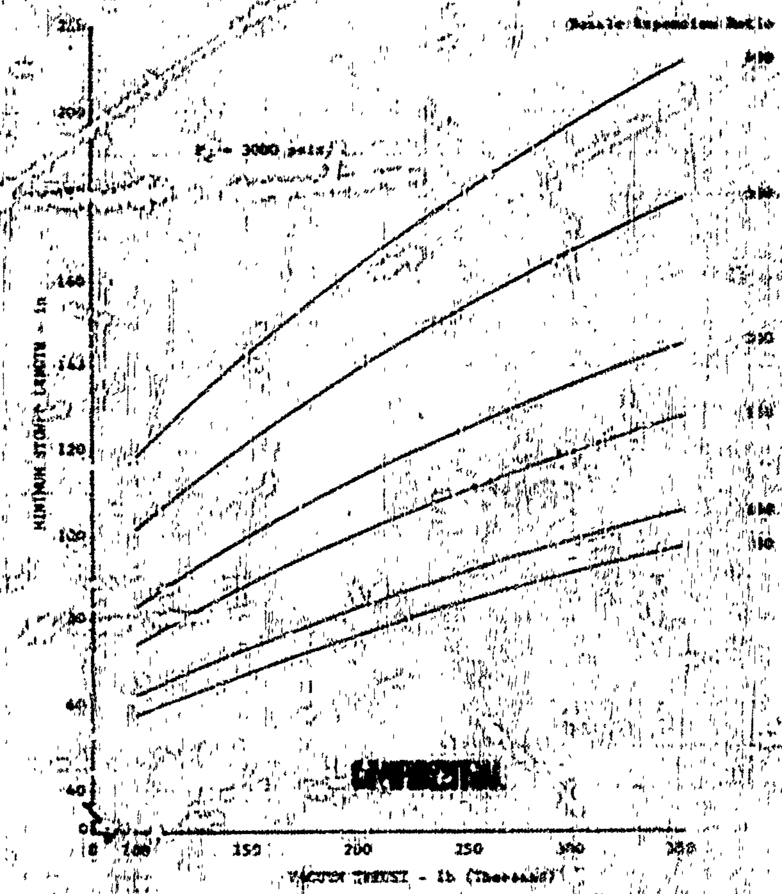

Figure 727. Minimum Stowed Length vs Vacuum Thrust for Engine With Maximum Performance tour Two-Position Nozzle DF 56259

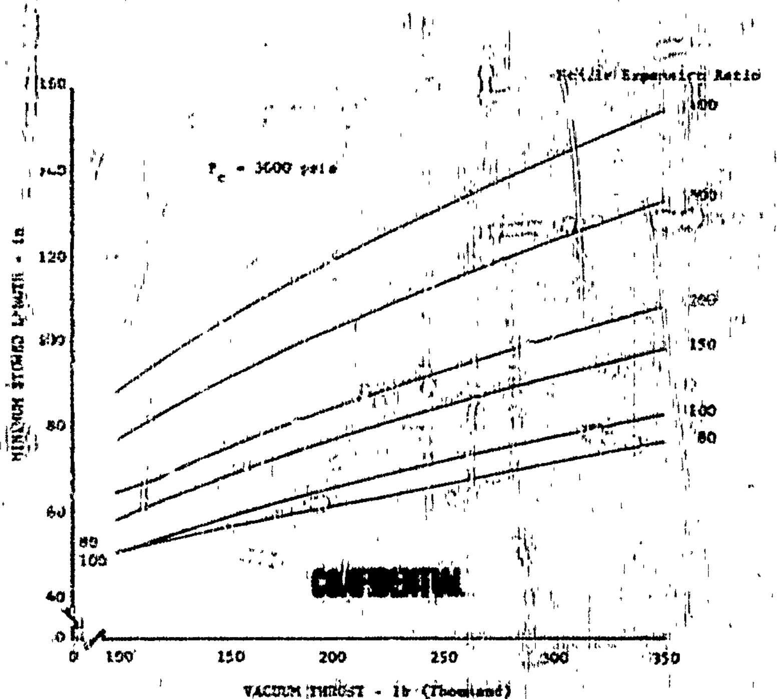

Figure 728. Minimum Stowed Length vs Vacuum Thrust for Engine With Minimum Surface Area Contour Two-Position Nozzl — DF 56258

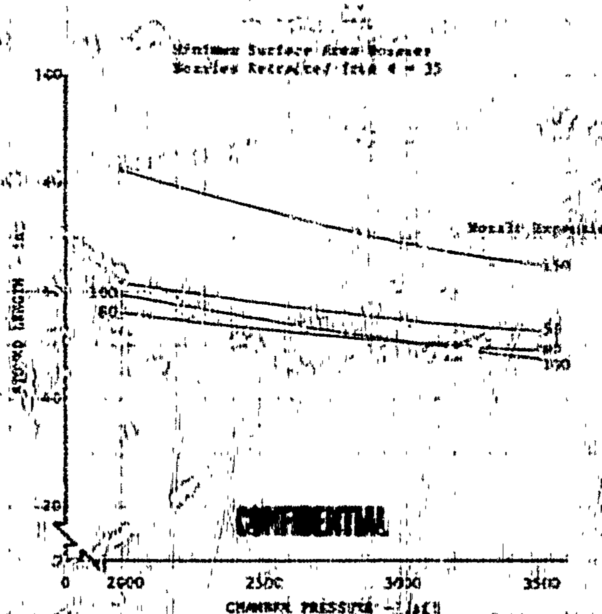

Figure 729. .towed Length vs Chamber Pressure for 100,000-lb Thrust Engine (ϵ_p = 35) — DF 56230

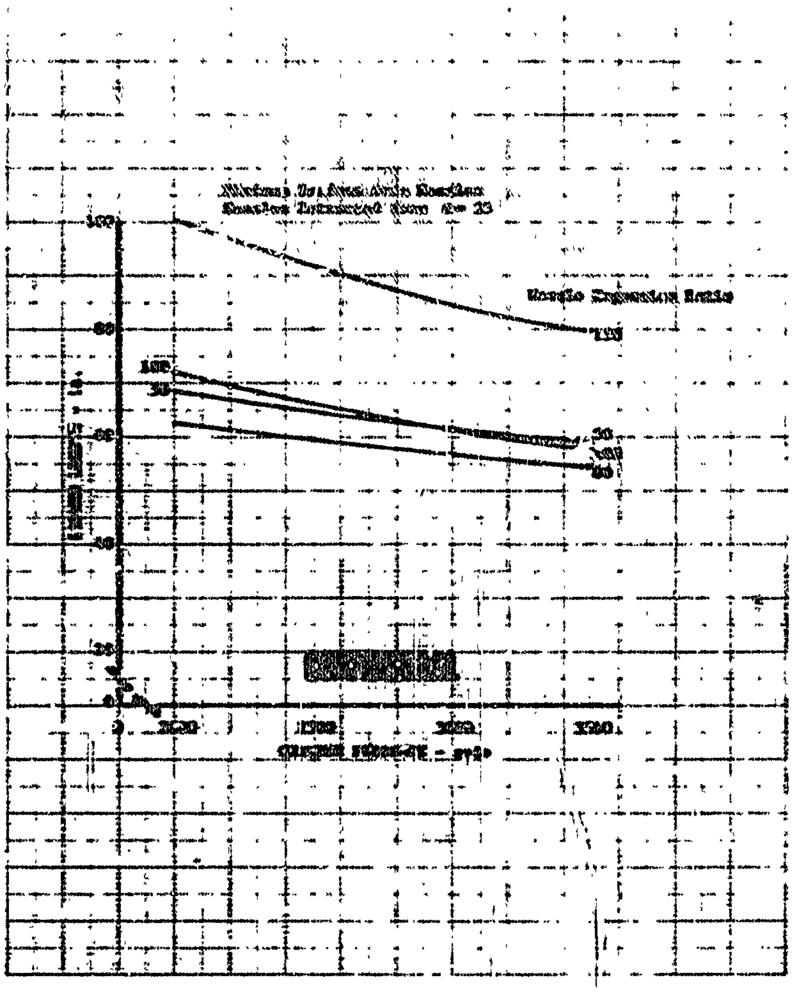

Figure 730. Stowed Length vs Chamber Pressure for 150,000-lb Thrust Engine ($\epsilon_p = 35$) DF 56229

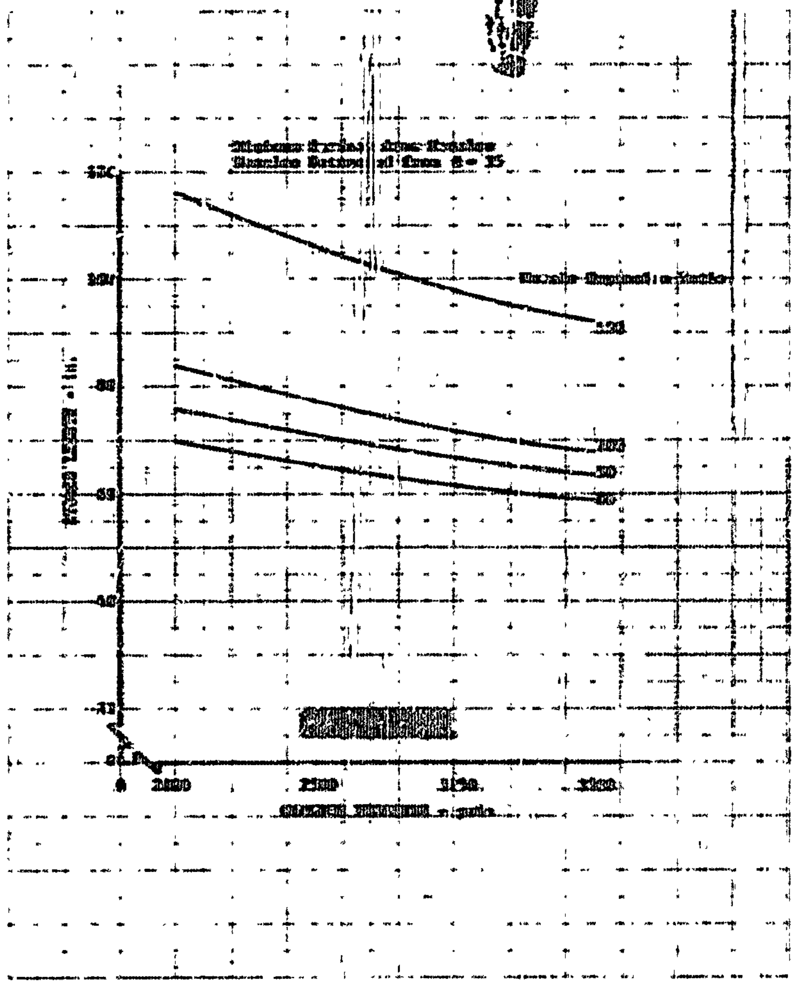

Figure 731. Stowed Length vs Chamber Pressure for 200,000-lb Thrust Engine ($\epsilon_p = 35$) DF 56228

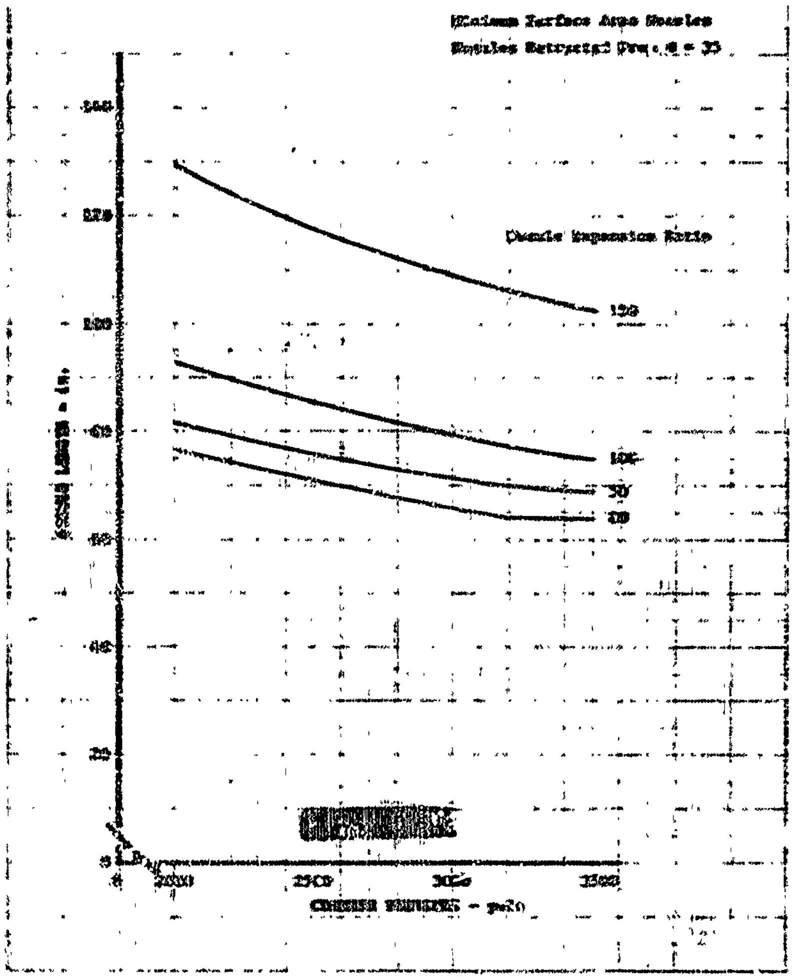

Figure 732. Stowed Length vs Chamber Pressure for 250,000-lb Thrust Engine ($\epsilon_p = 35$)

DF 56227

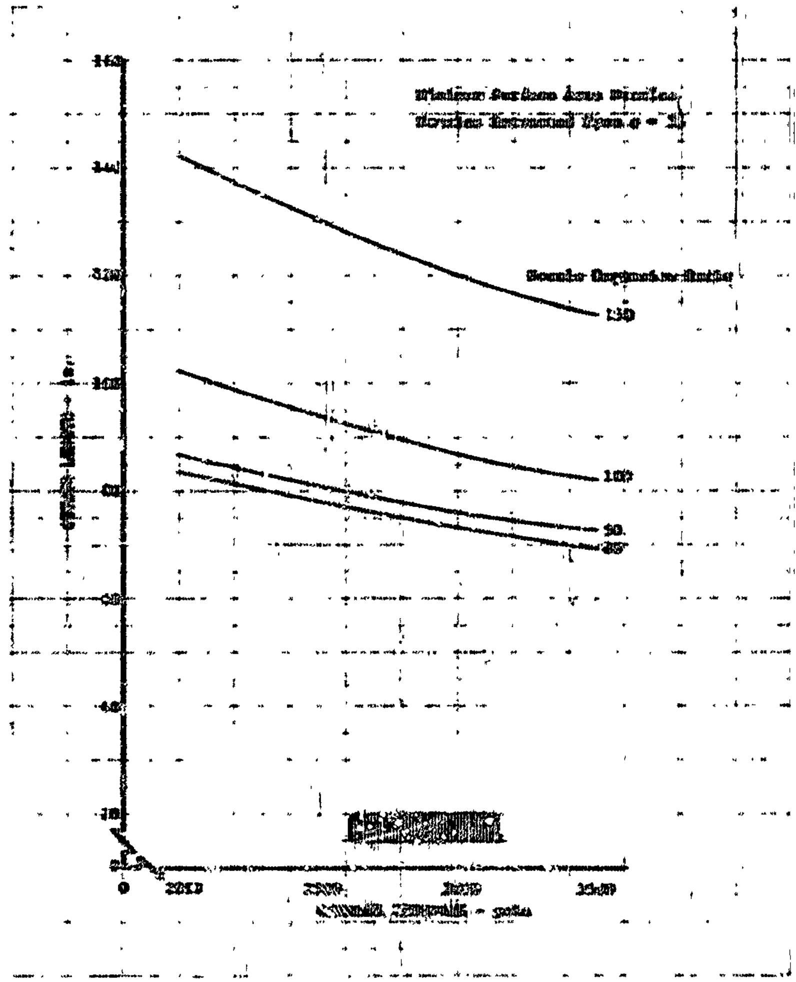

Figure 733. Stowed Length vs Chamber Pressure for 300,000-lb Thrust Engine ($\epsilon_p = 35$)

DF 56226

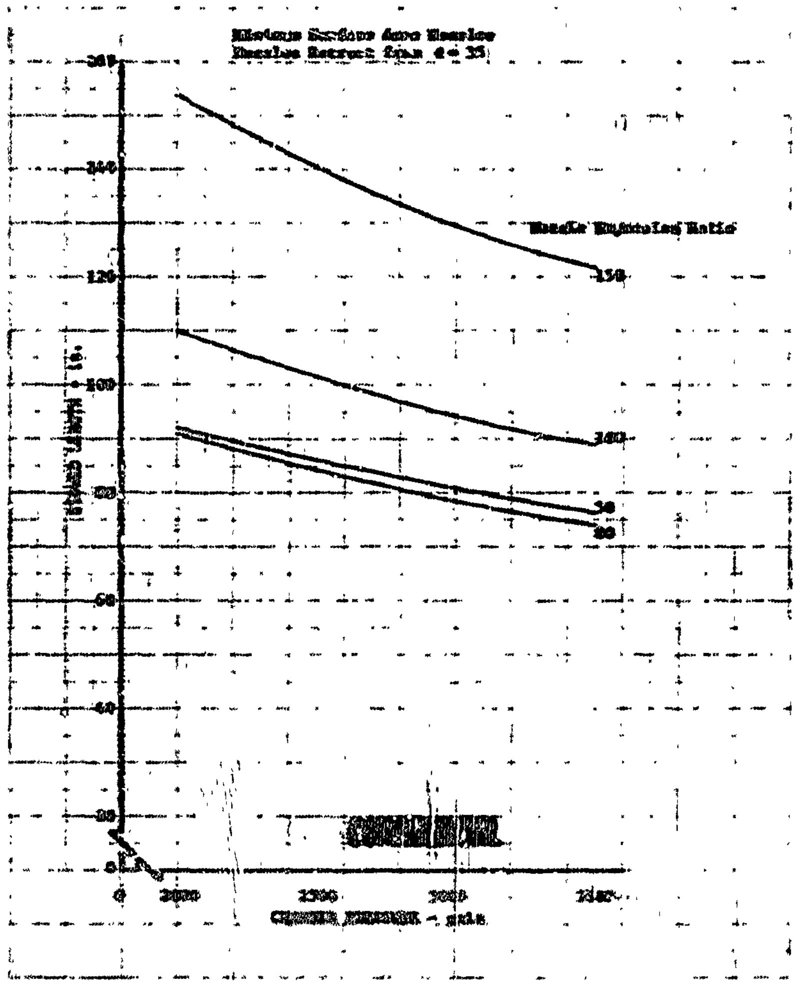

Figure 734. Stowed Length vs Chamber Pressure for 350,000-lb Thrust Engine ($\epsilon_p = 25$)

DF 56225

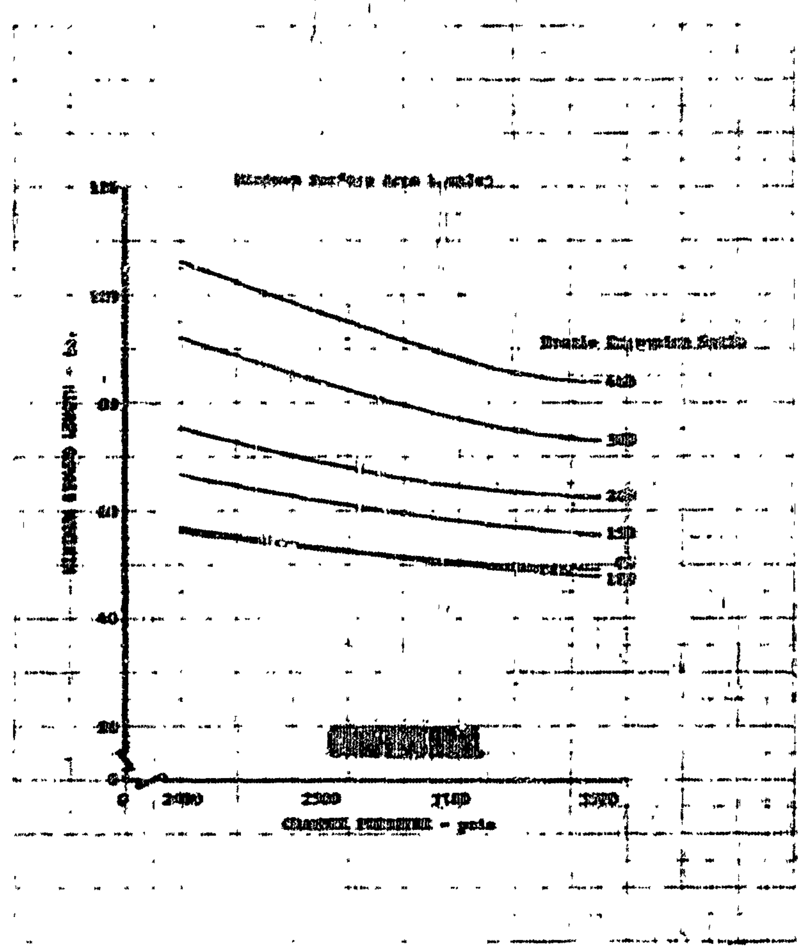

Figure 735. Minimum Stowed Length vs Chamber Pressure for 100,000-lb Thrust Engine

DF 56236

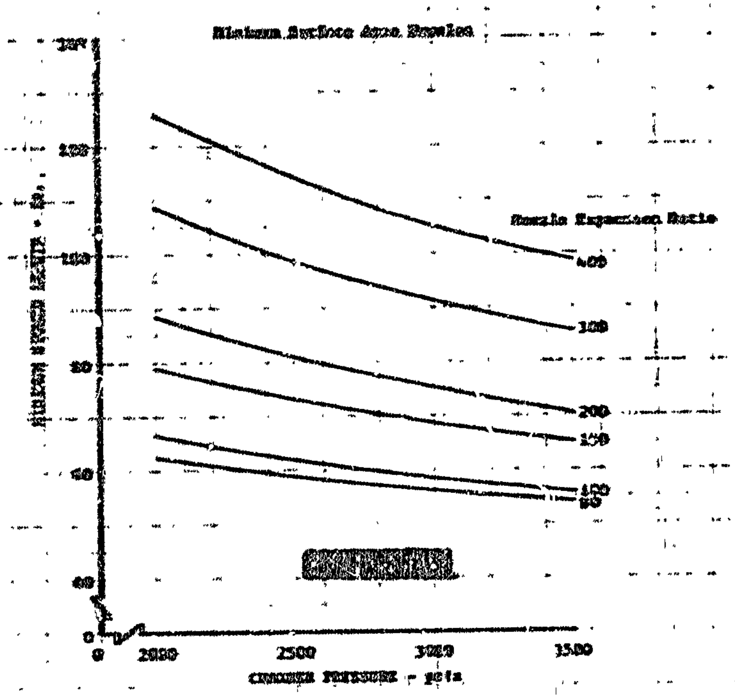

Figure 736. Minimum Stowed Length vs Chamber Pressure for 150,000-lb Thrust Engine

DF 56235

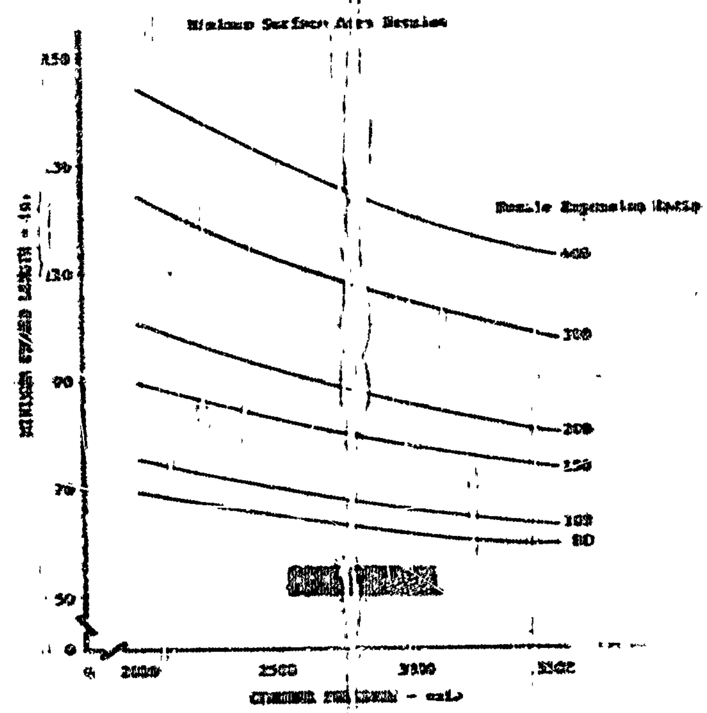

Figure 737. Minimum Stowed Length vs Chamber Pressure for 200,000-lb Thrust Engine

DF 56234

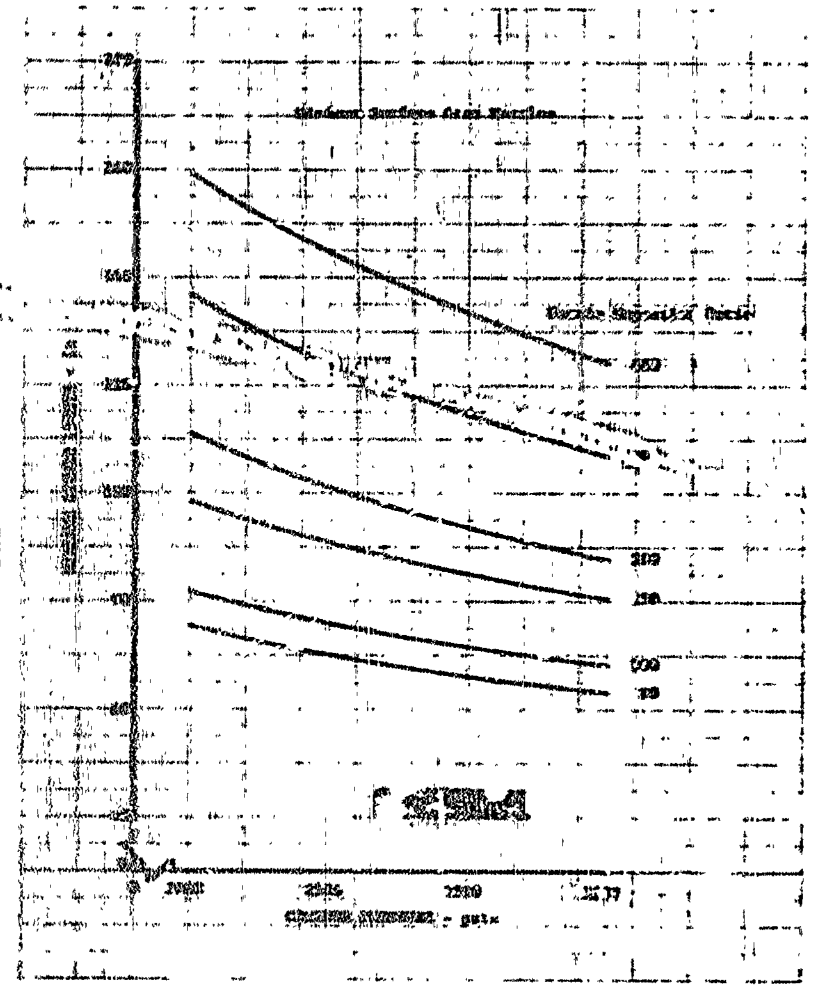

Figure 738. Minimum Stowed Length vs Chamber Pressure for 250,000-lb Thrust Engine

DF 56233

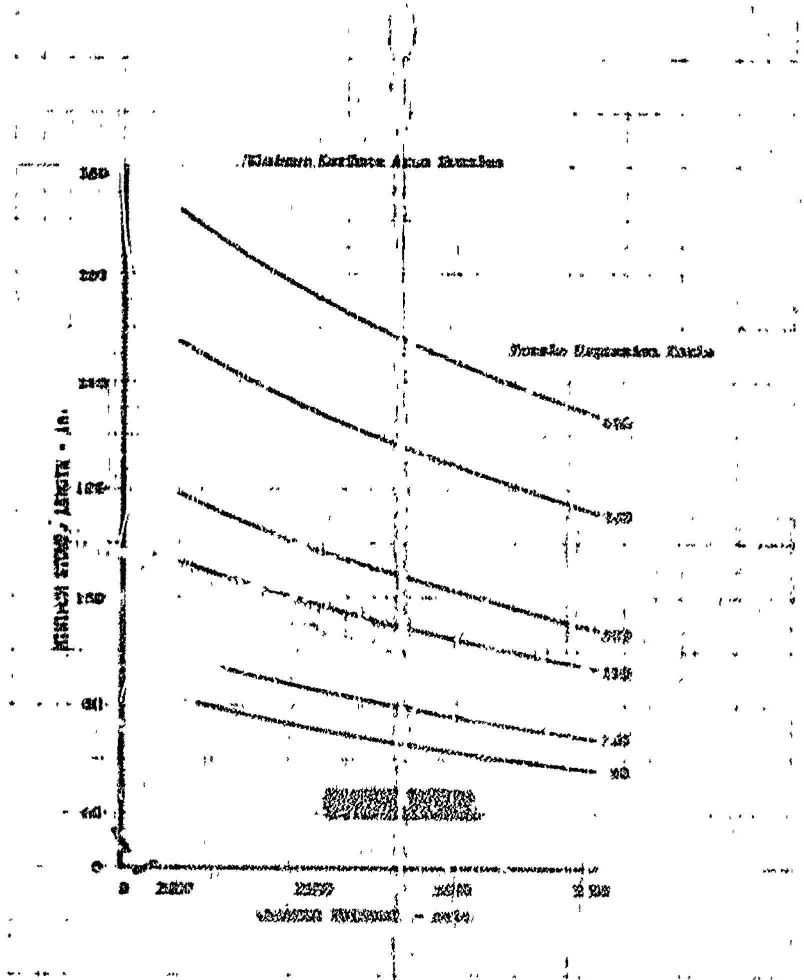

Figure 739. Minimum Stowed Length vs Chamber Pressure for 300,000-lb Thrust Engine

DF 56232

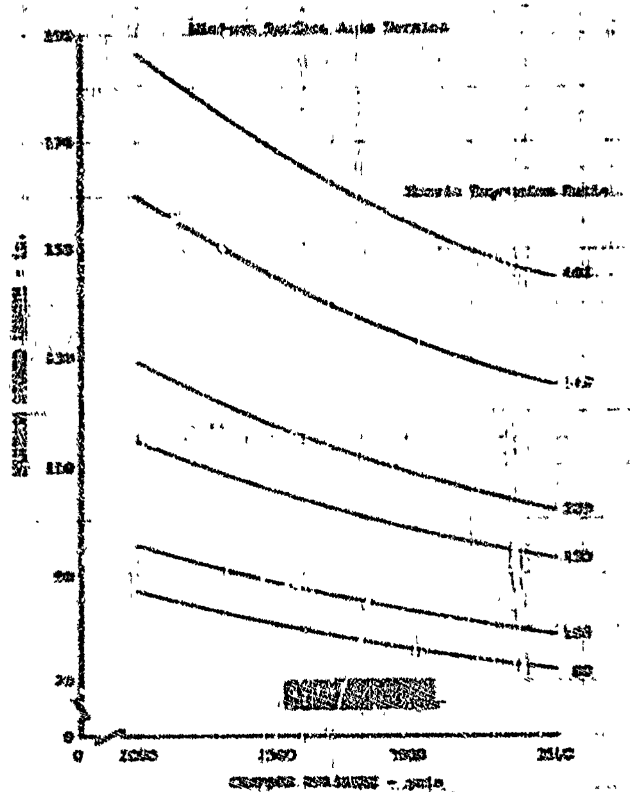

Figure 740. Minimum Stowed Length vs Chamber Pressure for 350,000-lb Thrust Engine DF 56233

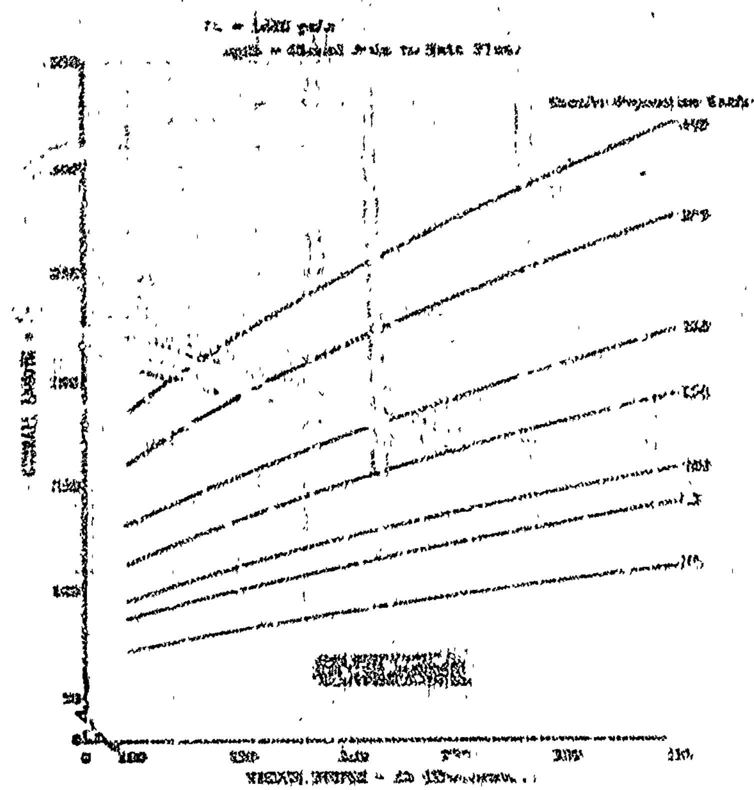

Figure 741. Overall Length vs Vacuum Thrust With Base Nozzle Contour DF 56212

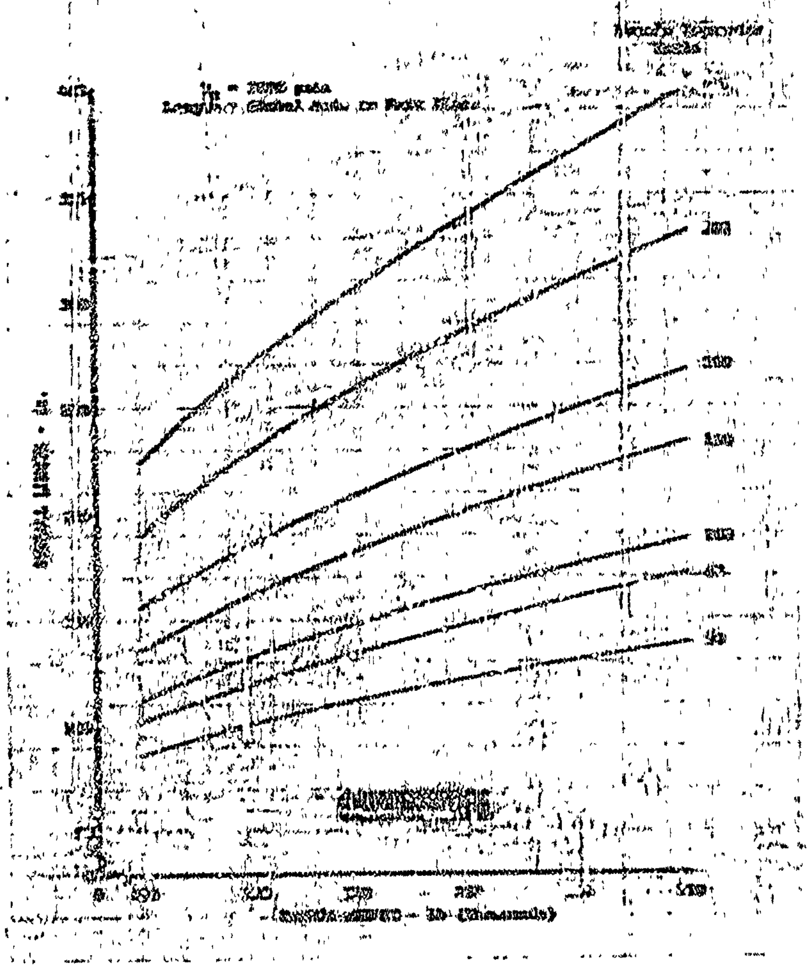

Figure 742. Overall Length vs Vacuum Thrust With Maximum Performance Nozzle Contour

DF 56260

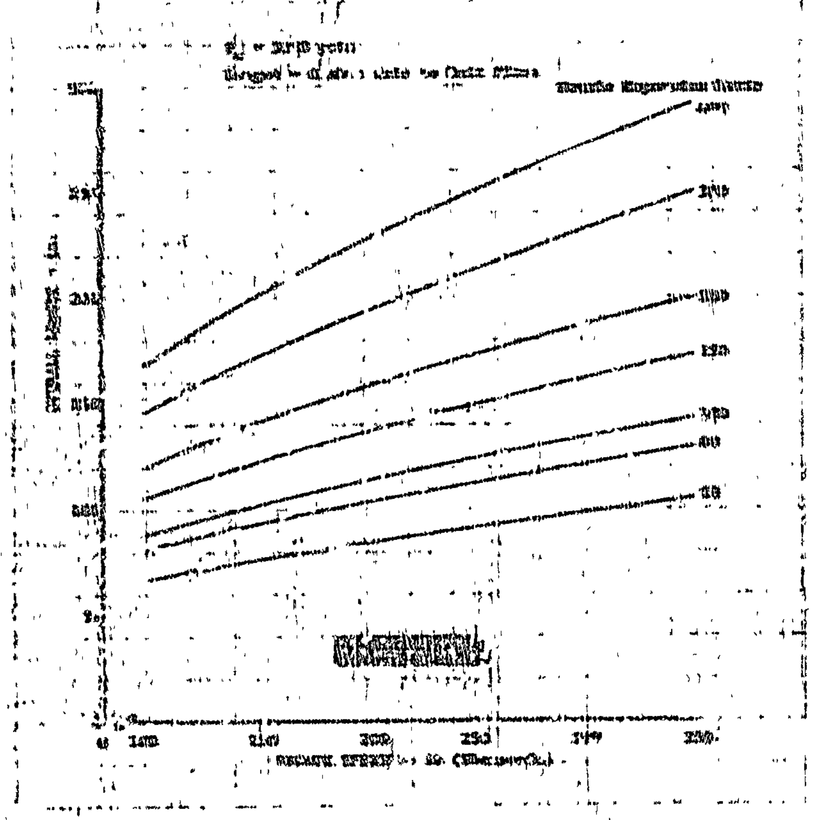

Figure 743. Overall Length vs Vacuum Thrust With Minimum Surface Area Nozzle Contour

DF 56211

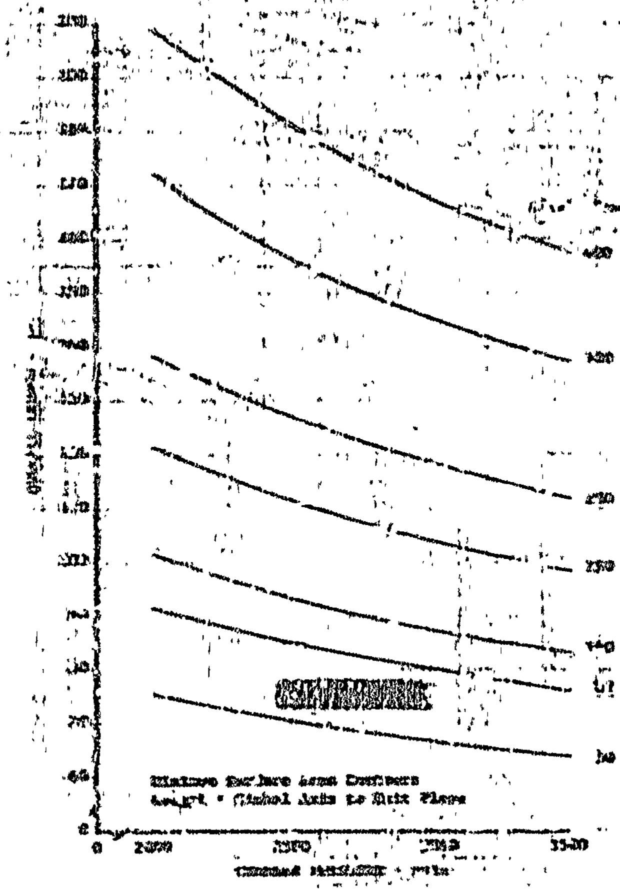

Figure 744. Overall Length vs Chamber Pressure for 1[illegible]0,000-lb Thrust Engine — DF 55003

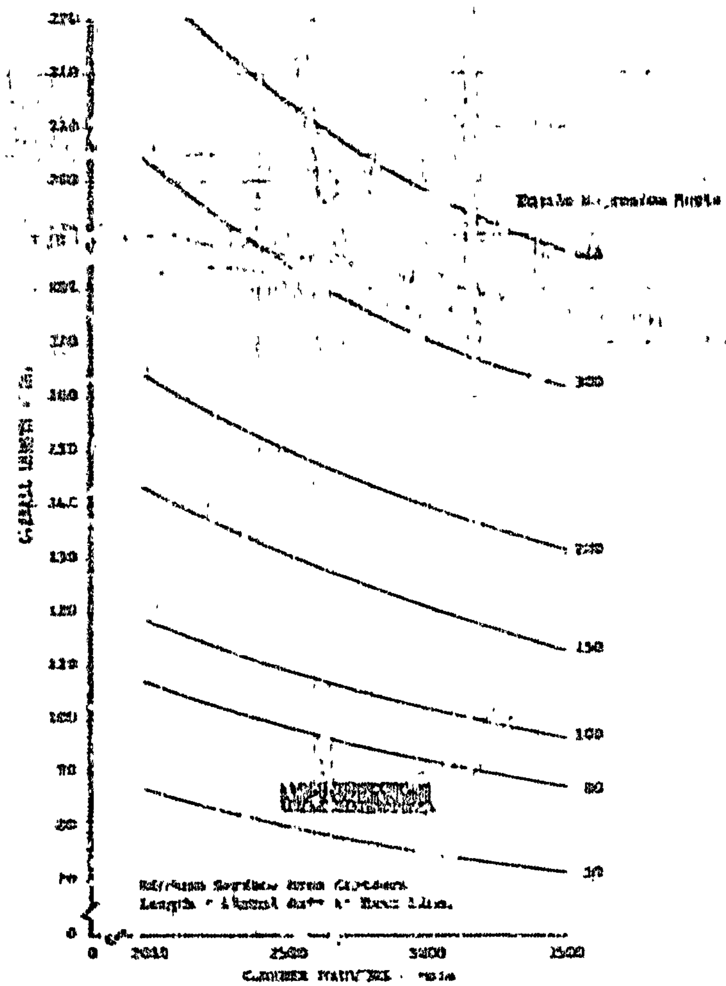

Figure 745. Overall Length vs Chamber Pressure for 150,000-lb Thrust Engine — DF 55402

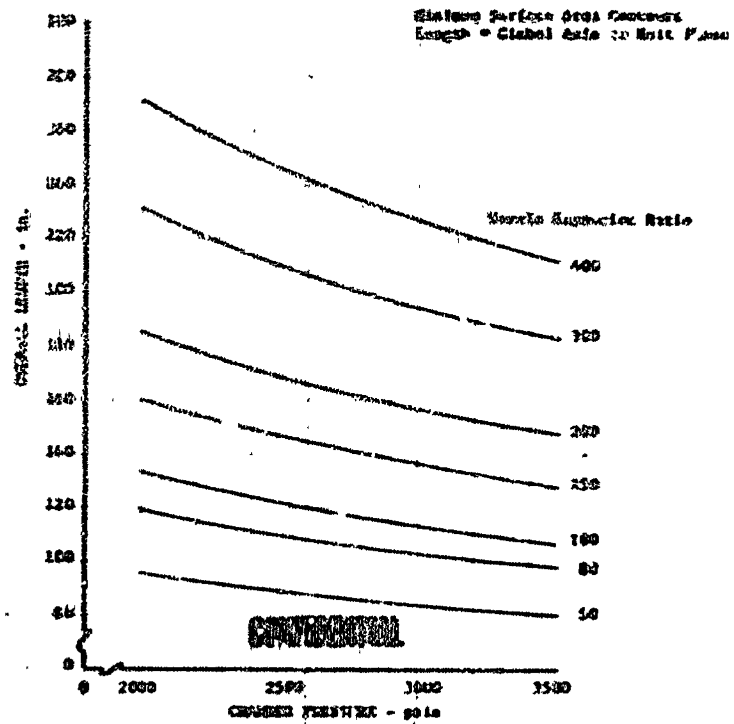

Figure 746. Overall Length vs Chamber Pressure for 200,000-lb Thrust Fngine

DF 55301

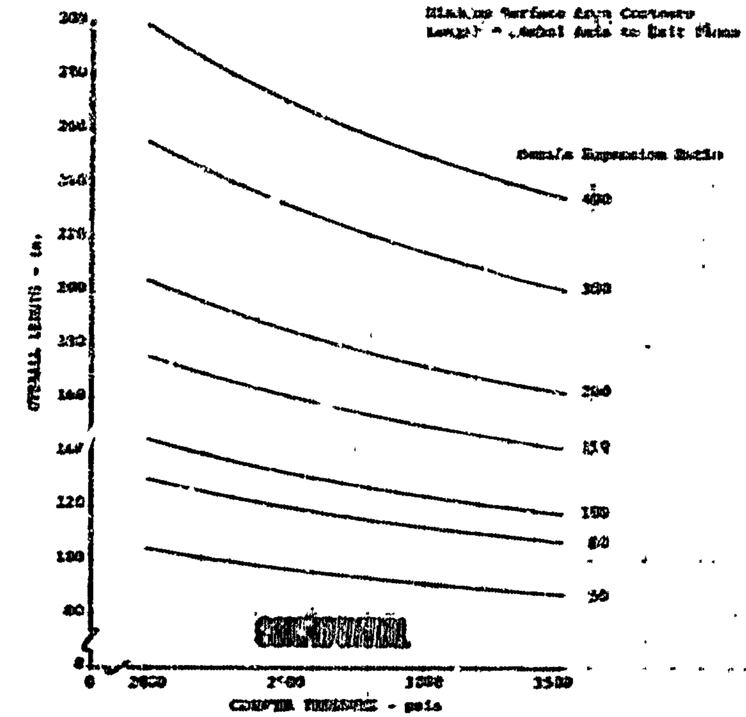

Figure 747. Overall Length vs Chamber Pressure for 250,000-lb Thrust Engine

DF 55800

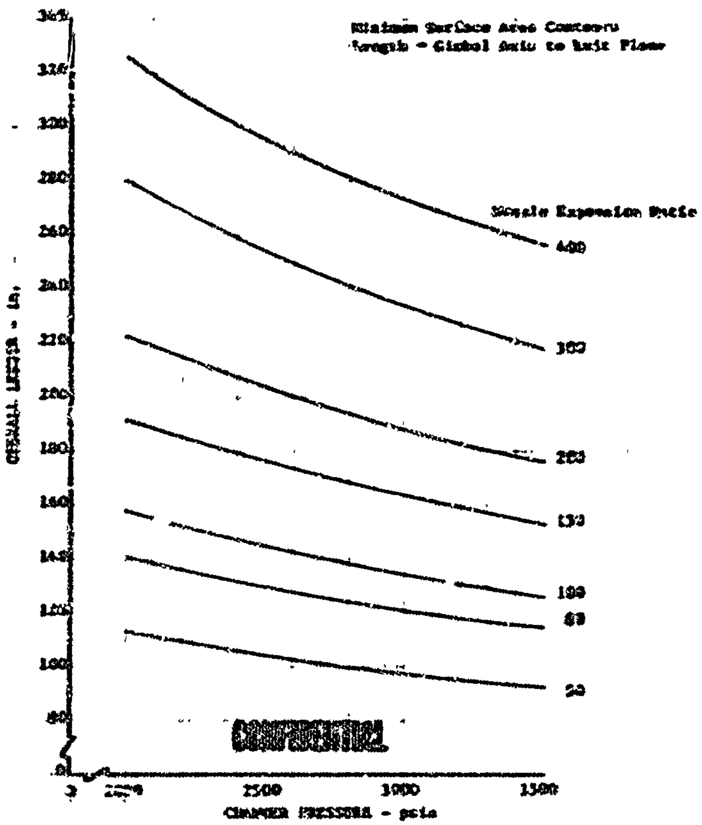

Figure 748. Overall Length vs Chamber Pressure for 300,000-lb Thrust Engine DF 55799

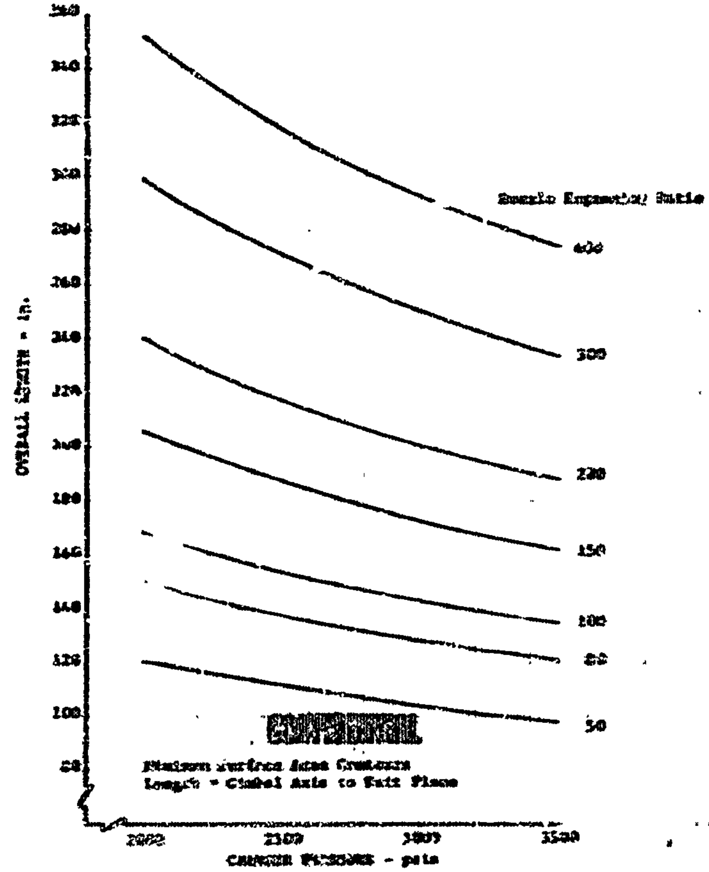

Figure 749. Overall Length vs Chamber Pressure for 350,000-lb Thrust Engine DF 55798

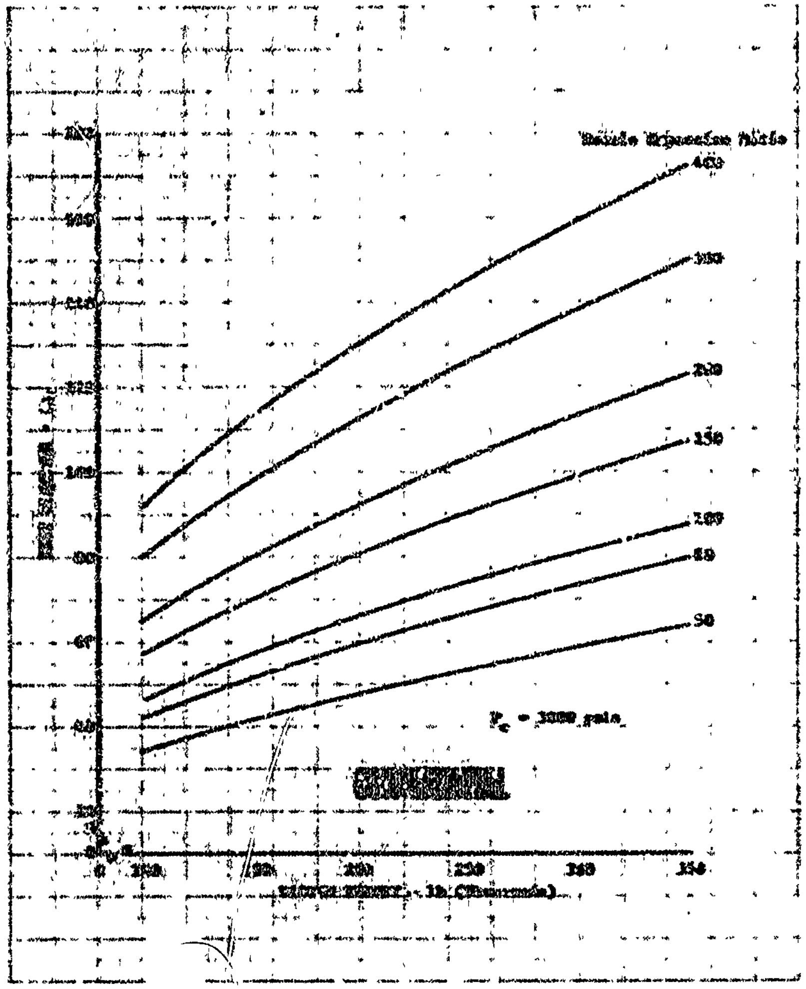

Figure 750. Overall Exit Diameter vs Vacuum Thrust DF 56257

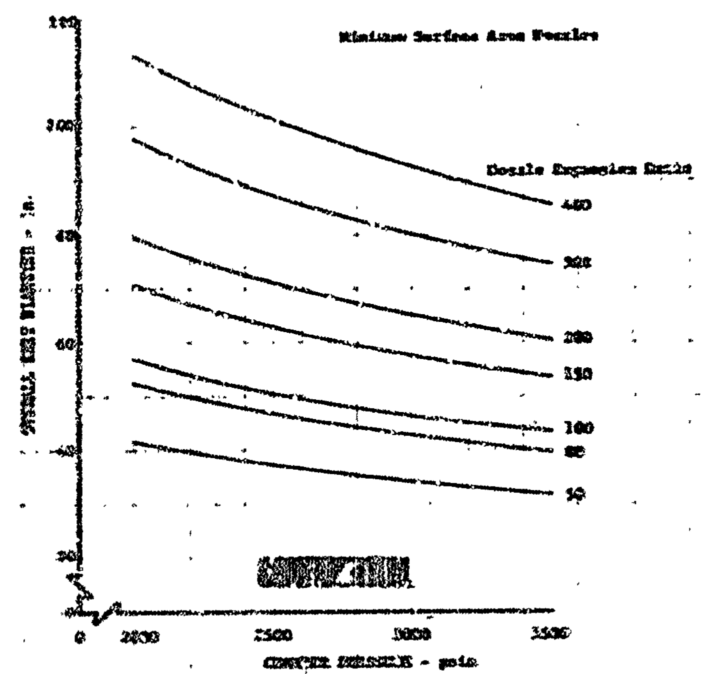

Figure 751. Overall Exit Diameter vs Chamber Pressure for 100,000-lb Thrust Engine DF 56218

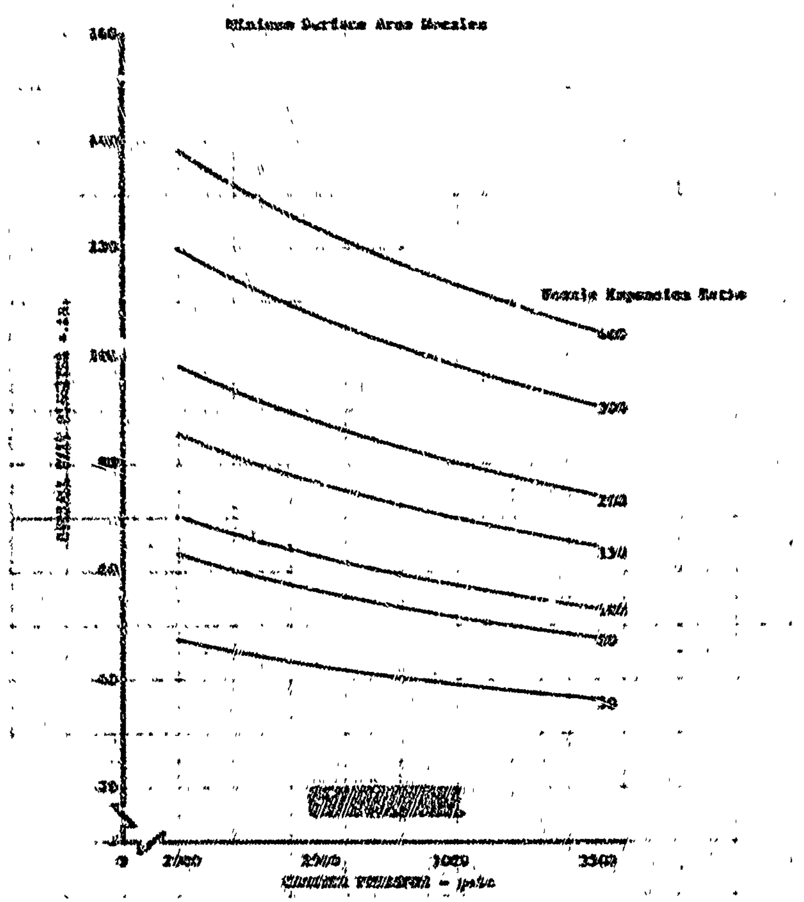

Figure 752. Overall Exit Diameter vs Chamber Pressure for 150,000-lb Thrust Engine

DF 56217

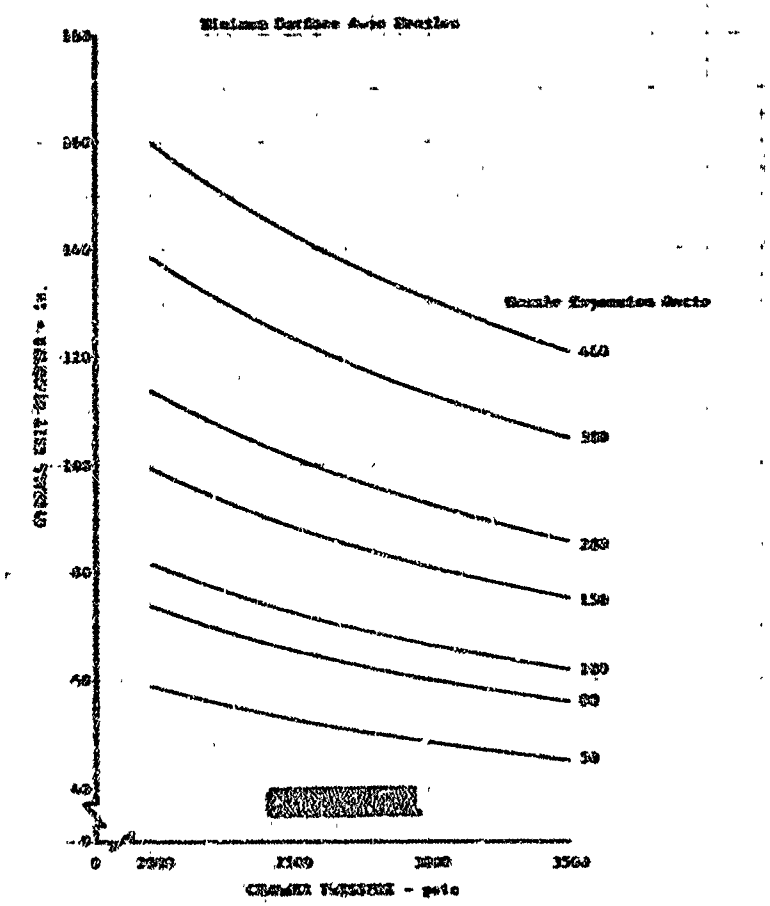

Figure 753. Overall Exit Diameter vs Chamber Pressure for 200,000-lb Thrust Engine

DF 56216

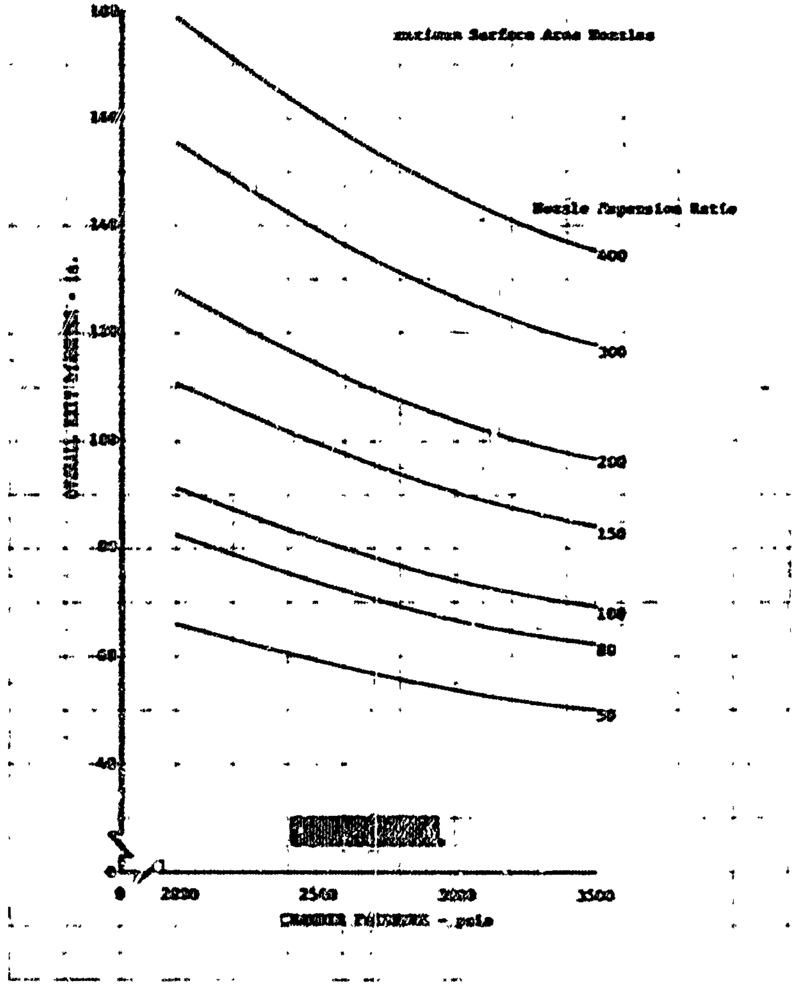

Figure 754. Overall Exit Diameter vs Chamber Pressure for 250,000-lb Thrust Engine

DF 56215

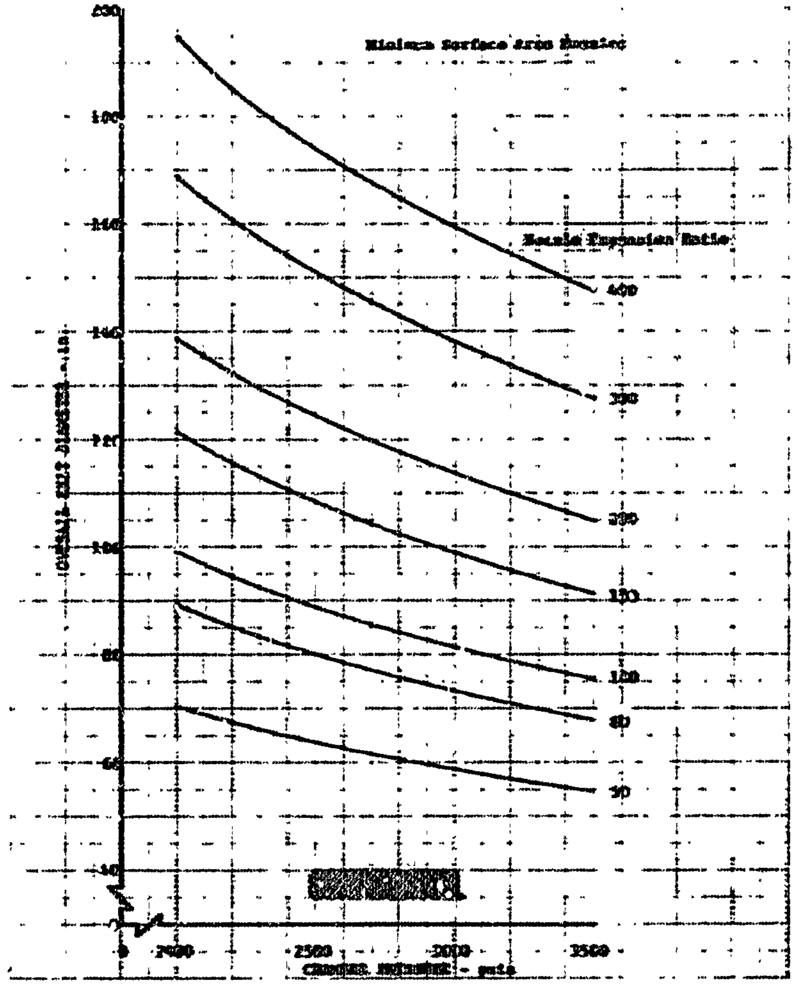

Figure 755. Overall Exit Diameter vs Chamber Pressure for 300,000-lb Thrust Engine

DF 56214

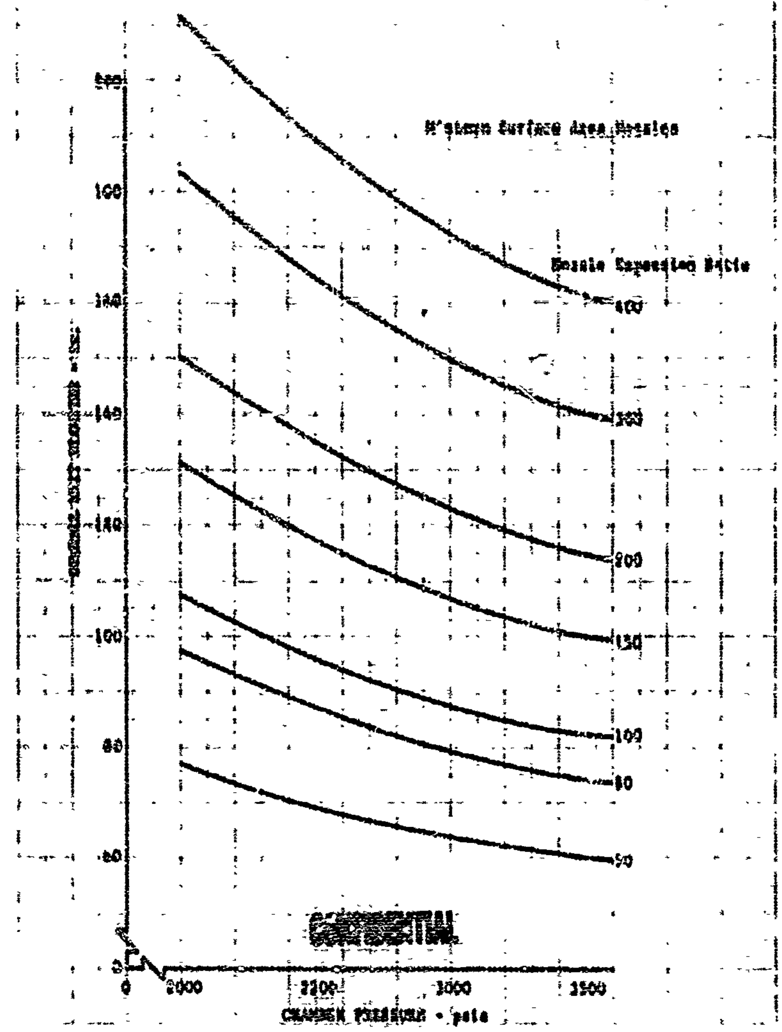

Figure 756. Overall Exit Diameter vs Chamber Pressure for 350,000-lb Thrust Engine DP 56213

APPENDIX IV
PERFORMANCE DATA REDUCTION

APPENDIX IV
PERFORMANCE DATA REDUCTION

(U) A treatment of the data, which are used to obtain the experimental performance parameters, is summarized in the following paragraphs.

A. NOZZLE THROAT AREA

1. Uncooled Chamber Tests

(U) Nozzle throat erosion during the uncooled tests requires a method for prorating the total erosion that occurs during a test to that which has occurred up to and during the data point time. Nozzle throat erosion is essentially eliminated except during the data period by using gaseous hydrogen film cooling during the transient conditions. The throat area at the data point was calculated from pre- and post-test throat diameters by assuming a constant diametric erosion rate during the data period when the coolant is turned off.

(U) To check the validity of the constant erosion rate assumption, a second method was used for comparison.

(U) The second method calculates the throat area from the equation:

$$A_x^*/A_o^* = k_1 \dot{w}_p / P_c,$$

where: k_1 is chosen to make A_x^*/A_o^* equal to unity immediately after the coolant is turned off.

(U) Because only minor changes in mixture ratio and chamber pressure occur during the period that the nozzle coolant is turned off, c* and η_c* are considered as constant. By assuming that the significant nozzle throat erosion occurs while the coolant is off and dividing A_x^* by the original throat area (A_o^*), the rate of change in A_x^* with coolant turned off can be estimated by the equation above.

(U) A comparison of the two methods is shown in figure 757.

(U) An estimate of the nozzle discharge coefficient, C_d, and resilient mechanical area change, ΔA^*, because of pressure and thermal gradients of test conditions were made to determine the aerodynamic throat area. The aerodynamic throat area, A*, is defined by the following equation.

$$A^* = (A_x^*)(1 + \Delta A^*/A_o^*)(C_d)$$

(U) The physical throat area change of the ATJ graphite nozzle insert used for the uncooled tests was estimated by computer analysis of the pressure and thermal gradients in the graphite nozzle throat insert. The nozzle insert was divided into a series of cylinders and the deformations caused by the temperature and pressure gradients were analyzed separately, and then superimposed. The analysis indicated that $\Delta A^*/A^*$ equals -0.009, a 0.9% throat area decrease. The compressive pressure loading on the outside diameter of the nozzle throat insert tended to decrease the throat area by 1.2% while thermal expansion tended to increase throat area by 0.3%.

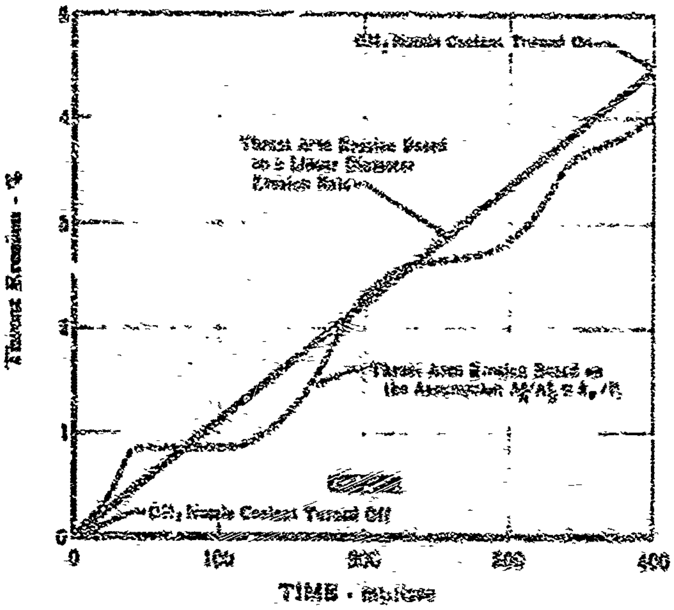

Figure 757. Nozzle Throat Estimation FD 17254A

(U) The discharge coefficients were determined from the nozzle inlet geometry by the relations shown in figure 758.[8]

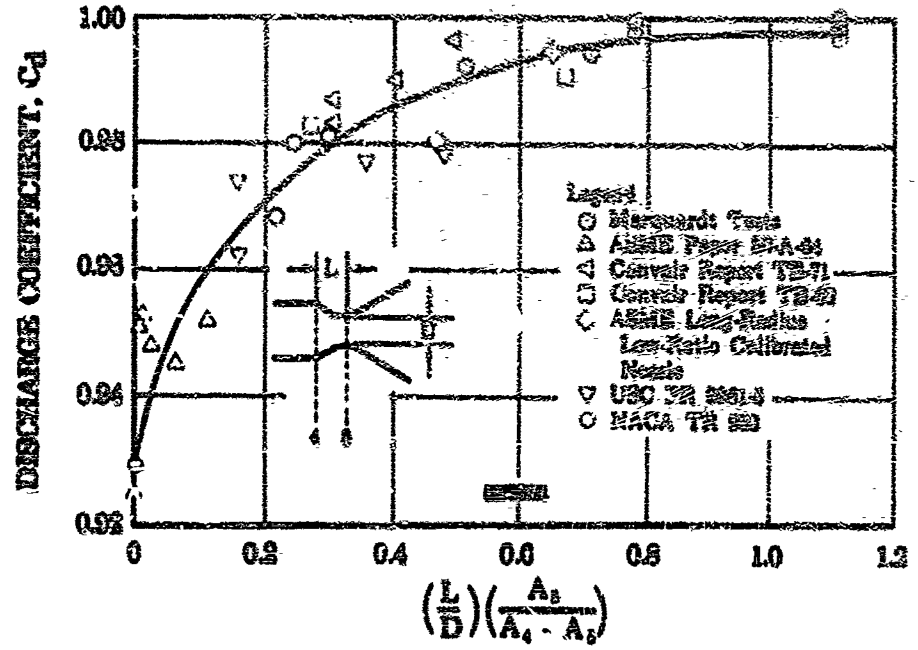

Figure 758. Discharge Coefficient vs Chamber Geometry FD 21118

(C) An estimate of nozzle throat discharge coefficient (C_d) for the contraction ratio of 5 chamber is 0.992.

---

8 Refer to Marquardt Report 5162, 1 August 1951.

2. Cooled Chamber Tests

(C) The cooled chamber, $\Delta A^*/A^*_0$, was assumed to be negligible because the cooled copper wafers are subject to less severe thermal gradients than the uncooled graphite nozzle insert.

(C) An estimate of the nozzle throat discharge coefficient for the contraction ratio of 3 chamber is 0.989.

B. NOZZLE EXIT AREA

1. 50K Model Tests

(U) The nozzle exit area was determined by physical measurements after every test.

2. 250K Tests

(U) The measured nozzle exit area $(A_e)_o$ was corrected for thermal expansion based on measured metal temperature.

$$A_e = (A_e)_o \text{ (expansion factor)}$$

C. NOZZLE AREA RATIO

(U) The nozzle area ratio was determined from the calculated aerodynamic throat and exit areas.

$$\epsilon = A_e/A^*$$

D. STAGNATION CHAMBER PRESSURE

(U) Main chamber pressure was measured as a static pressure at the injector face (P_{ci}) on the cooled chamber tests and by an additional static pressure tap (P_{cn}) at the entrance to the convergent nozzle section for the uncooled thrust chamber tests.

(U) For the uncooled chamber tests, the nozzle throat stagnation chamber pressure was calculated from measured nozzle entrance static pressure and the relation:

$$P_c = P_{cn} \times \text{function } (r, A_c/A^*)$$

(U) For the cooled chamber tests, a momentum balance determined the nozzle entrance static pressure from the injector face readings. The throat stagnation pressure was then calculated as described above.

(U) The momentum balance analysis assumed that the flow is parallel and homogeneous at the nozzle entrance. Neglecting wall friction, the equation is:

$$A_c P_{ci} + z = \dot{w}_p \frac{V}{g} + A_c P_{cn}$$

where:

x = Axial momentum of the propellants at the injector face
A_c = Combustion chamber area
P_{ci} = Static pressure at the injector face
v = Velocity at the nozzle entrance, $f(r, A_c/A^*)$
P_{cn} = Static pressure at the nozzle entrance.

(U) If each propellant is injected at an injector pressure differential ΔP, with an effective area A_{cd}, and inclined to the chamber axis at an angle the total momentum is:

$$x = (2A_{cd}\ \Delta P \cos\theta)_f + (2A_{cd}\ \Delta P \cos\theta)_o$$

(U) For the uncooled runs, the nozzle entrance static pressure was calculated to be approximately 58 psia less than the measured static pressure at the injector face. Corresponding pressure measurements verified this ~~static pressure loss to be 50 ± 5 psia; this verified the momentum~~ balance method used.

E. PROPELLANT FLOW RATE

(U) $\dot{w}_p = \dot{w}_o + \dot{w}_f$

where:

$\dot{w}$ = Volumetric flow rate x density

(U) Volumetric propellant flow rates are measured with turbine-type flowmeters or standard orifices. The propellant densities are established by temperature and pressure measurements at the flowmeters.

(U) Oxygen contamination was measured from samples taken immediately before and after each test. The oxidizer flow rate was corrected for the difference in densities of O_2, N_2, and A.

(U) Propellant leakages through stand valves and flange seals were measured with standard orifices.

F. MIXTURE RATIO

(U) $r = \dot{w}_o/\dot{w}_f$

G. THRUST

1. 50K Model Tests

(U) $F_{vac} = F_{meas} + P_a(A_s) + (A_e - A_s)P_s$

where:

A_s = Nozzle area at diffuser seal

P_s = Pressure acting on outside of nozzle skirt downstream of the diffuser seal.

(U) For the run test (50SC3C), which was conducted without a diffuser, separation occurred and a separation drag thrust correction was applied by graphically integrating the pressure area parameters downstream of the area ratio at which the separation occurred.

2. 250K Tests

(U) For the retracted nozzle tests the sea level thrust was measured directly.

(U) For the extended nozzle tests:

$$F_{vac} = F_{meas} + A_e \times P_{amb}.$$

H. CHAMBER HEAT LOSS

(U) The 50K uncooled tests were conducted with graphite and copper chamber liners. The graphite was uncooled but the copper liners were GH_2 film-cooled except at the data point. A heat transfer computer program was conducted to analyze both the graphite and copper chamber liner heat transfer using film coefficients as calculated by the Bartz[9] equation.

(C) The total heat flux was estimated to be 5000 and 4200 Btu/sec for the uncooled copper and graphite liners, respectively. The effect of these heat fluxes on characteristic velocity and vacuum impulse was estimated by a theoretical combustion program to be approximately 0.28 and 0.44% respectively.

I. NOZZLE HEAT LOSS

(C) For the uncooled nozzle tests the nozzle skirt downstream of an area ratio of 4.75 was film-cooled with water except at the data point. Analysis of the transient heat transfer was used to obtain a heat loss and heat loss profile.

(C) On five 250K tests (250SC7C through 250SC11C), the primary nozzle was hydrogen cooled from an area ratio of 4.75 to an area ratio of 20. The nozzle heat loss in this section was determined from measured coolant flow rates and inlet and discharge conditions.

(U) The effect of heat loss on performance was estimated by computing the theoretical performance for an equivalent loss of heat at discrete nozzle stations.

---

9 Bartz, D.R., "A Simple Equation for Rapid Estimation of Rocket Nozzle Convective Heat Transfer Coefficients," Jet Propulsion 27 (49) 1957.

J. PROPELLANT INJECTOR PARAMETERS

1. Fuel Injection Velocity

(U) In the following equations subscript "f" refers to the hydrogen in the preburner and to the preburner combustion products in the main burner.

$$V_f = \sqrt{\frac{P_t\ 2g\ \gamma_f}{\rho_f(\gamma_f - 1)} \left[\left(\frac{P_t}{P}\right)_f^{\frac{\gamma-1}{\gamma}} - 1\right] \Bigg/ \left(\frac{P_t}{P}\right)_f^{\frac{\gamma+1}{\gamma}}} \qquad \text{(250K Tests)}$$

$$V_f = \sqrt{\frac{2g\ \Delta P_f}{\rho_f}} \qquad \text{(50K Tests)}$$

2 Oxidizer Injection Velocity

(U) $$V_o = \sqrt{\frac{2g\ \Delta P_o}{\rho_o}}$$

3. Injection Velocity Ratio

(U) $$VR = \frac{V_f}{V_o}$$

d. Injection Momentum Ratio

(U) $$MR_{\substack{\text{main}\\ \text{burner}}} = \dot{w}_{fs}\ V_f \big/ \dot{w}_o V_o = \left(1 - \frac{\dot{w}_r}{\dot{w}_f}\right)\left(\frac{\dot{w}_f V_f}{\dot{w}_o V_o}\right)$$

where:

$\dot{w}_{fs}$ = Flow through the fuel slots around the oxygen elements

$\dot{w}_r/\dot{w}_f$ = A_{cd} Rigimesh injector face/A_{cd} Fuel total x 100 = % face cooling

(U) $MR_{preburner} = \dot{w}_f V_f / \dot{w}_o V_o$

K. SPECIFIC IMPULSE

(U) $I_s = F/\dot{w}_p$

L. IMPULSE EFFICIENCY

1. Nozzle Retracted

(U) $\eta_{I_{s1}} = 100(I'_{s1}/I_{s1})$

where I'_{sl} is a function of propellant inlet conditions, chamber pressure, exhaust pressure, overall mixture ratio, nozzle area ratio, oxidizer contamination, and nozzle and chamber heat loss; for one-dimensional isentropic flow and shifting equilibrium.

2. Nozzle Extended

(U) $$\eta_{I_{vac}} = 100(I_{vac}/I'_{vac})$$

where I'_{vac} is a function of propellant inlet conditions, chamber pressure overall mixture ratio, nozzle area ratio, oxidizer contamination, and nozzle and chamber heat loss; for one-dimensional isentropic flow and shifting equilibrium.

M. THRUST COEFFICIENT

(U) $$C_f = F/P_c A^*$$

N. THRUST COEFFICIENT EFFICIENCY

1. Nozzle Retracted

(U) $$\eta_{C_{F_{sl}}} = 100(C_{F_{sl}}/C'_{F_{sl}})$$

where $C'_{F_{sl}}$ is a function of propellant inlet conditions, chamber pressure, exhaust pressure, overall mixture ratio, nozzle area ratio, oxidizer contamination, and nozzle heat loss; for one-dimensional isentropic flow and shifting equilibrium.

2. Nozzle Extended

(U) $$\eta_{C_{F_{vac}}} = 100(C_{F_{vac}}/C'_{F_{vac}})$$

where $C'_{F_{vac}}$ is a function of propellant inlet conditions, chamber pressure, overall mixture ratio, nozzle area ratio, oxidizer contamination, and nozzle heat loss; for one-dimensional isentropic flow and shifting equilibrium.

O. CHARACTERISTIC VELOCITY

(U) $$c^* = P_c A^* g/\dot{w}_p$$

P. CHARACTERISTIC VELOCITY EFFICIENCY

(U) $$\eta_{c^*} = 100(c^*/c^{*\prime})$$

where $c^{*\prime}$ is a function of propellant inlet conditions, chamber pressure, throat mixture ratio, oxidizer contamination, and chamber heat loss (for uncooled tests); for one-dimensional isentropic flow and shifting equilibrium.

Q. TEST DURATION AND DATA POINT TIME

(U) Test duration and the data point times were selected by the techniques shown in figure 759.

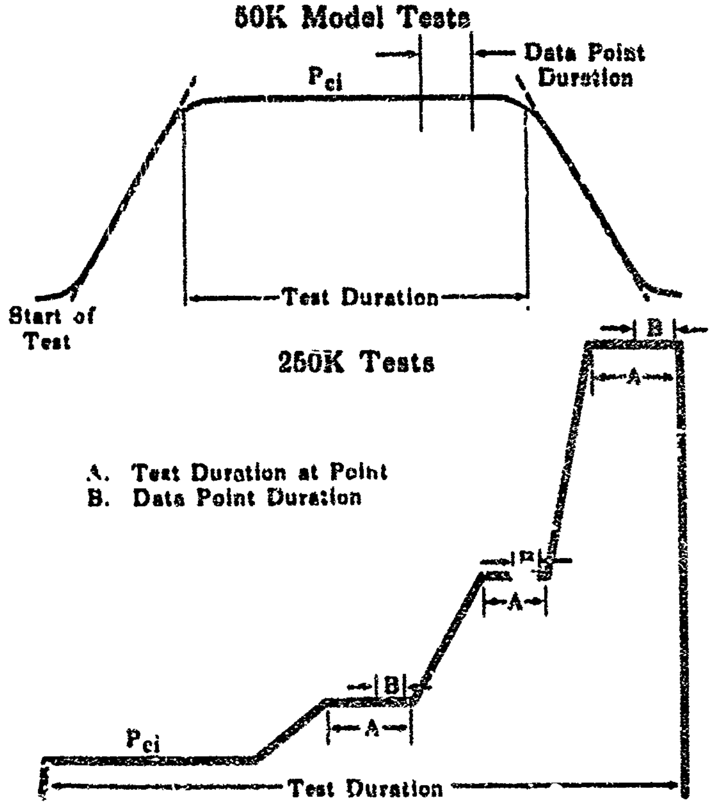

Figure 759. Typical P_c Tracer Showing Base for Firing Duration and Data Period FD 23065

R. TEST INSTRUMENTATION ERROR ANALYSIS

1. 50K Data

(U) An error analysis was made to estimate the accuracy of the combustion performance data. The method by Dr. J. N. Berretone[10], "Tolerancing by the Statistical or Differential Method," was used. According to Berretone's equation, the error, Δy, in the dependent variable y, is a function of the independent variables, x, and their estimated maximum probable errors Δx as shown by the relation:

$$\Delta y = \left[\sum_{1}^{N} \left(\partial y/\partial x_1\right)^2 \left(\Delta x_1\right)^2 + \left(\partial y/\partial x_2\right)^2 \left(\Delta x_2\right)^2 + \left(\partial y/\partial x_N\right)^2 \left(\Delta x_N\right)^2\right]^{1/2}$$

where N is the total number of independent variables.

[10] Chairman, Department of Statistics, Western Reserve University

(U) Maximum expected instrumentation errors (two standard deviations) for the 50,000-lbf thrust level tests on the B-2B test facility were:

Parameter	Maximum Expected Instrumentation Error
Chamber pressure*	± 0.41%
Flowmeter pressures	± 0.48%
LO_2 volumetric flow rate	± 0.64%
LH_2 volumetric flow rate	± 0.71%
GH_2 volumetric flow rate	± 1.4%
LO_2 flowmeter temperature	± 0.13°R
LH_2 flowmeter temperature	± 0.13°R
GH_2 flowmeter temperature	± 2.0°R
Thrust	± 0.36%

*Based on redundant pressure readings.

(U) The maximum expected error for nozzle throat area was ± 1.0% and ± 0.[illegible]% for the uncooled and cooled tests, respectively.

(C) Applying the error analysis equation yields the following estimated performance data errors:

Parameter	Uncooled Tests		Cooled Tests	
	Nominal Value	Estimated Error (% of Nominal)	Nominal Value	Estimated Error (% of Nominal)
F_{vac}	50,000 lb_f	± 0.42%	50,000 lb_f	± 0.42%
$\dot{w}_o$	96.2 lb/sec	± 1.16%	94.5 lb/sec	± 1.15%
$\dot{w}_f$	14.8 lb/sec	± 0.87%	14.2 lb/sec	± 0.87%
$\dot{w}_c$			3.0 lb/sec	± 1.5%
r	6.5	± 1.45%	5.5	± 1.38%
c*	7390 ft/sec	± 1.46%	7540 ft/sec	± 1.05%
$C_{F_{vac}}$	1.96	± 1.13%	1.92	± 0.58%
I_{vac}	449 sec	± 1.10%	448 sec	± 1.07%
c*'	7540 ft/sec	± 0.29%	7775 ft/sec	± 0.21%
$C'_{F_{vac}}$	2.00	± 0.21%	1.95	± 0.18%
I'_{vac}	468 sec	± 0.10%	471 sec	± 0.03%
η_{c^*}	98.0%	± 1.49%	97.0%	± 1.07%
$\eta_{C_{F_{vac}}}$	98.0%	± 1.15%	98.0%	± 0.60%
$\eta_{I_{vac}}$	96.0%	± 1.11%	95.0%	± 1.07%

2. 250K Data

(U) The error analysis made of the 250K data used the method based on the preliminary recommendations of the Interagency Chemical Rocket Propulsion Group, Measurement Uncertainty Committee, and provides four separate numbers. The factors considered are:

1. Precision Error (σ) - A measure of the scatter or nonrepeatability of a measurement. The precision error of a measurement is reported as one sample standard deviation. It is a statistic calculated directly from redundant measurement data or indirectly as a linear combination of variance estimates.

2. Degrees of Freedom (DF) - The effective sample size used in estimating the precision error. The degrees of freedom associated with the precision error is reported and reflects the sample size and the method used to obtain the precision error estimate. If the estimate is a root sum square of other estimates based on different sample sizes, the Welch-Satterthwaite[11] method is used to estimate the degrees of freedom. If the degrees of freedom exceeds 30, it is not reported (except that DF > 30).

3. Bias (B) - The systematic error of the measurement. All known biases are removed; the remaining bias is unknown in both magnitude and sign. The error is reported as an upper limit or upper bound based on a best engineering judgment. These limits are ordinarily in the form ± B. B is not a statistic (i.e., not data).

4. Uncertainty (U) - An arbitrary measure of the system accuracy or closeness of the measurement to the truth. This is calculated from

$$U = \sqrt{B^2 + (t_{95;DF}\sigma)^2}$$

where:

$t_{95;DF}$ = The 95% value based on a t distribution for the degrees of freedom (DF) reported in (2).
B = Bias from (3)
σ = Precision error from (1)

The uncertainty is calculated as a linear combination of bias and precision error. This term does not have statistical validity but is useful as a single number representing accuracy.

(U) The errors of calculated parameters based on measured parameters are calculated using the method of partial derivatives and the statistical theory of propagation of error. The precision error for a calculated value, x, which is a function of two other variables y, z, i.e., x = f(y,z) is calculated using a Taylor series expansion for a function of two variables. Thus

$$\sigma_x = \sqrt{\left(\frac{\partial f}{\partial y}\sigma_y\right)^2 + \left(\frac{\partial f}{\partial z}\sigma_z\right)^2}$$

[11] K. A. Brownlee, Statistical Theory and Methodology in Science and Engineering," John Wiley & Sons, New York City, N. Y., 1960 pp 230-240.

(U) The maximum expected measurement errors for the 250,000-lb thrust level tests on the E-8 test facility were:

Parameter	Precision (1σ)	Bias (Maximum Estimated)
Chamber pressure	± 0.22%	± 0.23%
Flowmeter pressure	± 0.09%	± 0.18%
LO_2 flow rate (total)	± 0.20%	± 1.32%
LO_2 flow rate (preburner)	± 0.21%	± 1.52%
LO_2 flow rate (main burner)	± 0.20%	± 1.33%
LH_2 flow rate (preburner)	± 0.21%	± 1.67%
GH_2 flow rate (preburner)	± 0.33%	± 3.00%
GH_2 flow rate (coolant)	± 0.17%	± 2.50%
LO_2 flowmeter temperature	± 0.05°R	± 0.10°R
LH_2 flowmeter temperature	± 0.02°R	± 0.05°R
GH_2 flowmeter temperature	± 0.14°R	± 1.31°R
Thrust	± 0.19%	--
A_t	± 0.07%	--
A_e	± 0.09%	--

(C) Applying the error analysis yields the following estimated performance data errors:

Parameter	Nominal Value*	Precision (1σ)	Bias (Maximum Estimated)	Uncertainty (U)
F_{vac}	246,290	± 0.16%	--	± 0.31%
$\dot{w}_o$	467.7	± 0.14%	± 0.89%	± 0.93%
$\dot{w}_f$	74.3	± 0.18%	± 2.20%	± 2.22%
$\dot{w}_c$	5.3	± 0.17%	± 2.50%	± 2.52%
r	5.88	± 0.22%	± 1.67%	± 1.72%
c^*	7556	± 0.26%	± 0.82%	± 0.97%
$C_{F_{vac}}$	1.918	± 0.26%	± 0.23%	± 0.56%
I_{vac}	450	± 0.20%	± 0.79%	± 0.88%
$c^{*\prime}$	7695	± 0.04	± 0.31%	± 0.32%
$C'_{F_{vac}}$	1.941	± 0.03	± 0.23%	± 0.24%
I'_{vac}	465	± 0.01	± 0.06%	± 0.07%
η_{c^*}	98.2	± 0.26%	± 0.87%	± 1.02%
$\eta_{C_{F_{vac}}}$	98.8	± 0.26%	± 0.32%	± 0.61%
$\eta_{I_{vac}}$	96.7	± 0.20%	± 0.79%	± 0.86%

*Based on test No. 250SC7C, 100% thrust data.

Note: The degrees of freedom were greater than 30.

(U) The above analyses of the 50% and 250% data apply only to instrumentation and other measuring techniques to which maximum expected errors can be estimated with a high degree of confidence. The effect of other factors such as heat loss, contamination effects, imperfect steady-state conditions, and inexact knowledge of the thermodynamic nozzle throat area behavior can only be approximated and increase the actual maximum expected errors over the values given.

S. ANALYTICAL PERFORMANCE MODELS

1. Combustion Gas Profile

(U) A combustion gas profile model was used to determine the effect on performance of combustion chamber mixture ratio profile (incomplete mixing) exclusive of the effect of transpiration cooling.

(U) The propellants, chamber pressure, exhaust nozzle area ratio, and average engine mixture ratio are selected, and the theoretical characteristic velocity and thrust coefficient calculated as reference values. The reaction products are distribution divided into nineteen stream tubes of equal mass fraction. A parabolic mixture ratio about the mean mixture ratio is arbitrarily assumed. A mixture ratio of some arbitrary increment below the average engine mixture ratio is selected, and the required mixture ratio for a corresponding stream tube above average engine mixture ratio is calculated as follows:

(U) The weight fraction of fuel and oxidizer based on the engine mixture ratio are:

$$X_{f_a} = \frac{1}{1 + r_{oa}} \text{ and } X_{o_a} = \frac{r_{oa}}{1 + r_{oa}}$$

(U) The weight fractions of the total fuel and total oxidizer in a lower mixture ratio stream tube were:

$$X_{f_1} = \frac{Y_1}{1 + r_1} \text{ and } X_{o_1} = \frac{Y_1 r_1}{1 + r_1}$$

(U) the weight fraction of total fuel and oxidizer in the higher mixture stream tube is:

$$X_{f_h} = X_{f_a} - X_{f_1} \text{ and } X_{o_h} = X_{o_a} - X_{o_1}$$

and the mixture ratio is:

$$r_h = \frac{X_{o_2}}{X_{f_h}}$$

(U) Having determined the mixture ratio for all the stream tubes, the performance for the unmixed case is calculated. First, the throat condition for the simultaneous expansion of the stream tubes is found by minimizing the flow area for the sum of the stream tubes.

$$\dot{w} = \rho A V = \text{constant}$$

$$A = \frac{\dot{w}}{\rho V} = \text{minimum at nozzle throat}$$

or

$$A^* = \frac{Y_1}{\rho_1 V_1} + \frac{Y_2}{\rho_2 V_2} + \ldots + \frac{Y_{19}}{\rho_{19} V_{19}} = \text{minimum} \qquad (12)$$

(U) Gas densities and velocities are found by determining equilibrium performance with expansion to a series of pressures near the estimated throat pressure. An area is calculated and the throat pressure is determined for the minimum value solution of equation (12).

(U) A similar procedure is then used to determine the vacuum specific impulse based on expansion to the area ratio of interest. For a given exit pressure the area ratio is:

$$\frac{A_e}{A^*} = \frac{Y_{1_e}/\rho_{1_e} V_{1_e} + Y_{2_e}/\rho_{2_e} V_{2_e} + \ldots + Y_{19_e}/\rho_{19_e} V_{19_e}}{Y_1^*/\rho_1^* V_1^* + Y_2^*/\rho_2^* V_2^* + \ldots + Y_{19}^*/\rho_{19}^* V_{19}^*} \qquad (13)$$

(U) For several pressures near the estimated exit pressure the density and velocity are found with the combustion deck. The exit pressure corresponding to the area ratio of interest is found by interpolation.

(U) I_{vac} and c^* are calculated for each stream tube with the equilibrium performance deck for the determined throat pressure and nozzle exit pressure. The unmixed performance is then calculated by taking weighted averages of the stream tubes.

$$c^* = Y_1 c_1^* + Y_2 c_2^* + \ldots + Y_{19} c_{19}^*$$

$$I_{vac} = Y_1 I_{vac\ 1} + Y_2 I_{vac\ 2} + \ldots + Y_{19} I_{vac\ 19}$$

(U) The unmixed characteristic velocity and vacuum specific impulse efficiency relative to the completely mixed case are:

$$\eta_{c^*} = \frac{c^*}{c^{*'}} \text{ and } \eta_{I_{vac}} = \frac{I_{vac}}{I'_{vac}}$$

where $c^{*'}$ and I'_{vac} are theoretical values at the average m[illegible] ratio, and the thrust coefficient efficiency is:

$$\eta_{C_{F_{vac}}} = \frac{\eta_{I_{vac}}}{\eta_{c^*}}$$

(U) η_{c^*}, η_{Cp}, and $\eta_{I_{vac}}$, as functions of mixture ratio profile at constant engine mixture ratio can be determined by assuming different increments of mixture ratio, $r_{oa} - r_i$, and repeating the calculations.

2. Transpiration Cooling Mixture Ratio Profile Model

(U) An analytical model that assumes partial mixing of the injector combustion gases and hydrogen coolant was used to estimate the effect of transpiration cooling on performance. A mixture ratio profile for the flow passing through the throat section is assumed as shown in figure 760. The profile is calculated by assuming:

1. The mixture ratio varies linearly with area across a diffusion layer from the wall to the mainstream.
2. The local gas temperature across the profile is equal to the ideal combustion temperature at the local mixture ratio.
3. The stream tube mass fraction is proportional to tube area fraction.

(U) The profile in the diffusion layer is divided into i concentric stream tubes of equal area. The area of each tube (ΔA_i^*) is determined by summing the weighted average of the percent fuel of each tube (including the mainstream) and equating the sum to the average overall percent fuel value at the throat, as shown in the following equation:

$$\sum_i (\%\ \text{fuel})_i\ \Delta A_i^* = (\text{Overall Throat \% fuel})\ A^* \qquad (14)$$

(U) The predicted characteristic velocity (c^*) is determined by summing the mass fraction contribution of the theoretical characteristic velocities of each stream tube.

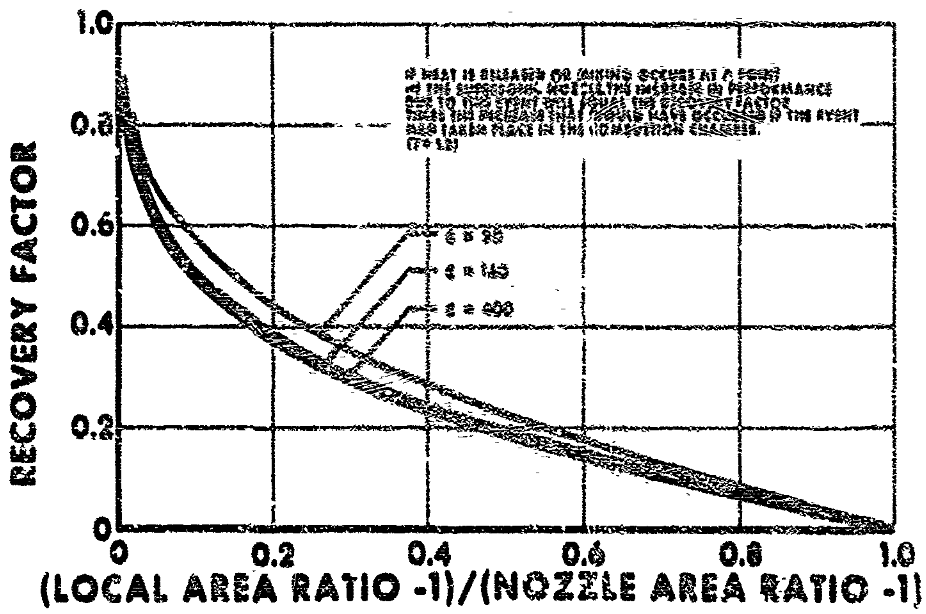

Figure 760. Mixture Ratio Profile FD 14021

(U) Base specific impulse is the summation of the specific impulses corresponding to the various stream tube mixture ratios at the throat as expressed by the following equation:

$$I_{S_{\text{Throat (Base)}}} = \left[\frac{\text{Total Engine Flow} - \text{Transpiration Cooling Downstream of Throat}}{\text{Total Engine Flow}} \right] \sum_i (I_S)_i \left(\frac{\Delta A_i^*}{A^*} \right) \qquad (15)$$

(U) Because a portion of the transpiration cooling flow is injected through the nozzle wall downstream of the throat, the continuing diffusion of the cooling flow into the main flow (burning or releasing of energy) alters this base impulse.

(U) Specific impulse is calculated at the cross section where the transpiration cooling flow terminates in the nozzle by the same procedure as that described for the throat section. Sections in the nozzle downstream of the end of transpiration cooling are examined also. New mixture ratio profiles are constructed and their resulting specific impulses calculated. The new profiles are determined by assuming that the diffusion layer increases at a constant rate for every unit length/unit diameter (L/D) in the nozzle. The difference between the thickness of the diffusion layer at the end of the transpiration cooled section and at the throat divided by the $\Sigma(\Delta L/D)$ at the end of the cooling section is the radial growth per increment of L/D. Therefore, at any other section in the nozzle the $\Sigma(\Delta L/D)$ of that section will yield the increase in diffusion layer thickness over the value at the throat. $\Sigma(\Delta L/D)$ vs expansion ratio for a typical bell nozzle is illustrated in figure 761.

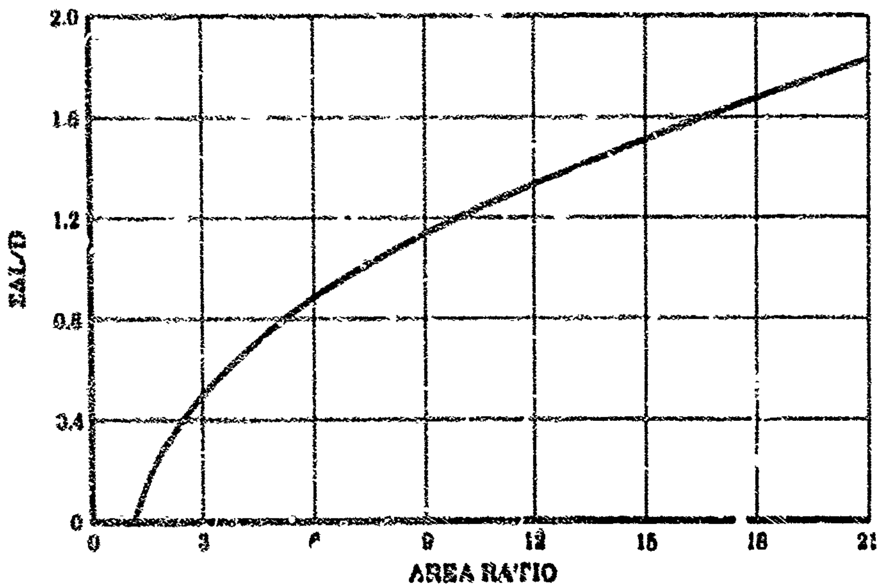

Figure 761. $\Sigma(\Delta L/D)$ vs Area Ratio FD 14020

(U) The relative impulse contribution (ΔI) calculated at each section is correlated by a recovery factor, RF, (refer to figure 762) to obtain an impulse gain associated with the mixing in the nozzle. This increase in impulse added to the base impulse calculated at the throat as shown in equation (16) is the total predicted specific impulse for the nozzle.

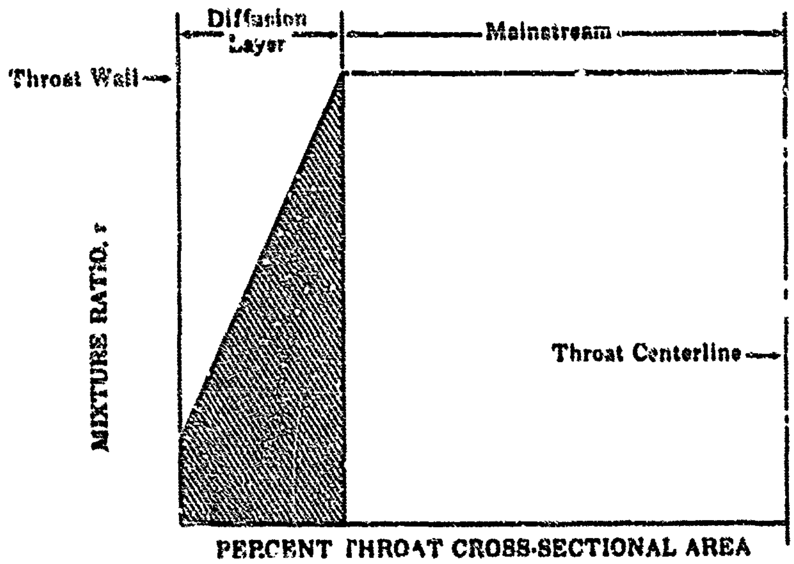

Figure 762. Nozzle Recovery Factor FD 5204

$$I_S = I_{S\ \text{Throat (base)}} + RF_1 \left[\Delta I\right]_{\epsilon = 1}^{\epsilon = ET} + RF_2 \left[\Delta I\right]_{\epsilon = ET}^{\epsilon = \epsilon_1} + \ldots + RF_n \left[\Delta I\right]_{\epsilon = E_{n-2}}^{\epsilon = \epsilon_x} \qquad (16)$$

where:

RF = Recovery factor
ET = Area at end of transpiration cooling
ϵ_x = Nozzle exit area ratio

(U) The theoretical predicted thrust coefficient (C_F) is found by taking the ratio of specific impulse to the c^* predicted by the model.

APPENDIX V
ROCKET EXHAUST SAMPLING PROBE

(C) Correlation of the high pressure test data with theoretical analytical models such as the combustion gas profile model discussed in Appendix II suggests that a significant source of performance loss (3.0% at r = 6.5 based on 50K tests) is attributable to the main chamber combustion gas mixture ratio profile. The assumed profile at r = 6.5 is shown in figure 763.

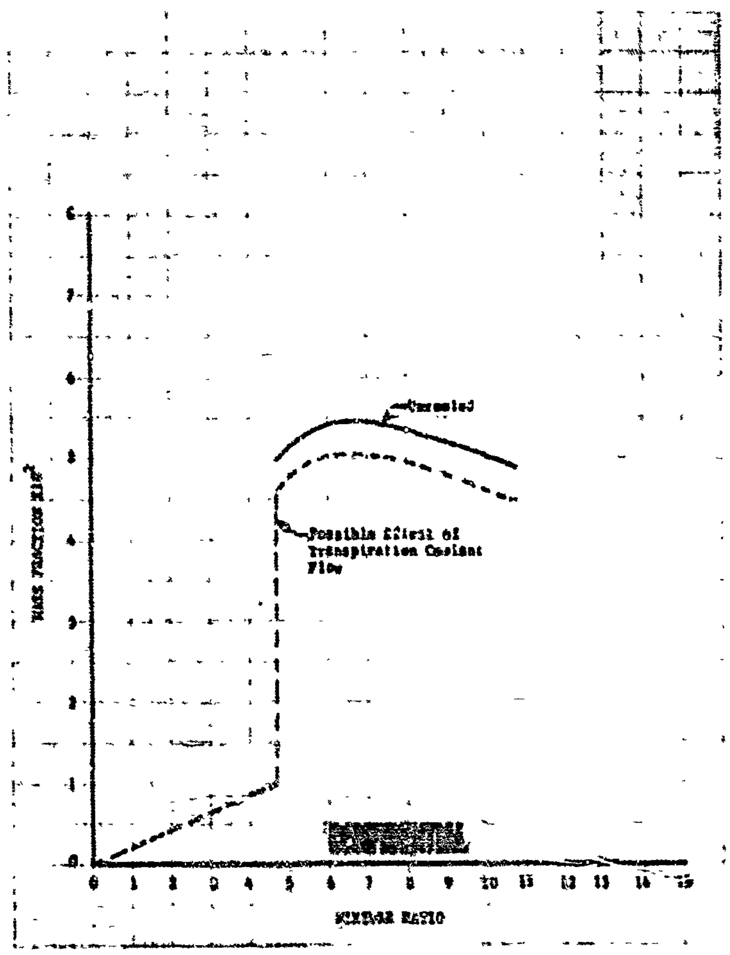

Figure 763. Mixture Ratio Profile Predicted by Combustion Gas Profile Model for r_{inj} = 6.5 and P_c = 3000 psi DF 59677

(U) A probe with four radial sampling ports, shown in figure 764, was used to evaluate the mixture ratio profiles at the exit plane of the secondary nozzle.

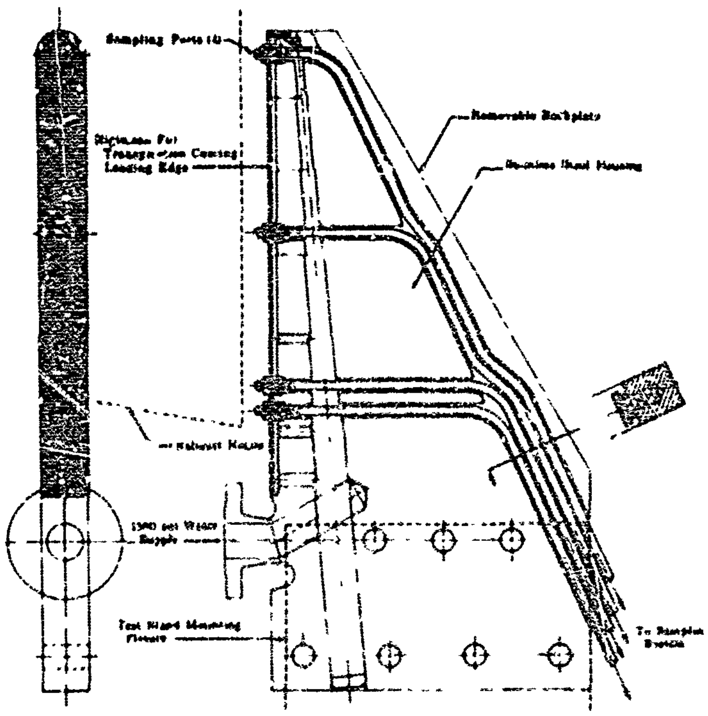

Figure 764. Rocket Exhaust Gas Sampling Probe FD 20173A

(U) The sampling system is shown schematically and installed on the test stand in figures 765 and 766, respectively. Probe tip radial locations are shown in figure 767. Two techniques were employed for profile determination:

1. Continuous monitoring resonator technique
2. Trapped gas sample chromatograph analyses.

(U) The resonator technique is based on the principle that a resonator frequency is proportional to the speed of sound in the media, which is a function of the gas temperature, molecular weight, and specific heat ratio. The gas temperatures and resonator frequencies were measured and used to calculate the molecular weight (mixture ratio). The resonators were frequency-calibrated and the frequency measured by a vibration pickup. The relationship of frequency to mixture ratio and gas temperature is shown for resonator No. 4 in figure 768. In the gas analysis technique, a sample is trapped in the sampling loop of a solenoid-actuated sampling valve and transferred to the chromatograph by a helium carrier, where the constituents are separated by differences in their affinity for a molecular sieve material. The quantity of each constituent is then determined electrically by measuring the changes in the resistance of a heated element, which is affected by the thermal conductivity of the gas. Samples were taken at full thrust with the nozzle extended.

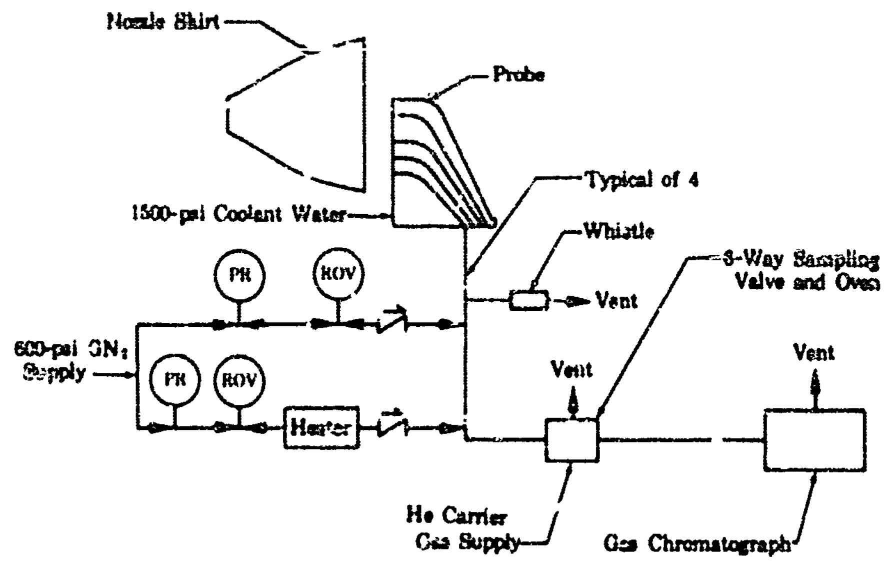

Figure 765. Rocket Exhaust Combustion Gas Sampling System FD 22465

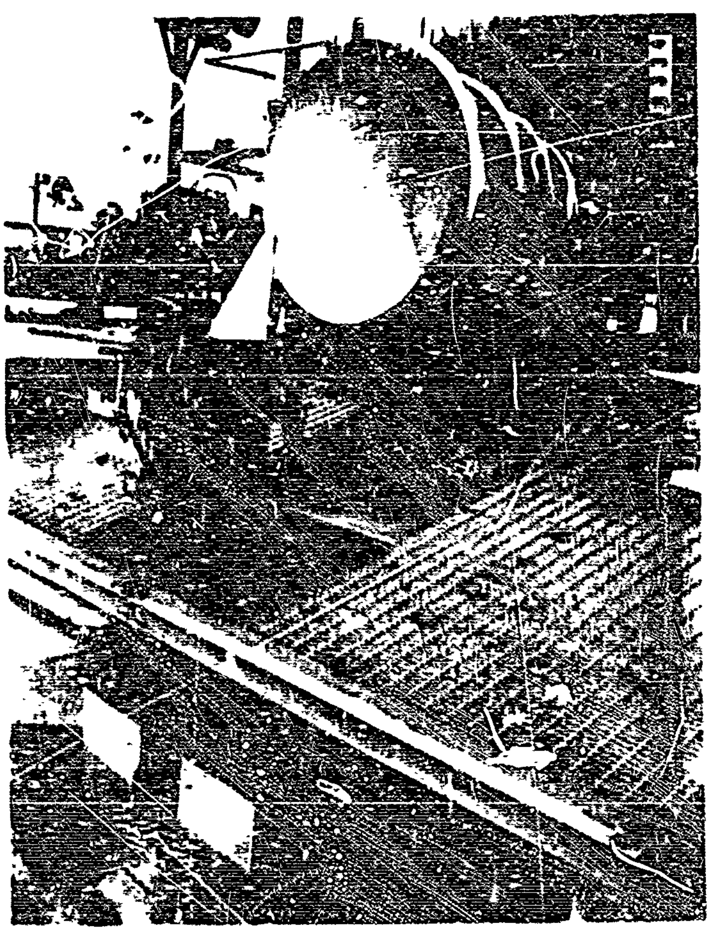

Figure 766. Exhaust Gas Sampling System Installed in Test Stand FE 71324

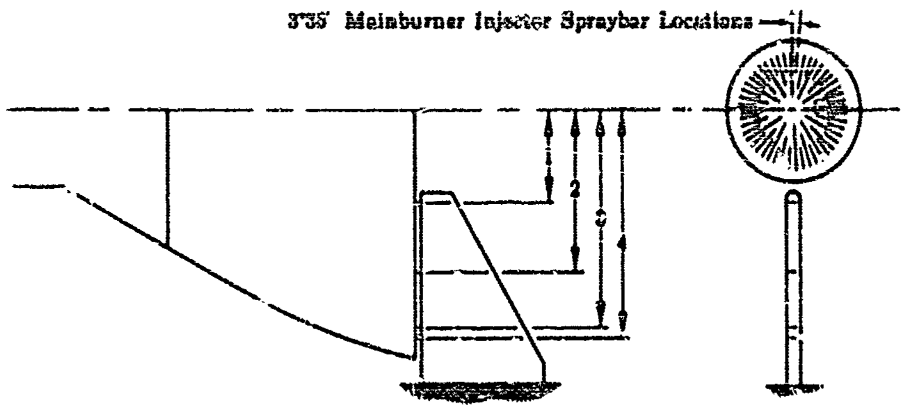

PROBE RADIAL LOCATIONS

Run No.	250SC2C-250SC6C	250SC7C-250SC11C
Probe No. 1	12.443	10.443
Probe No. 2	20.550	18.550
Probe No. 3	27.160	25.160
Probe No. 4	28.250	26.250

Figure 767. Probe Tip Locations FD 23012

(C) The probe leading edge was water-cooled Rigimesh and the sampling tubes were water cooled internally in the housing. Samples were taken during seven tests (250SC2C through 250SC6C, 250SC8C, and 250SC11C). Valid data were not obtained for the first five tests because of insufficient hot gas purge time to adequately heat the lines and prevent condensation. The GN_2 heating system did not provide the capacity to preheat the system significantly above ambient (130°F maximum). Purge time was increased from 4 to 7.75 seconds and system temperatures were increased, although not enough to prevent condensation in all cases. Valid resonator data were obtained at location No. 4 during the last two tests and are shown plotted in figure 768. The chromatograph data cannot be used quantitatively because temperatures at the sample valve remained too low to prevent condensation. However, a significant variation in hydrogen and the fact that some oxygen was captured, as shown in figures 769 and 770, substantiates the theory that a significant mixture ratio profile exists.

(U) The hardware was in good condition after testing, as shown in figure 771. Some erosion of the sampling tips and of the Rigimesh face occurred where the shock wave from the sampling ports impinged on the housing. The probe will be modified to allow more coolant in these areas for future tests. The sampling system will be modified to ensure adequately high system temperatures (>300°F) to prevent water condensation.

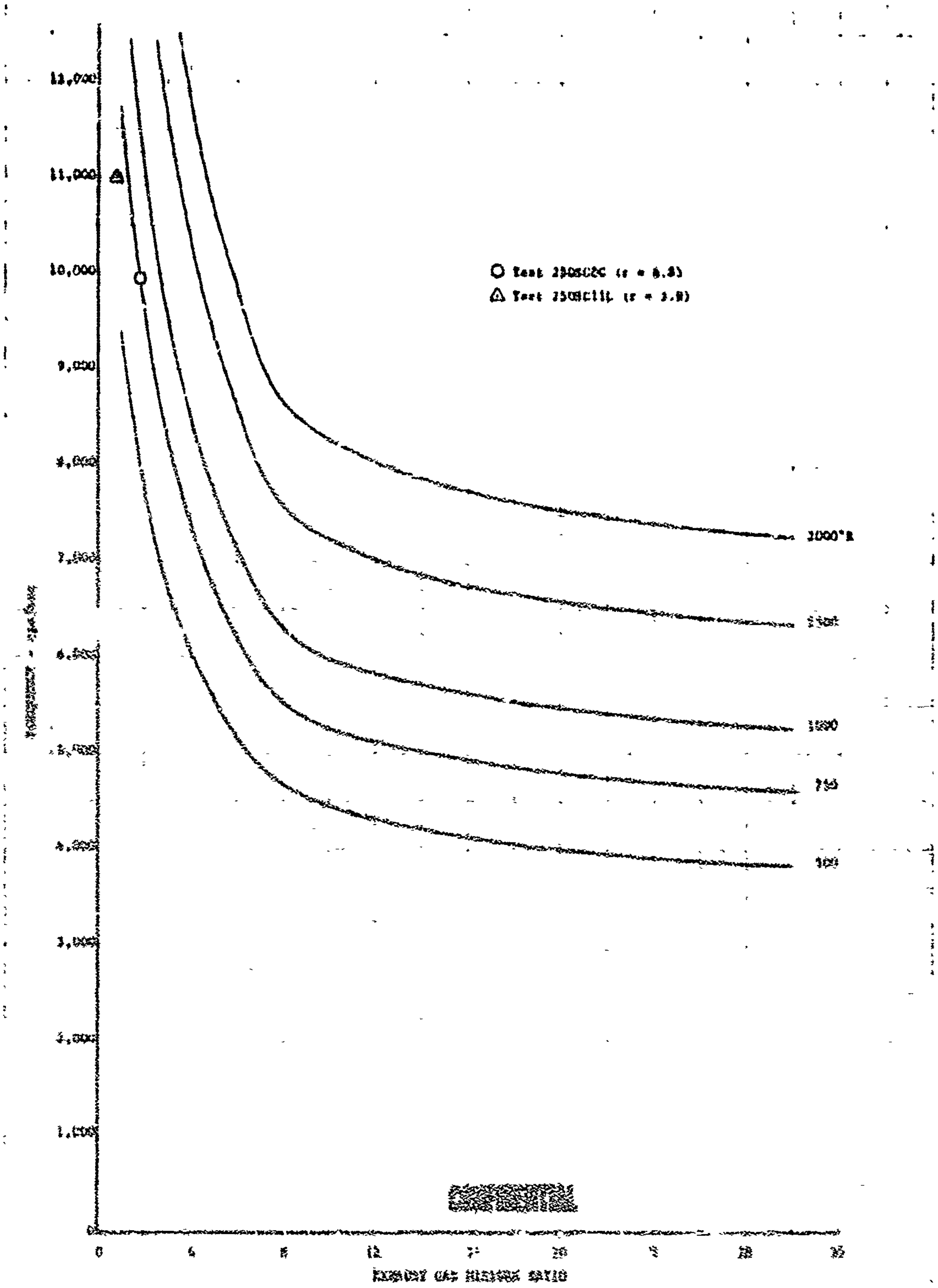

Figure 768. 250K Exhaust Gas Analysis DF 79678

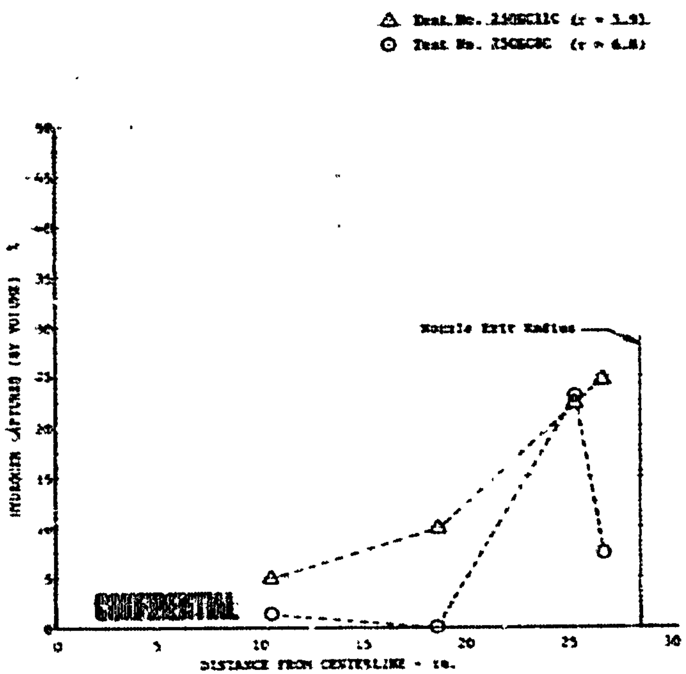

Figure 769. Percent Free Hydrogen (Captured by Sampling Probe) vs Radial Distance From Centerline at Nozzle Exit DF 59390

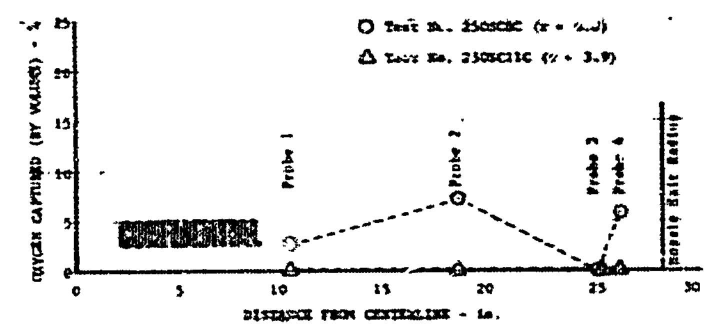

Figure 770. Percent Oxygen (Captured by Sampling Probe) vs Radial Distance From Centerline at Nozzle Exit DF 59391

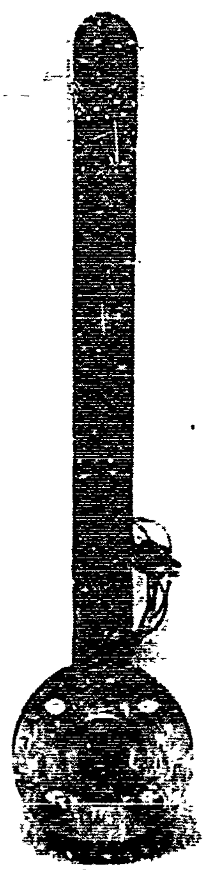

Figure 771. Post-Test Condition of Exhaust Gas Sampling Probe FE 72210

REFERENCES

1. Eckert and Drake, "Heat and Mass Transfer."

2. M. W. Rubensin, "The Influence of Surface Injection on Heat Transfer....," NASA RMA 55L13.

3. E. Bartle and B. Leadon, "The Effectiveness as a Universal Measure of Mass Transfer Cooling for a Turbulent Layer."

4. AFBMA Standards, Section 9, The Anti-Friction Bearing Manufacturers Association, Inc., New York, New York, 1957.

UNCLASSIFIED
Security Classification

DOCUMENT CONTROL DATA - R&D

(Security classification of title, body of abstract and indexing annotation must be entered when the overall report is classified)

1 ORIGINATING ACTIVITY (Corporate author) Pratt & Whitney Aircraft Division of United Aircraft Corporation Florida Research and Development Center	2a REPORT SECURITY CLASSIFICATION CONFIDENTIAL 2b GROUP 4

3 REPORT TITLE

FINAL REPORT
ADVANCED CRYOGENIC ROCKET ENGINE PROGRAM
STAGED-COMBUSTION CONCEPT

4 DESCRIPTIVE NOTES (Type of report and inclusive dates)

Final Report, 1 March 1966 to 30 September 1967

5 AUTHOR(S) (Last name, first name, initial)

Atherton, Robert R.

6 REPORT DATE	7a TOTAL NO OF PAGES	7b NO OF REFS
15 December 1967	814	4

8a CONTRACT OR GRANT NO AF 04(611)-11401 b PROJECT NO c 681C d BPSN 63681C	9a ORIGINATOR'S REPORT NUMBER(S) PWA FR-2597 9b OTHER REPORT NO(S) (Any other numbers that may be assigned this report) AFRPL-TR-67-298

10 AVAILABILITY/LIMITATION NOTICES In addition to security requirements which must be met this document is subject to special export controls and each transmittal to foreign governments or foreign nationals may be made only with prior approval of AFRPL (RPPR/STINFO) Edwards, California 93523

11 SUPPLEMENTARY NOTES Patent Secrecy "Special" and "A" permits	12 SPONSORING MILITARY ACTIVITY Propulsion Laboratory Research and Technology Division, Edwards, California Air Force Systems Command, USAF

13 ABSTRACT

Phase 1 of the Advanced Development Program for a High Performance Oxygen/Hydrogen Rocket Engine, which was sponsored by the Air Force Rocket Propulsion Laboratory at Pratt & Whitney Aircraft, was an evaluation of the critical technology associated with the staged-combustion bell nozzle engine system. Experimental evaluation was conducted in the areas of preburner, main chamber, nozzle, turbopump bearings, and engine controls. In addition, engine system (module) preliminary design and applications studies were conducted. In the Module Design Study, a system cycle balance, steady-state off-design analyses, transient analyses, component and system design studies, a weight study, and a parametric engine study were completed. The Applications Study was completed, and a separate final report, AFRPL-TR-67-270, was issued. Under the Cooling Investigation, 50K staged combustion tests were conducted that demonstrated high impulse efficiency and the two-position translating nozzle. Under the Turbopump Component Investigation, endurance testing of the hydrogen turbopump bearing demonstrated long life is feasible, but roller skewing remains a significant problem. Under the Module Control System investigation, the oxidizer flow divider valve, the mixture ratio valve, and ignition systems were designed, manufactured, and tested with the preburner and main burner. Continued development is needed to improve seal performance. The Preburner Demonstration investigation was completed, and ignition, control, and dynamic combustion stability were demonstrated, however, additional development is required to reduce the hot gas temperature profile. Under the 250K Staged Combustion investigation, the 250K main chamber was tested, and the performance and feasibility of the full-scale tandem concept, including the two-position nozzle and dynamic combustion stability, was demonstrated at various thrust levels

DD FORM 1 JAN 64 1473

UNCLASSIFIED
Security Classification

14. KEY WORDS	LINK A ROLE	LINK A WT	LINK B ROLE	LINK B WT	LINK C ROLE	LINK C WT
Advanced Development Program						
High Performance Oxygen/Hydrogen Rocket Engine						
250K Demonstrator Engine						
High-Pressure, Staged-Combustion, Bell-Nozzle Engine						
Design and Analysis						
Module Design						
Application Study						
Fabrication and Test						
Critical Component Evaluation						
Performance Evaluation						
Cooling Investigation						
Main Chamber						
Preburner						
Turbopump Bearings						
Controls						

INSTRUCTIONS

1. **ORIGINATING ACTIVITY.** Enter the name and address of the contractor, subcontractor, grantee, Department of Defense activity or other organization *(corporate author)* issuing the report.

2a. **REPORT SECURITY CLASSIFICATION:** Enter the overall security classification of the report. Indicate whether "Restricted Data" is included. Marking is to be in accordance with appropriate security regulations.

2b. **GROUP:** Automatic downgrading is specified in DoD Directive 5200.10 and Armed Forces Industrial Manual. Enter the group number. Also, when applicable, show that optional markings have been used for Group 3 and Group 4 as authorized.

3. **REPORT TITLE:** Enter the complete report title in all capital letters. Titles in all cases should be unclassified. If a meaningful title cannot be selected without classification, show title classification in all capitals in parenthesis immediately following the title.

4. **DESCRIPTIVE NOTES:** If appropriate, enter the type of report, e.g., interim, progress, summary, annual, or final. Give the inclusive dates when a specific reporting period is covered.

5. **AUTHOR(S):** Enter the name(s) of author(s) as shown on or in the report. Enter last name, first name, middle initial. If military, show rank and branch of service. The name of the principal author is an absolute minimum requirement.

6. **REPORT DATE:** Enter the date of the report as day, month, year, or month, year. If more than one date appears on the report, use date of publication.

7a. **TOTAL NUMBER OF PAGES:** The total page count should follow normal pagination procedures, i.e., enter the number of pages containing information.

7b. **NUMBER OF REFERENCES:** Enter the total number of references cited in the report.

8a. **CONTRACT OR GRANT NUMBER:** If appropriate, enter the applicable number of the contract or grant under which the report was written.

8b, 8c, & 8d. **PROJECT NUMBER:** Enter the appropriate military department identification, such as project number, subproject number, system numbers, task number, etc.

9a. **ORIGINATOR'S REPORT NUMBER(S):** Enter the official report number by which the document will be identified and controlled by the originating activity. This number must be unique to this report.

9b. **OTHER REPORT NUMBER(S):** If the report has been assigned any other report numbers *(either by the originator or by the sponsor)*, also enter this number(s).

10. **AVAILABILITY/LIMITATION NOTICES:** Enter any limitations on further dissemination of the report, other than those imposed by security classification, using standard statements such as:

(1) "Qualified requesters may obtain copies of this report from DDC."

(2) "Foreign announcement and dissemination of this report by DDC is not authorized."

(3) "U. S. Government agencies may obtain copies of this report directly from DDC. Other qualified DDC users shall request through ________."

(4) "U. S. military agencies may obtain copies of this report directly from DDC. Other qualified users shall request through ________."

(5) "All distribution of this report is controlled. Qualified DDC users shall request through ________."

If the report has been furnished to the Office of Technical Services, Department of Commerce, for sale to the public, indicate this fact and enter the price, if known.

11. **SUPPLEMENTARY NOTES:** Use for additional explanatory notes.

12. **SPONSORING MILITARY ACTIVITY:** Enter the name of the departmental project office or laboratory sponsoring *(paying for)* the research and development. Include address.

13. **ABSTRACT:** Enter an abstract giving a brief and factual summary of the document indicative of the report, even though it may also appear elsewhere in the body of the technical report. If additional space is required, a continuation sheet shall be attached.

It is highly desirable that the abstract of classified reports be unclassified. Each paragraph of the abstract shall end with an indication of the military security classification of the information in the paragraph, represented as *(TS), (S), (C), or (U)*.

There is no limitation on the length of the abstract. However, the suggested length is from 150 to 225 words.

14. **KEY WORDS:** Key words are technically meaningful terms or short phrases that characterize a report and may be used as index entries for cataloging the report. Key words must be selected so that no security classification is required. Identifiers, such as equipment model designation, trade name, military project code name, geographic location, may be used as key words but will be followed by an indication of technical context. The assignment of links, roles, and weights is optional.

SUPPLEMENTARY

INFORMATION

AD-385 912

DIVISION OF UNITED AIRCRAFT CORPORATION

OCT - 7 1968

In reply please refer to:
MFS:RPSmh:Cont. Adm.

Mrs. Mary Racovich, FTMKR-3
Directorate of Materiel
Procurement Division
Edwards Air Force Base, California 93523

Reference: (a) N/F PWA FP 67-11, 250K High Performance Reusable Oxygen/Hydrogen Rocket Engine, dated 21 August 1967.

(b) N/F PWA FR-1810, Components Design Handbook, Advanced Development Program for a High Performance Oxygen/Hydrogen Rocket Engine, dated 30 June 1966.

(c) PWA FR-1911, Quarterly Report No. 1, Advanced Cryogenic Rocket Engine Program Staged - Combustion Concept, dated June 1966.

(d) N/F PWA FR-1928, Quarterly Report No. 1, 250K Thrust Chamber Technology Program, dated 30 June 1966.

(e) N/F PWA FR-2372, Final Report - Advanced Engine Design Study, Bell, (AEB), dated July 31, 1967.

(f) PWA FR-2597, Advanced Cryogenic Rocket Engine Program Staged - Combustion Concept - Final Report, dated December 1967.

Dear Mrs. Racovich:

The U. S. Patent Office has issued a Secrecy Order with a modifying "Security Requirements Permit" against United Aircraft Corporation's U. S. Patent Application No. 725,954, entitled "Dual Slot Swirler Injector Element." This Secrecy Order relates to a single throttleable injection element that provides a wide range of throttleability. You are advised that the referenced documents contain information relating to this concept.

A "Security Requirements Permit" limits disclosure of the subject matter involved to the security requirements of the Government contract which imposes the highest level of security classification thereon. The highest level of security classification on the subject matter of this application is "Confidential". Disclosure of the invention or any material information with respect thereto is prohibited except by written consent of the Commissioner of Patents or as authorized by the permit. By statute, violation of a Secrecy Order is punishable by a fine not to exceed $10,000 and/or imprisonment for not more than two years.

If this invention has been disclosed to others, the recipients of this letter are requested to notify them of the issuance of the Secrecy Order and "Security Requirements Permit" and of the penalties for violation.

Very truly yours,

UNITED AIRCRAFT CORPORATION
Pratt & Whitney Aircraft Division

M. F. Samples

M. F. Samples
Senior Contract Administrator
Florida Research and Development Center

cc: see attached.